Unveiling cosmic-ray mysteries through radio: modeling and analysis of radio signals detected with GRAND

LPNHE PARIS
IAP
SCIENCES SORBONNE UNIVERSITÉ

Marion Guelfand

GRAND

PhD Defense Talk
Sorbonne University, Jussieu Campus, Paris
September 17, 2025

Supervisors:
Olivier Martineau - Kumiko Kotera - Simon Prunet

The puzzle of cosmic rays

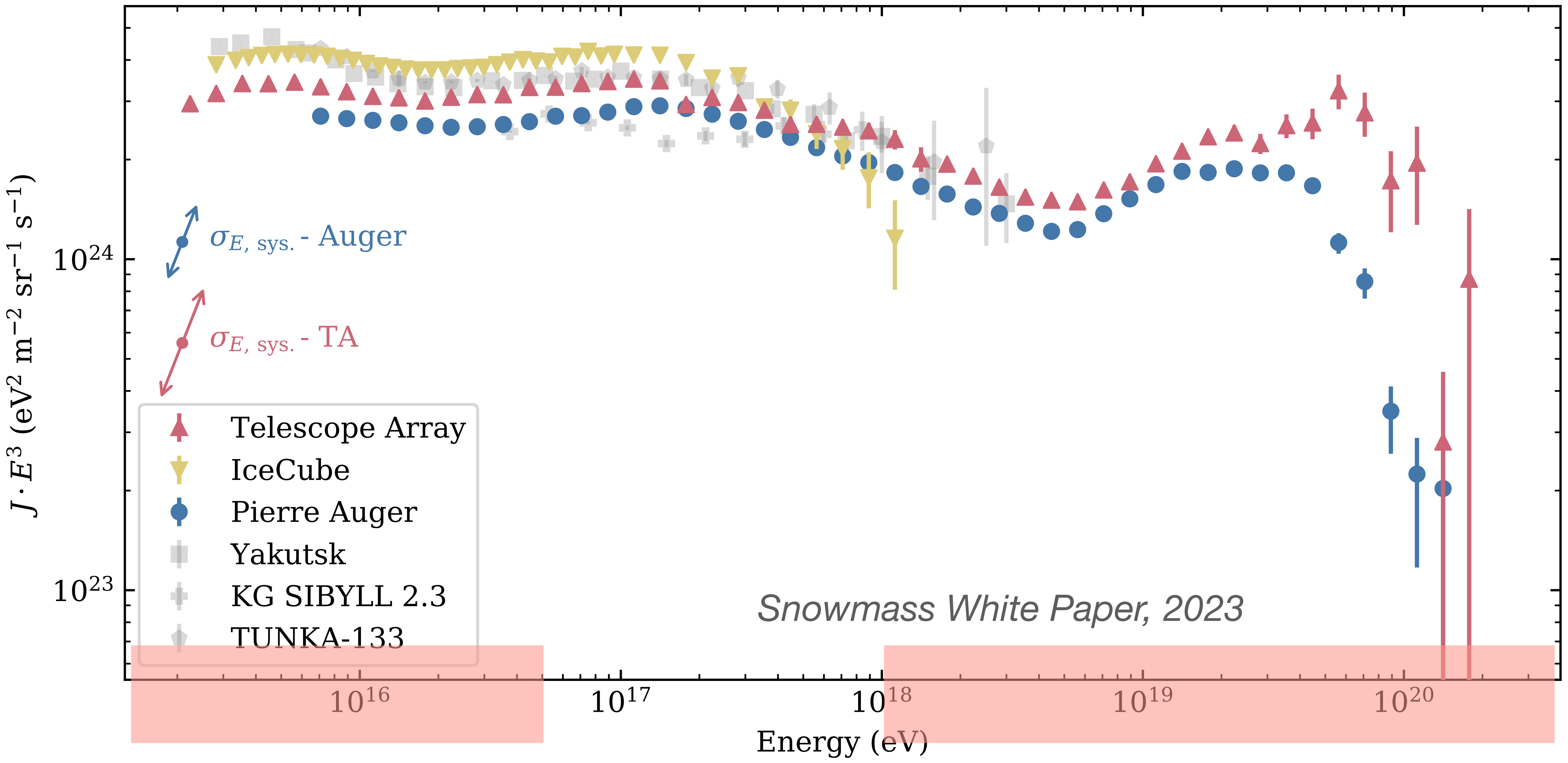

Produced in the Galaxy (Milky Way)

Produced in other galaxies… But how? Which sources?

- Cosmic rays (CRs)

High energy nuclei

Galactic origin: $E \lesssim 10^{16.5}$ eV

- Ultra high energy cosmic rays (UHECRs): $E > 10^{18}$ eV

Extragalactic origin

Most energetic particles in the Universe

What are the sources that produces UHECRs?

$E_{\mathrm{UHECR}} \sim 3.10^{20}$ eV
~ 50 J

$E_{\mathrm{LHC}} \sim 10^{13}$ eV
$\sim 1.6\,\mu$J

The puzzle of cosmic rays

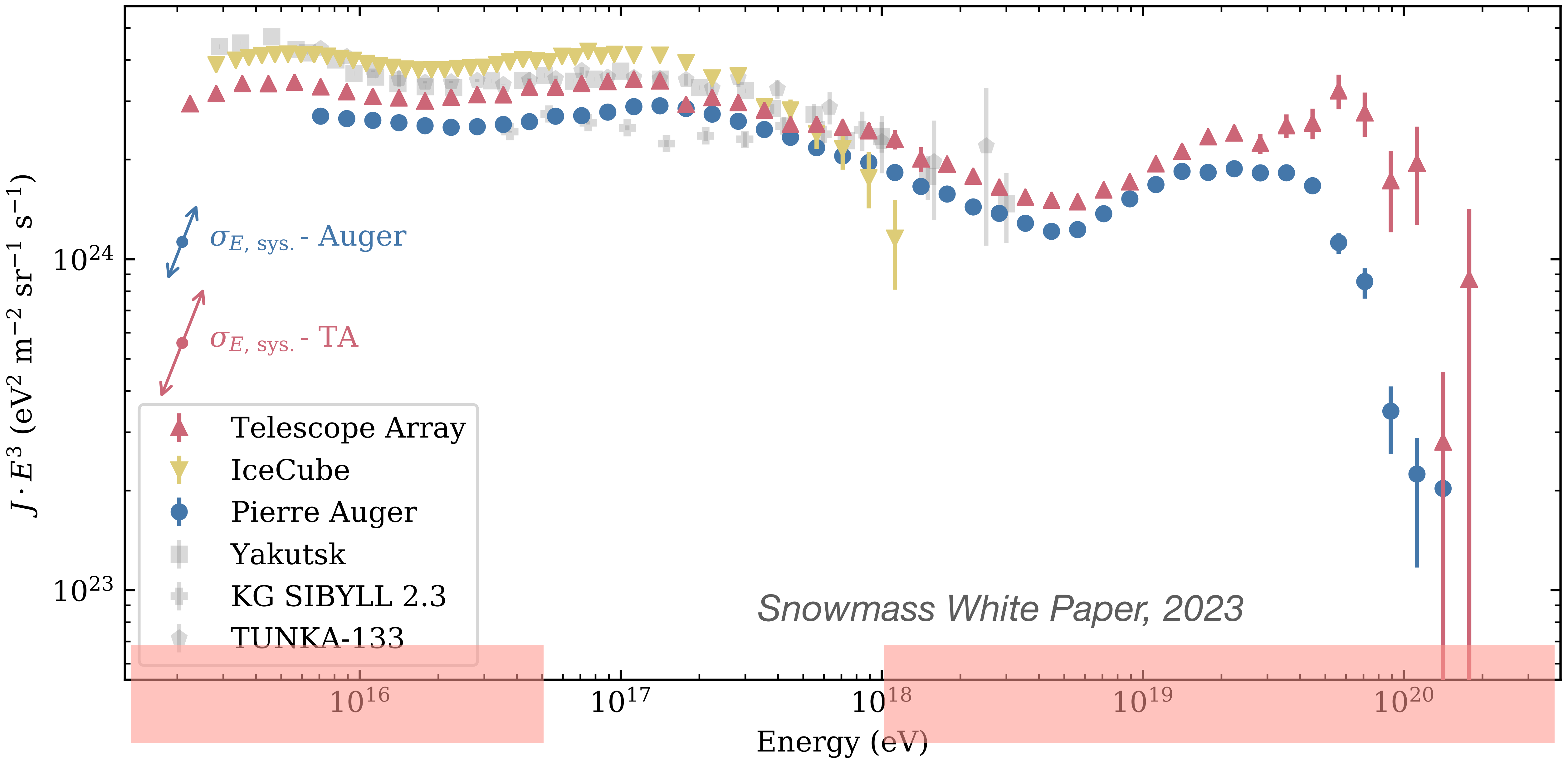

Produced in the Galaxy
(Milky Way)

Produced in other galaxies…
But how? Which sources?

- Cosmic rays (CRs)

High energy nuclei

Galactic origin: $E \lesssim 10^{16.5}$ eV

- Ultra high energy cosmic rays (UHECRs): $E > 10^{18}$ eV

Extragalactic origin

Most energetic particles in the Universe

What are the sources that produces UHECRs?

The UHECR puzzle
- Deflected: charged particles
- Attenuated during propagation
- Very low fluxes —> only indirect detection

$E_{\text{UHECR}} \sim 3.10^{20}$ eV
~ 50 J

$E_{\text{LHC}} \sim 10^{13}$ eV
$\sim 1.6\,\mu$J

The ultra high energy (UHE) multi-messengers

UHE gamma rays γ

- Undefleted ✓
- Short horizon
- Undetected

UHE neutrinos ν ($E \geq 10^{17}$ eV)

- Undeflected ✓
- Deep horizon (small cross section) ✓
- Hadronic interactions ✓

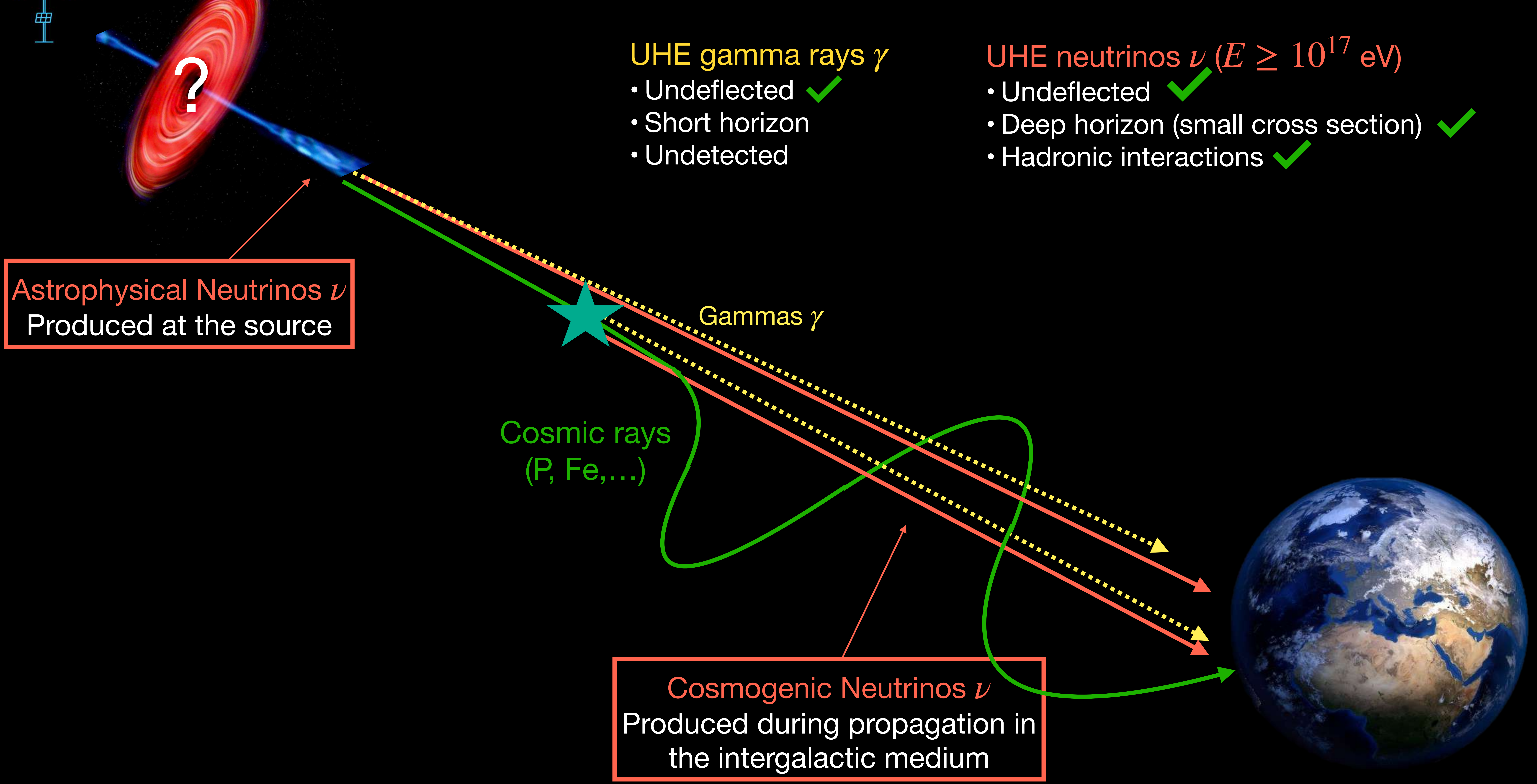

The ultra high energy (UHE) multi-messengers

UHE gamma rays γ
- Undeflected ✓
- Short horizon
- Undetected

UHE neutrinos ν ($E \geq 10^{17}$ eV)
- Undeflected ✓
- Deep horizon (small cross section) ✓
- Hadronic interactions ✓

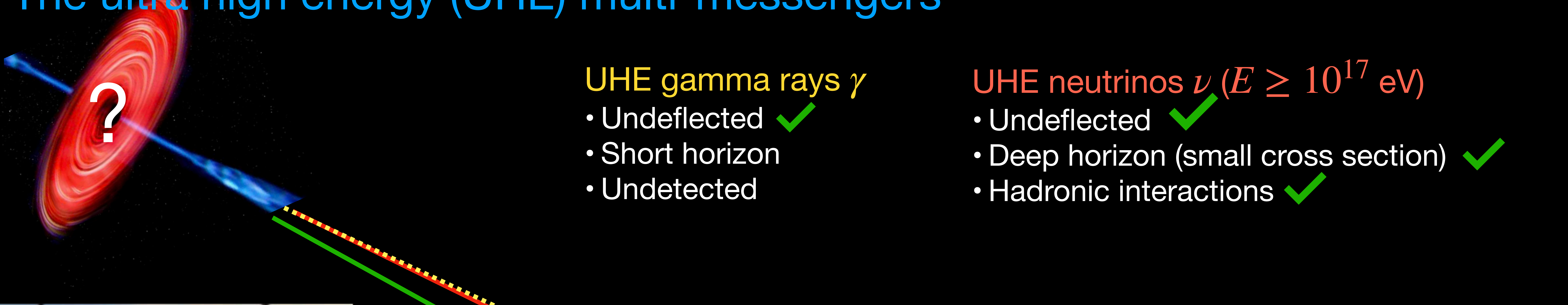

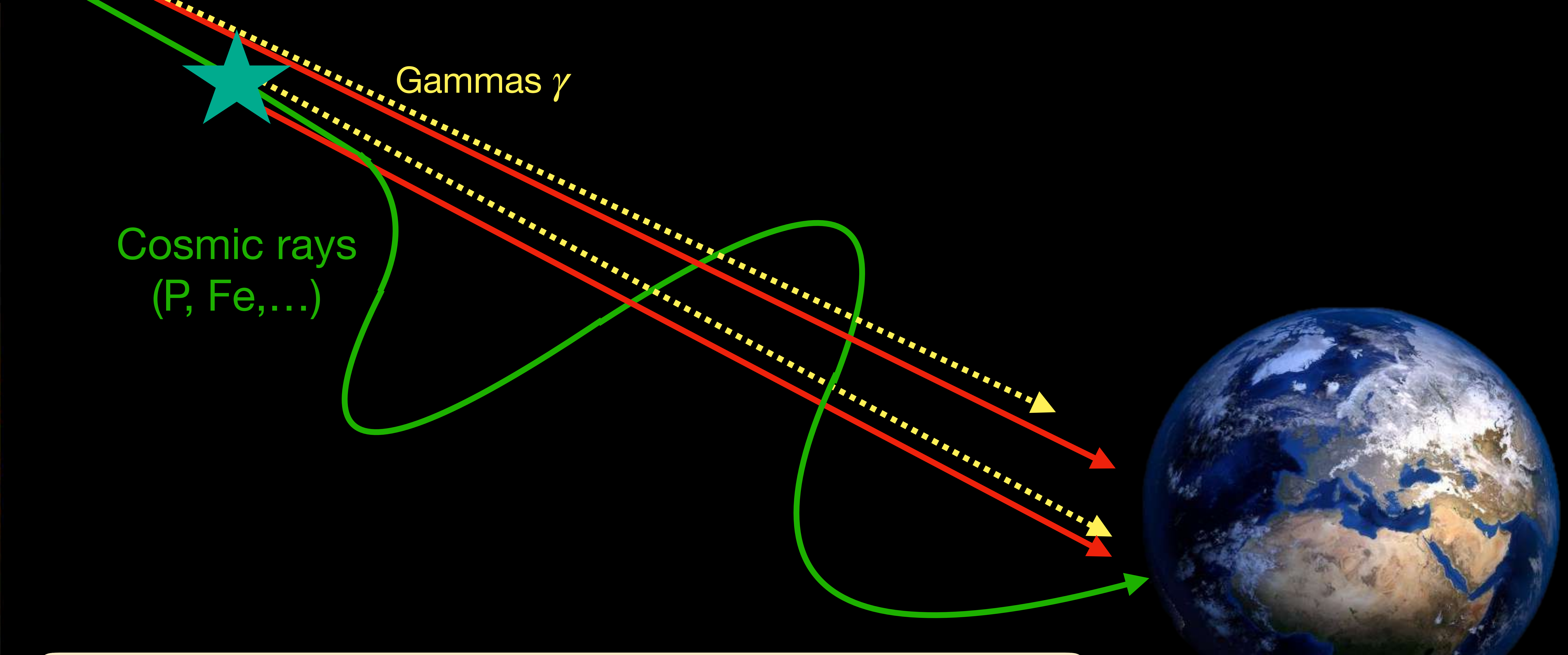

February 2025: First detection of UHE neutrinos by KM3NeT

An evolving science case

- UHE ν frontier: largely unexplored (very low fluxes)
  - **Smoking gun evidence for the origin of UHECRs**

- **Multi-messenger astronomy:**
Understanding UHE Universe and probe UHE transient source

Credit: NASA GSFC & Caltech/MIT/LIGO Lab

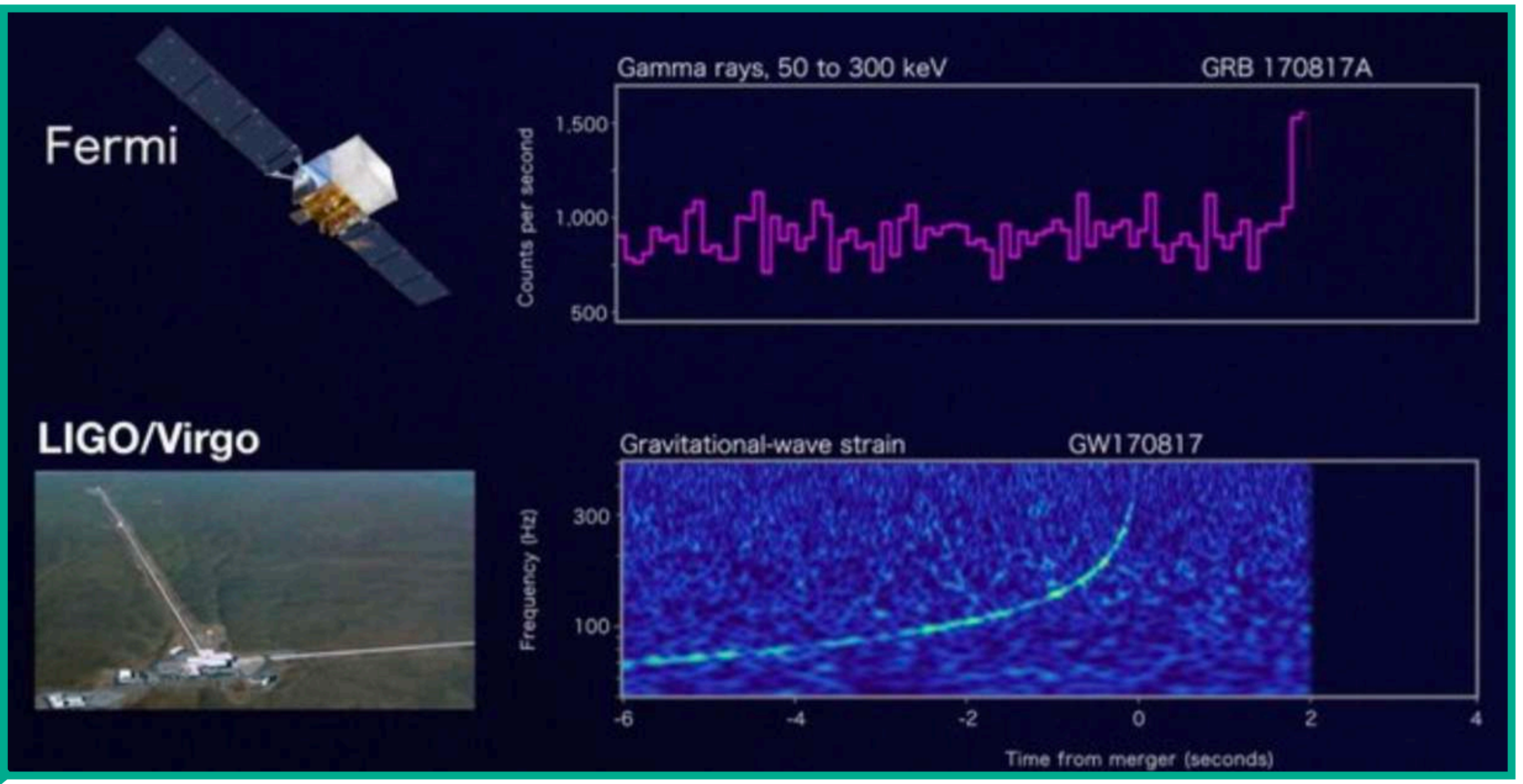

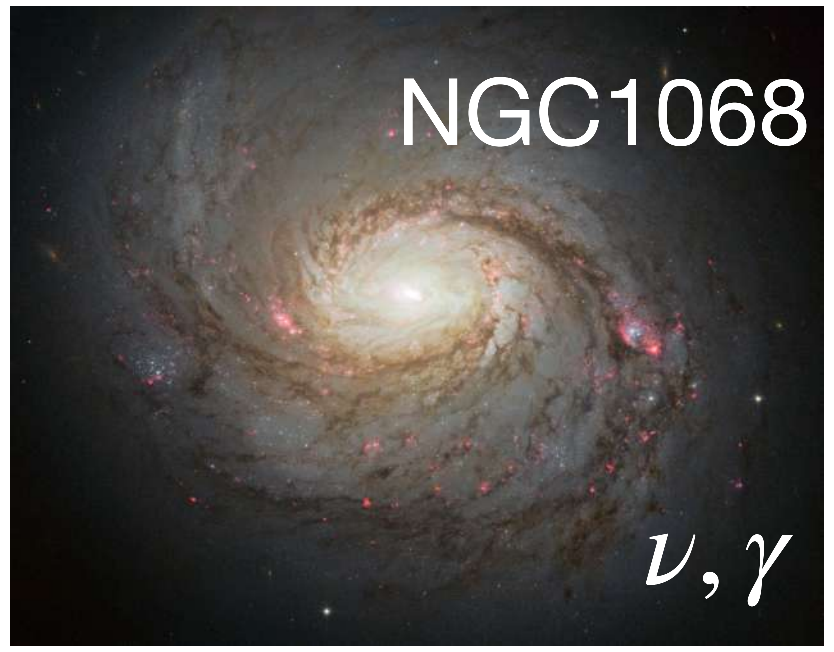

Active Galactic Nuclei (2022)

Binary neutron star merger (2017)

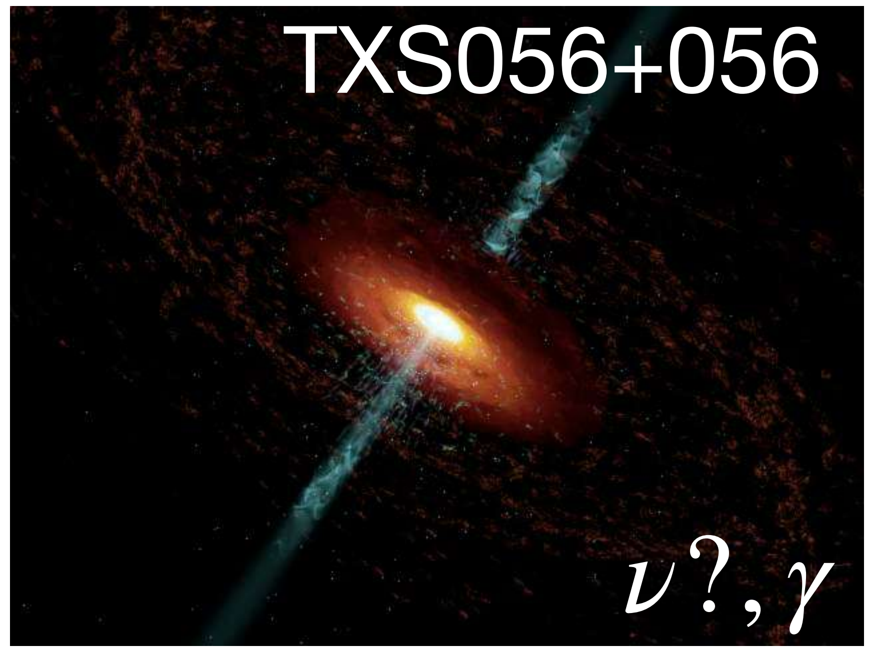

Blazar Flare (2017)

Next generation experiments will need:
- **Gigantic detection surfaces** to improve sensitivity
- Wide instantaneous field of view
- **Sub-degree angular resolution**

UHE neutrino detection methods

- **In ice/water** pioneering neutrino detectors
(IceCube, ANTARES, KM3NeT)
Dense medium $\longrightarrow$ enhanced interaction probability

IceCube: first cosmic ν detected (2013): **only 2 > PeV energies**
Limits: size (extension IceCubeGen2 radio, 2032)
$\sim 1^\circ$ angular resolution

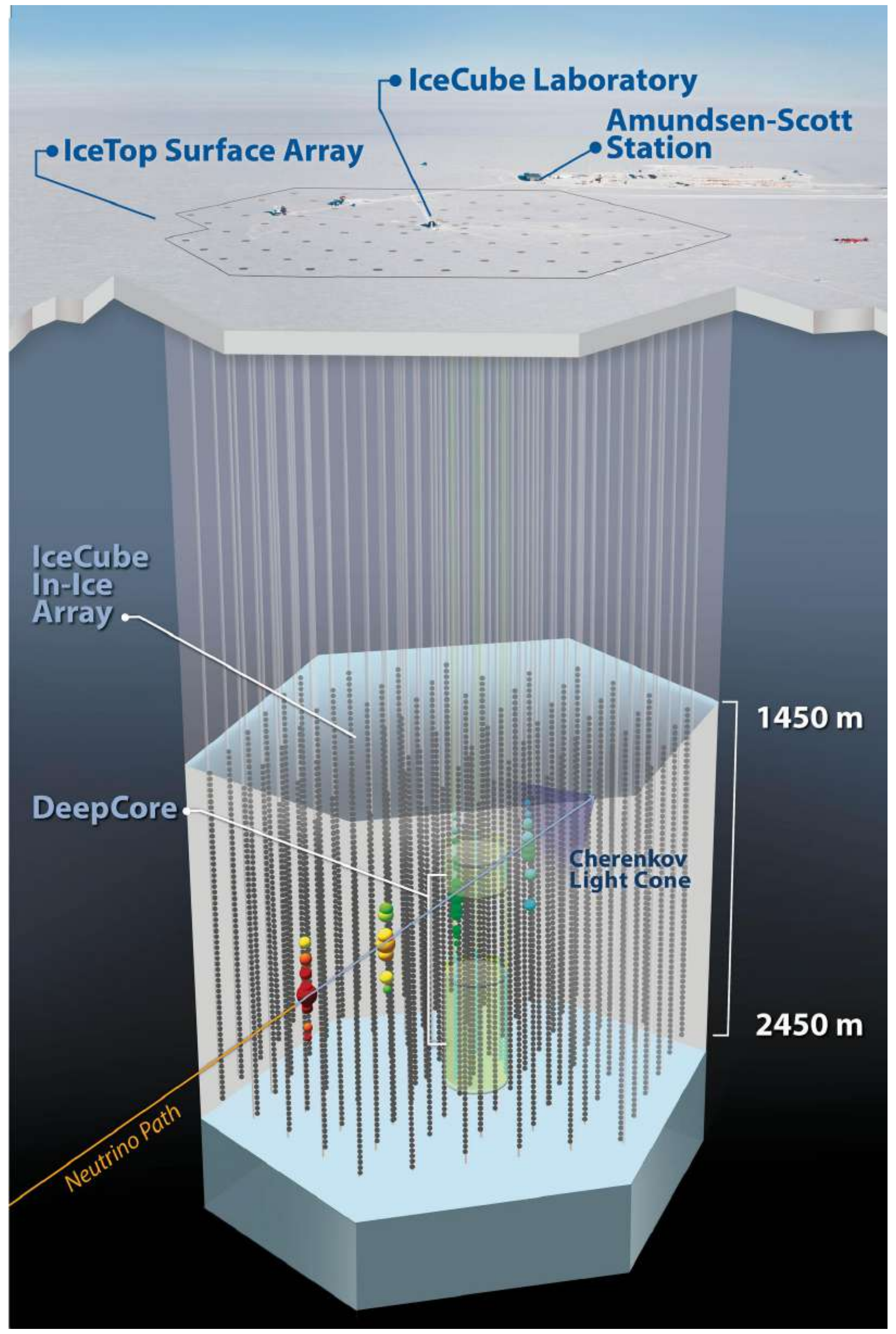

IceCube Neutrino Observatory

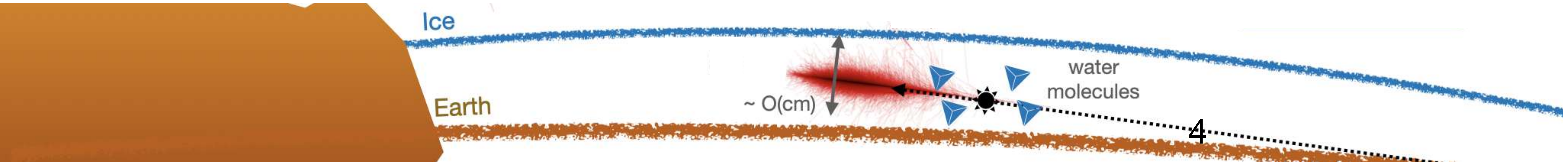

UHE neutrino detection methods

- In air detectors:

UHE ν_τ: interact in Earth crust ⟶ produce τ-particle ⟶ τ decay
UHECRs: interact in atmosphere

- Production of an extensive air shower (EAS)
- Emission mechanisms: Cherenkov light, fluorescence light in air, **radio emission**

Radio detection:
Efficient, scalable, robust, cheap, 100% duty cycle
Ideal for giant arrays to probe low fluxes

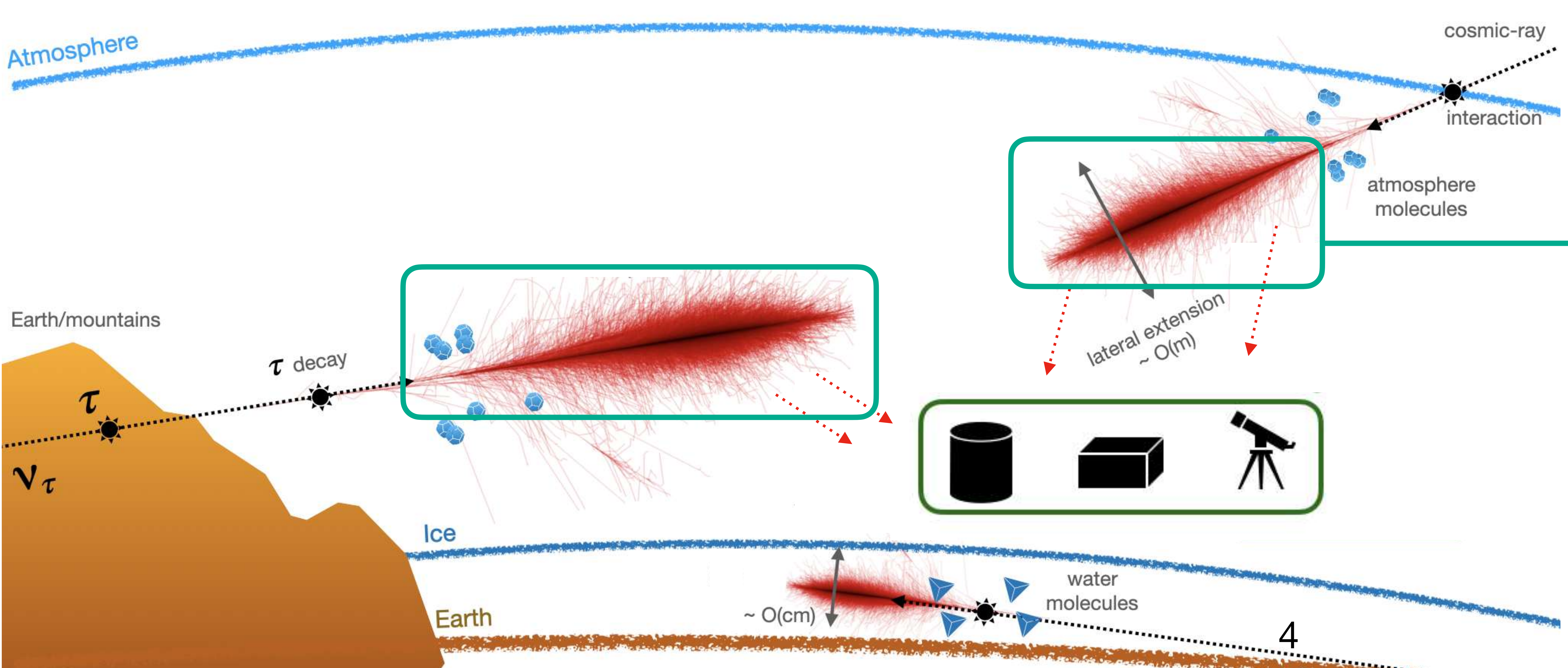

Particle cascade (called **extensive air shower** in air)

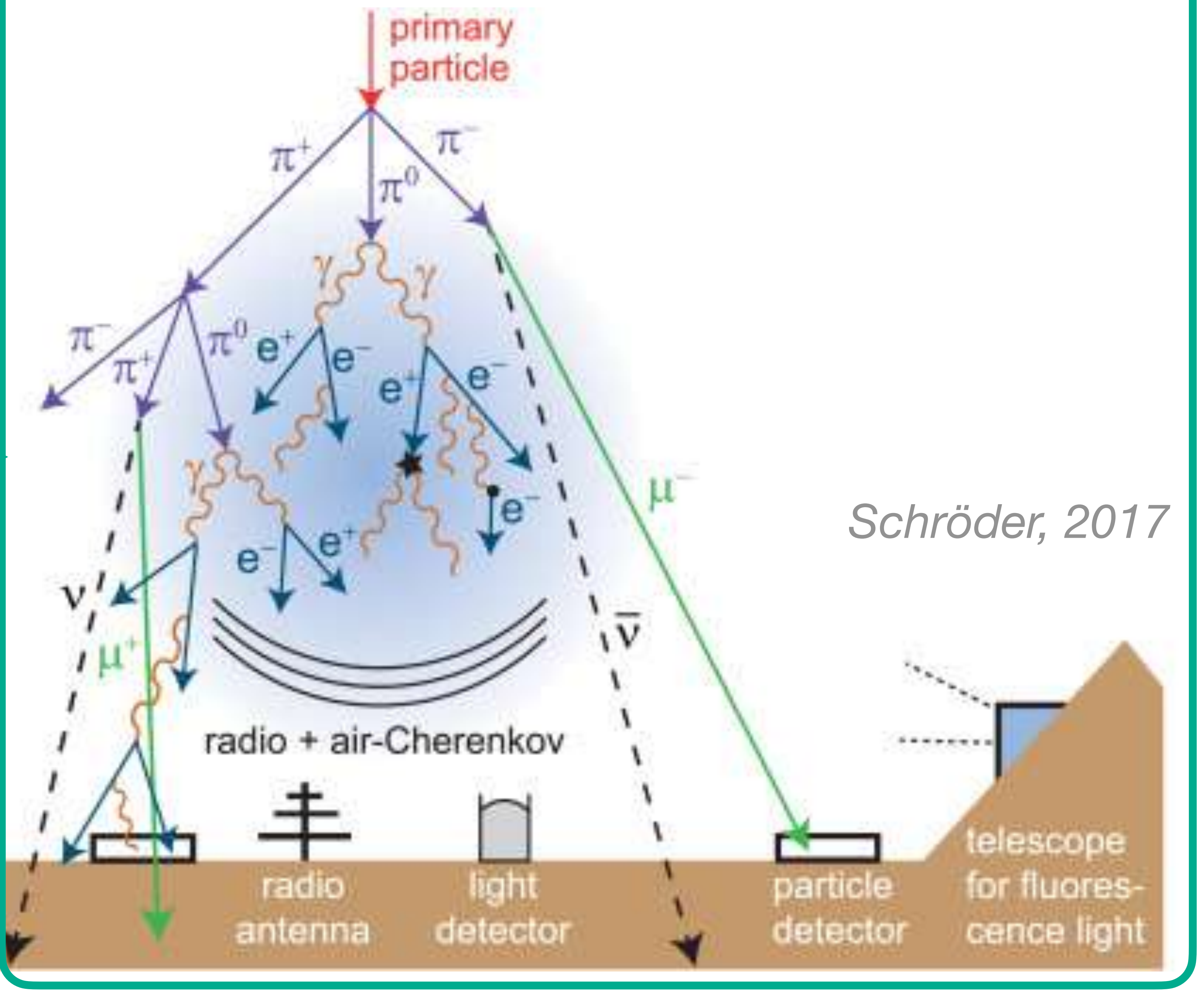

Schröder, 2017

The Giant Radio Array for Neutrino Detection (GRAND)

Baseline design:

200’000 radio antennas over 200'000 km² in 20 sub-arrays at favorable sites worldwide

The Giant Radio Array for Neutrino Detection (GRAND)

Baseline design:

200’000 radio antennas over 200'000 km² in 20 sub-arrays at favorable sites worldwide

Detection of very inclined air showers

Large footprints on ground

Sparse antenna array

Very **large observatory** for improved sensitivity

The Giant Radio Array for Neutrino Detection (GRAND)

Baseline design:

200’000 radio antennas over 200'000 km² in 20 sub-arrays at favorable sites worldwide

GRAND @ Nançay

GRANDProto300

GRAND @ Auger

Detection of very inclined air showers

Large footprints on ground

Sparse antenna array

Very **large observatory** for improved sensitivity

The GRANDProto300 (GP300) Prototype

Guelfand for the GRAND collaboration, Proceeding Moriond 2024, arXiv:2501.01851

Goals: **Validate detection principle**: **autonomous** radio detection

Science: cosmic rays $10^{16.5} - 10^{18}$ eV.

Transition region between Galactic ⟷ Extragalactic cosmic rays

Alves Batista, Guépin, Guelfand, Kotera, Marcowith, in prep

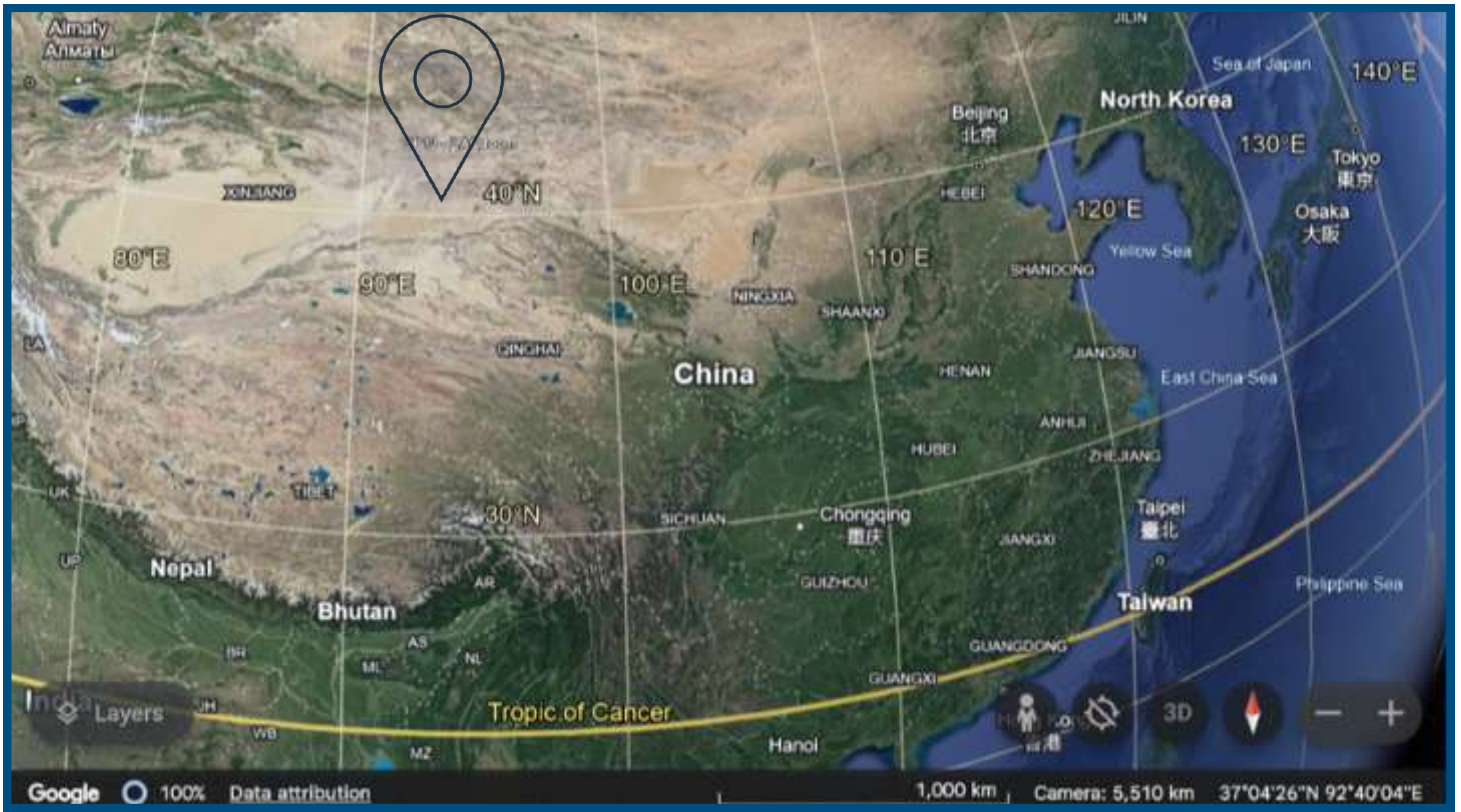

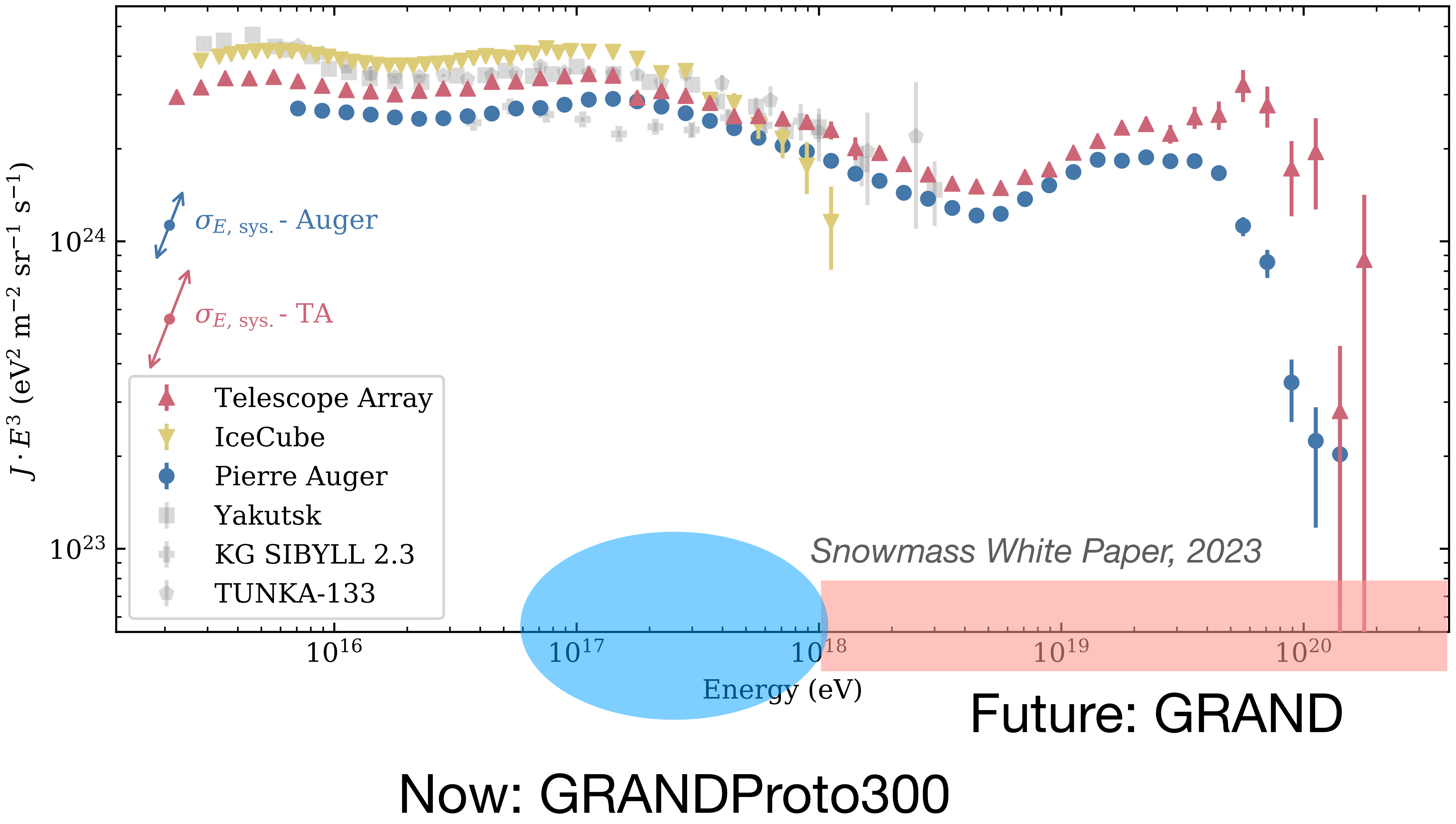

The GRANDProto300 (GP300) Prototype

__Guelfand__ for the GRAND collaboration, Proceeding Moriond 2024, arXiv:2501.01851

Goals: **Validate detection principle**: **autonomous** radio detection

Science: cosmic rays $10^{16.5} - 10^{18}$ eV.

Transition region between Galactic ⟷ Extragalactic cosmic rays

Final stage: 300 antennas over 200 km^2

Status: 65 antennas deployed and running

Clean environment, stable & homogeneous detector

- End of commissioning phase, **cosmic ray search** starting

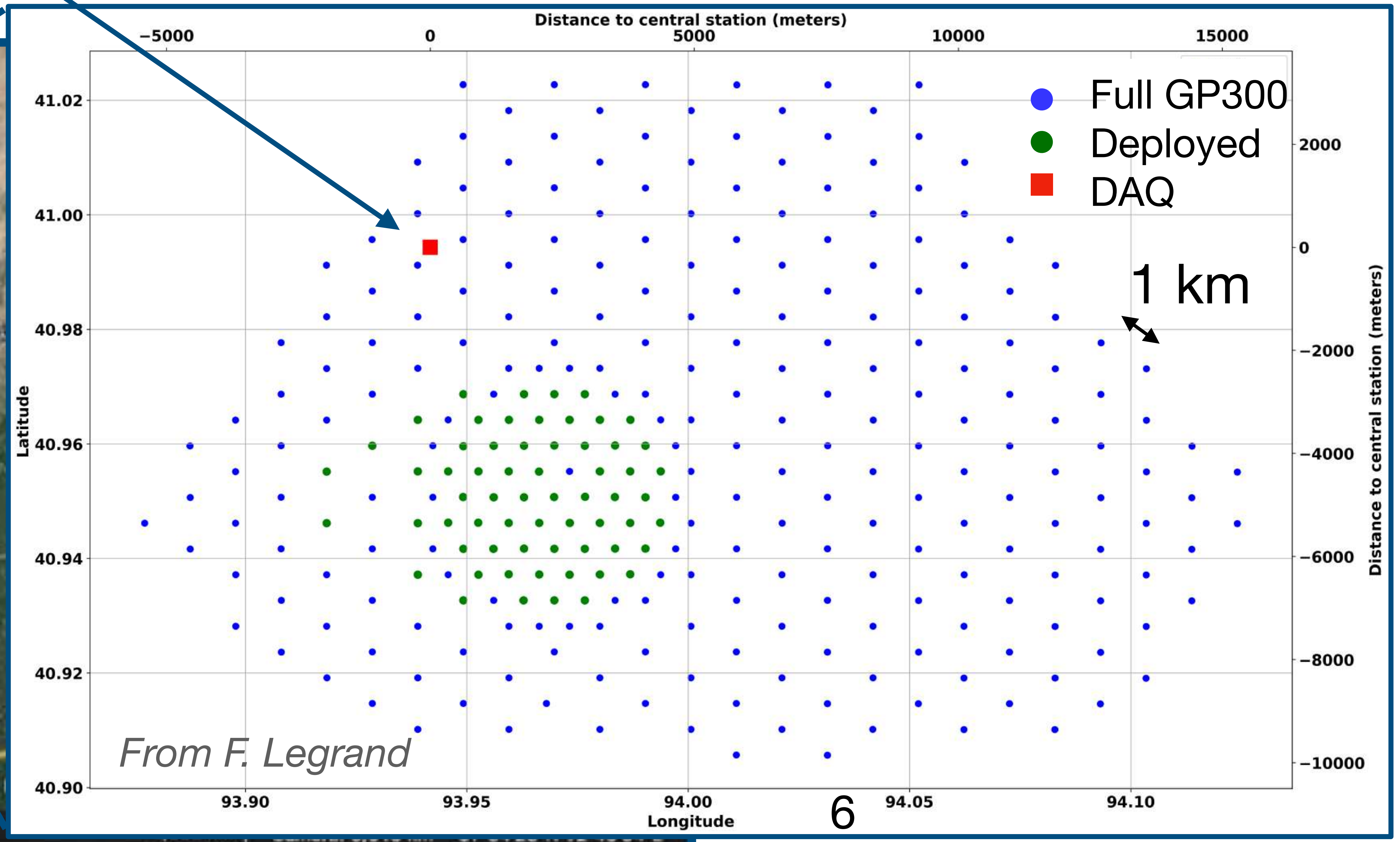

1.4m

3.5m

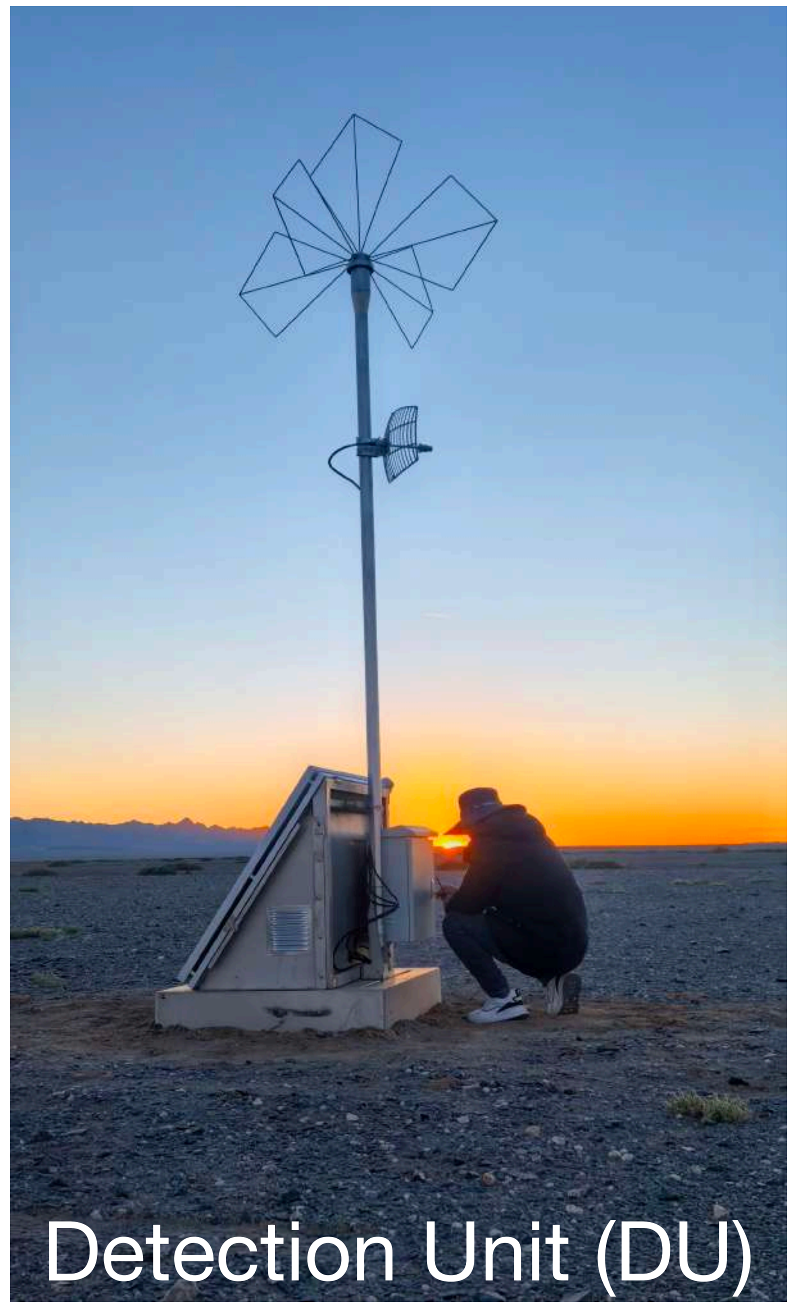

GRAND and the challenges of radio detection

I.Physical modeling of inclined air showers
and their radio emission

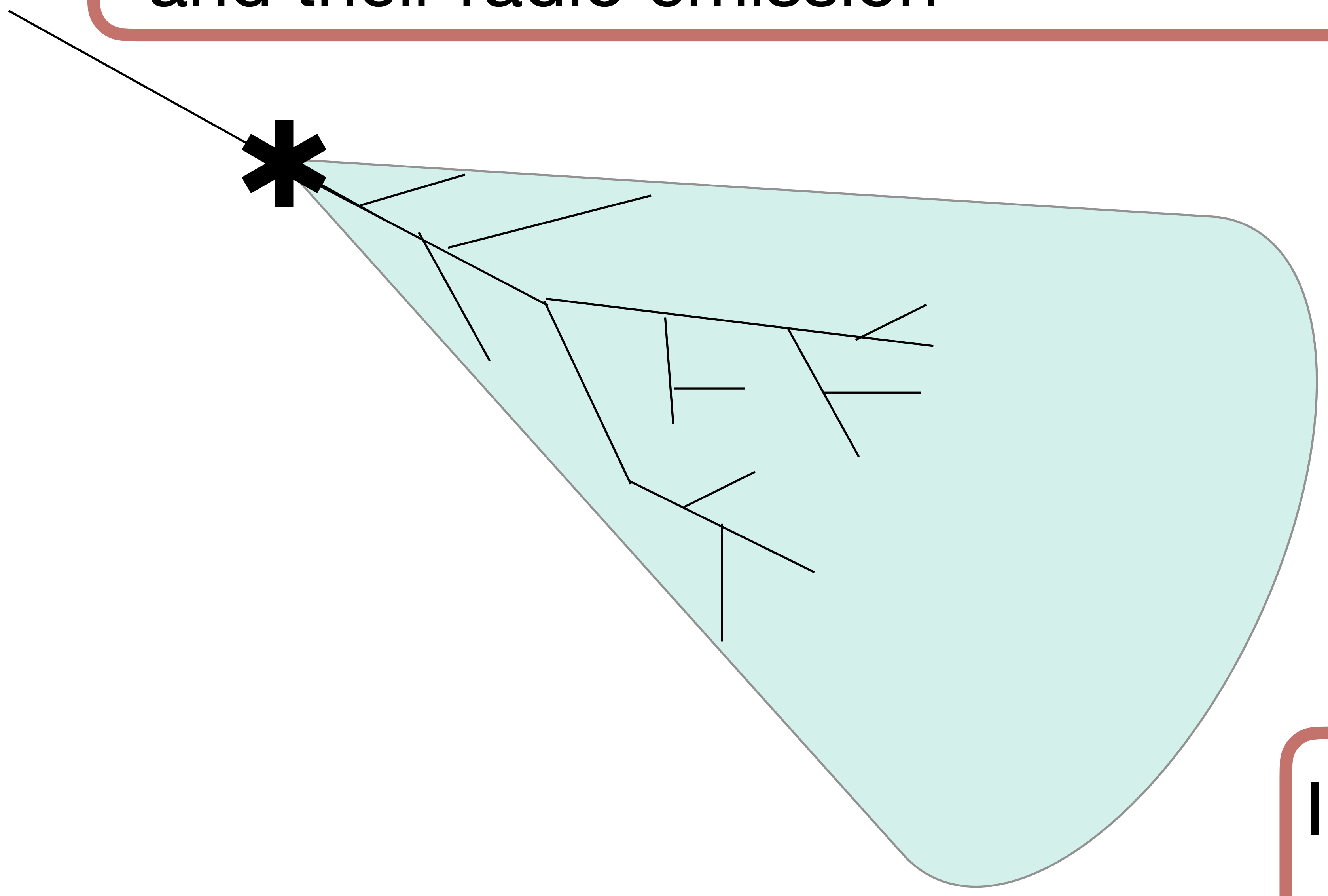

III. Reconstruction of cosmic particle
properties for very inclined showers

II. Autonomous trigger: find the radio
signal inside the noise

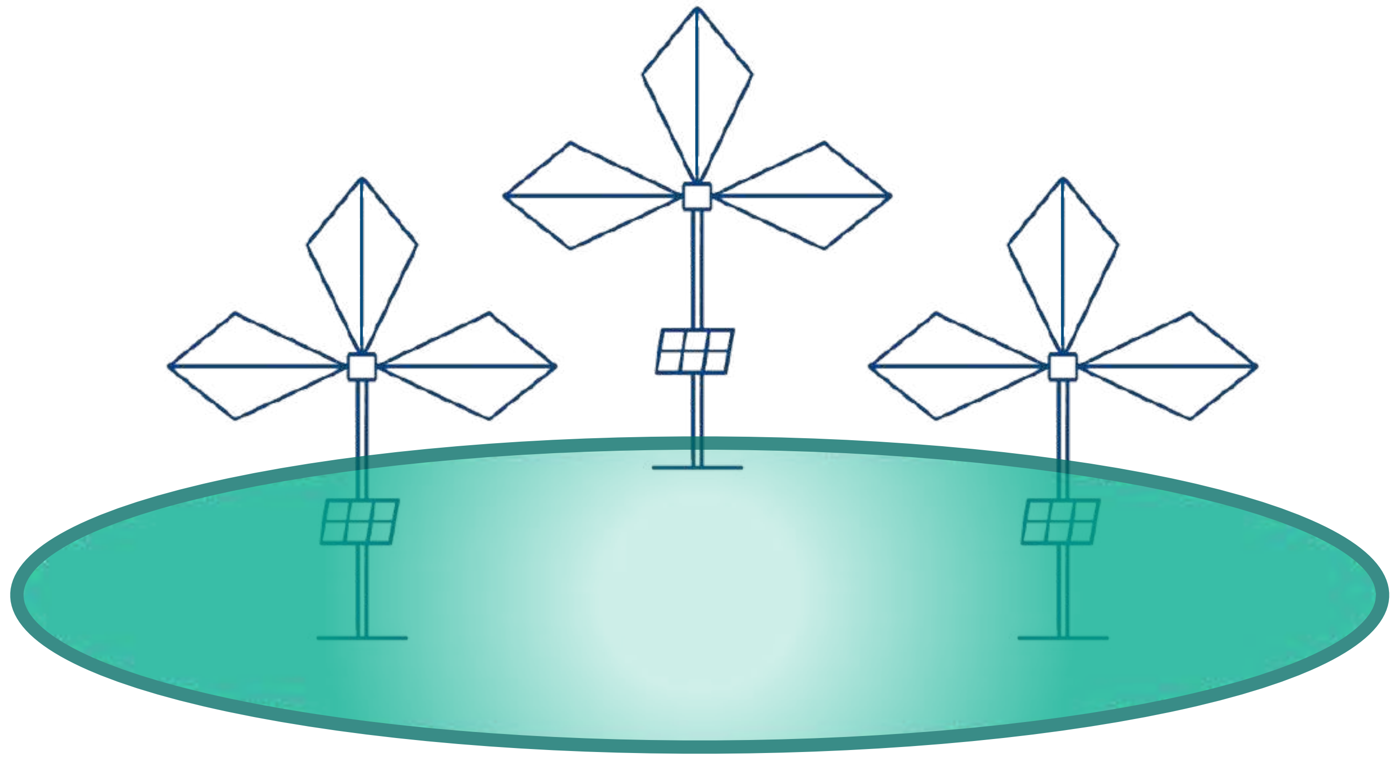

GRAND and the challenges of radio detection

I.Physical modeling of inclined air showers and their radio emission

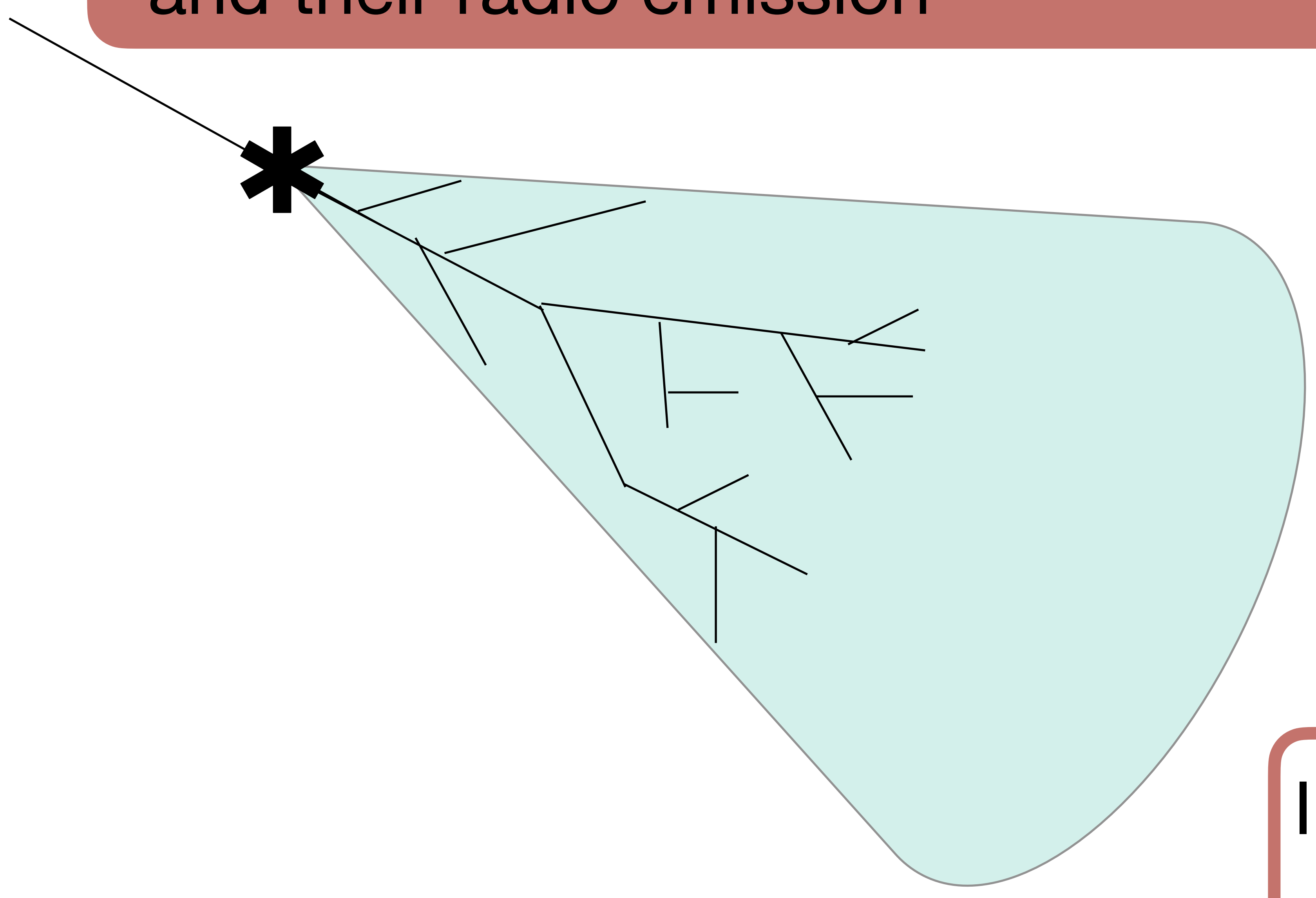

III. Reconstruction of cosmic particle properties for very inclined showers

II. Autonomous trigger: find the radio signal inside the noise

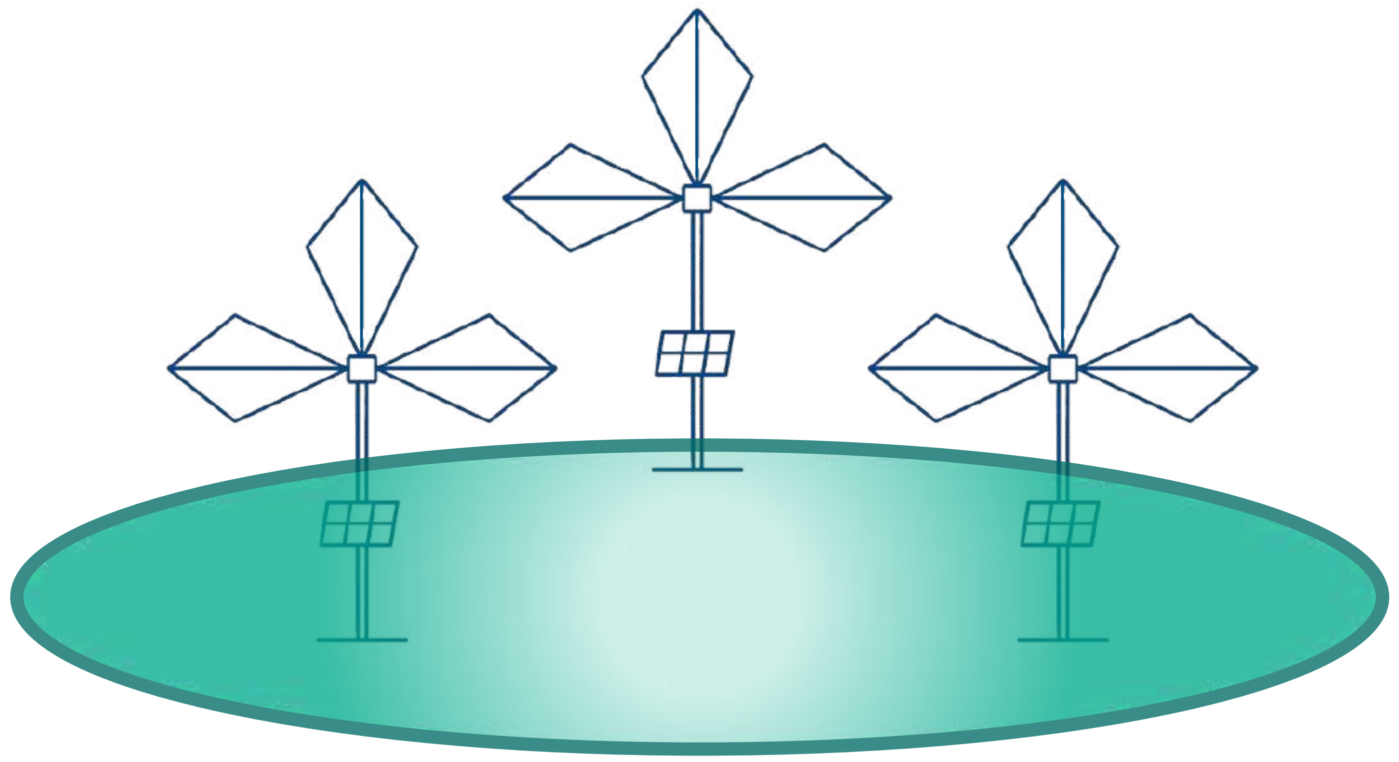

Radio signal induced by extensive air showers: classical picture

Vertical showers ($\theta < 60°$): extensively studied

Shower plane

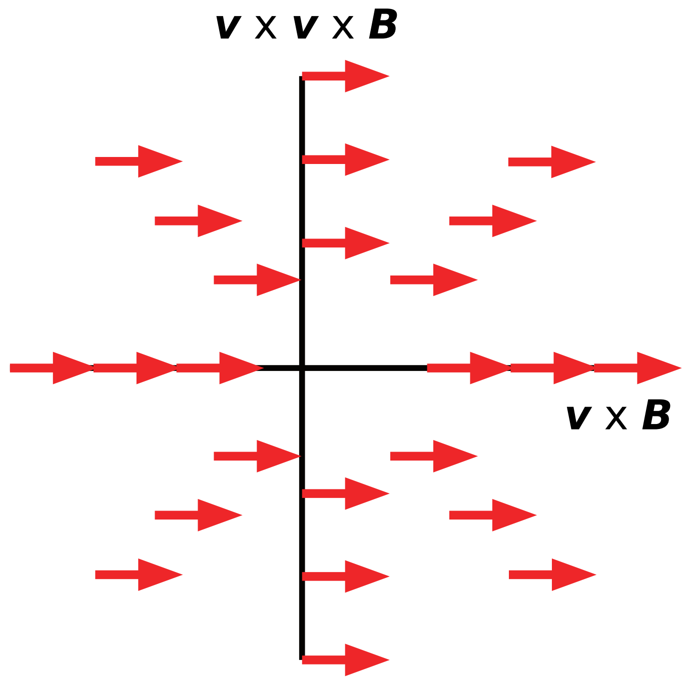

Geomagnetic emission

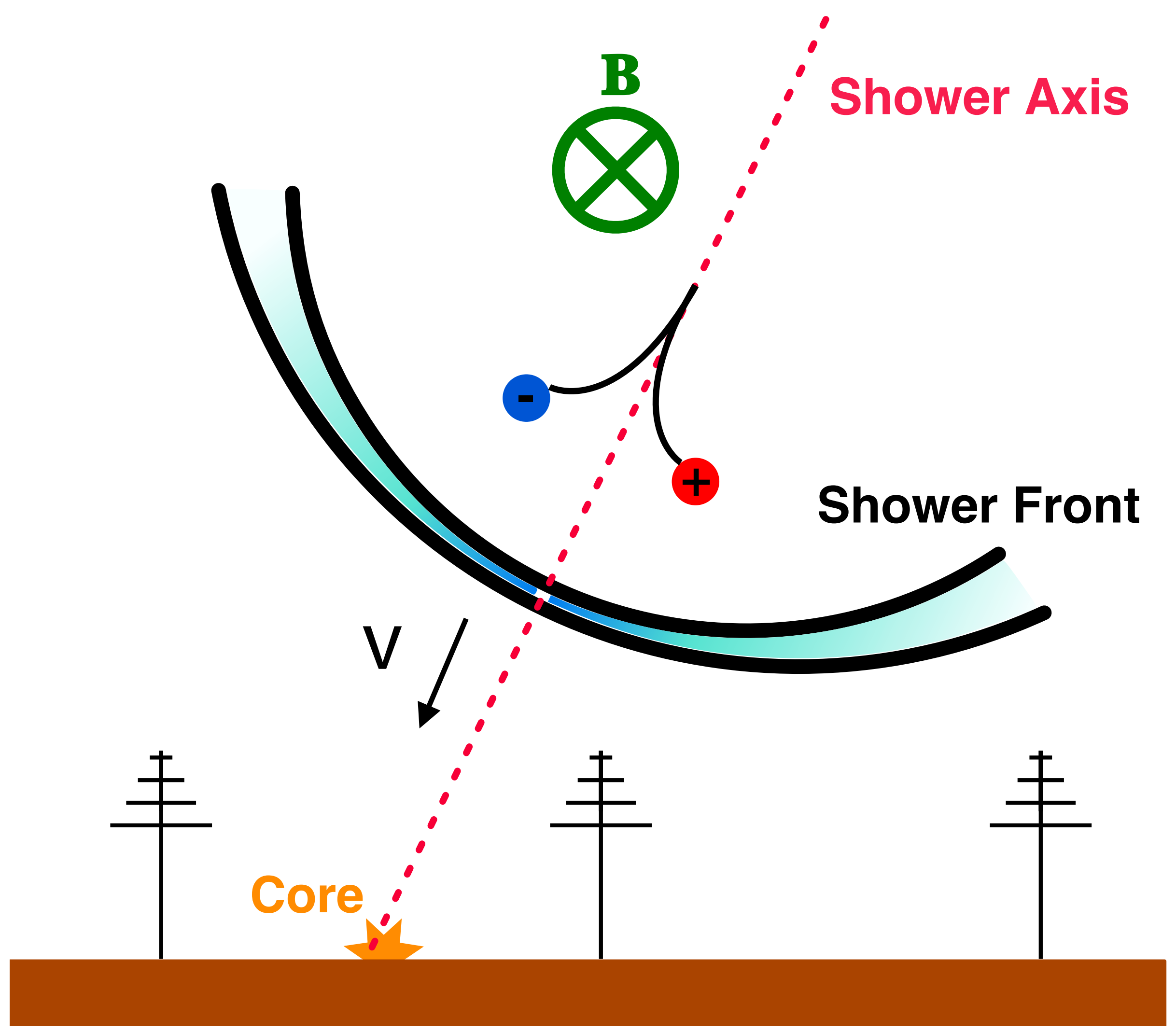

Huege, 2016

Askaryan emission

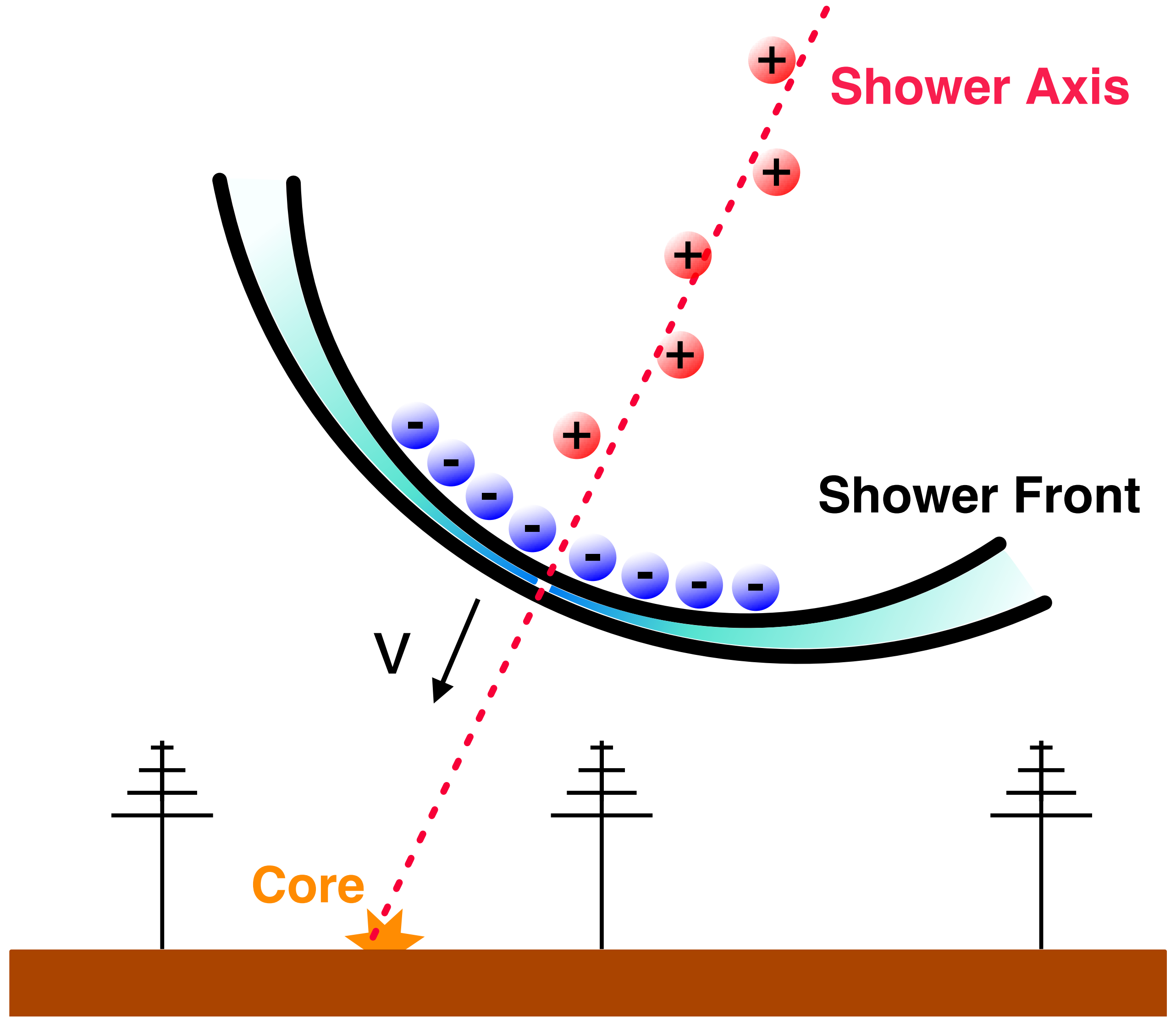

Shower plane

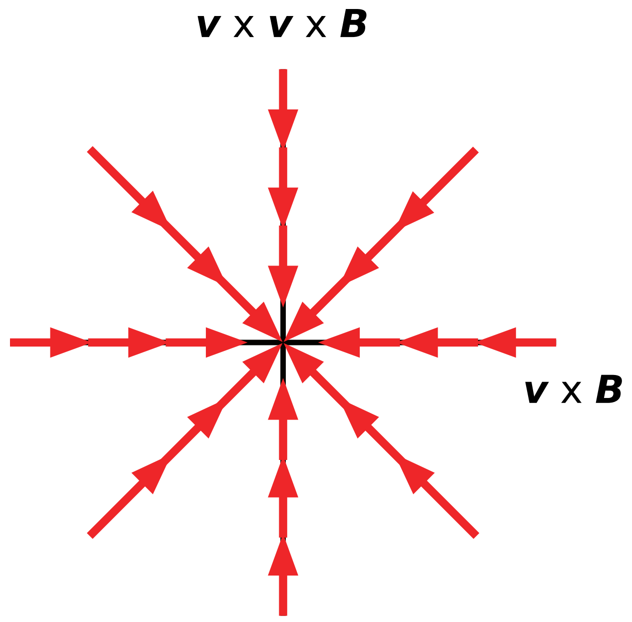

Lorentz force: $L_{\text{Lorentz}} = q\vec{v} \times \vec{B}$

Transverse motion of electrons and positrons

Electric field polarized along -$\vec{v} \times \vec{B}$

Main contribution to radio signal in air (~90%)

Accumulation of electrons close to the shower wavefront

Electric field radially polarized

Particle distribution of extensive air showers (EAS) linked to emission mechanisms

Competitive processes in air showers

Lateral extent: Distribution of particles in $\vec{v} \times \vec{B}$ direction

Lorentz force: $L_{\text{Lorentz}} = q\vec{v} \times \vec{B}$

Transverse motion of electrons and positrons

Multiple Coulomb Scattering, radiation losses (Bremsstrahlung, Ionisation) due to air molecules

Molière Radius: $R_{\text{Molière}} \sim \dfrac{9.6\,\text{g.cm}^{-2}}{\rho_{\text{air}}}$

Specific signatures for very inclined air showers

New challenges:

Development over longer trajectories

Develop higher in the atmosphere (lower ρ_{air})

Shower particles have larger mean free path for collisions

Enhanced effect of $\mathbf{B}_{\mathbf{Earth}}$

Affect spatial particle distribution and radio emission?

Analytical estimate of lateral extent for very inclined air showers

New challenges:

Development over longer trajectories

Develop higher in the atmosphere (lower ρ_{air})

Shower particles have larger mean free path for collisions

Lateral extent: Distribution of particles in $\vec{v} \times \vec{B}$ direction

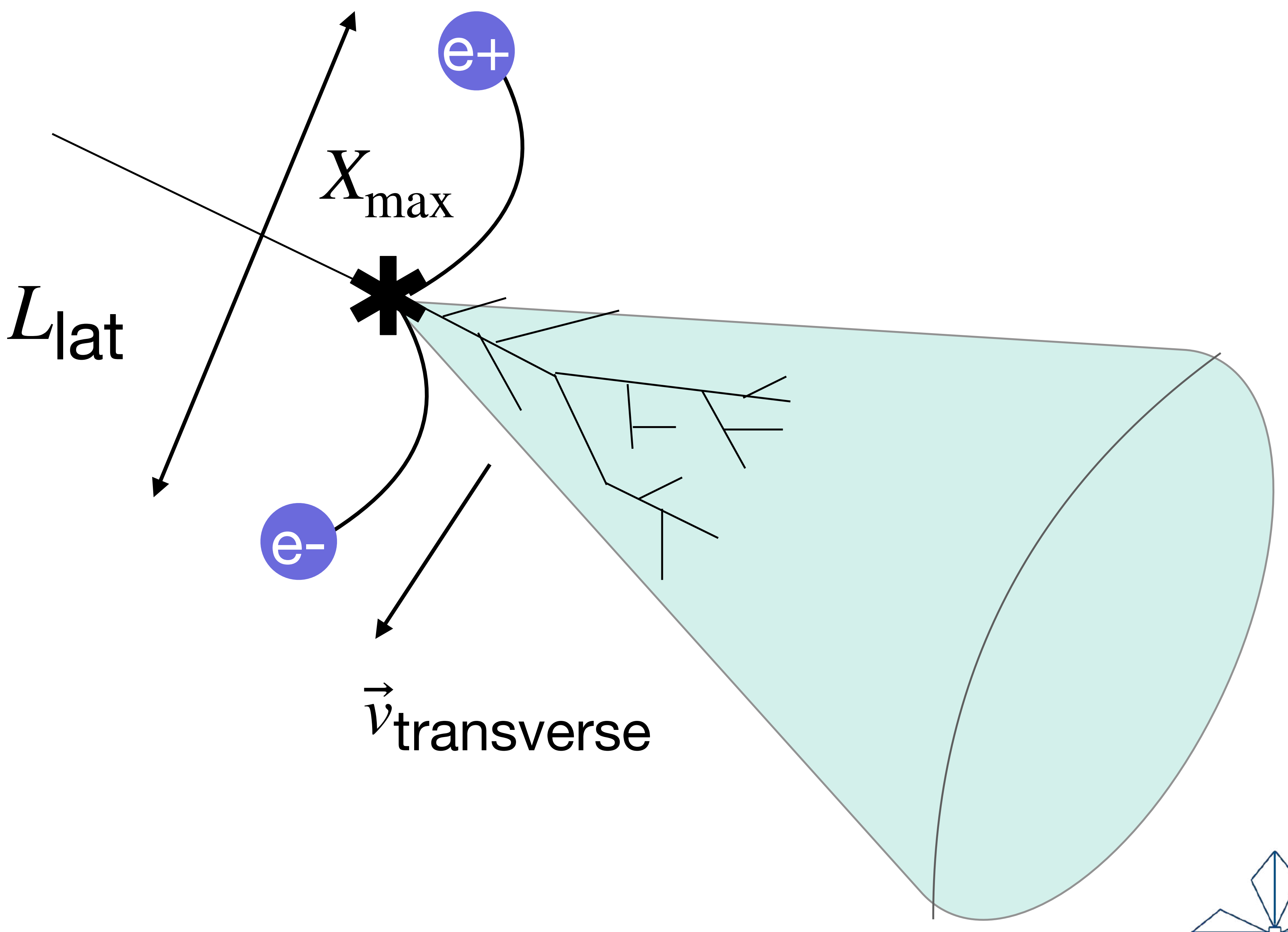

Scholten et al., 2007

$$v_{\text{transverse}}(t) = \frac{\tau c^3 e B_{\text{Earth}}}{E_0}(e^{-t/\tau} - 1)$$

$$x_{\text{transverse}}(t) = \frac{\tau^2 c^3 e B_{\text{Earth}}}{E_0}(e^{-t/\tau} - 1 - \frac{t}{\tau})$$

$$L_{\text{lat}} = 2x_{\text{transverse}}(t = \tau)$$

τ : Bremsstrahlung energy loss timescale

E_0: shower particle energy

$$L_{\text{lat}} \sim 30\,\text{m} \left(\frac{\rho_{\text{air}}}{1\,\text{kg}\,\text{m}^{-3}}\right)^{-2} \left(\frac{B_{\text{Earth}}}{50\,\mu\text{T}}\right) \left(\frac{E_0}{100\,\text{MeV}}\right)^{-1}$$

Lateral extent driven by deflection due to Earth magnetic field

Model validation: comparisons with Monte-Carlo numerical simulations

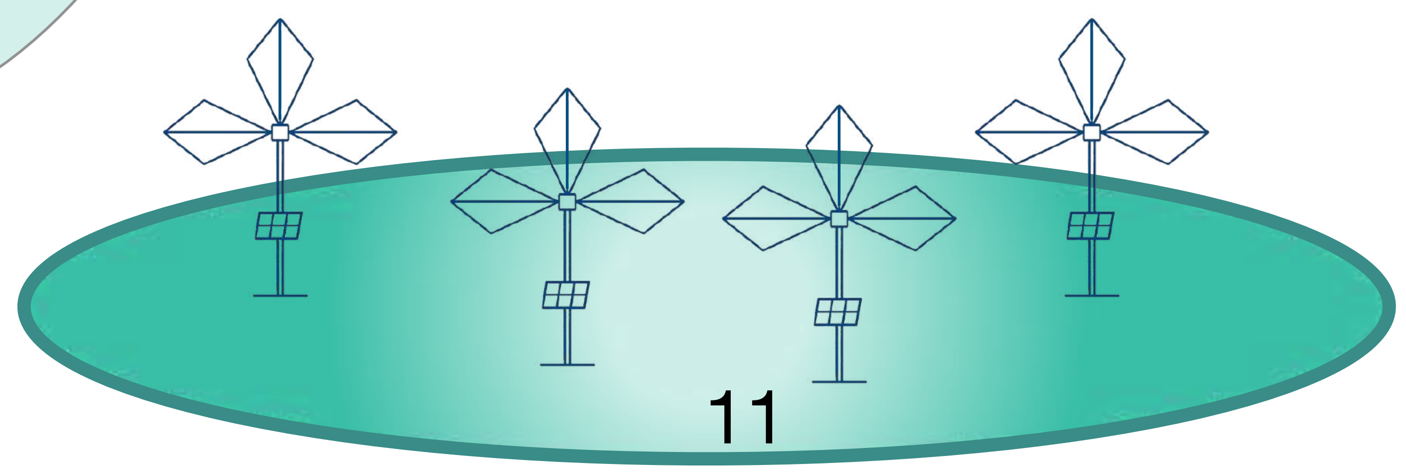

Lateral extent of air showers from simulations

Monte Carlo codes: ZHAireS & CoREAS
Simulations of **cosmic ray induced** air showers

$\theta = 60°$

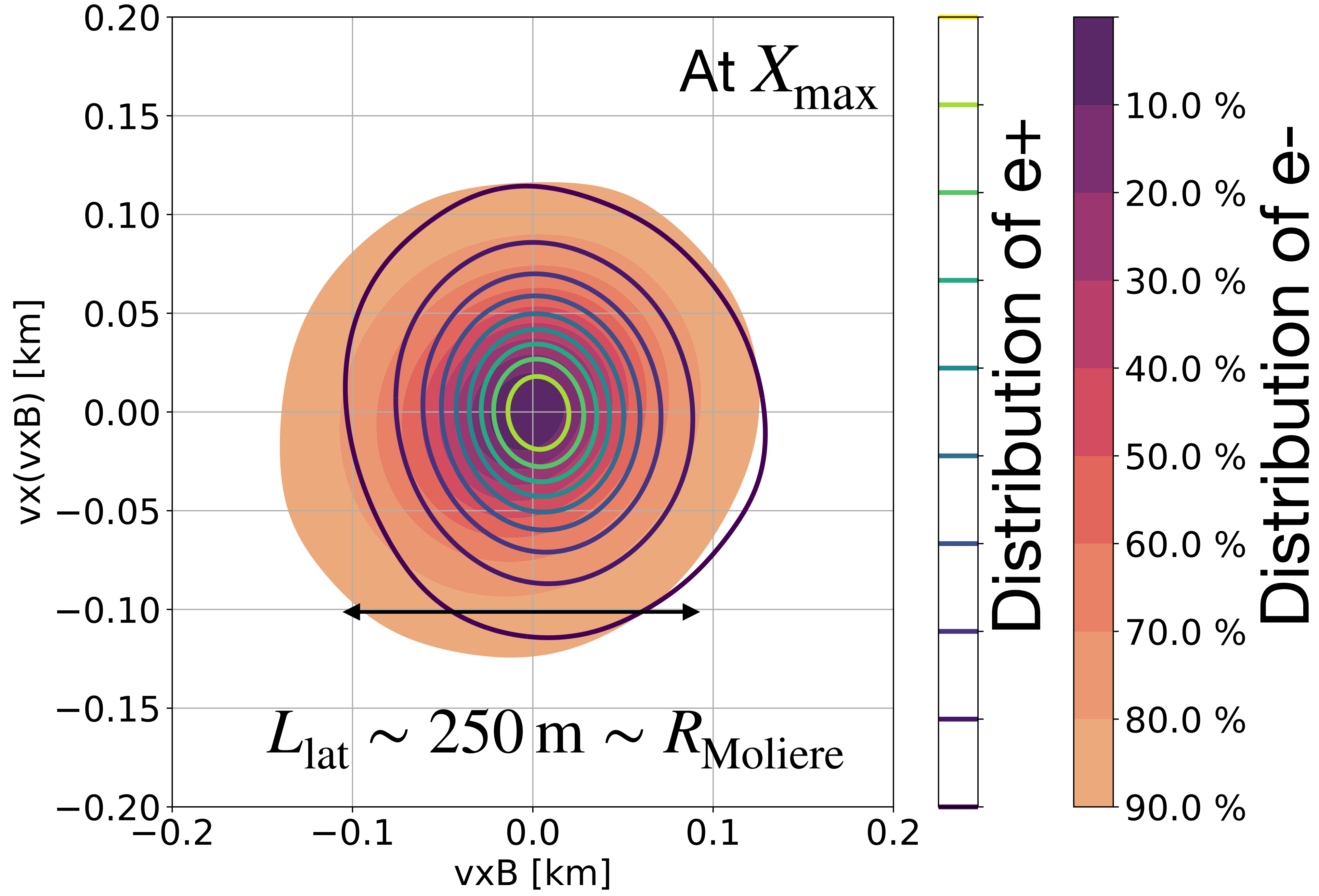

High ρ_{air} and strong B_{Earth}

Very inclined: $\theta = 87°$

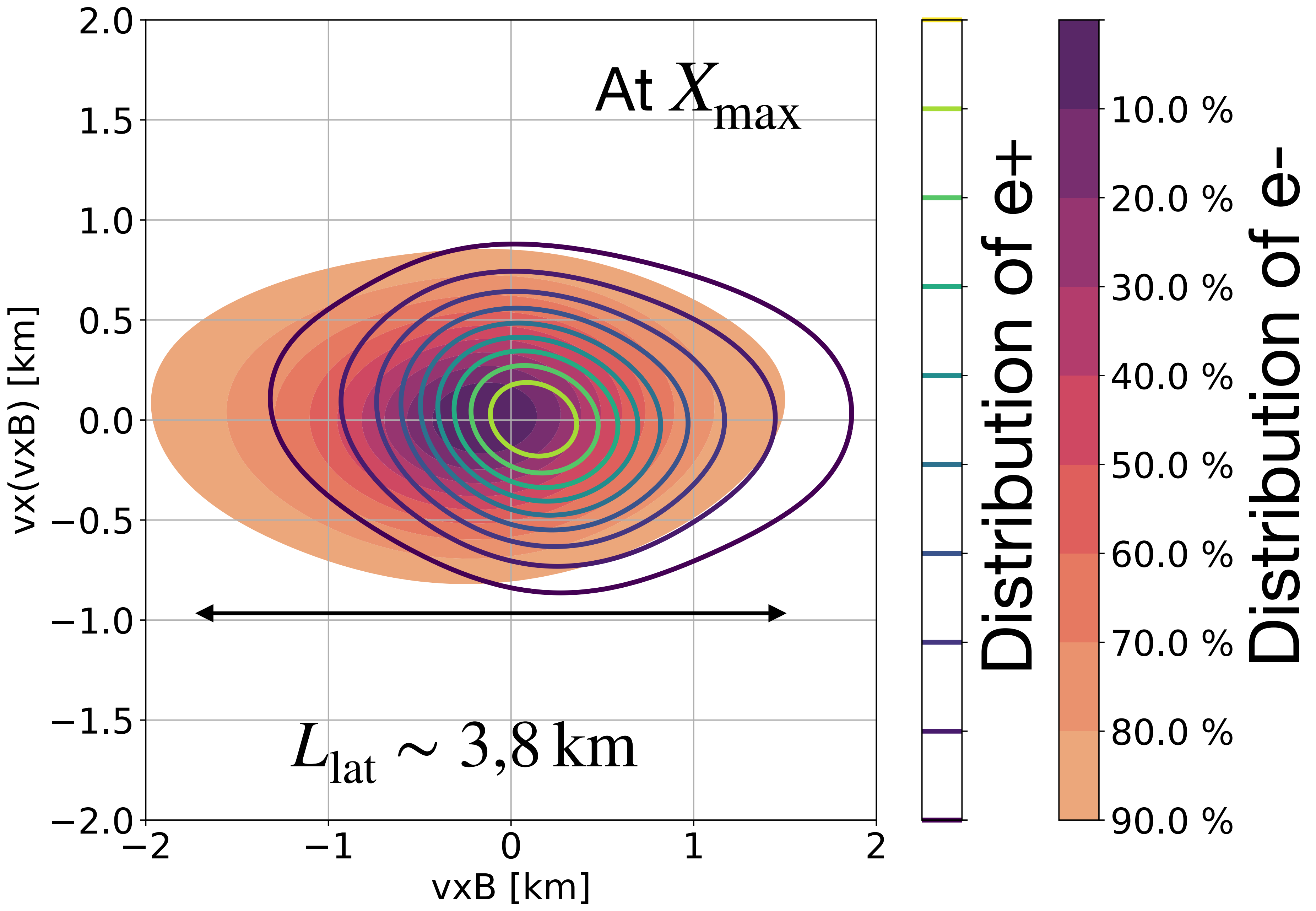

$R_{Moliere} \sim 800\,\mathrm{m}$ for $\rho_{air} = 0{,}12\,\mathrm{kg\,.\,m^{-3}}$ $(\theta = 87°)$

Low ρ_{air} and strong B_{Earth}

Drastic lateral extent increase

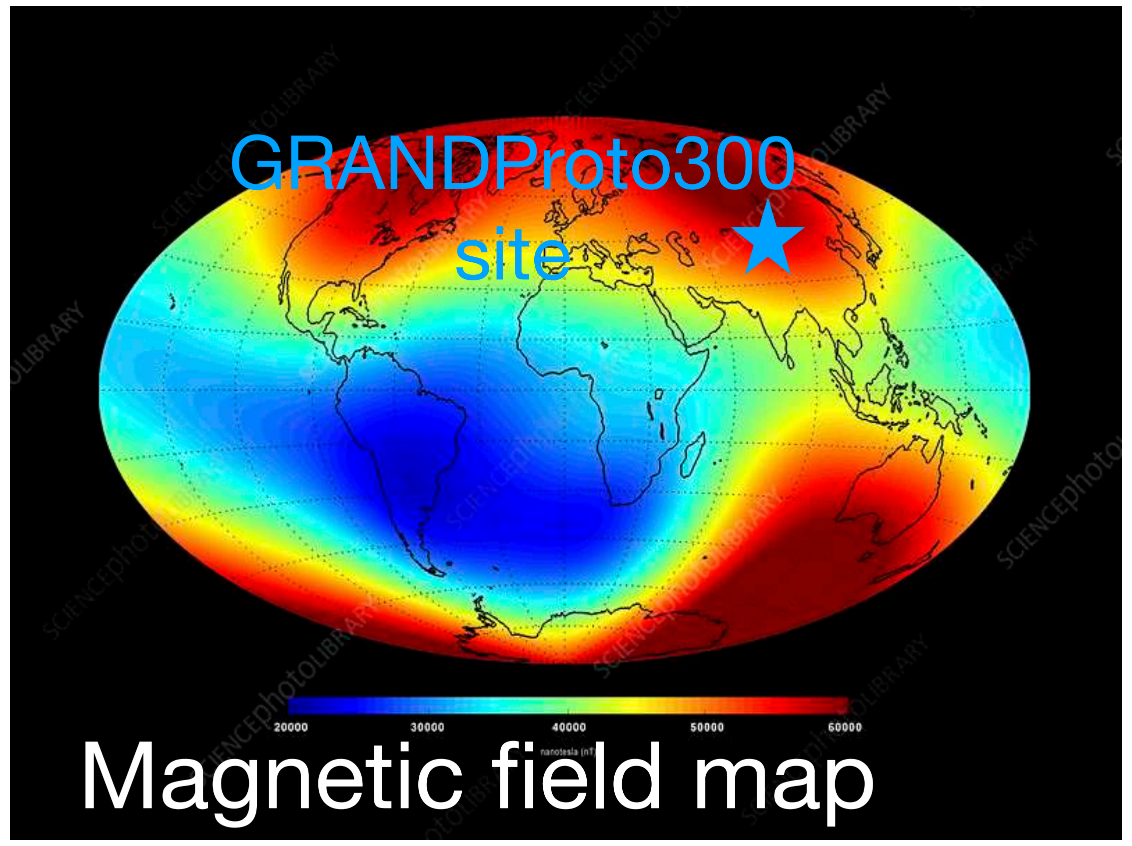

$B_{Earth} \sim 50\mu$T
(GRANDProto300)

Lateral extent: Distribution of particles in $\vec{v} \times \vec{B}$ direction

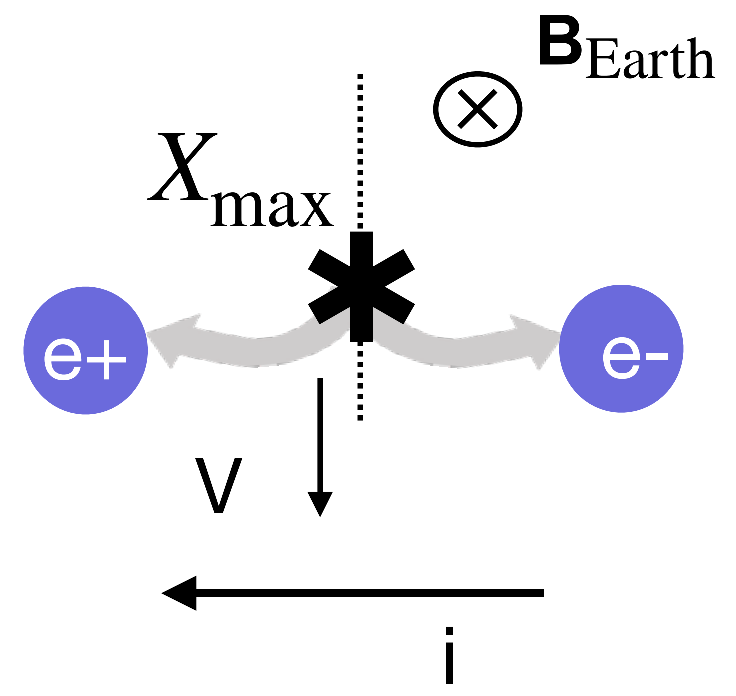

Lorentz Force: $L_{Lorentz} = q\vec{v} \times \vec{B}$

Lateral extent as a function of inclination: two regimes

***Guelfand** et al, JCAP (2024), arXiv:2310.19612*

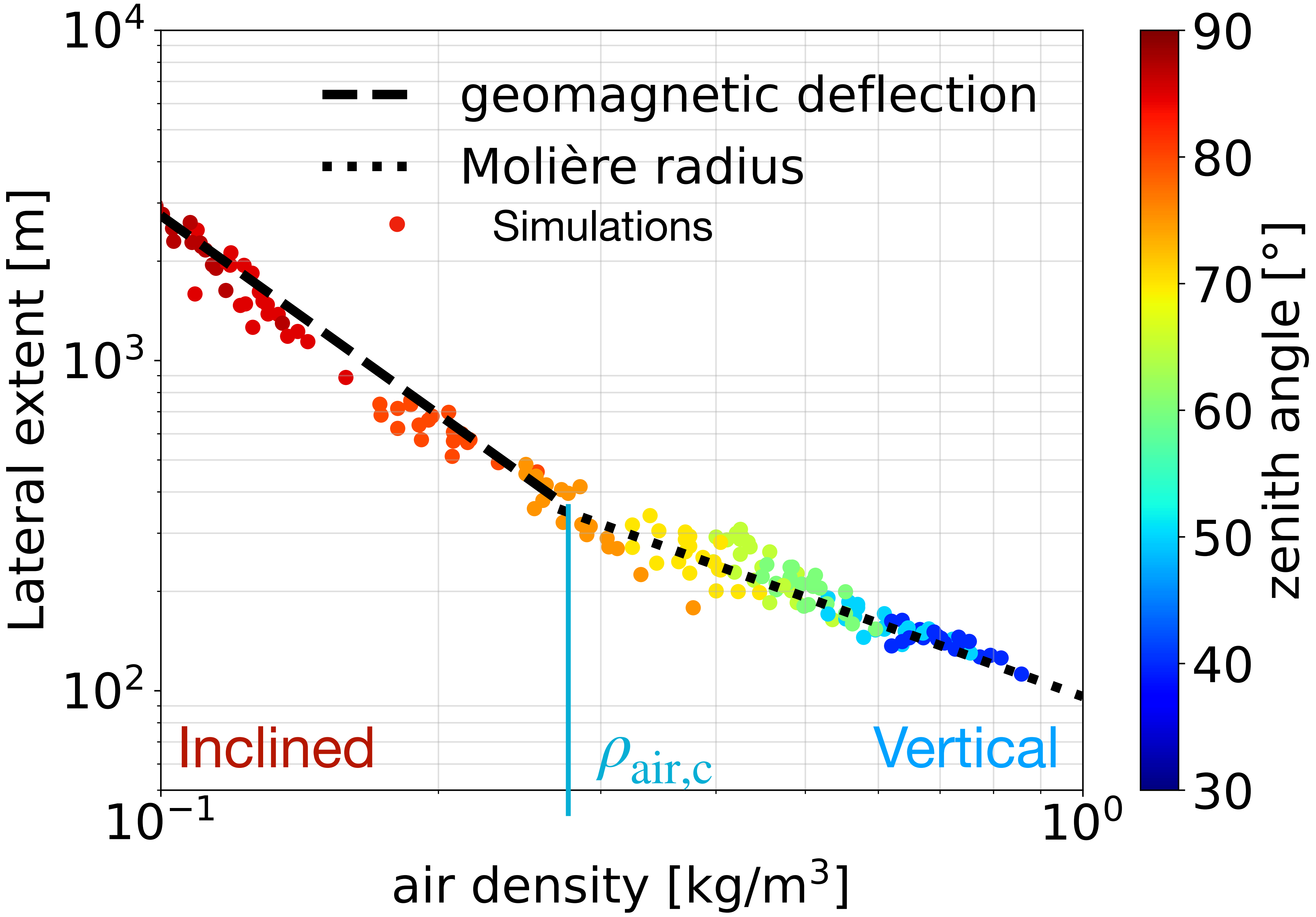

Two distinct regimes at low and high inclination: **simulations + analytical modeling**:

- vertical air showers driven by **multiple scattering:**

$$L_{\mathrm{lat}} = R_{\text{Molière}} \sim 96\,\mathrm{m}\,\left(\frac{\rho_{\mathrm{air}}}{1\,\mathrm{kg\,m^{-3}}}\right)^{-1}$$

- Very inclined air showers driven by **geomagnetic deflection:**

$$L_{\mathrm{lat}} \sim 30\,\mathrm{m}\left(\frac{\rho_{\mathrm{air}}}{1\,\mathrm{kg\,m^{-3}}}\right)^{-2}\left(\frac{B}{50\,\mu\mathrm{T}}\right)\left(\frac{E_0}{100\,\mathrm{MeV}}\right)^{-1}$$

Coherence loss in the radio signal

Simulated radio signal **filtered in 50-200 MHz** (GRAND frequency band)

Radiation energy: $E_{\mathrm{rad}} = c\epsilon_0 \int_0^{2\pi} \mathrm{d}\phi \int_0^{\infty} r\mathrm{d}r ||\vec{E}(r,\phi)||^2$ Radio signal = electric field

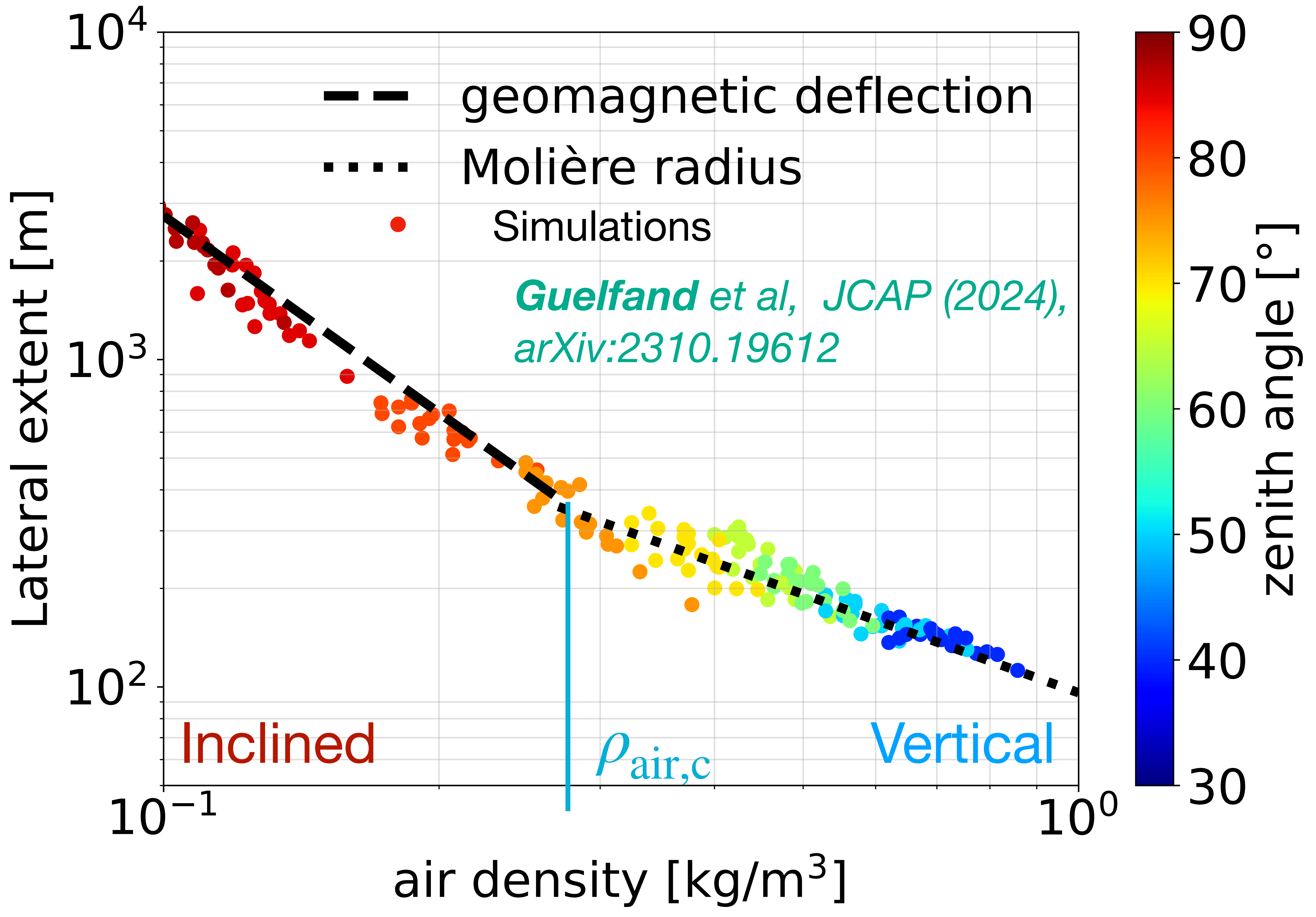

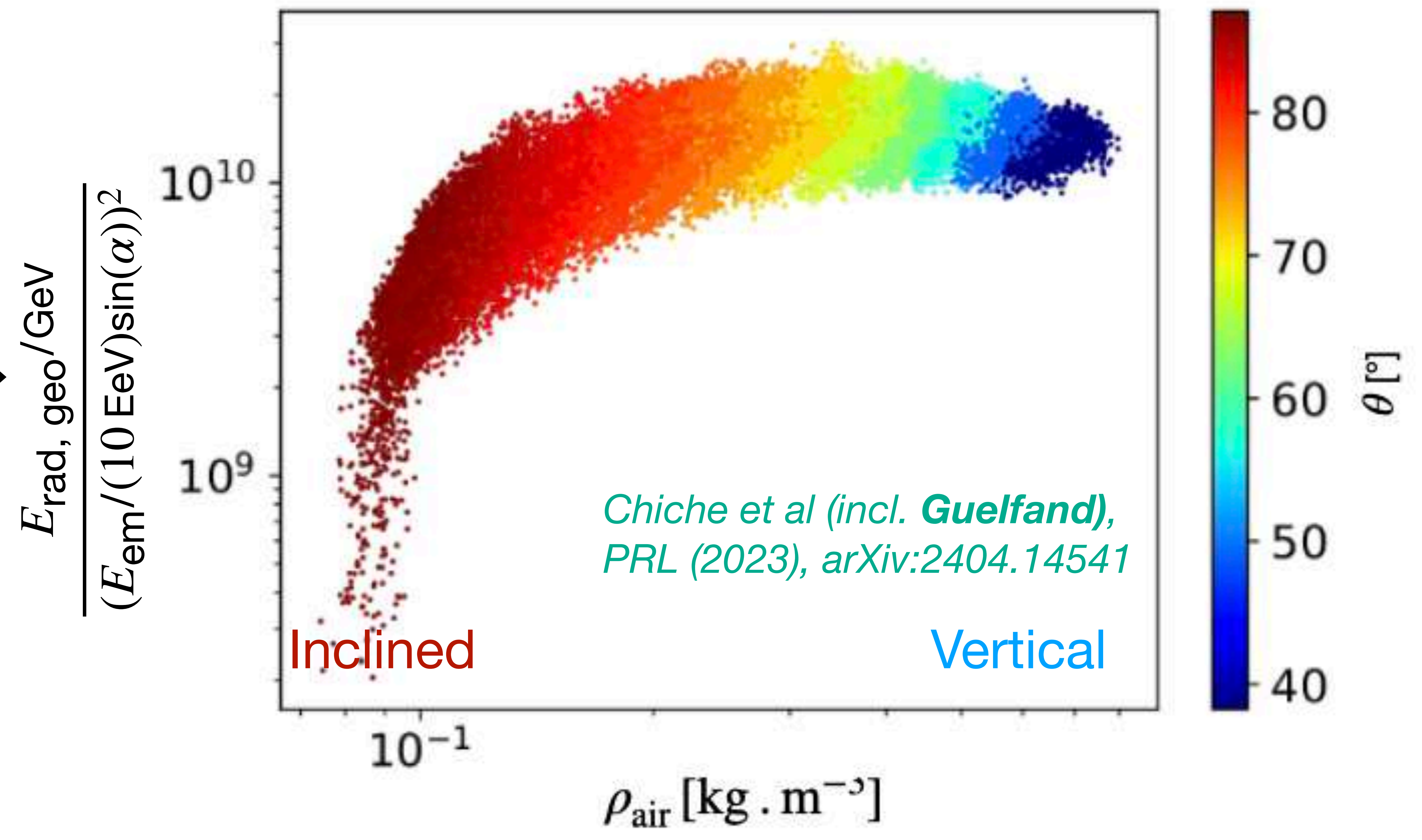

Coherence loss in the radio signal

Simulated radio signal **filtered in 50-200 MHz** (GRAND frequency band)

Radiation energy: $E_{\rm rad} = c\epsilon_0 \int_0^{2\pi} \mathrm{d}\phi \int_0^{\infty} r\mathrm{d}r \|\vec{E}(r,\phi)\|^2$

Radio signal = electric field

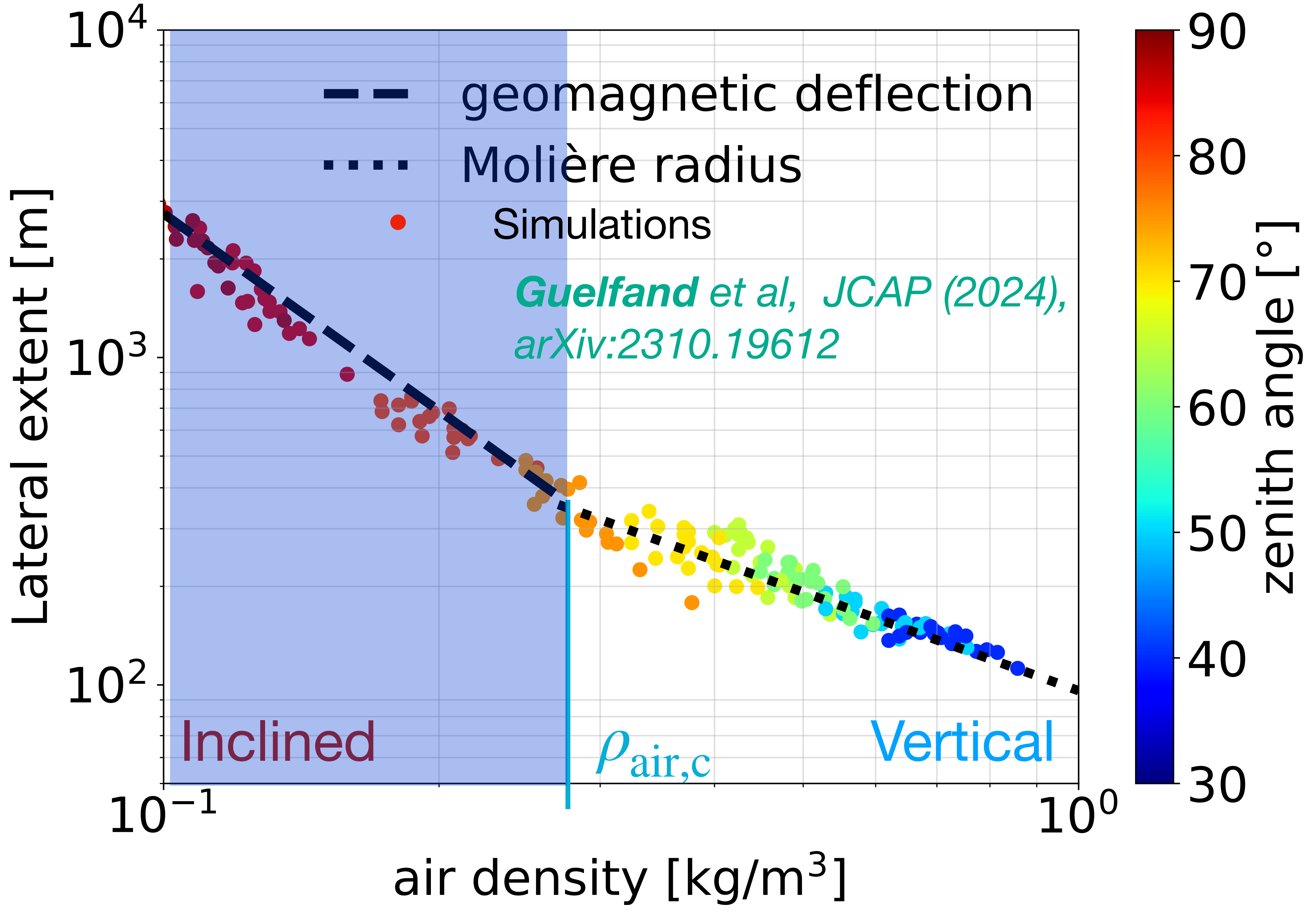

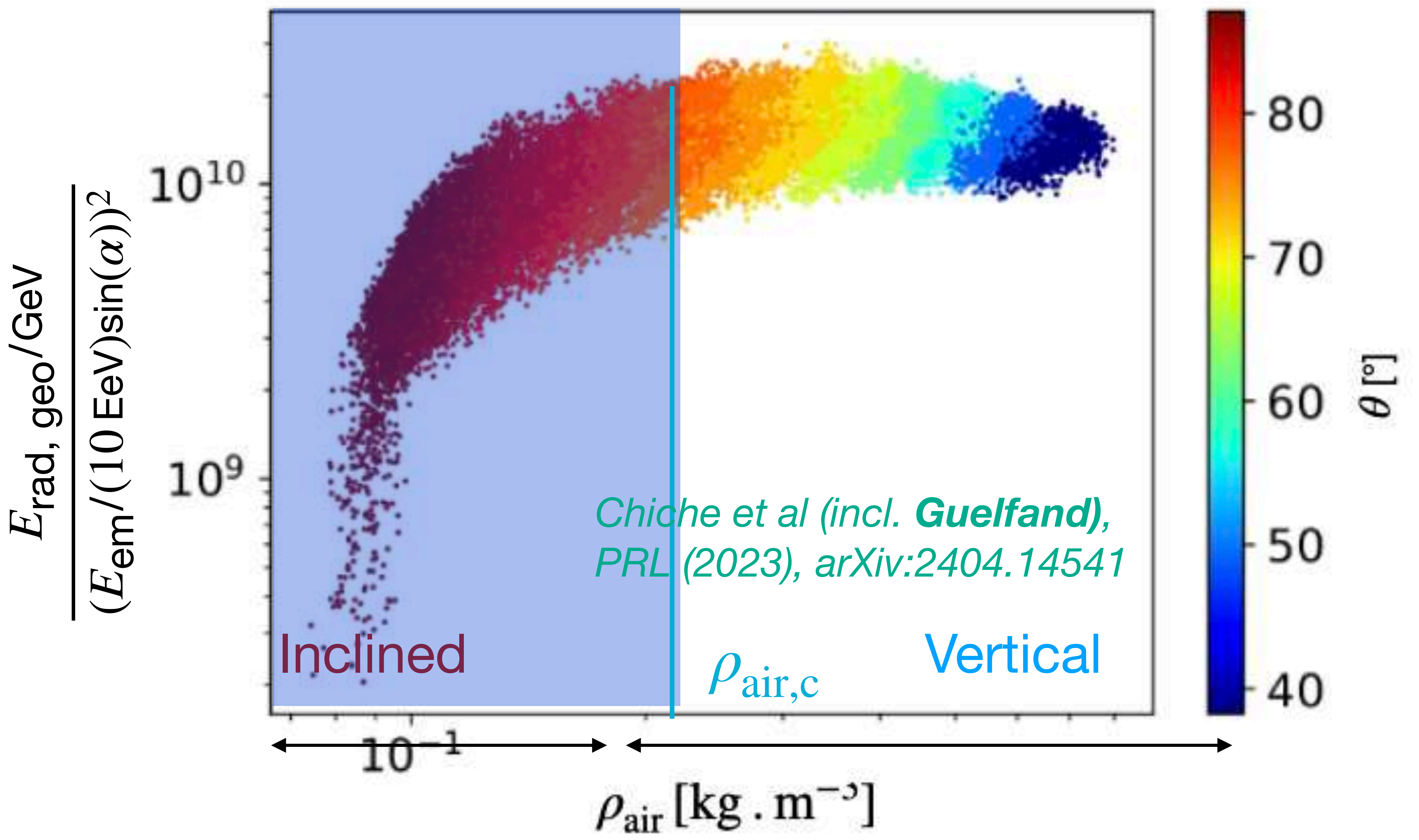

Coherence loss

Coherent radiation

New regime in lateral extent ⟷ transition to incoherent radio emission**: spatial coherence loss**

$$L_{\rm coh} \sim 30\,\mathrm{m} \left(\frac{\nu}{100\,\mathrm{MHz}}\right)^{-1} \left(\frac{d_{\rm obs}}{10\,\mathrm{km}}\right) \left(\frac{L_{\rm lat}}{10^3\,\mathrm{m}}\right)^{-1}$$

spatial coherence loss: $\dfrac{L_{\rm lat}}{L_{\rm coh}} > 1$

Coherence loss in the radio signal

Simulated radio signal **filtered in 50-200 MHz** (GRAND frequency band)

Radiation energy: $E_{\rm rad} = c\epsilon_0 \int_0^{2\pi} \mathrm{d}\phi \int_0^{\infty} r\mathrm{d}r \|\vec{E}(r,\phi)\|^2$

Radio signal = electric field

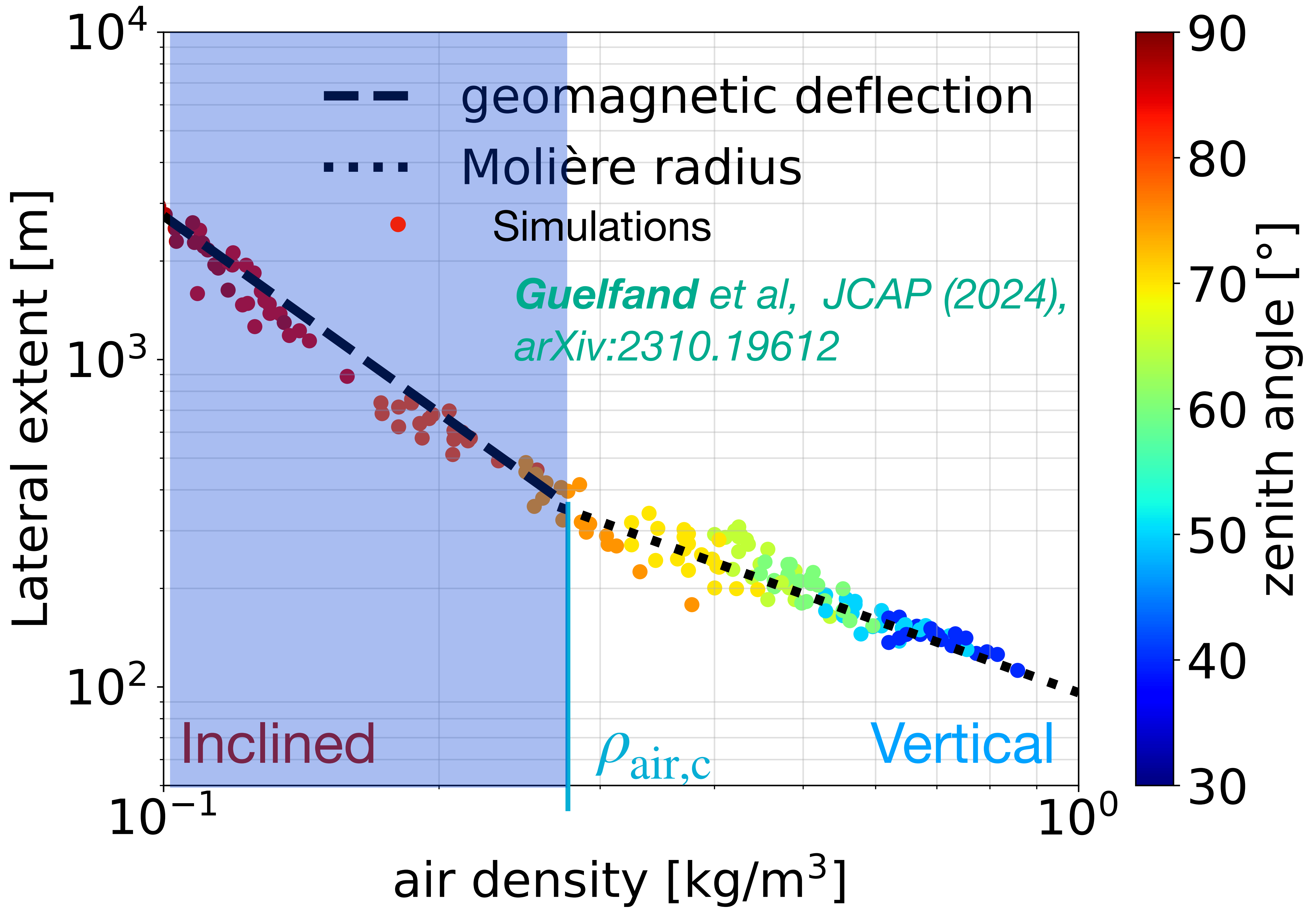

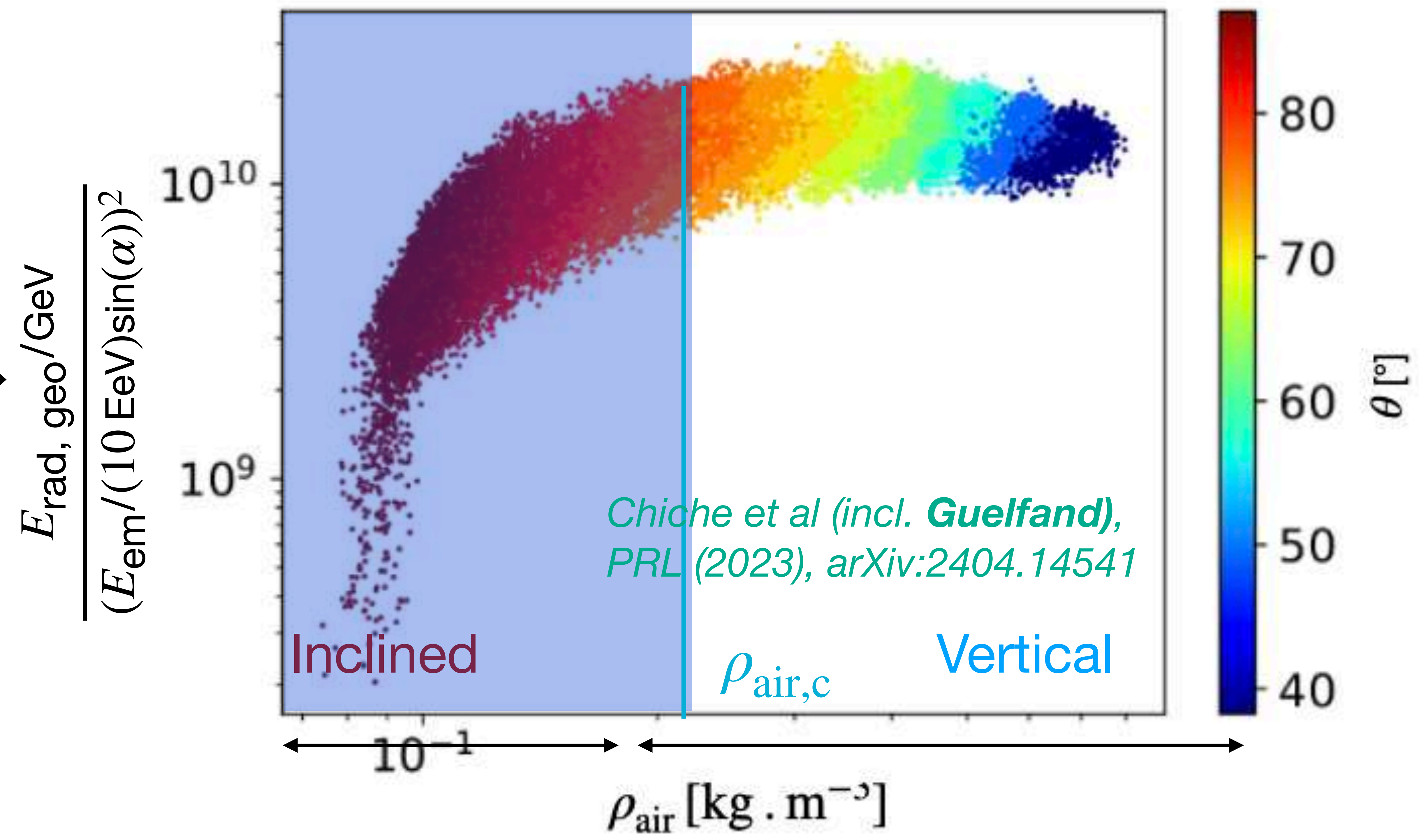

Coherence loss

Coherent radiation

$$L_{\rm coh} \sim 30\,\mathrm{m} \left(\frac{\nu}{100\,\mathrm{MHz}}\right)^{-1} \left(\frac{d_{\rm obs}}{10\,\mathrm{km}}\right) \left(\frac{L_{\rm lat}}{10^3\,\mathrm{m}}\right)^{-1}$$

New regime in lateral extent ⟷ transition to incoherent radio emission**: spatial coherence loss**

- Could affect detection and reconstruction strategies
- Could allow to **discriminate between cosmic rays and neutrinos**

spatial coherence loss: $\dfrac{L_{\rm lat}}{L_{\rm coh}} > 1$

GRAND and the challenges of radio detection

I.Physical modeling of inclined air showers and their radio emission

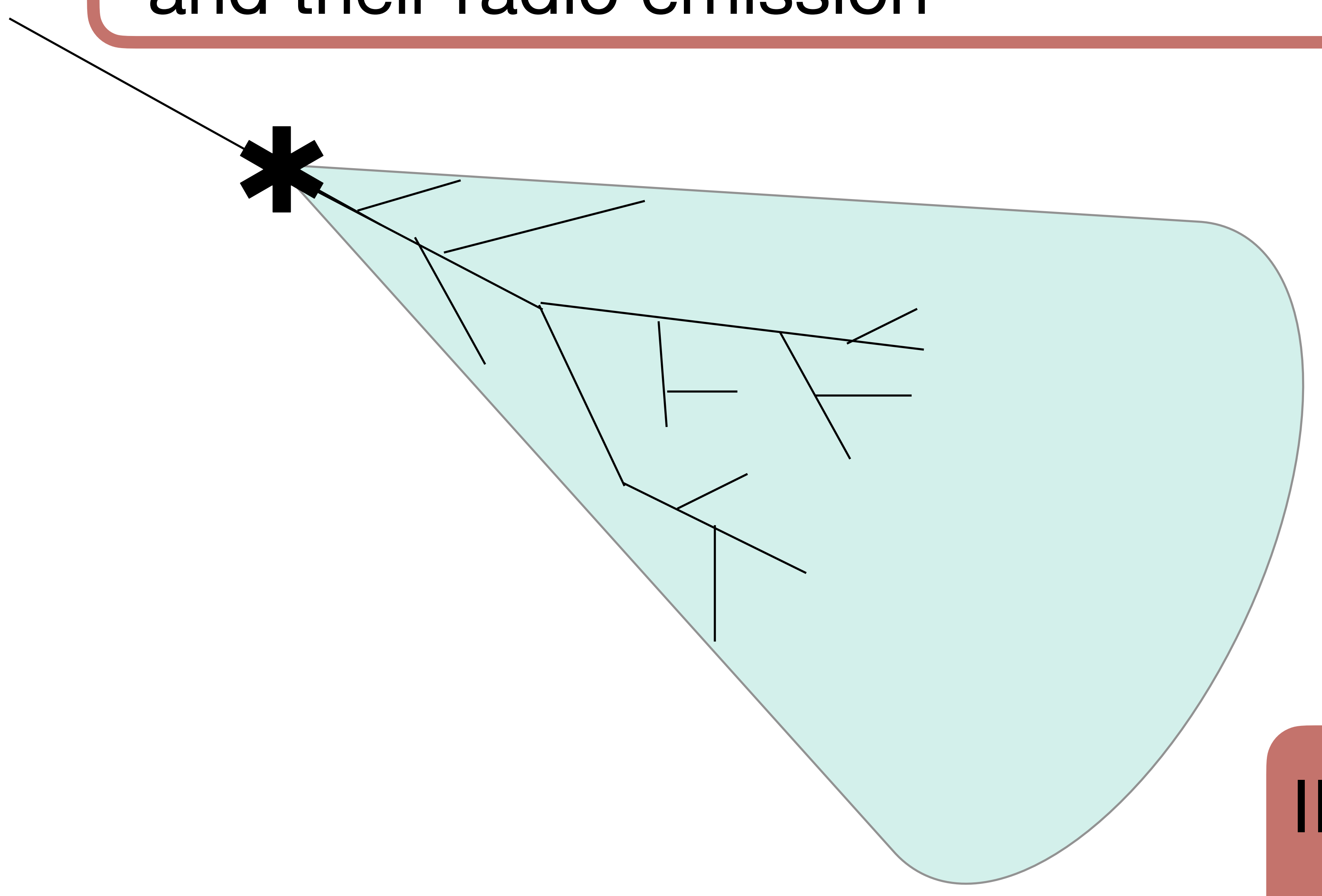

III. Reconstruction of cosmic particle properties for very inclined showers

II. Autonomous trigger: find the radio signal inside the noise

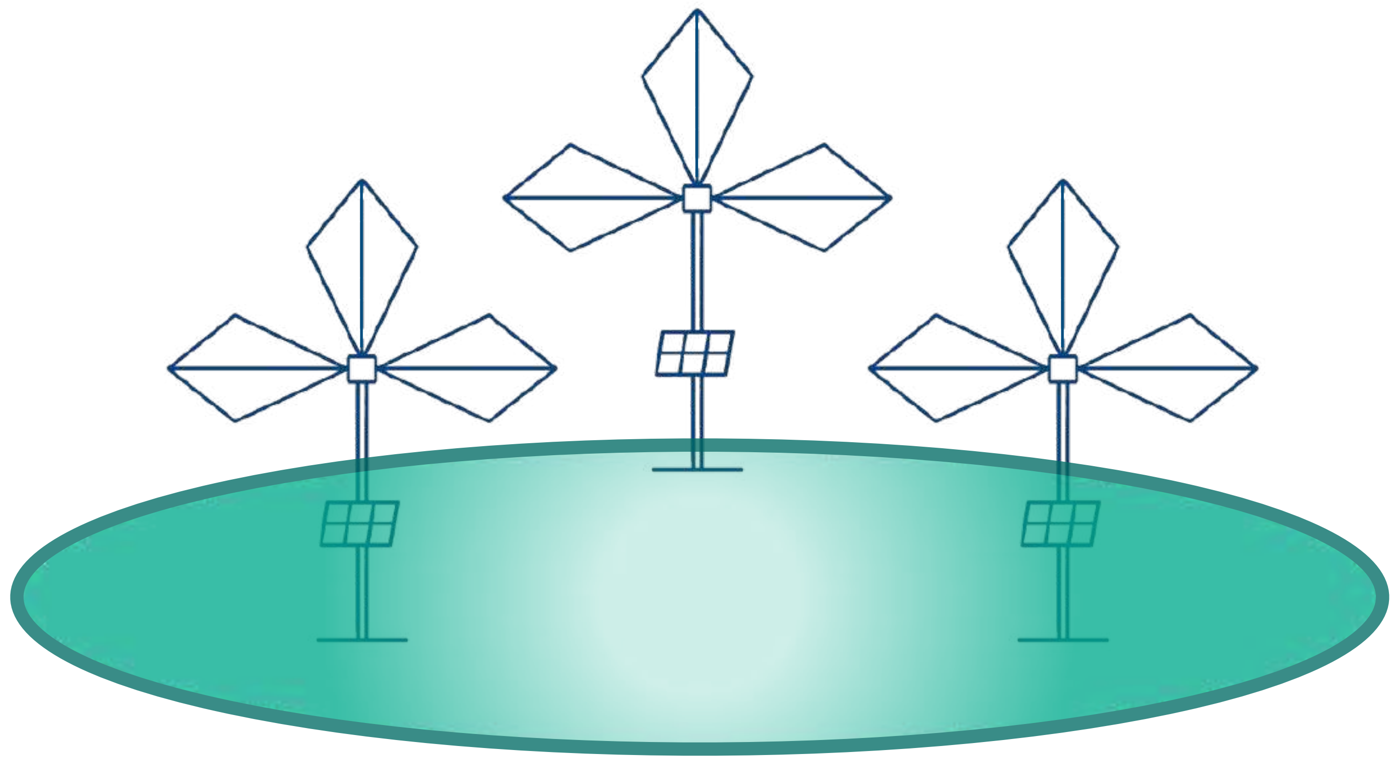

Autonomous radio detection of extensive air showers (EAS)

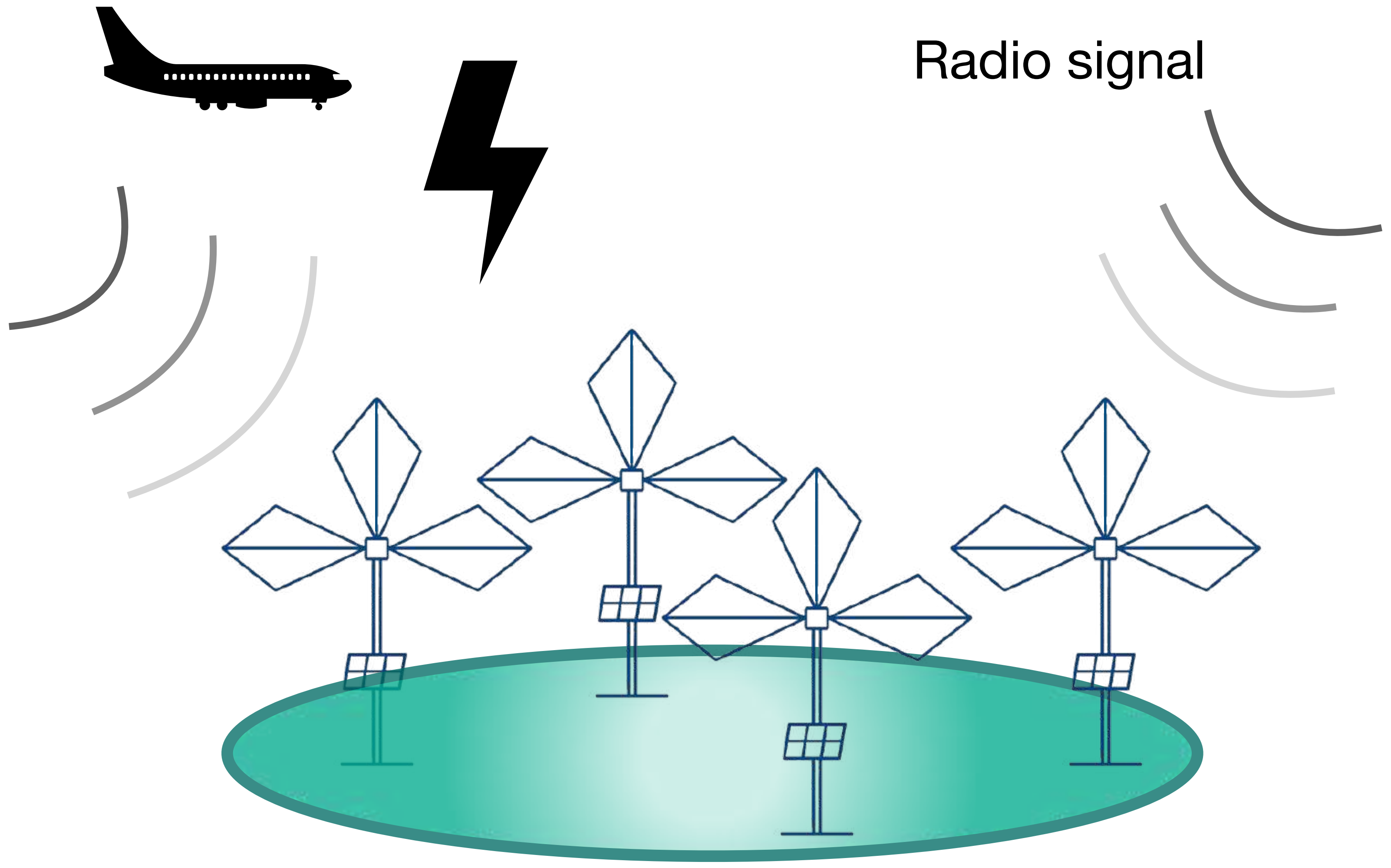

Autonomous radio detection of extensive air showers (EAS)

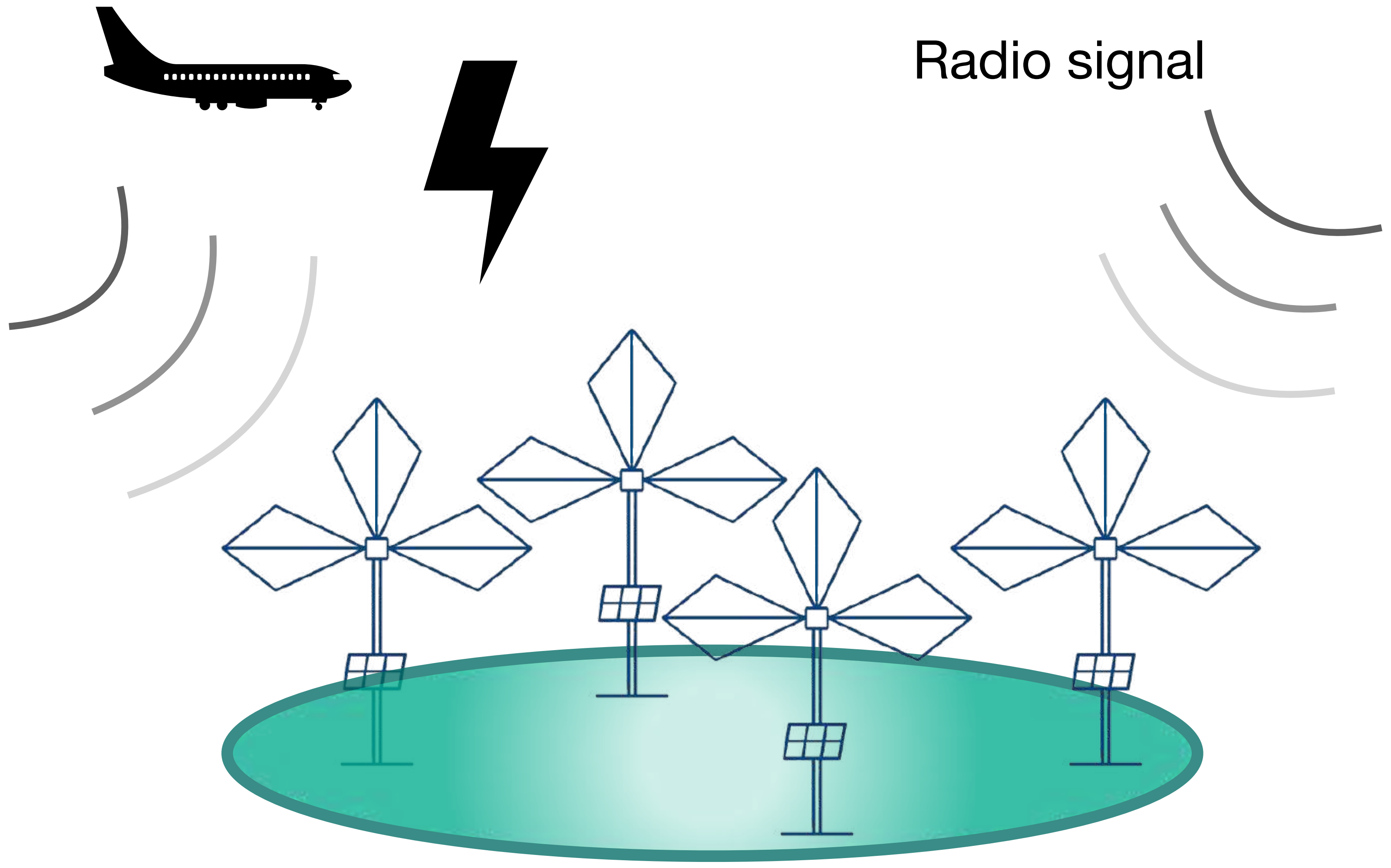

Stationary noise: Galactic noise

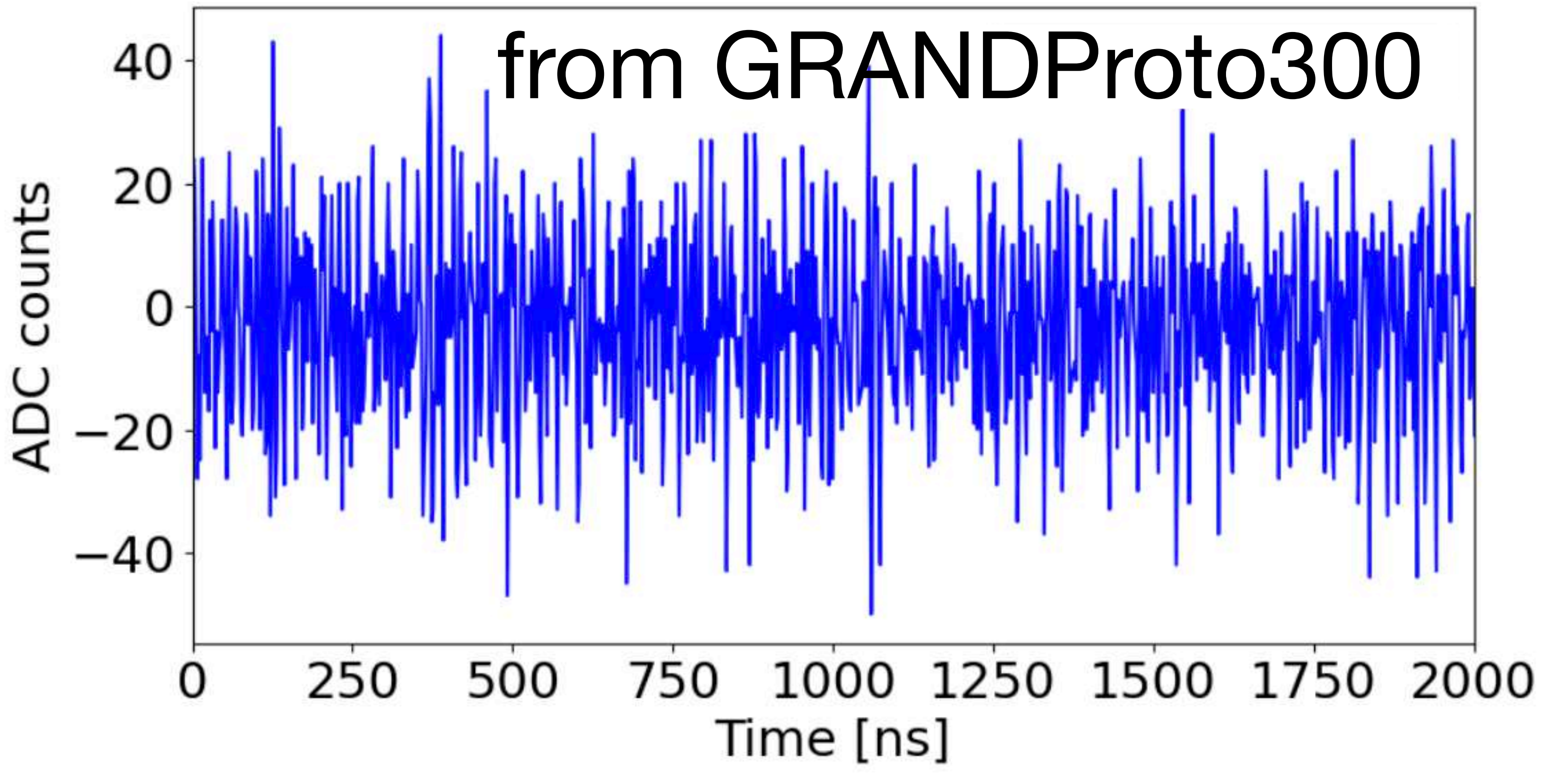

Autonomous radio detection of extensive air showers (EAS)

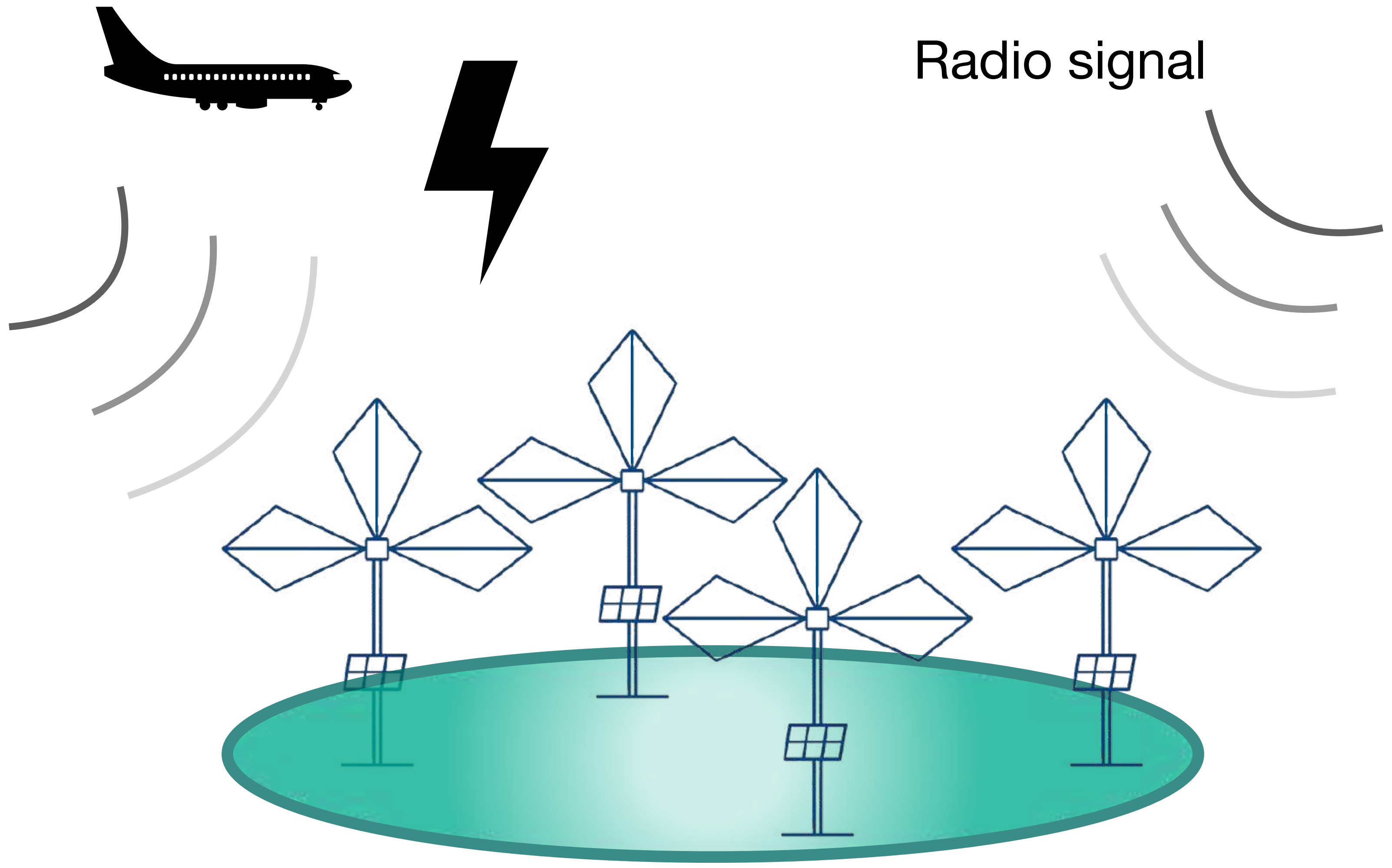

Stationary noise: Galactic noise

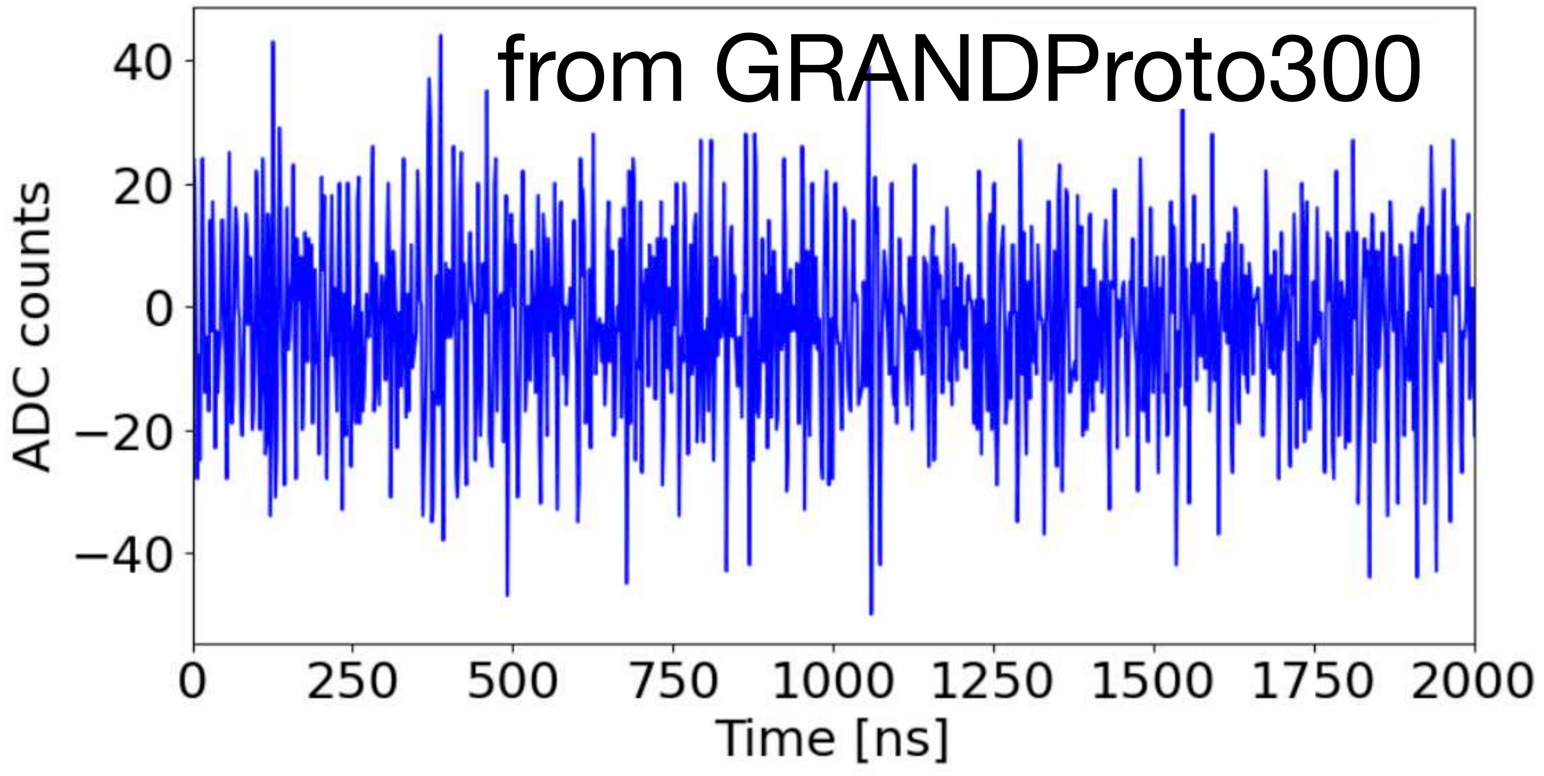

Transient noise: thunderstorms, power lines, aircrafts…

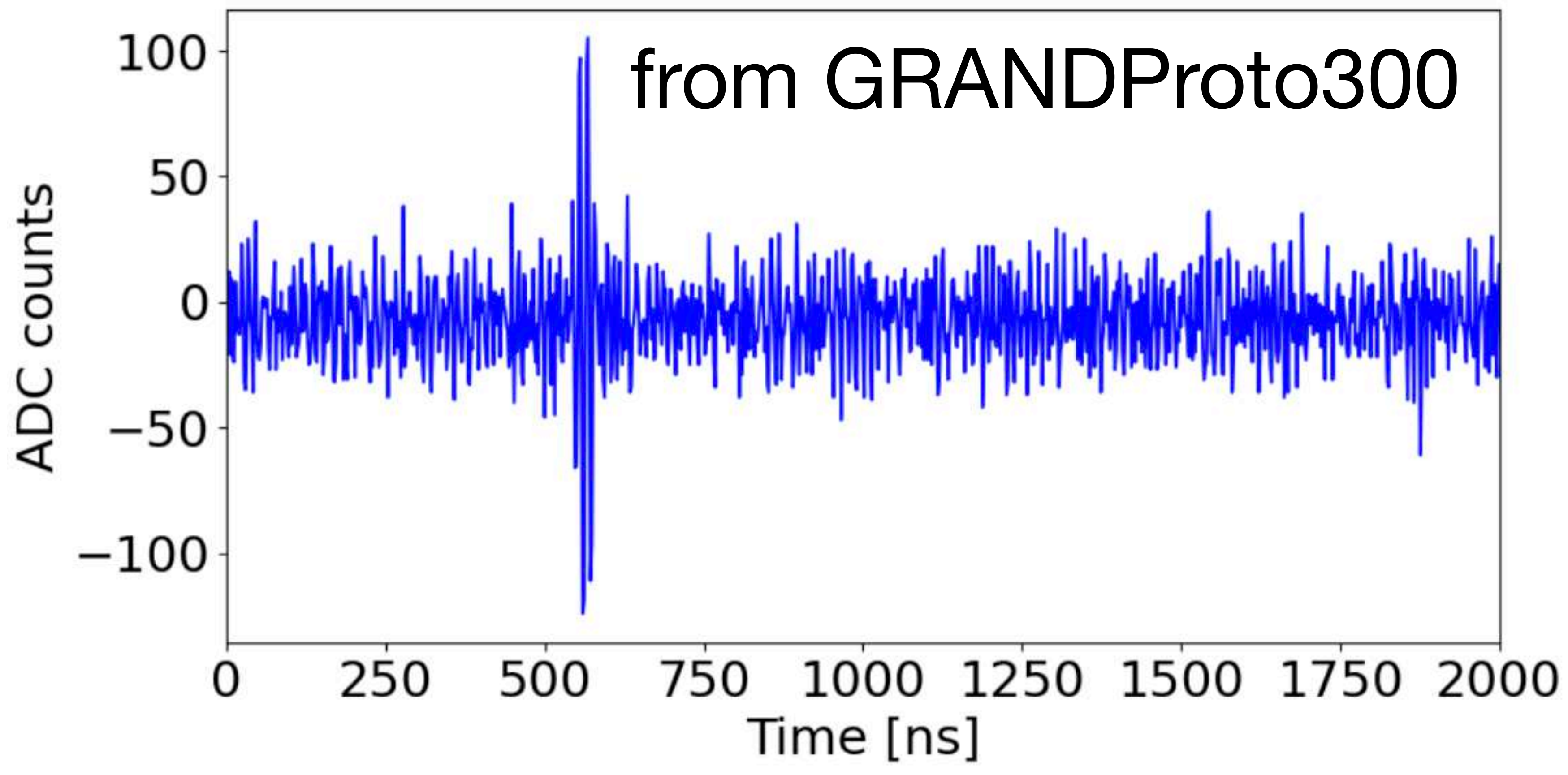

Autonomous radio detection of extensive air showers (EAS)

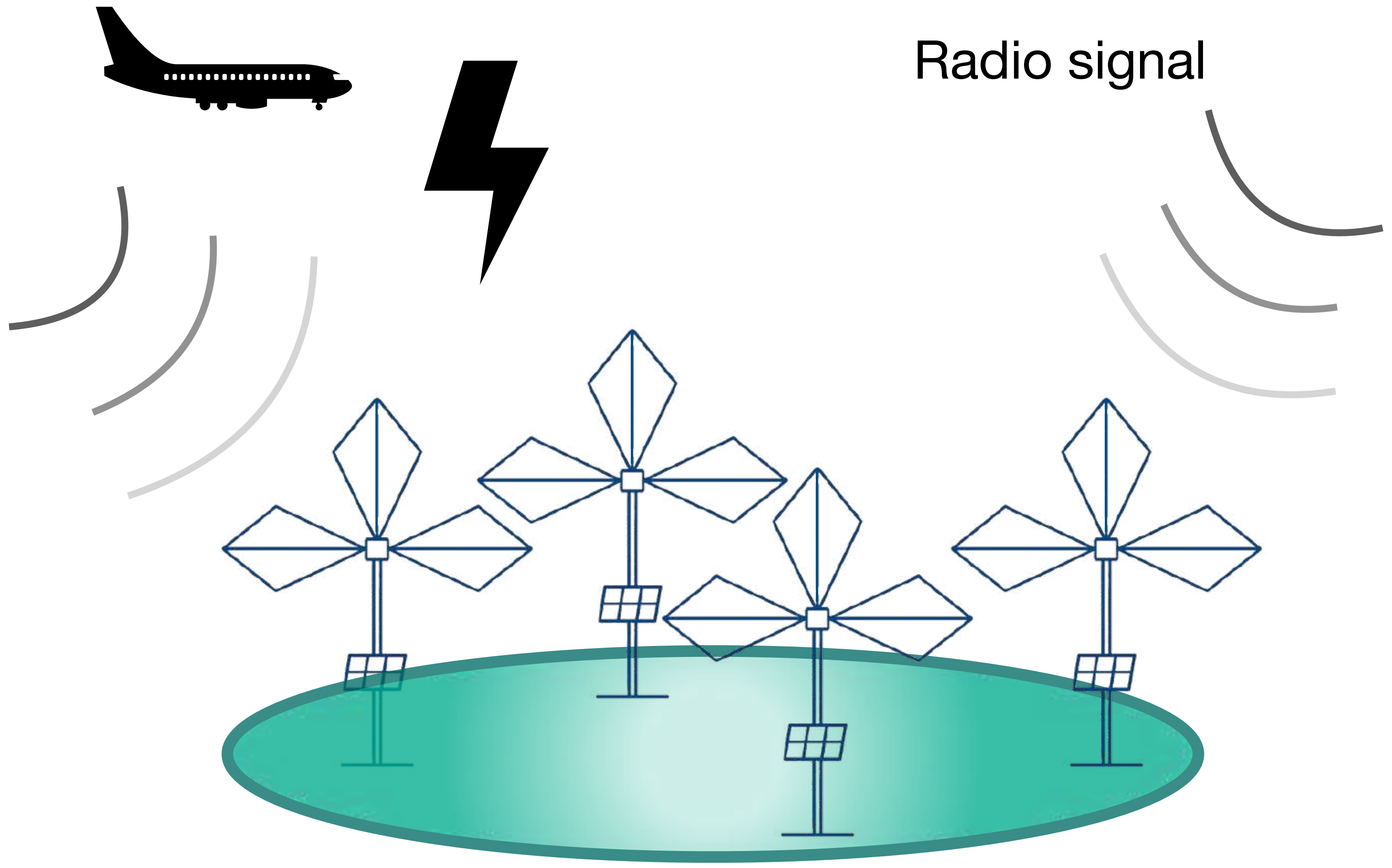

Stationary noise: Galactic noise

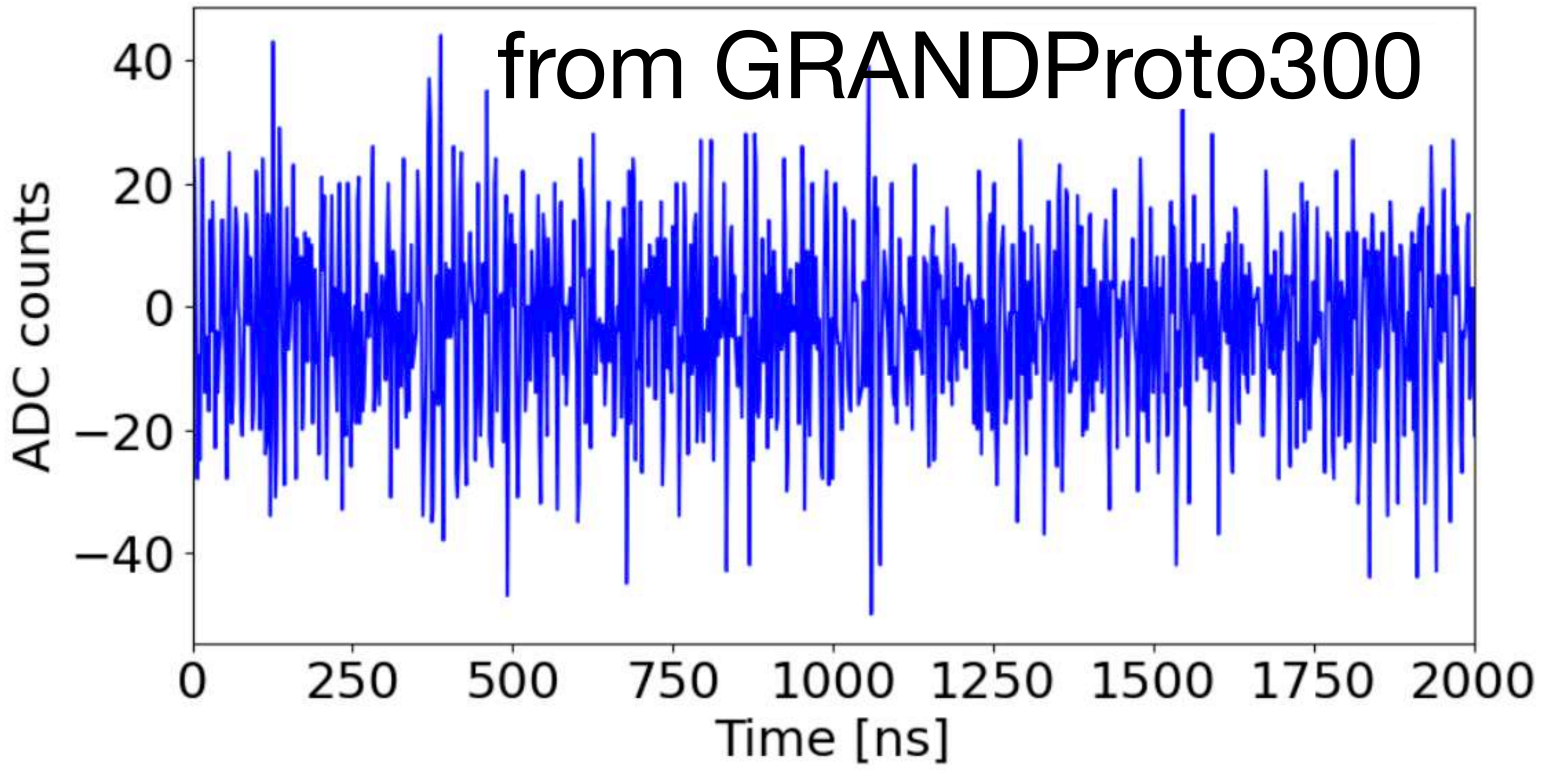

Simulated EAS signal: transient
Duration: ~ 100 ns

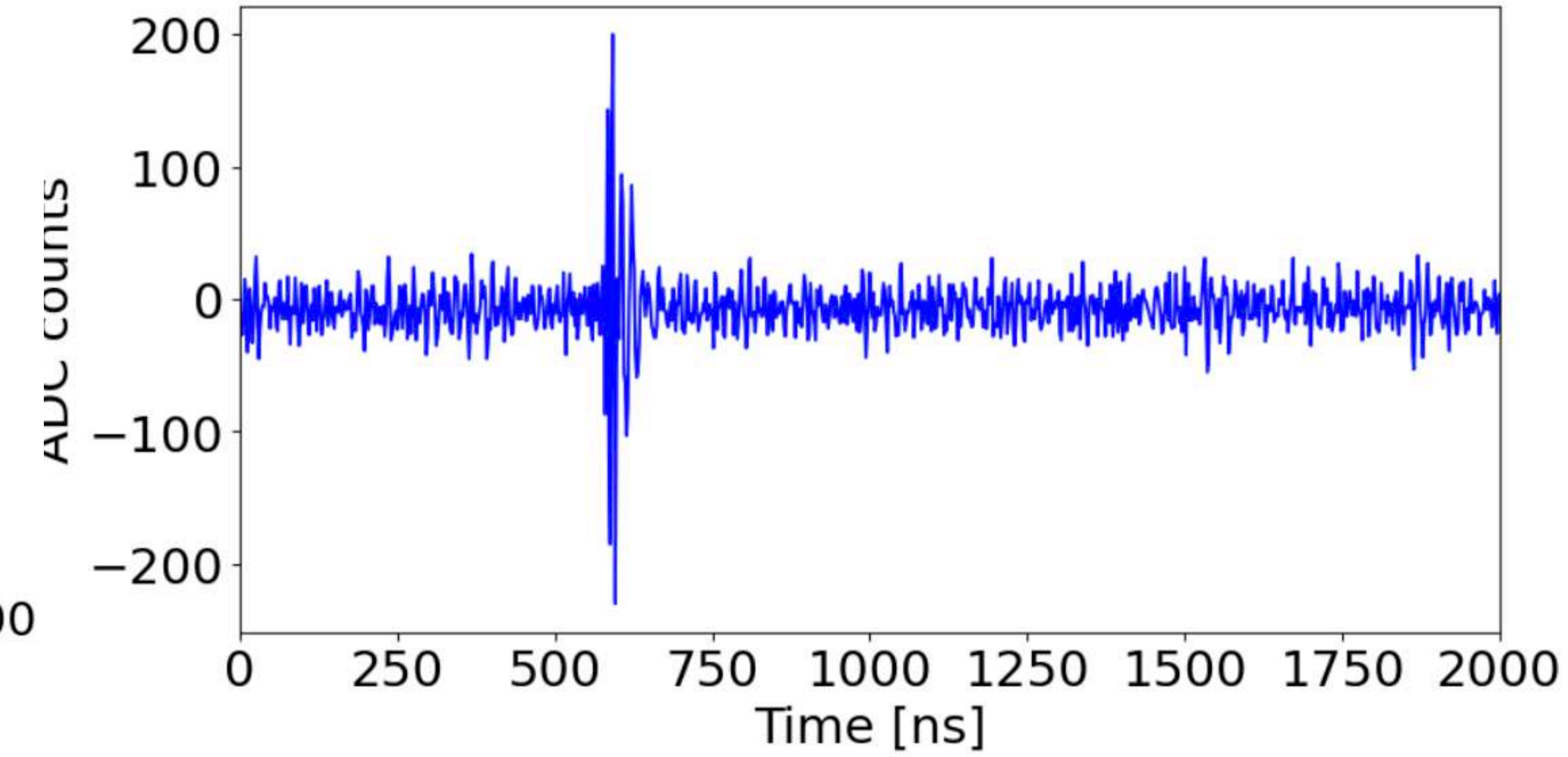

Transient noise: thunderstorms, power lines, aircrafts…

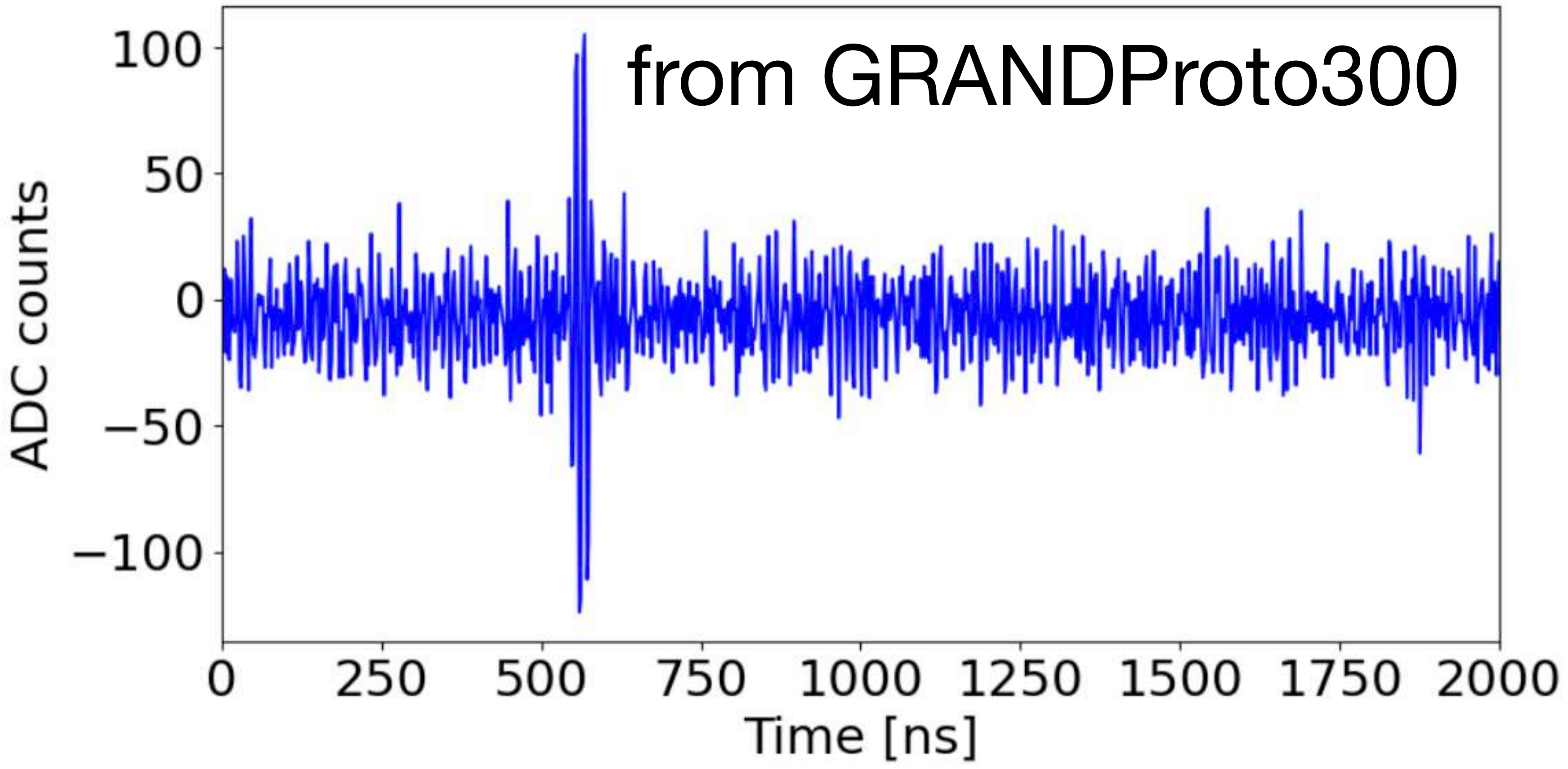

Autonomous radio detection of extensive air showers (EAS)

Autonomous Trigger

Radio signal only (giant arrays)

Extract EAS from noise

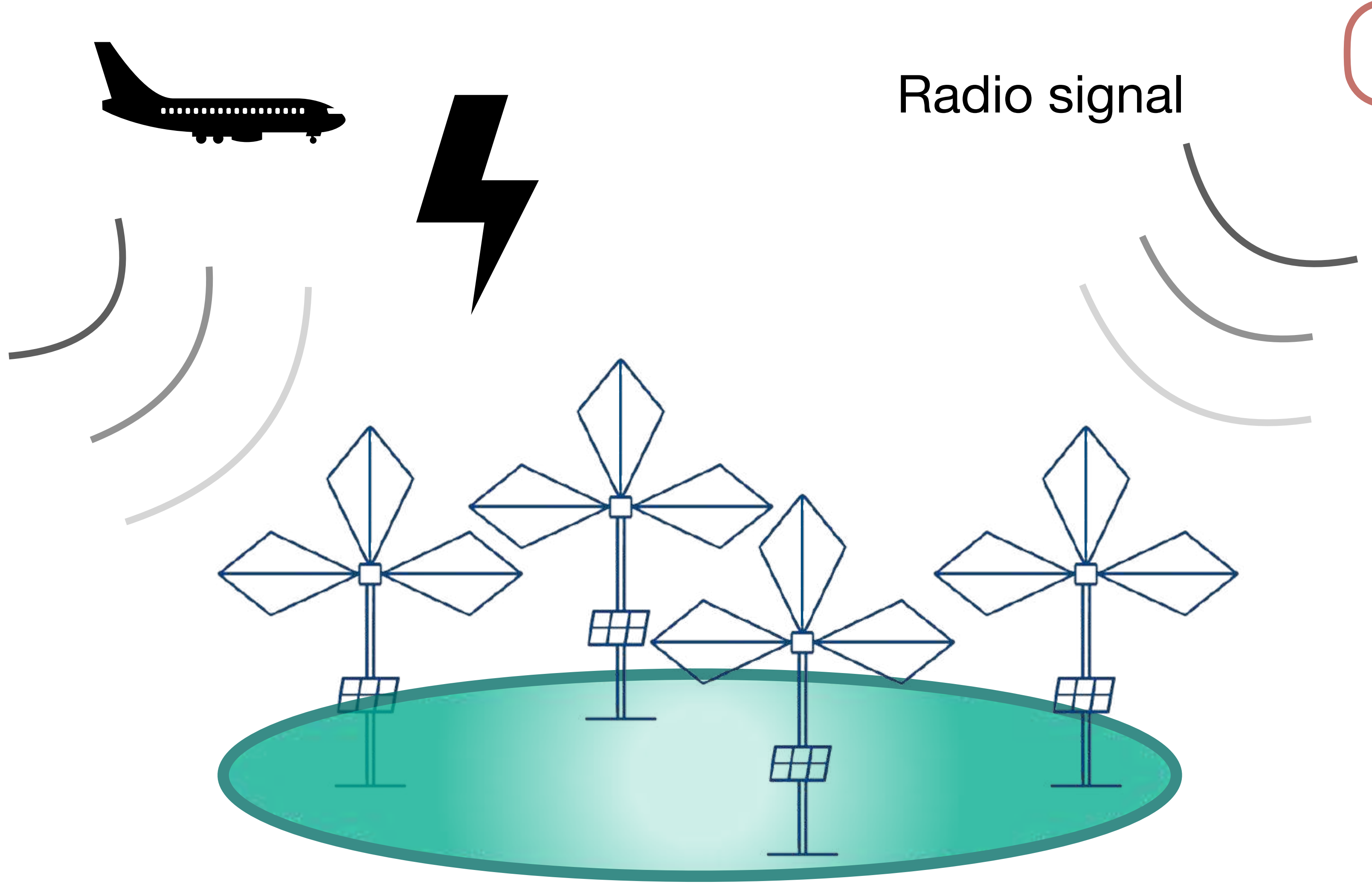

Stationary noise: Galactic noise

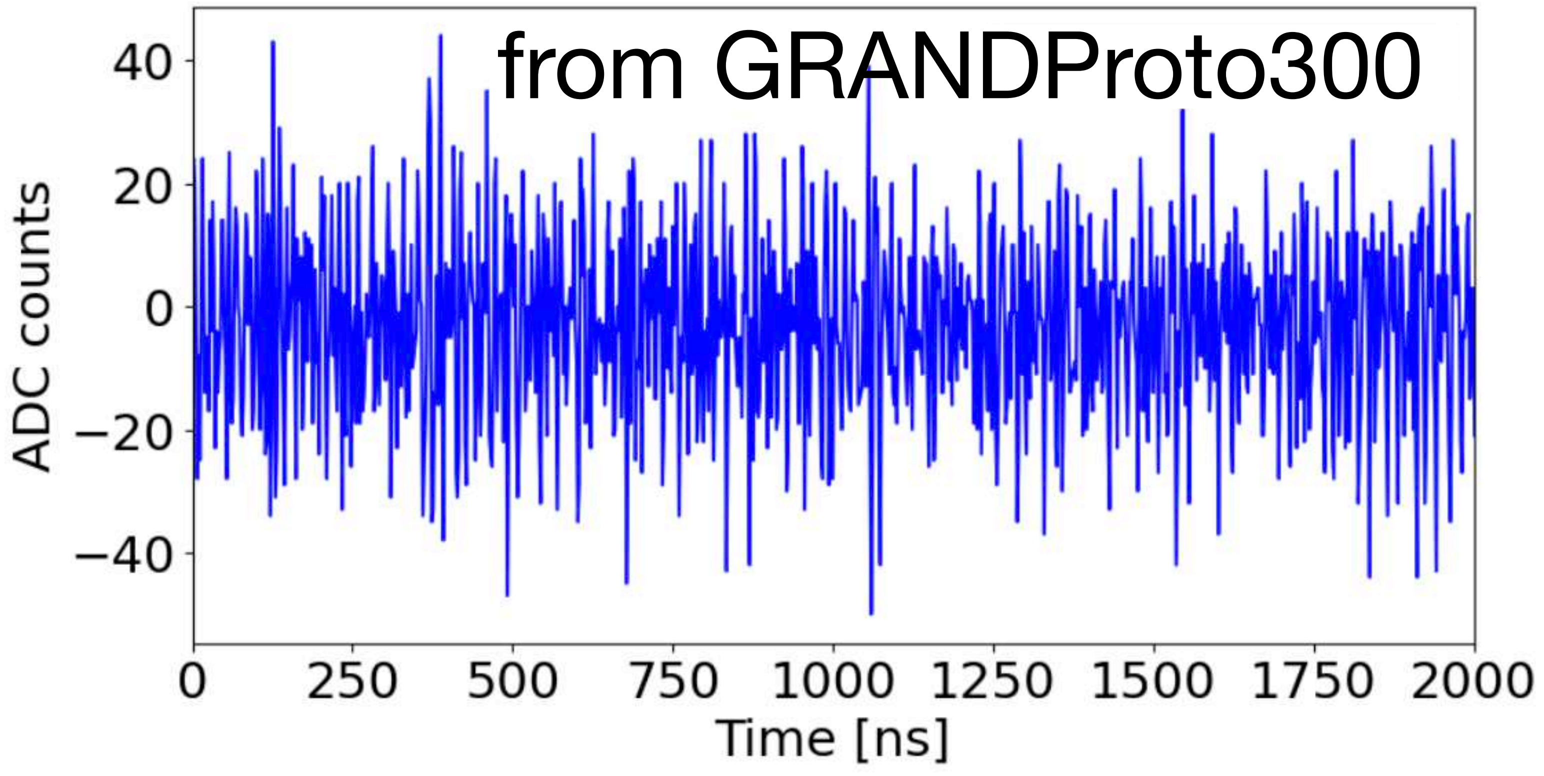

Simulated EAS signal: transient
Duration: ~ 100 ns

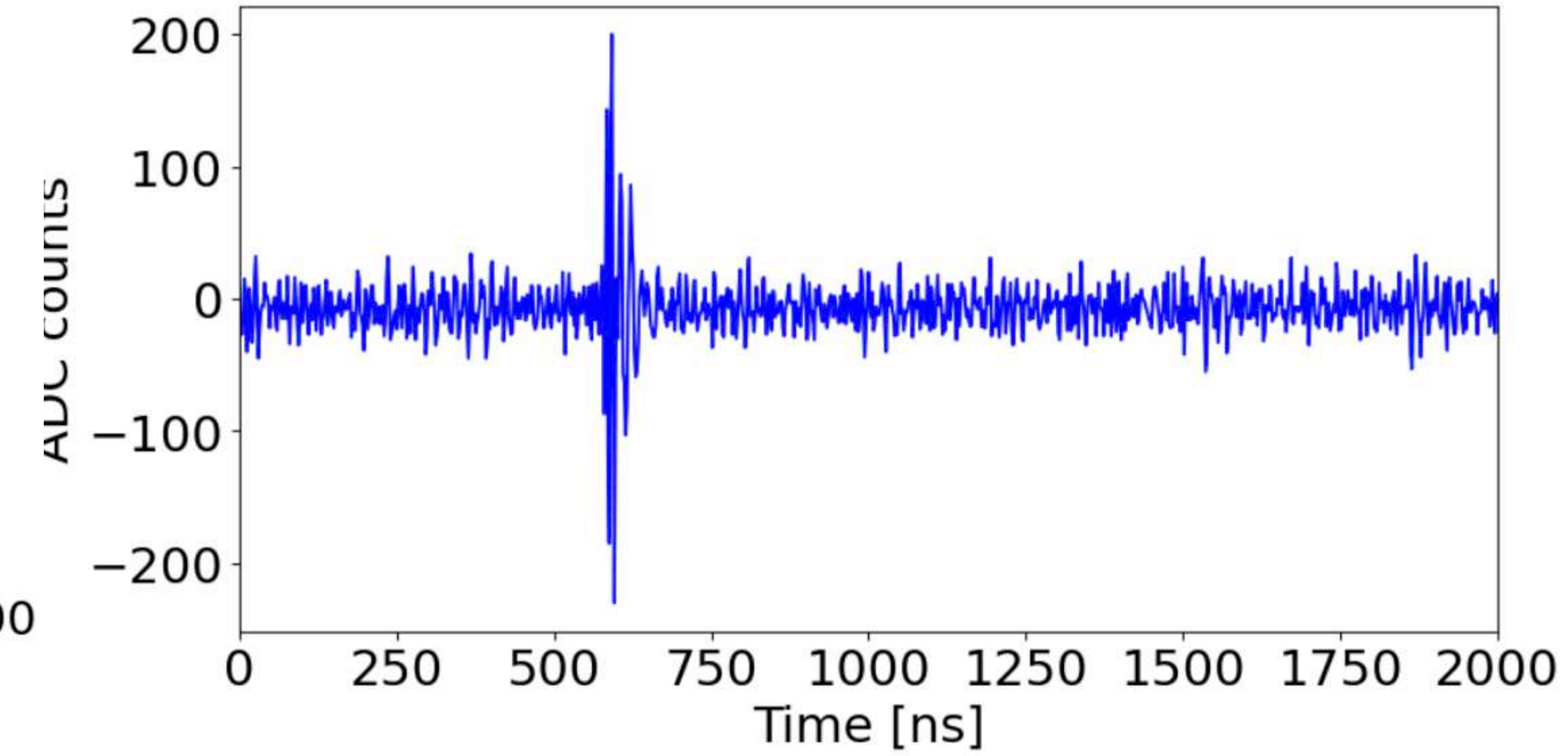

Transient noise: thunderstorms, power lines, aircrafts…

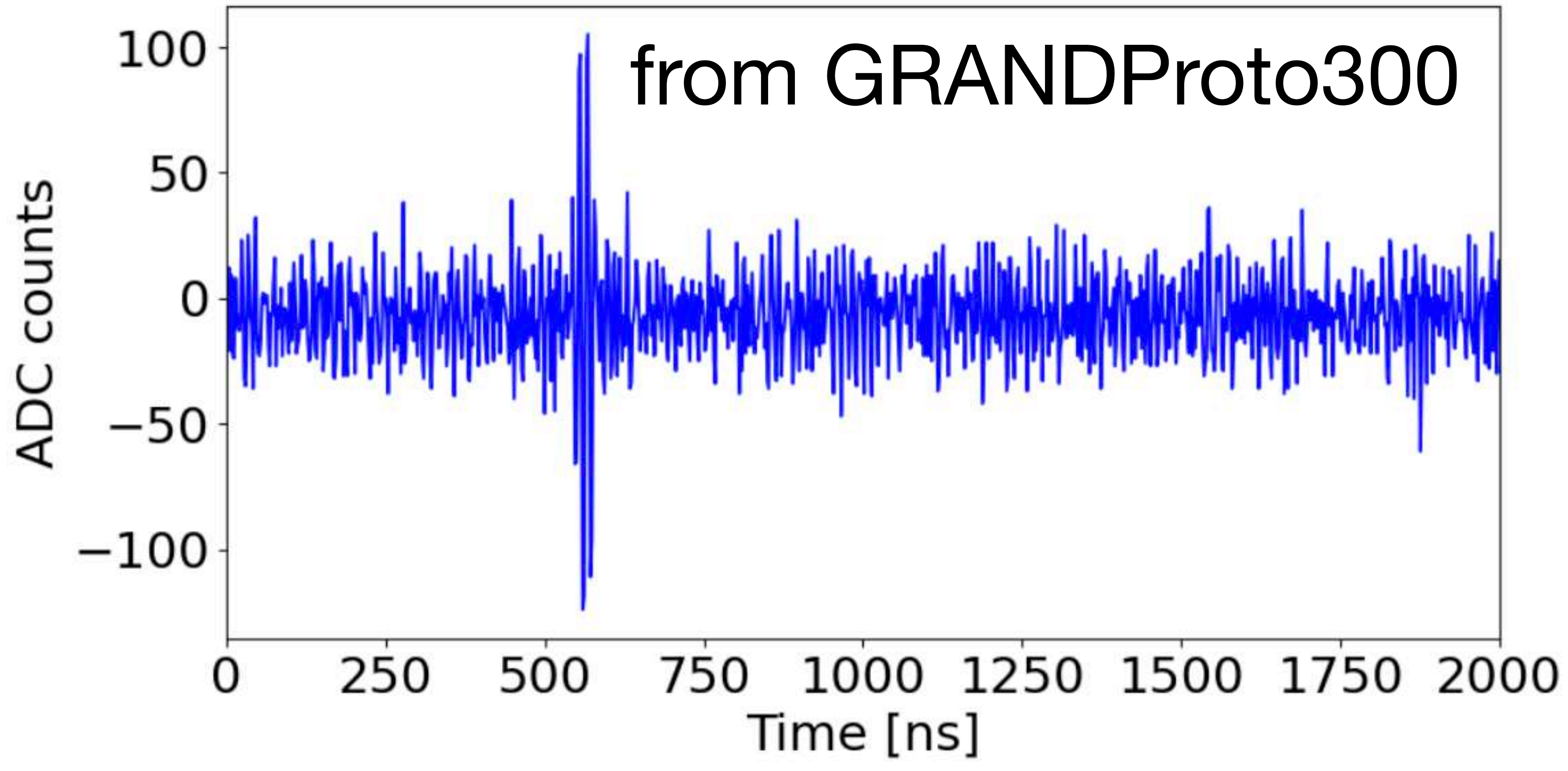

Autonomous radio detection of extensive air showers (EAS)

Autonomous Trigger

Radio signal only (giant arrays)

Extract EAS from noise

Trade-off between **efficiency** and **purity**
- Purity critical: Limited bandwidth because of large array size

Stationary noise: Galactic noise

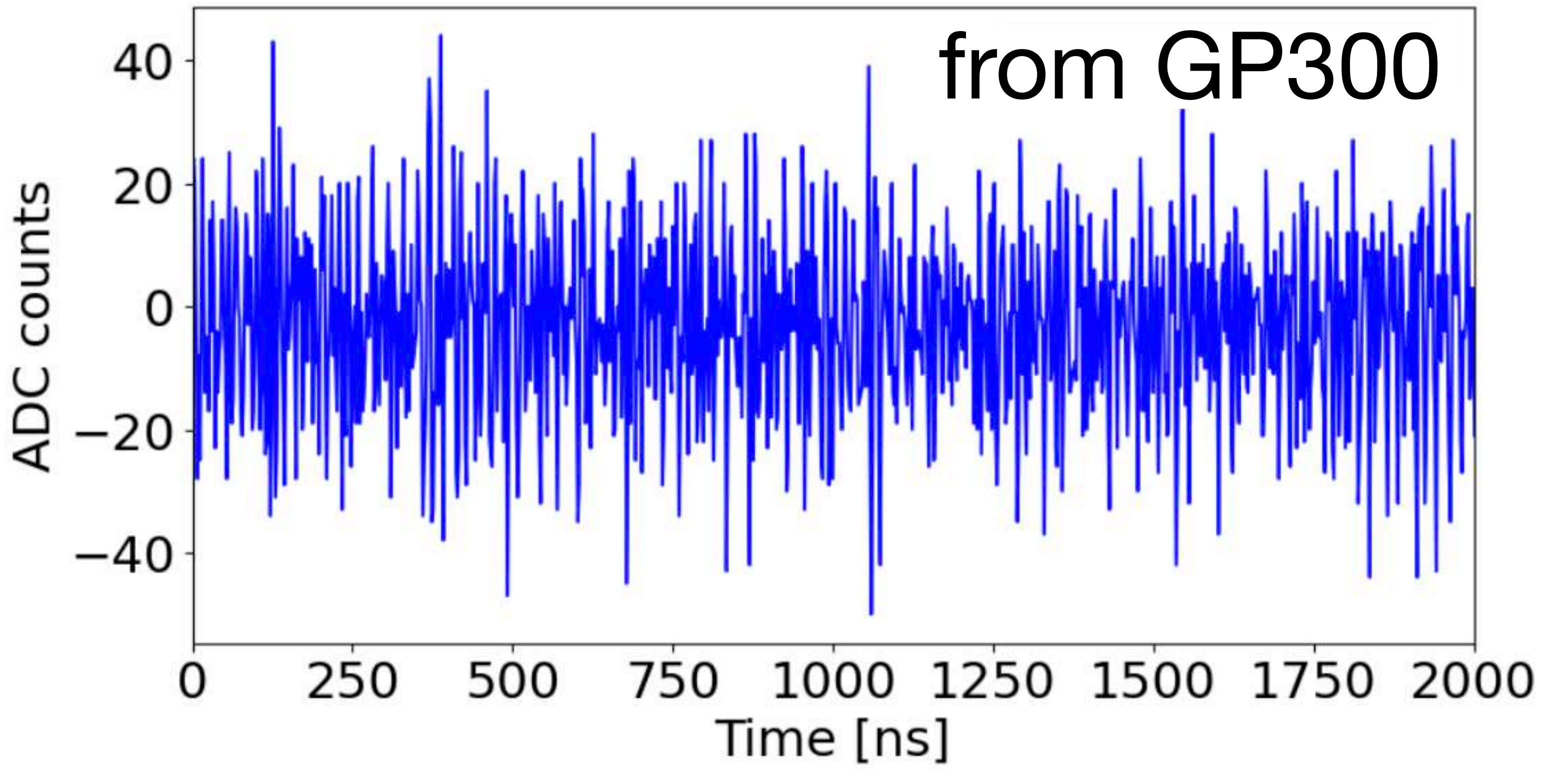

Simulated EAS signal: transient

Duration: ~ 100 ns

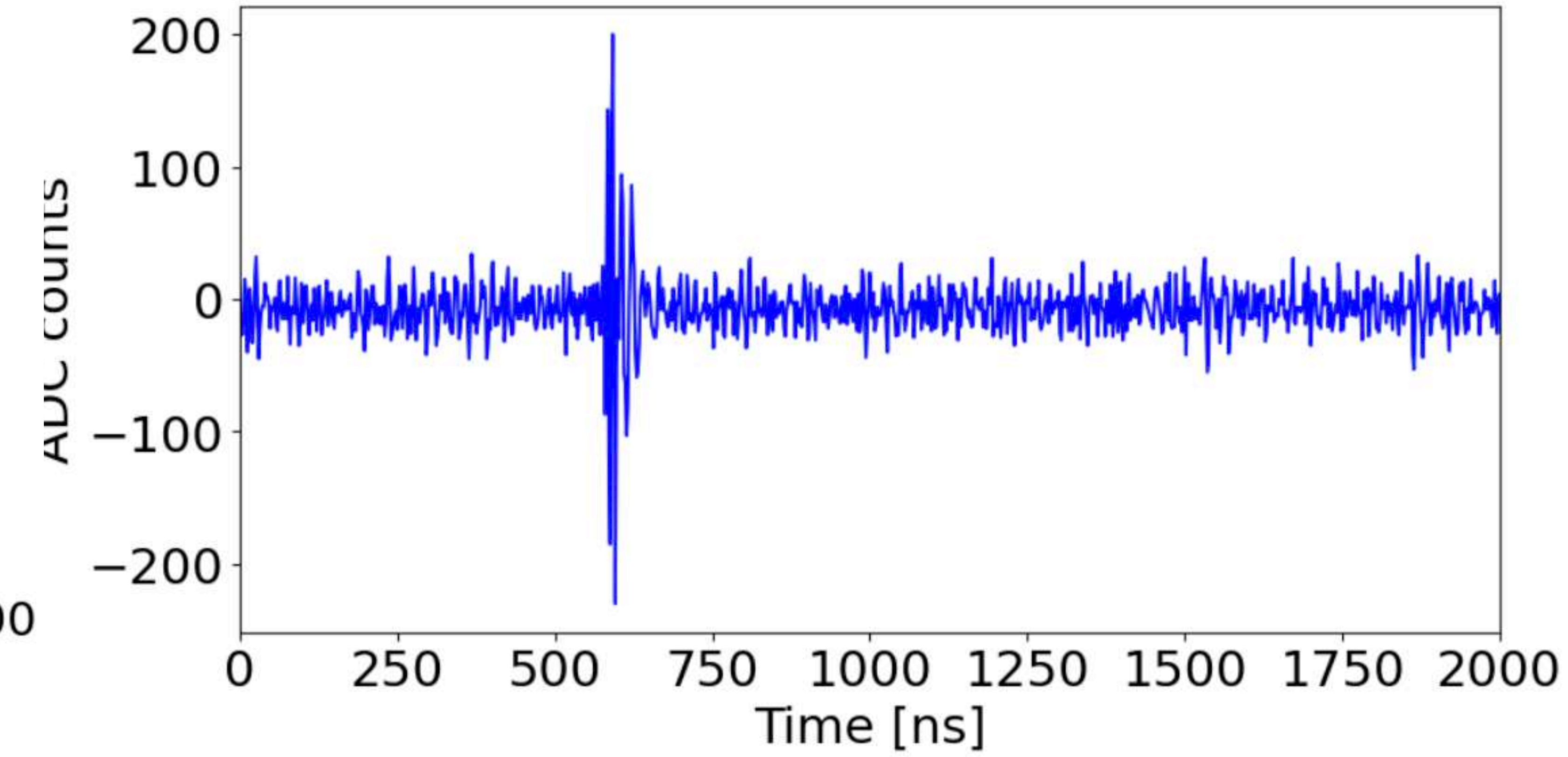

Transient noise: thunderstorms, power lines, aircrafts…

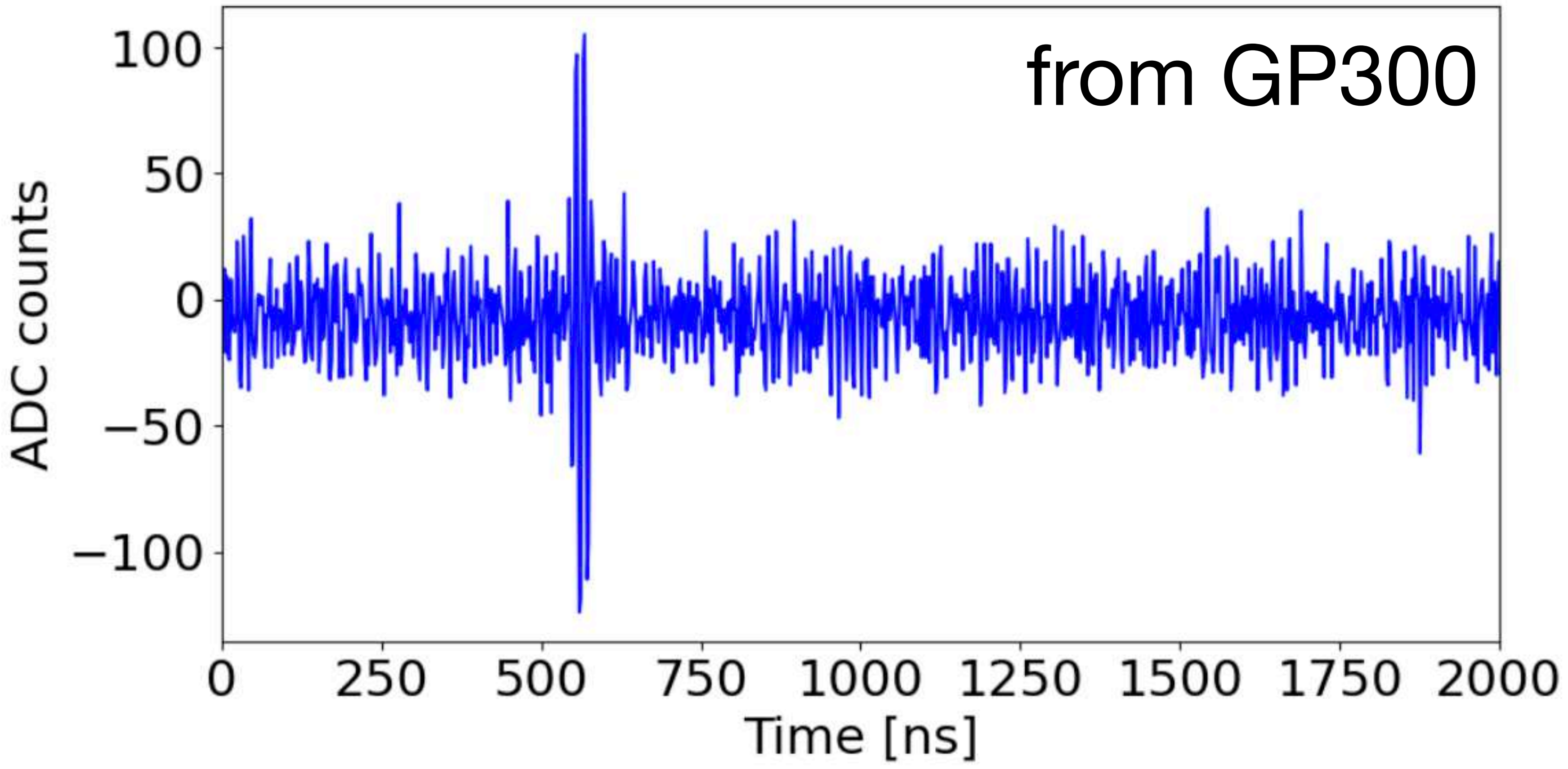

The electronics at GRANDProto300

3. Central Processing Units (CPU)
Field-Programmable Gate Array (FPGA)

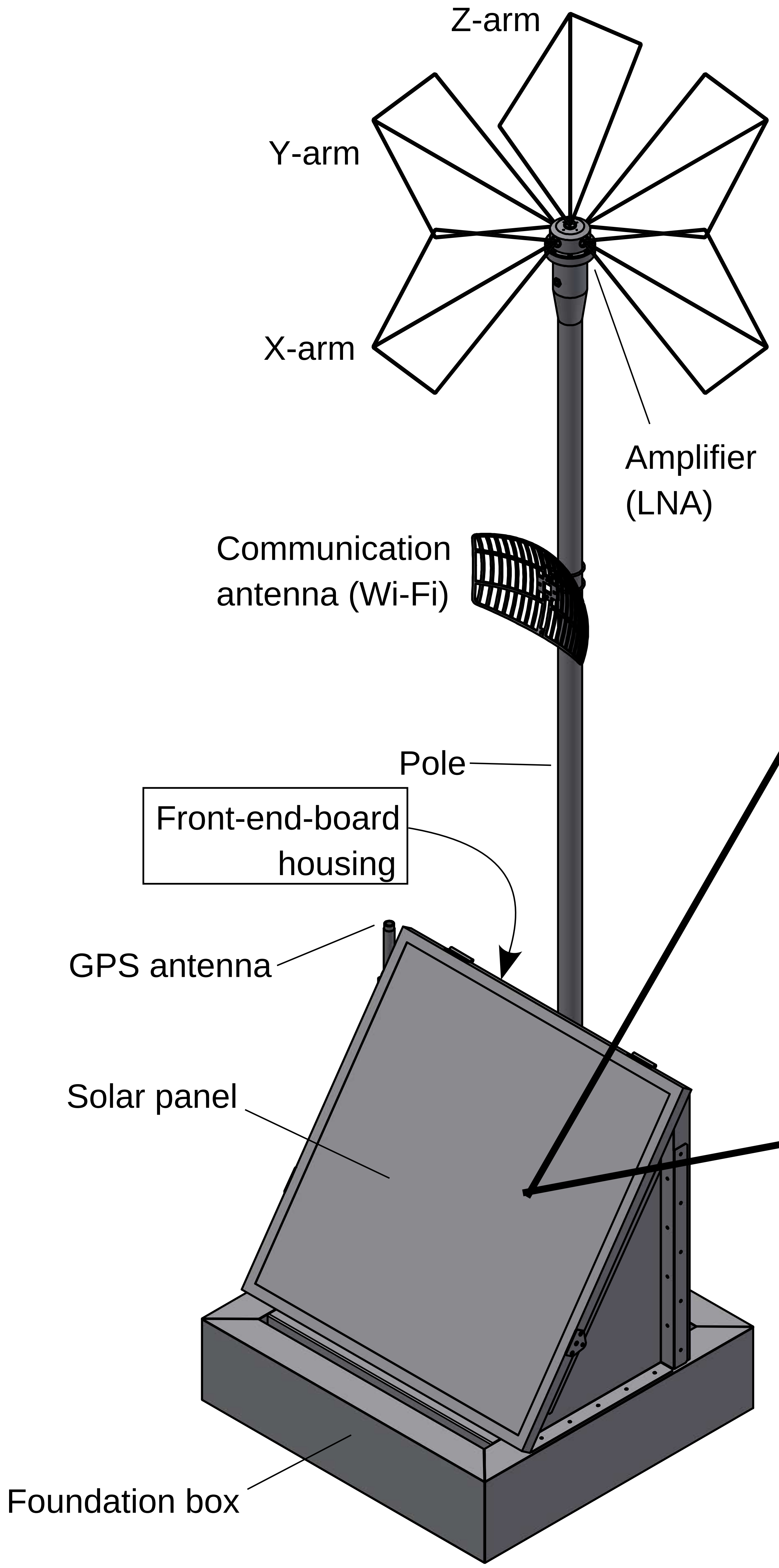

5. Ethernet chip

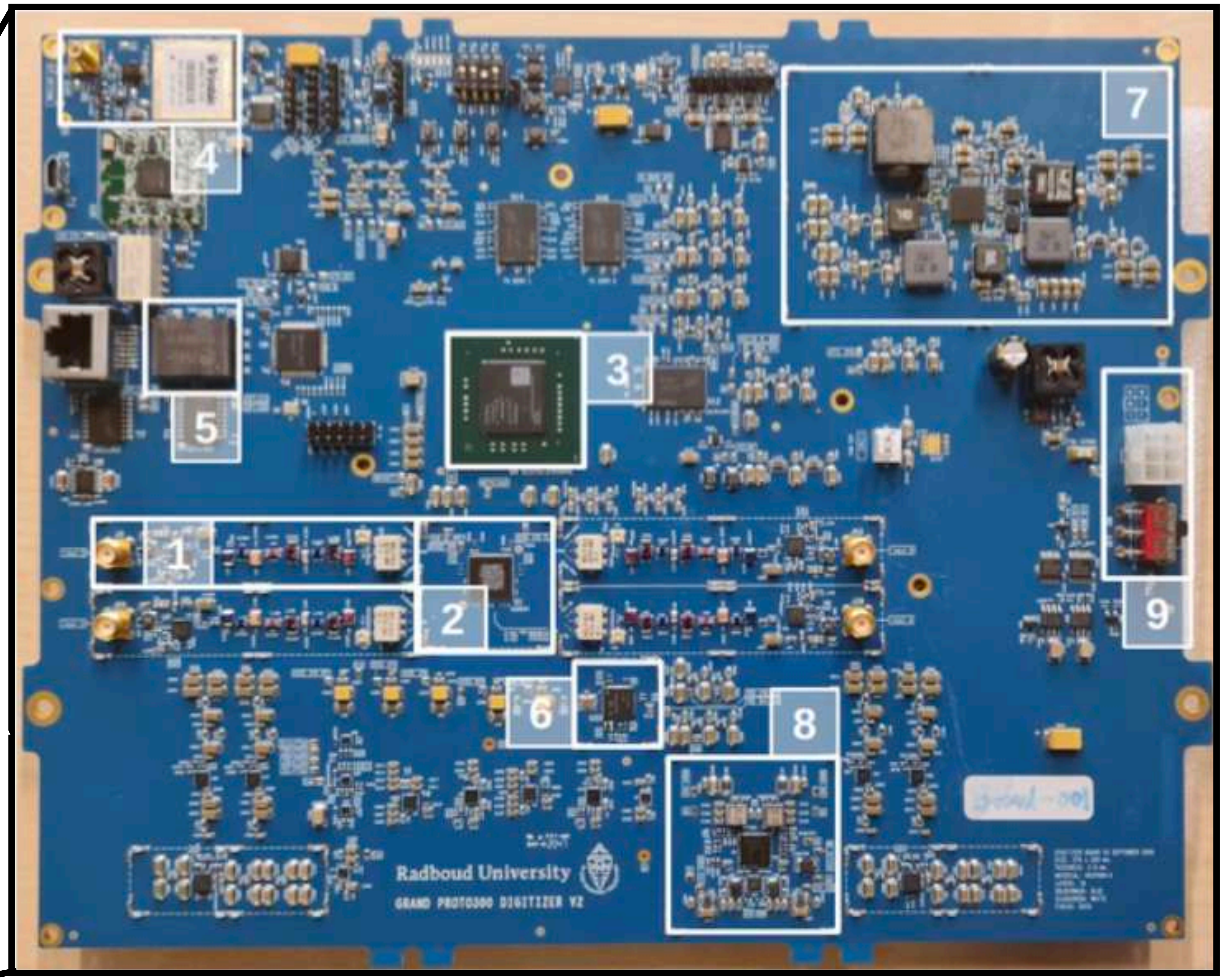

7. Digital power

9. Power connector

8. Analog power

1. Signal input & Analog filter (50-200 MHz)

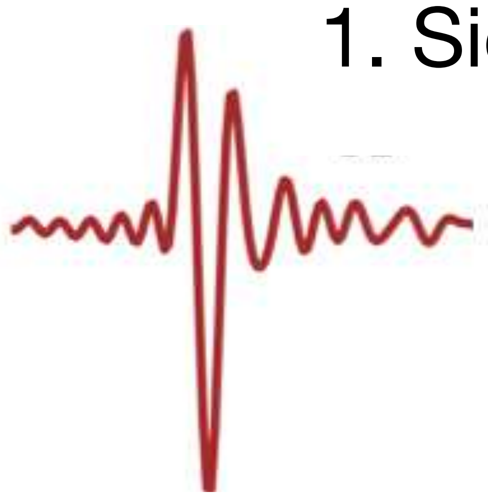

Voltage signal

2. Analog-to-Digital Converter

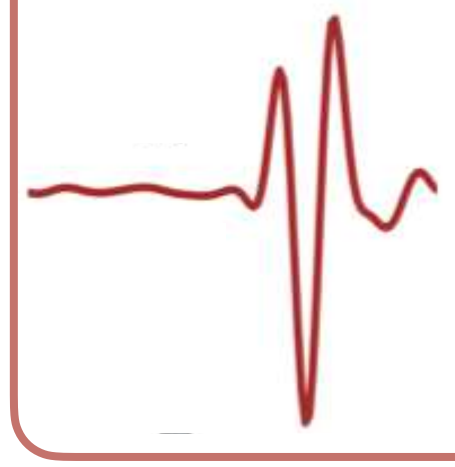

ADC signal

The current trigger system at GRANDProto300

First Level Trigger (FLT) on FPGA
Signal-over-threshold trigger

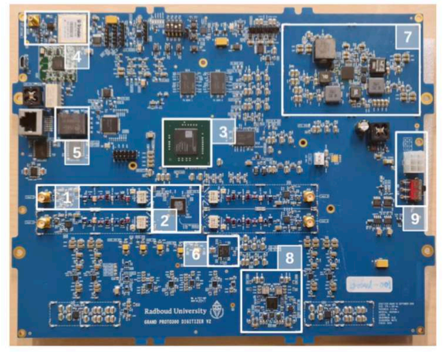

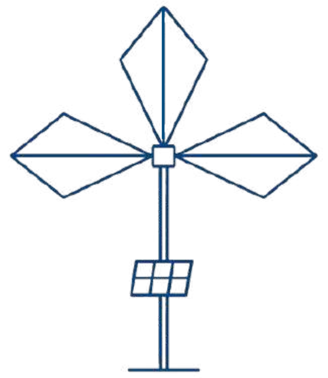

At the antenna level

Wi-Fi
data transfert

Second Level Trigger (SLT)
Coincidences within 10 μs time window between at least 5 antennas

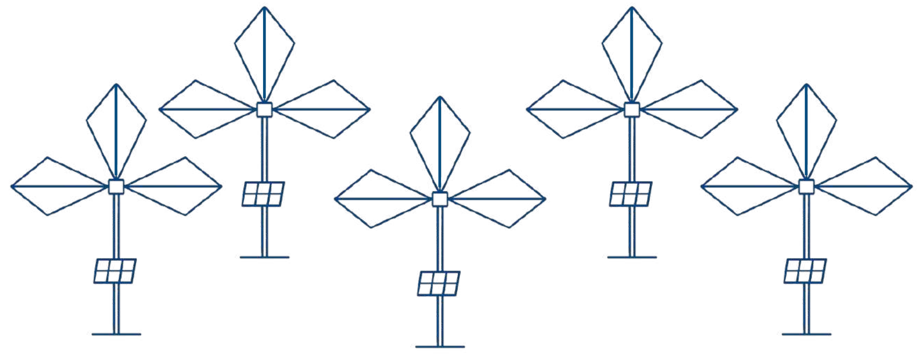

At the detector level

Central DAQ
Coincident data (CD) stored

- Offline analysis

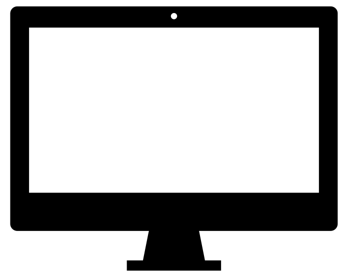

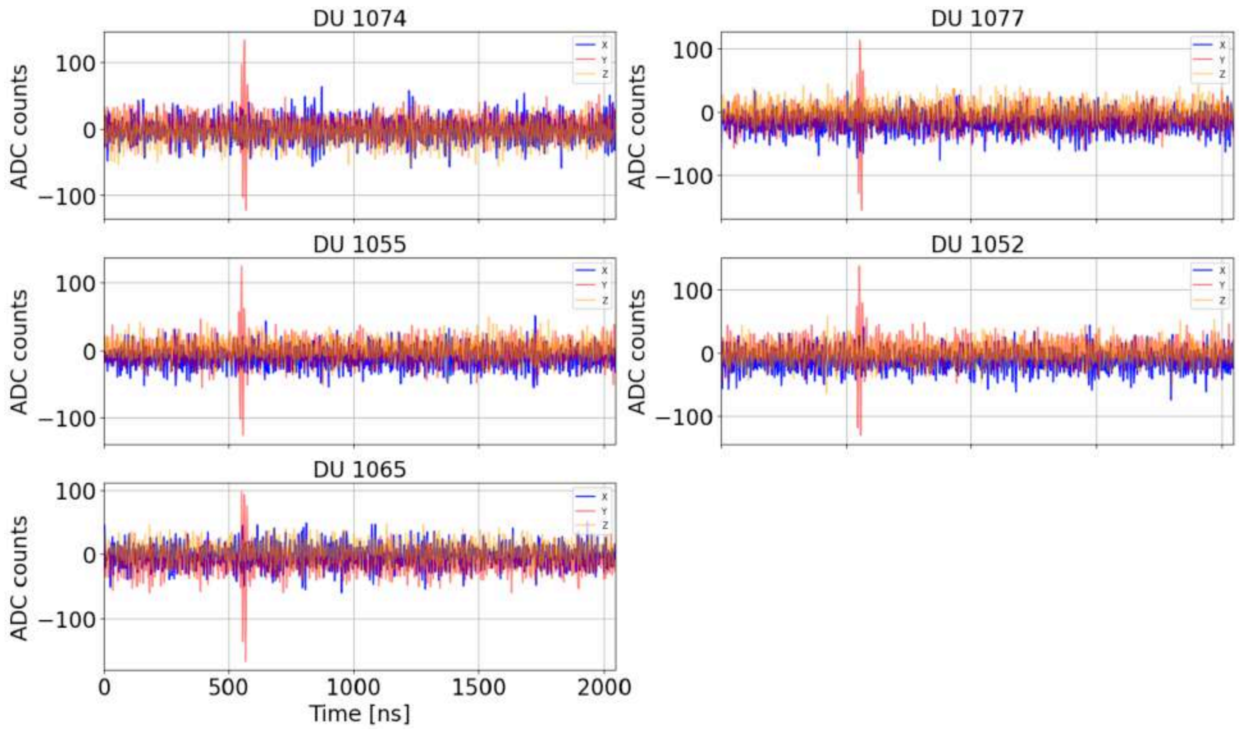

The current trigger system at GRANDProto300

First Level Trigger (FLT) on FPGA
Signal-over-threshold trigger

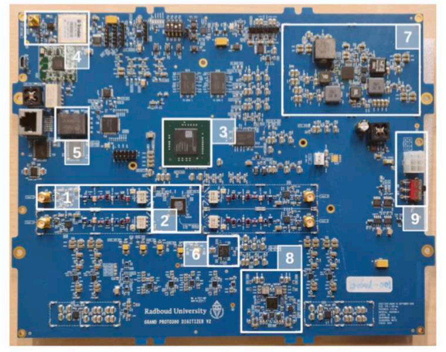

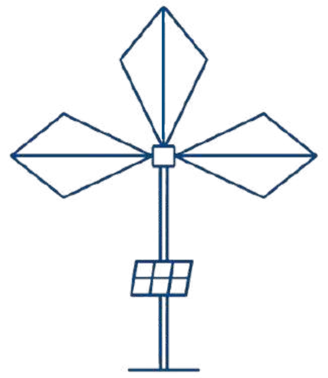

At the antenna level

Wi-Fi
data transfert

Second Level Trigger (SLT)
Coincidences within 10 μs time window
between at least 5 antennas

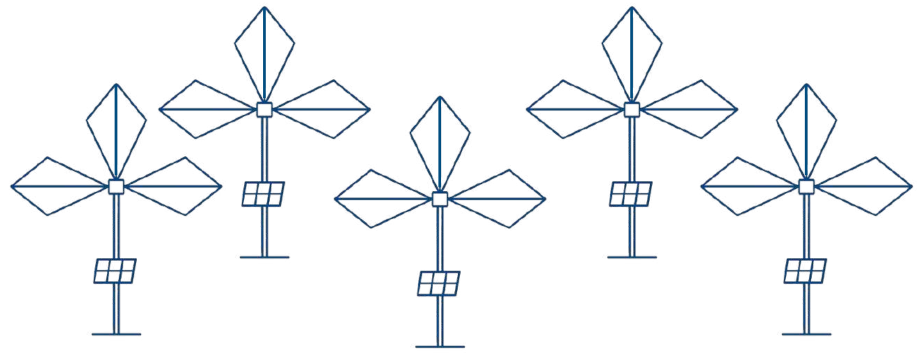

At the detector level

Central DAQ
Coincident data (CD) stored

‣ Offline analysis

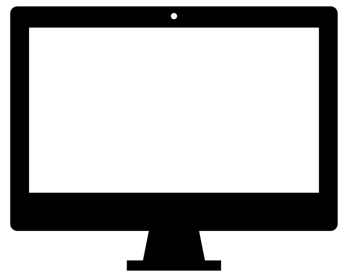

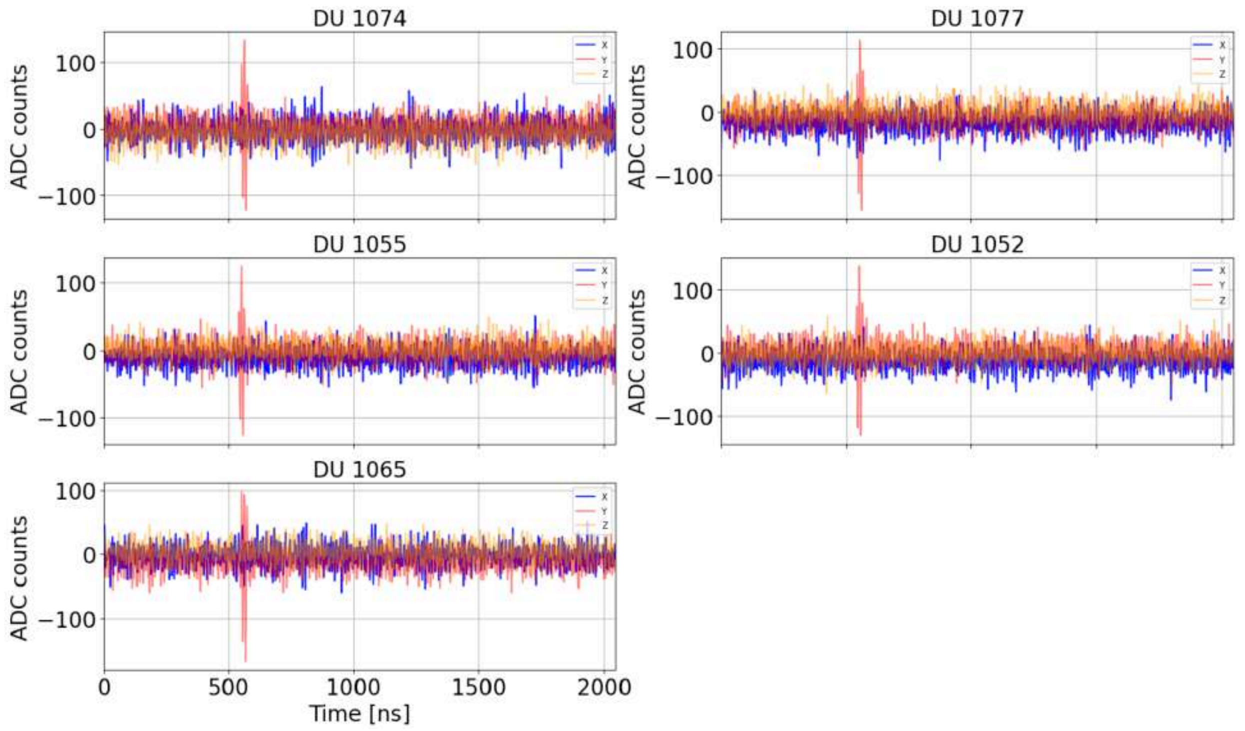

Data acquisition since Dec 2024 on GRANDProto300
‣ Fewer cosmic ray events than expected among coincident data (CD)
My work**:** tune parameters on First Level Trigger: best balance between **efficiency** and **purity?**

The First Level Trigger: logic

First Level Trigger: Double threshold, 5 parameters

- Th1: first signal amplitude threshold
- T_{period} (500ns): time window during which the trace is analyzed after the first Th1

- Th2: second threshold
- T_{sepmax}: The maximum duration allowed for two consecutive peaks (both exceeding Th2)
- NC: number of crossings allowed that exceeds Th2 (**including Th1 peak**)

Adapted from X. Tian

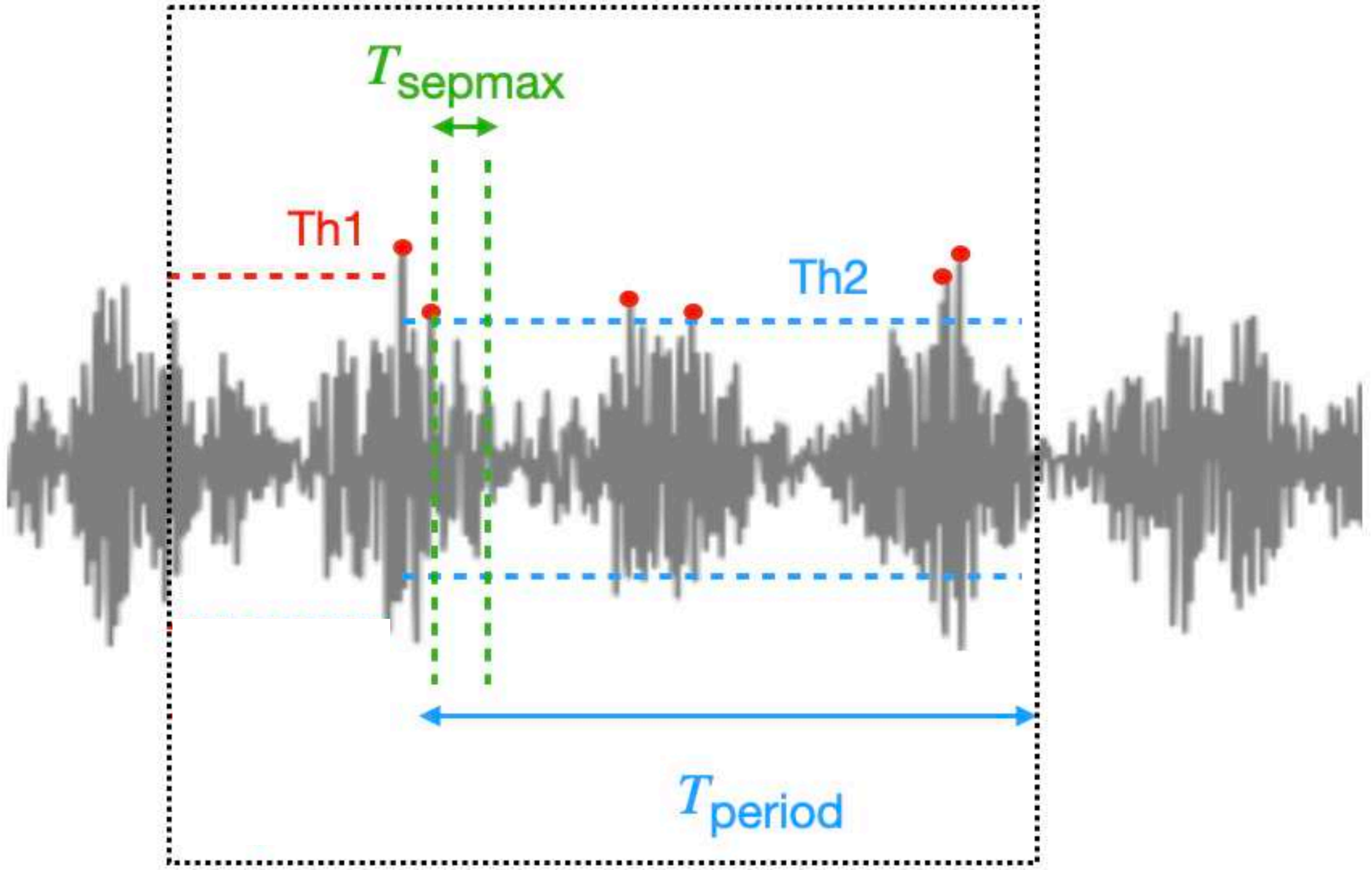

Parameters optimization: efficiency

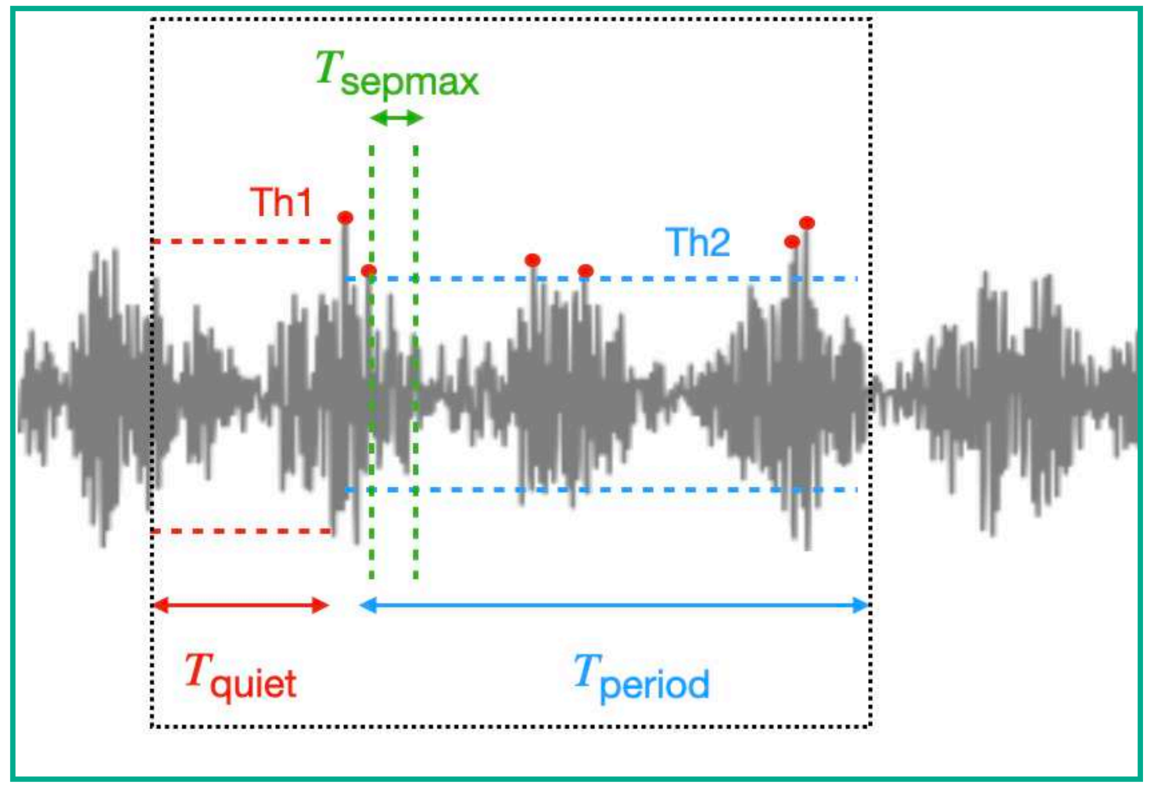

Reproduce First Level Trigger offline

GRAND realistic simulations:

$\sim 10^3$ GRAND cosmic-ray simulations ($\sim 120{,}000$ traces)

- Simulated electric fields with ZHAireS
- Process through simulated detector response
- Add **measured noise** on GRANDProto300 site
- **Digital filtering**

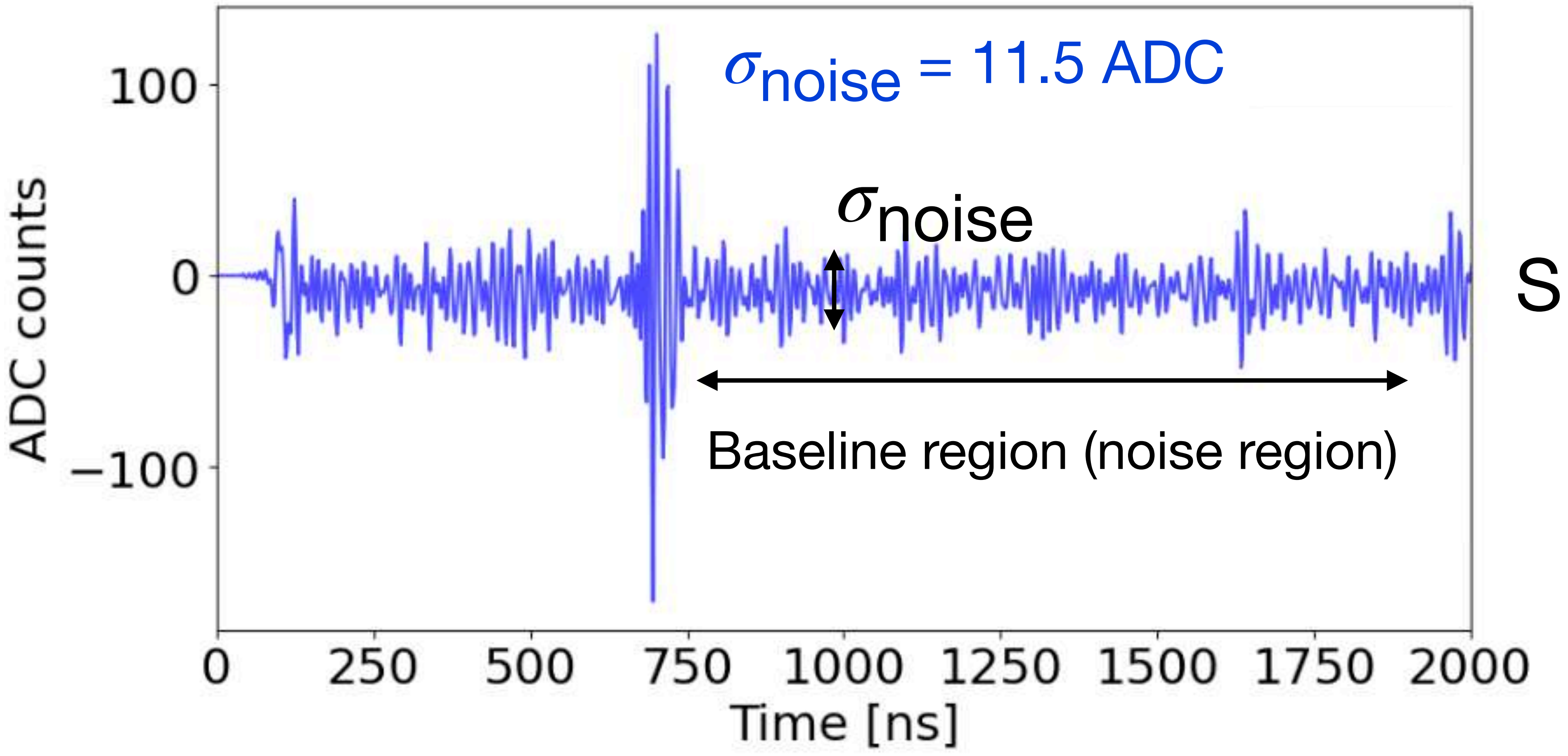

$$\text{SNR} = \frac{A_{\text{max}}}{\sigma_{\text{noise}}}$$

Parameters optimization: efficiency

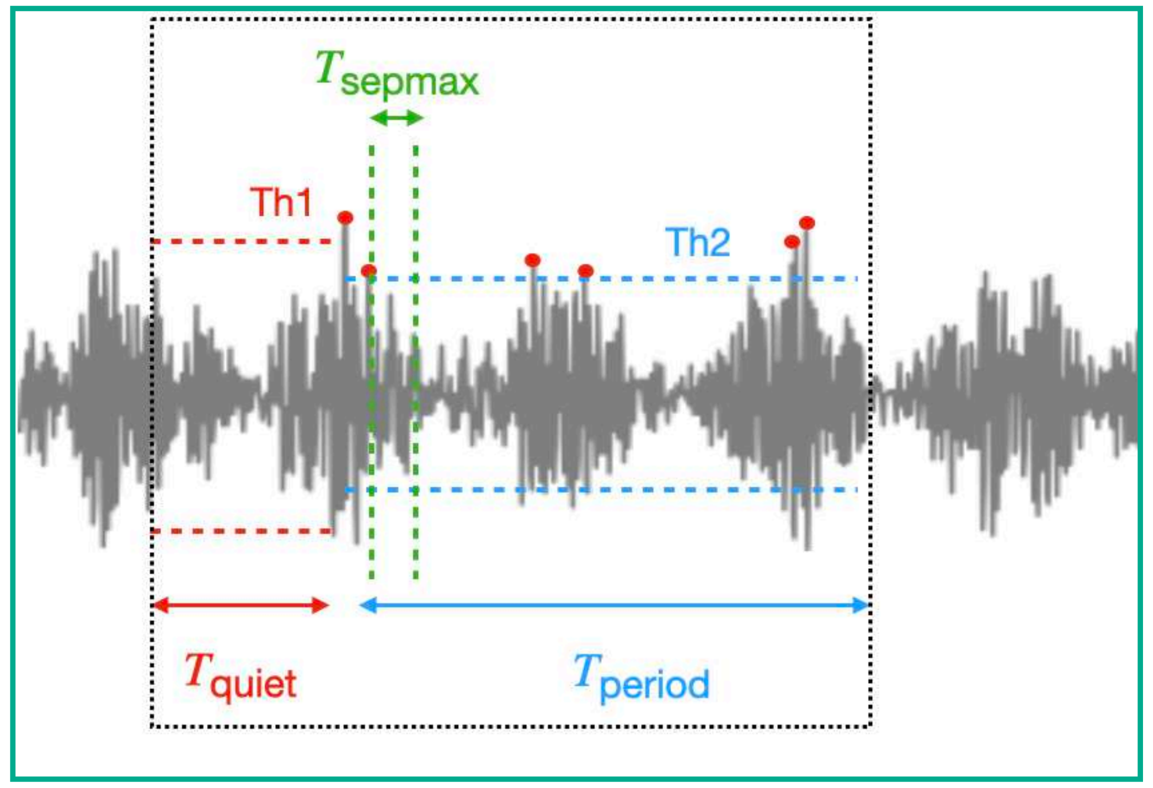

Reproduce First Level Trigger offline

Optimal (my work):
Th1 $\sim 5\sigma$
Th2 $\sim 4\sigma$
T_{sepmax} = 50 ns
NC between 2 and 7

On-site (before my analysis):
Th1 = 70 ADC ($\sim 6.5\sigma$)
Th2 = 35 ADC ($\sim 3\sigma$)
T_{sepmax} = 15 ns
NC between 2 and 7

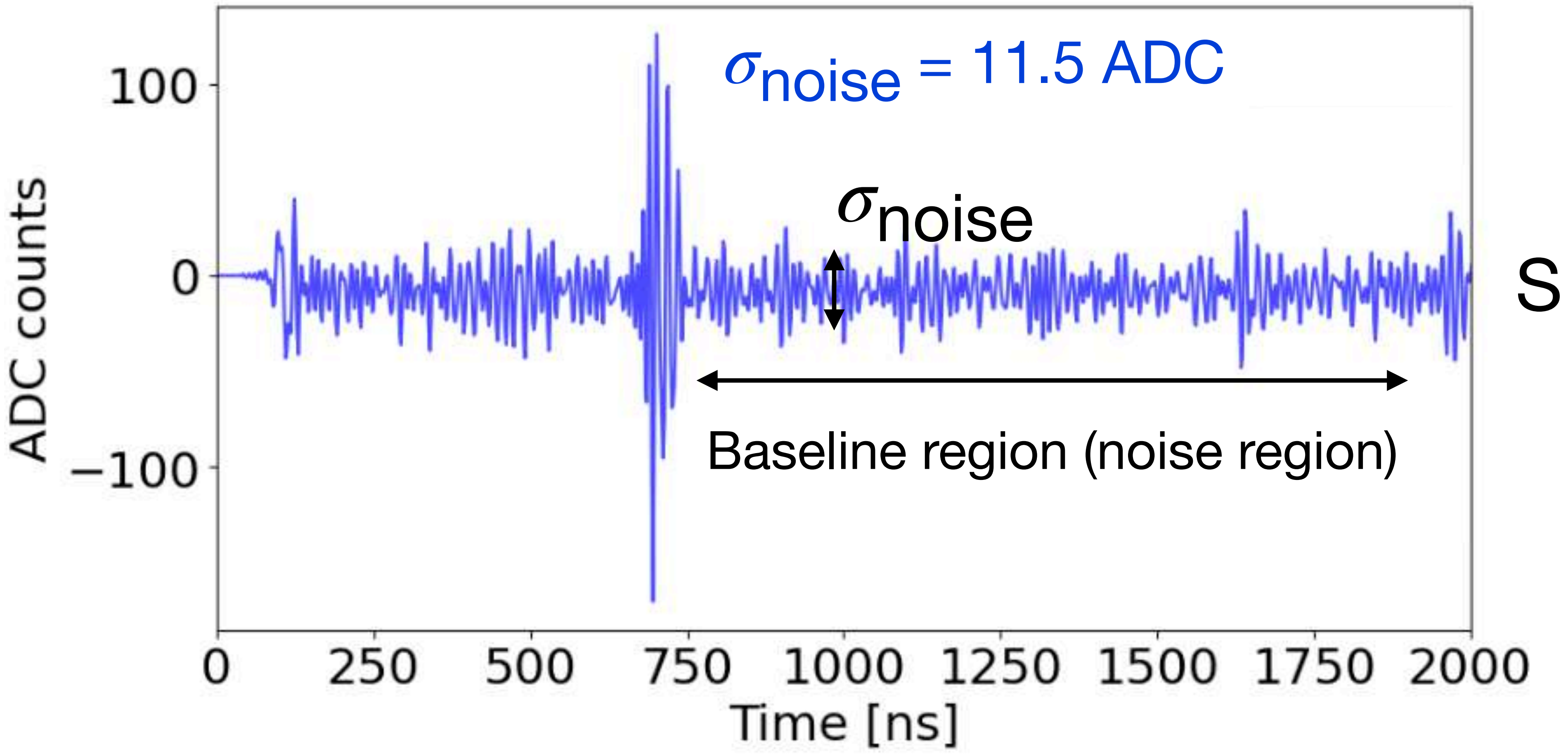

$$\text{SNR} = \frac{A_{\text{max}}}{\sigma_{\text{noise}}}$$

Parameters optimization: efficiency

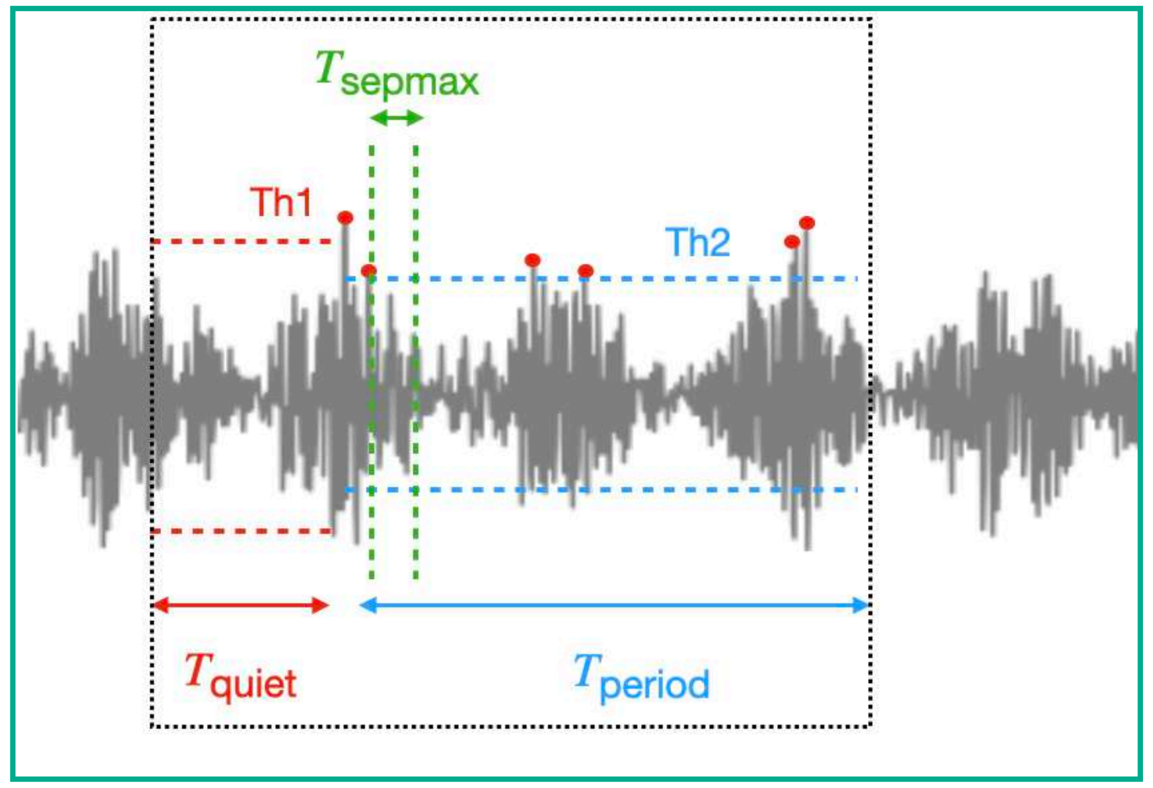

Reproduce First Level Trigger offline

Optimal (my work):
Th1 $\sim 5\sigma$
Th2 $\sim 4\sigma$
$T_{\text{sepmax}} = 50$ ns
NC between 2 and 7

On-site (before my analysis):
Th1 = 70 ADC ($\sim 6.5\sigma$)
Th2 = 35 ADC ($\sim 3\sigma$)
$T_{\text{sepmax}} = 15$ ns
NC between 2 and 7

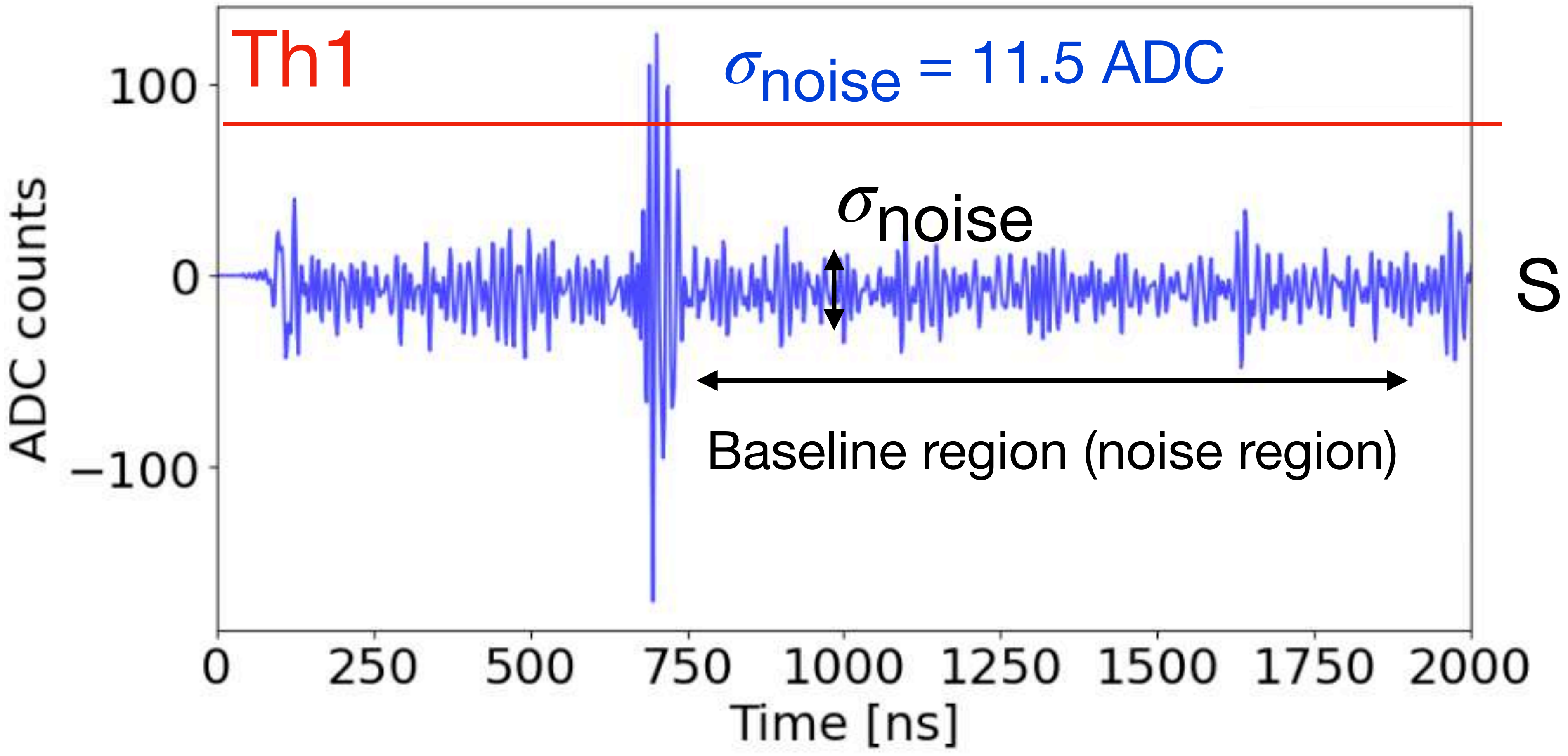

$$\text{SNR} = \frac{A_{\text{max}}}{\sigma_{\text{noise}}}$$

Th1: main driven parameter
Chose if the signal will be analyzed
Best practice: do not set absolute ADC value

Parameters optimization: efficiency

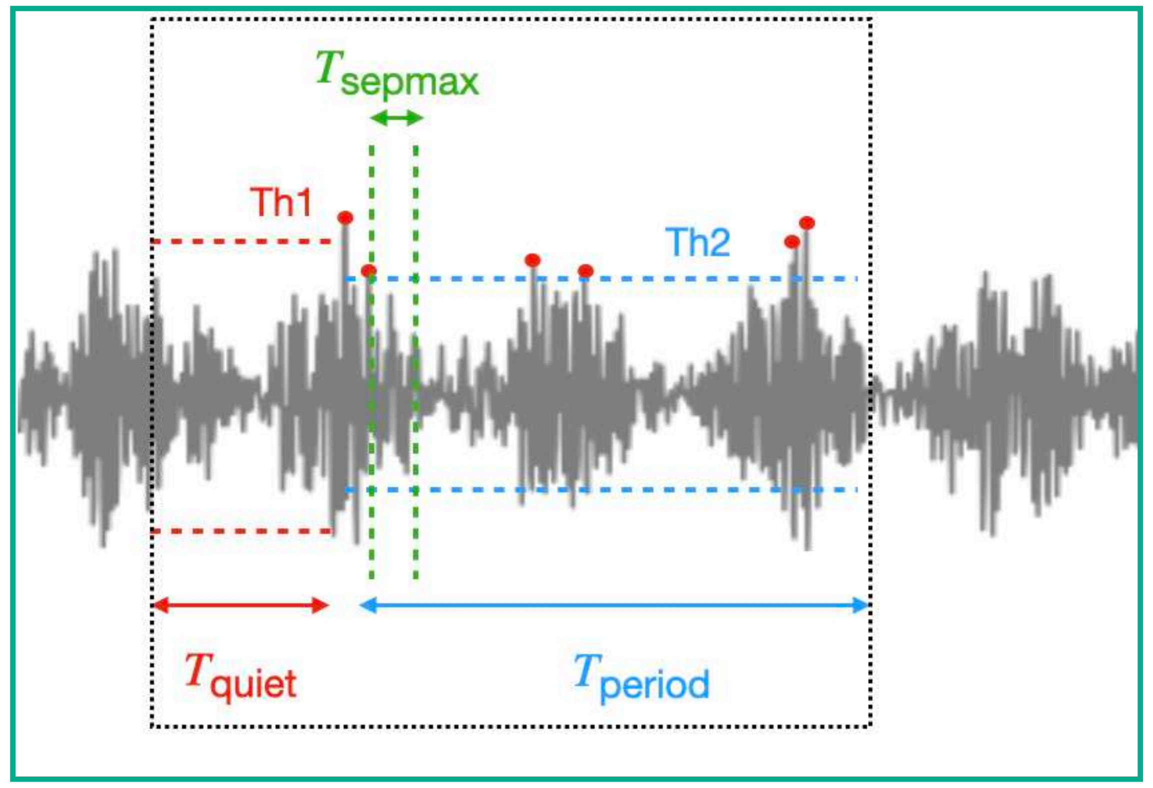

Reproduce First Level Trigger offline

Optimal (my work):
Th1 $\sim 5\sigma$
Th2 $\sim 4\sigma$
T_{sepmax} = 50 ns
NC between 2 and 7

On-site (before my analysis):
Th1 = 70 ADC ($\sim 6.5\sigma$)
Th2 = 35 ADC ($\sim 3\sigma$)
T_{sepmax} = 15 ns
NC between 2 and 7

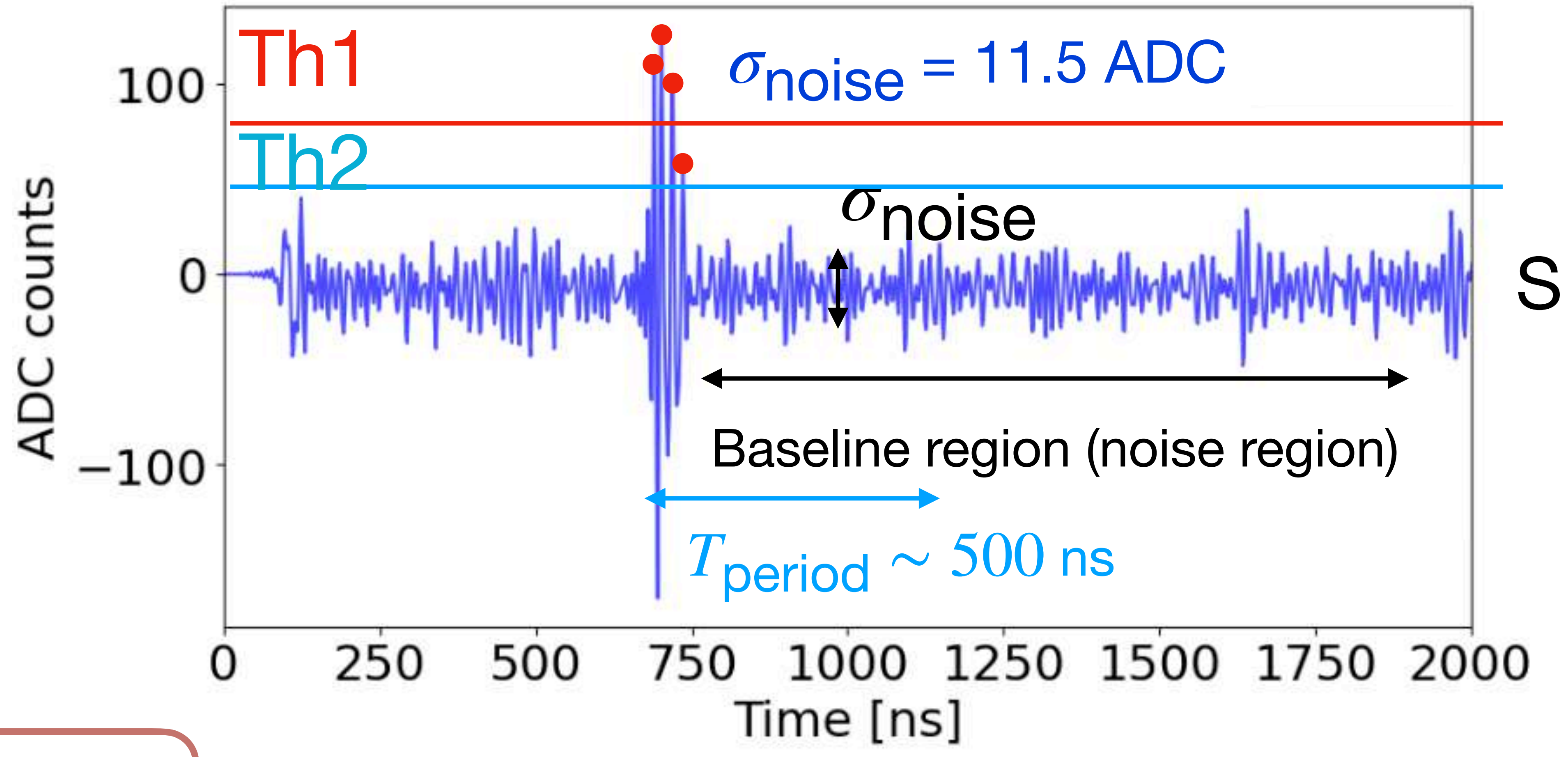

$$\text{SNR} = \frac{A_{\text{max}}}{\sigma_{\text{noise}}}$$

Th2: trade-off
Set high enough to suppress noise peaks in the baseline
Set low enough to detect the secondary pulse(s) within the main signal
Because NC min = 2 (avoid trigger on single sample)
Best practice: do not set absolute ADC value

Parameters optimization: efficiency

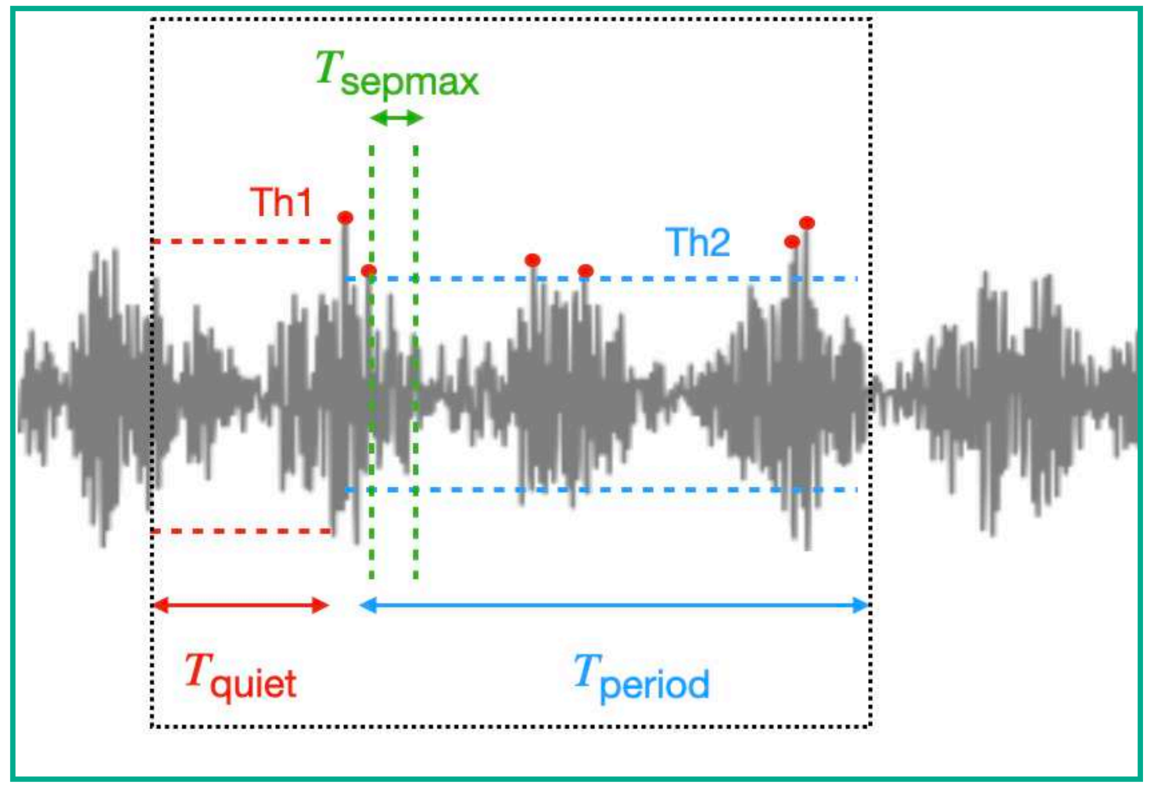

Reproduce First Level Trigger offline

Optimal (my work):
Th1 $\sim 5\sigma$
Th2 $\sim 4\sigma$
$T_{\textbf{sepmax}}$ **= 50 ns**
NC between 2 and 7

On-site (before my analysis):
Th1 = 70 ADC ($\sim 6.5\sigma$)
Th2 = 35 ADC ($\sim 3\sigma$)
T_{sepmax} = 15 ns
NC between 2 and 7

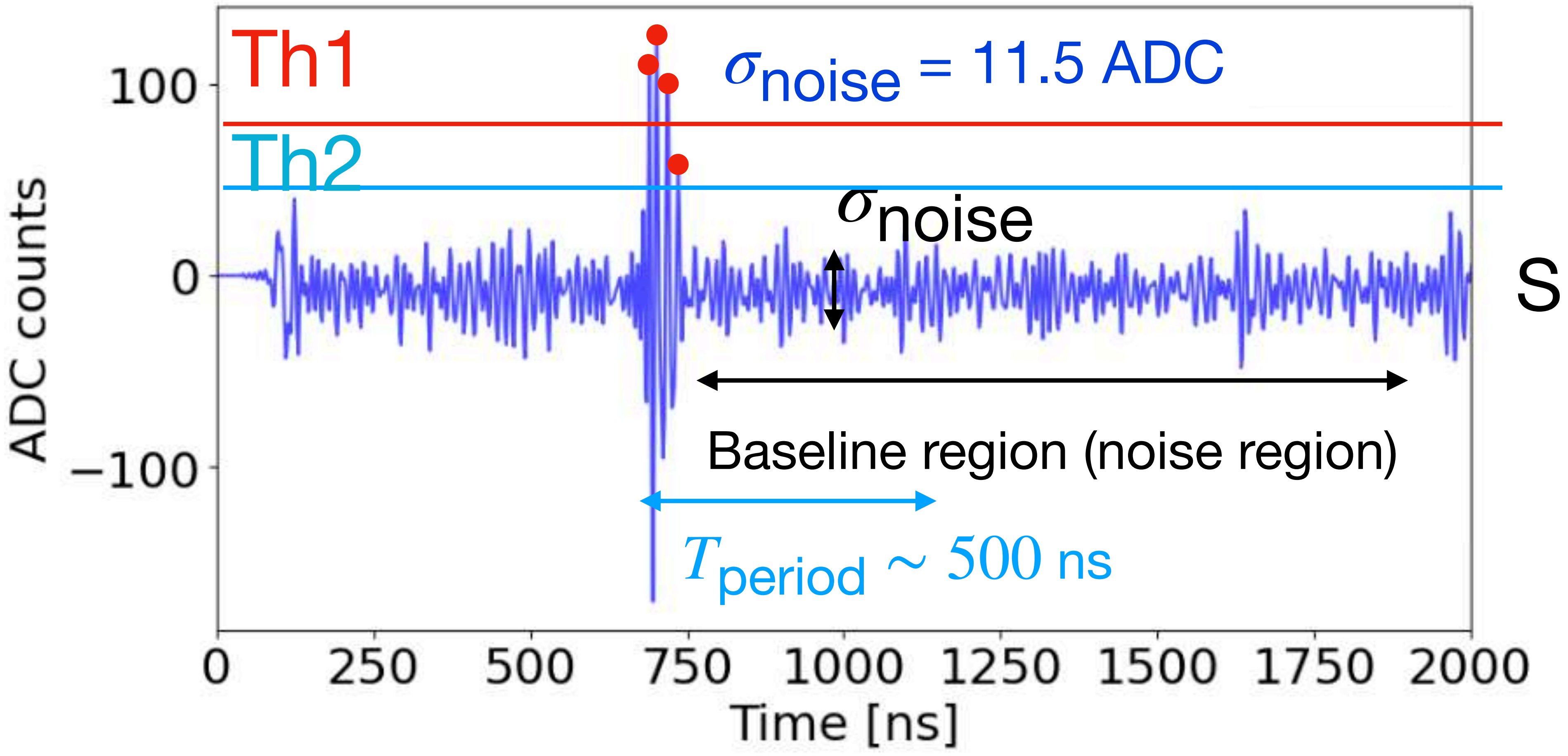

$$\text{SNR} = \frac{A_{\max}}{\sigma_{\text{noise}}}$$

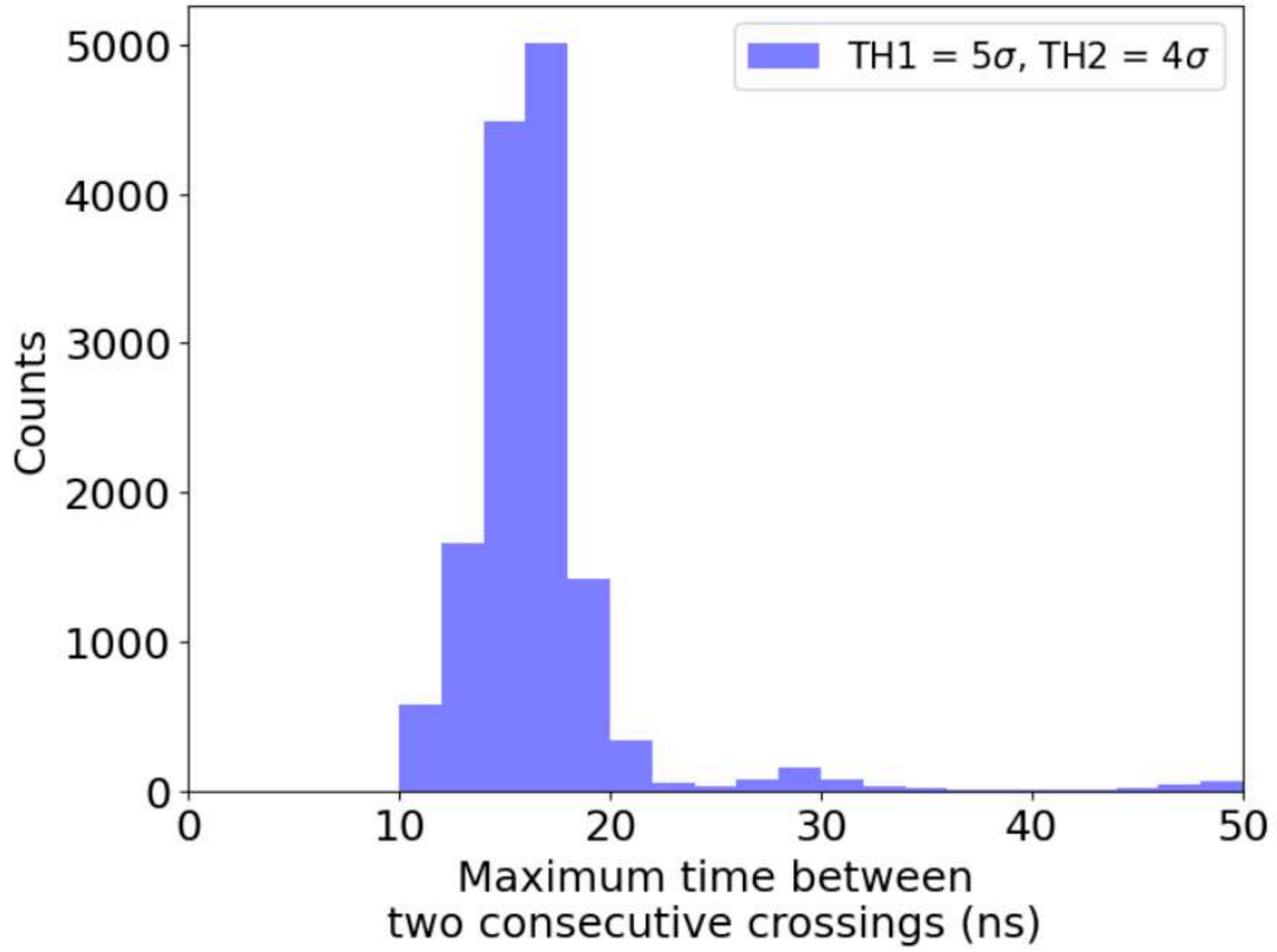

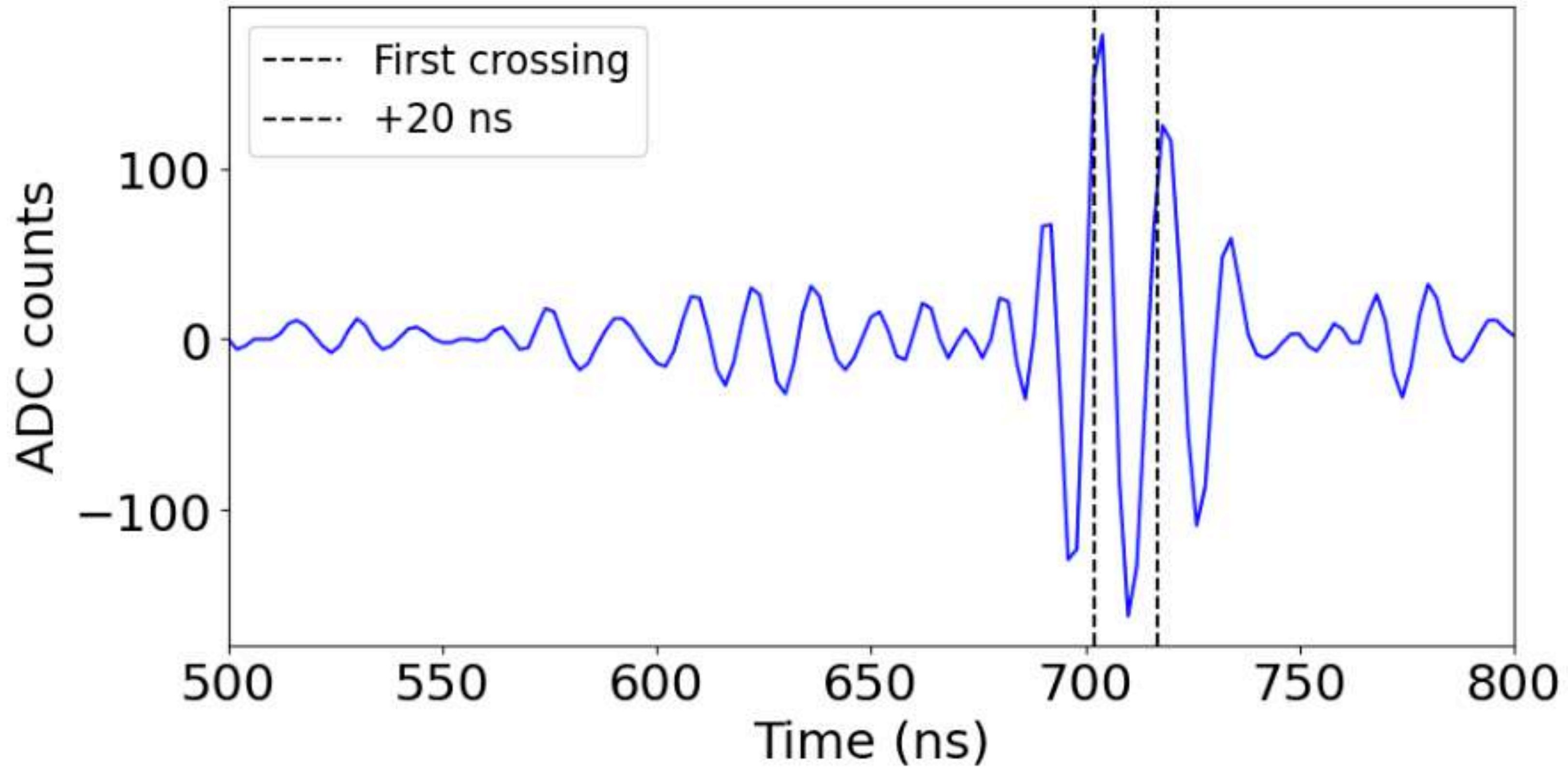

Best practice: $T_{\text{sepmax}} > 20$ ns !

Parameters optimization: efficiency

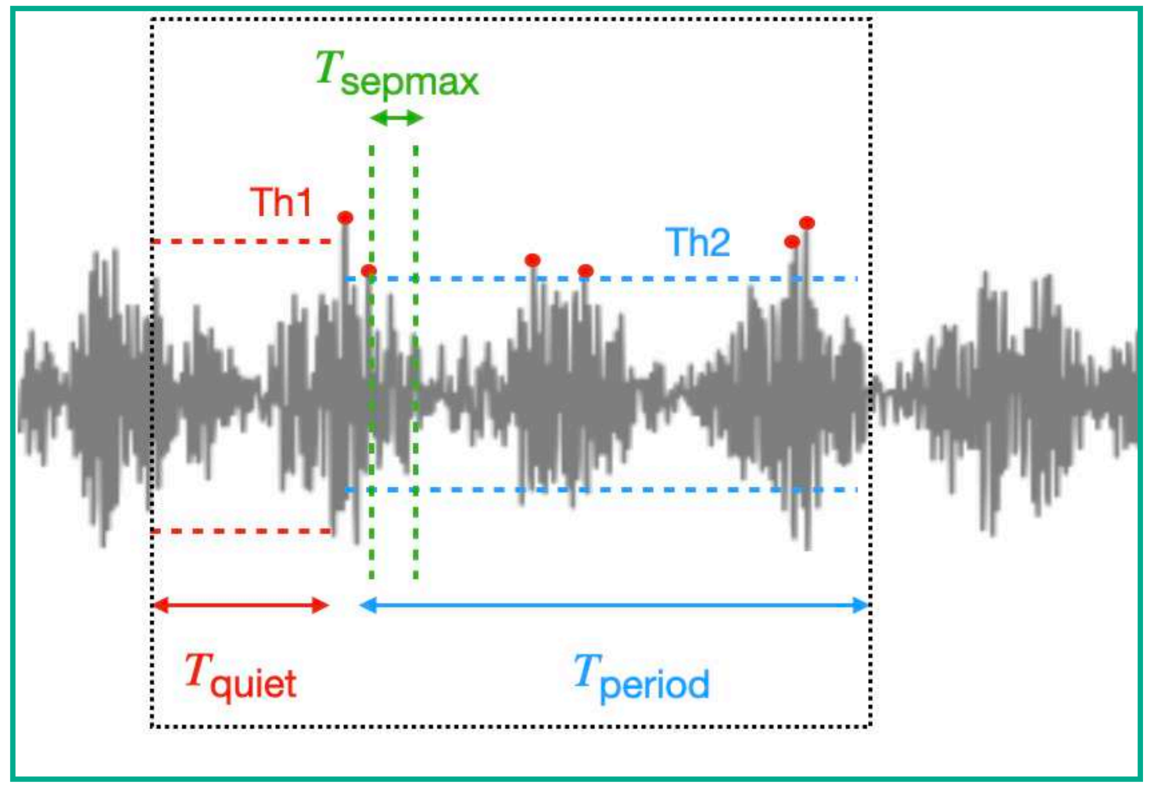

Reproduce First Level Trigger offline

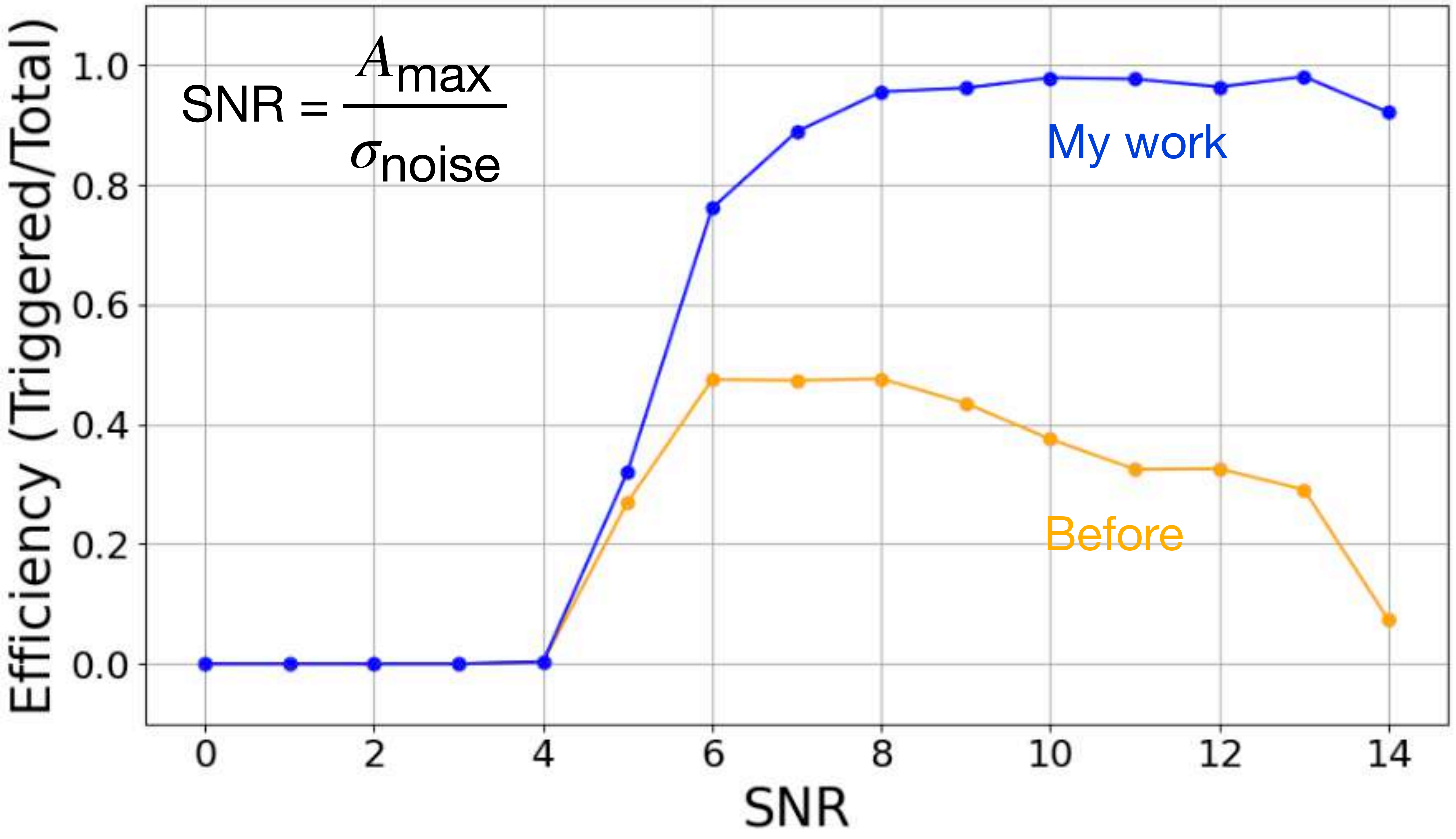

Optimal (my work):

Th1 $\sim 5\sigma$

Th2 $\sim 4\sigma$

T_{sepmax} = 50 ns

NC between 2 and 7

On-site (before my analysis):

Th1 = 70 ADC ($\sim 6.5\sigma$)

Th2 = 35 ADC ($\sim 3\sigma$)

T_{sepmax} = 15 ns

NC between 2 and 7

Parameters optimization: purity

On-site experimental noise (GRANDProto300)

Trigger rate with optimal parameters:
- Digital filtering: 73 Hz
- (Raw data: 516 Hz)

Optimal (my work):
Th1 $\sim 5\sigma$
Th2 $\sim 4\sigma$
T**sepmax = 50 ns**
NC between 2 and 7

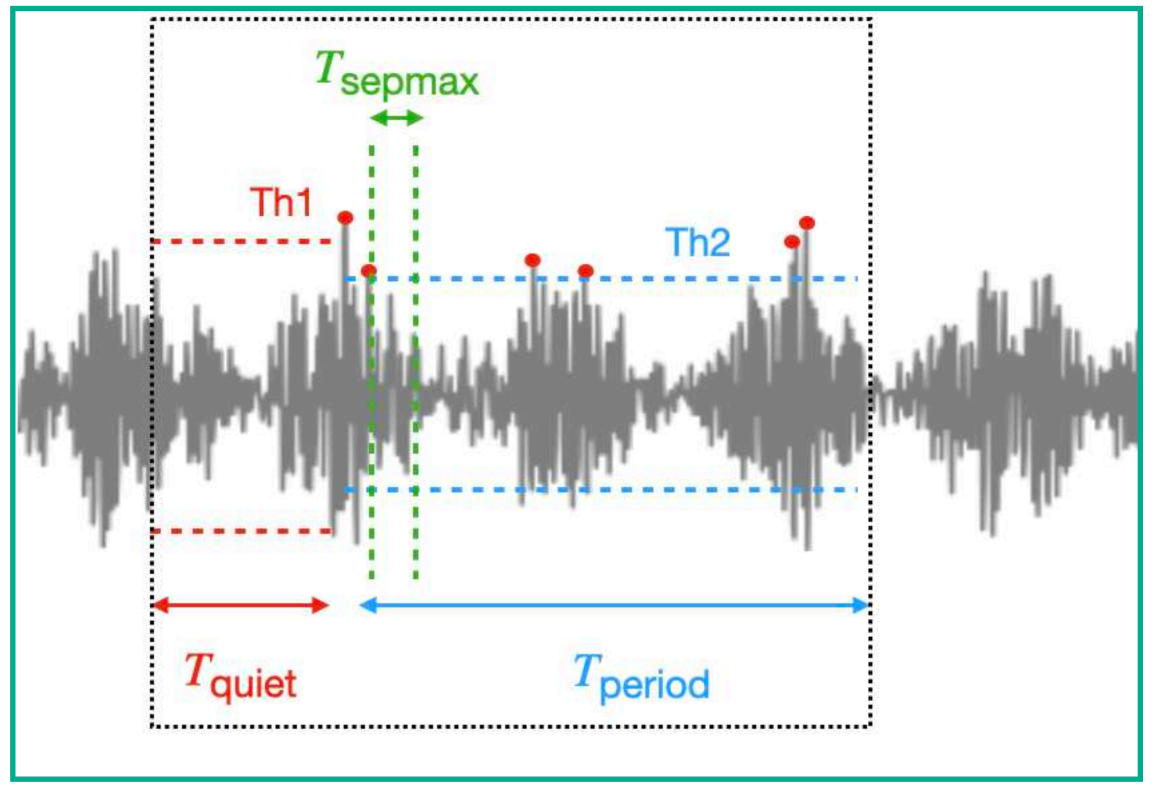

Parameters optimization: purity

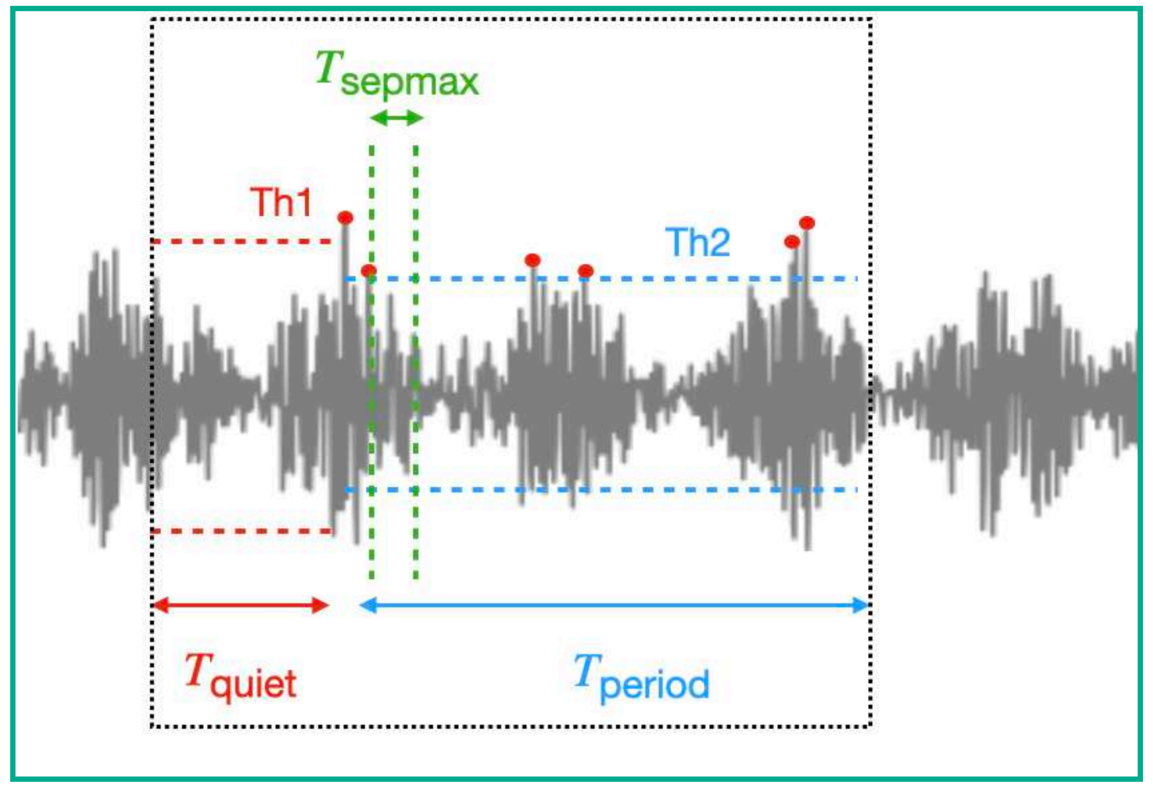

On-site experimental noise (GRANDProto300)

Trigger rate with optimal parameters:
- Digital filtering: 73 Hz
- Raw data: 516 Hz

Optimal (my work):
Th1 $\sim 5\sigma$
Th2 $\sim 4\sigma$
T**sepmax = 50 ns**
NC between 2 and 7

Triggered transient background event

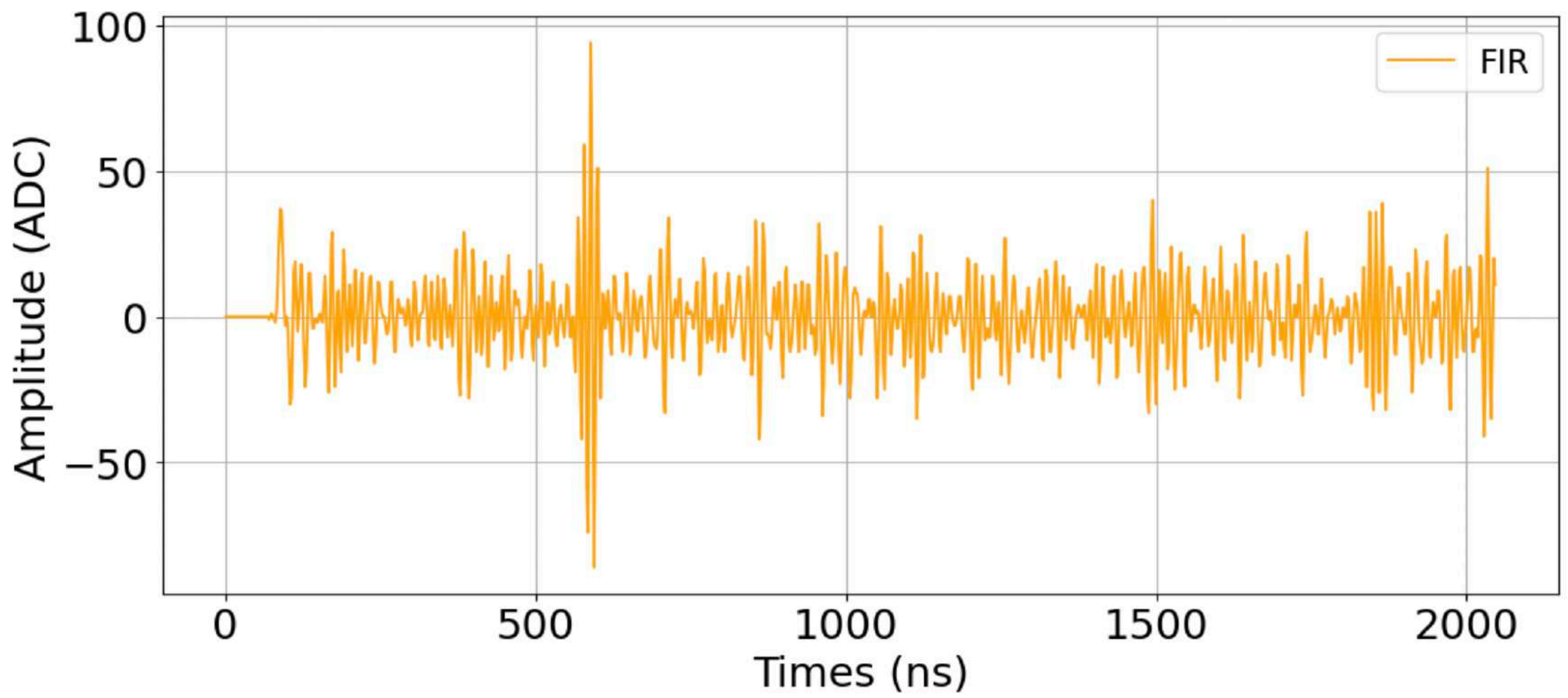

Parameters optimization: purity

On-site experimental noise (GRANDProto300)

Trigger rate with optimal parameters:
- Digital filtering: 73 Hz
- Raw data: 516 Hz

Optimal (my work):
Th1 $\sim 5\sigma$
Th2 $\sim 4\sigma$
$T_{\mathbf{sepmax}}$ **= 50 ns**
NC between 2 and 7

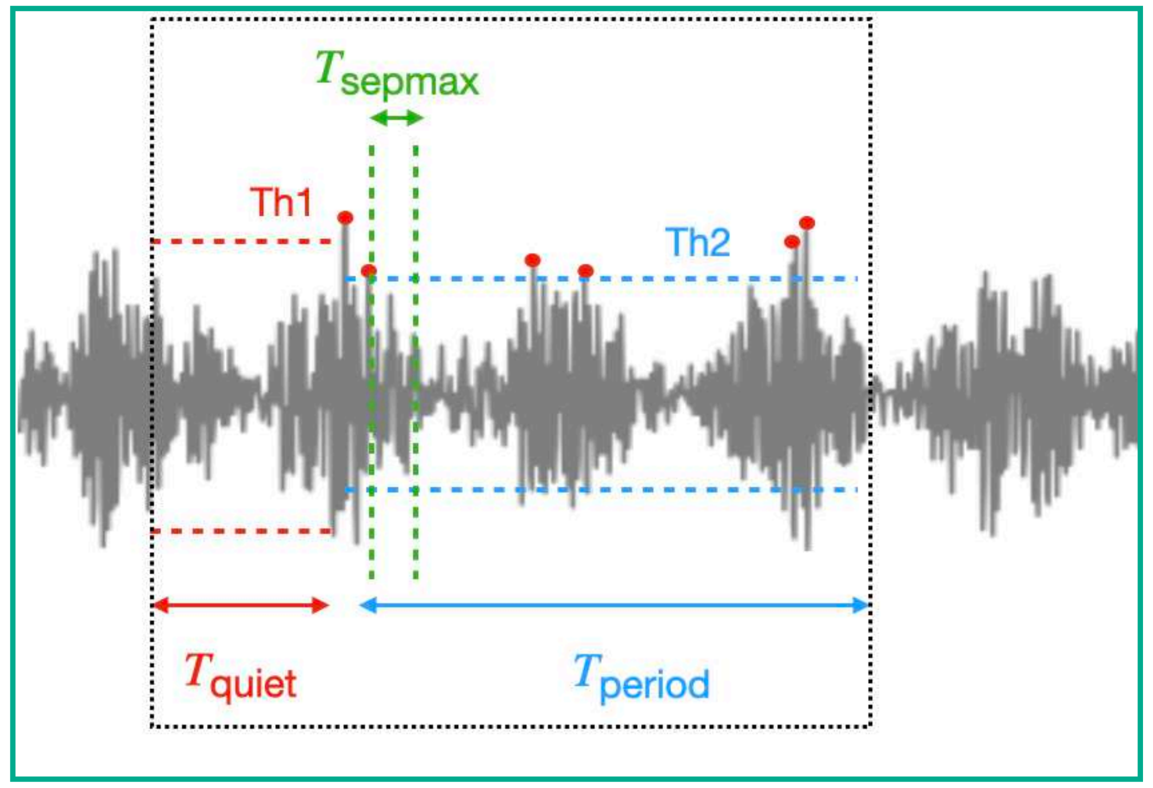

Triggered transient background event

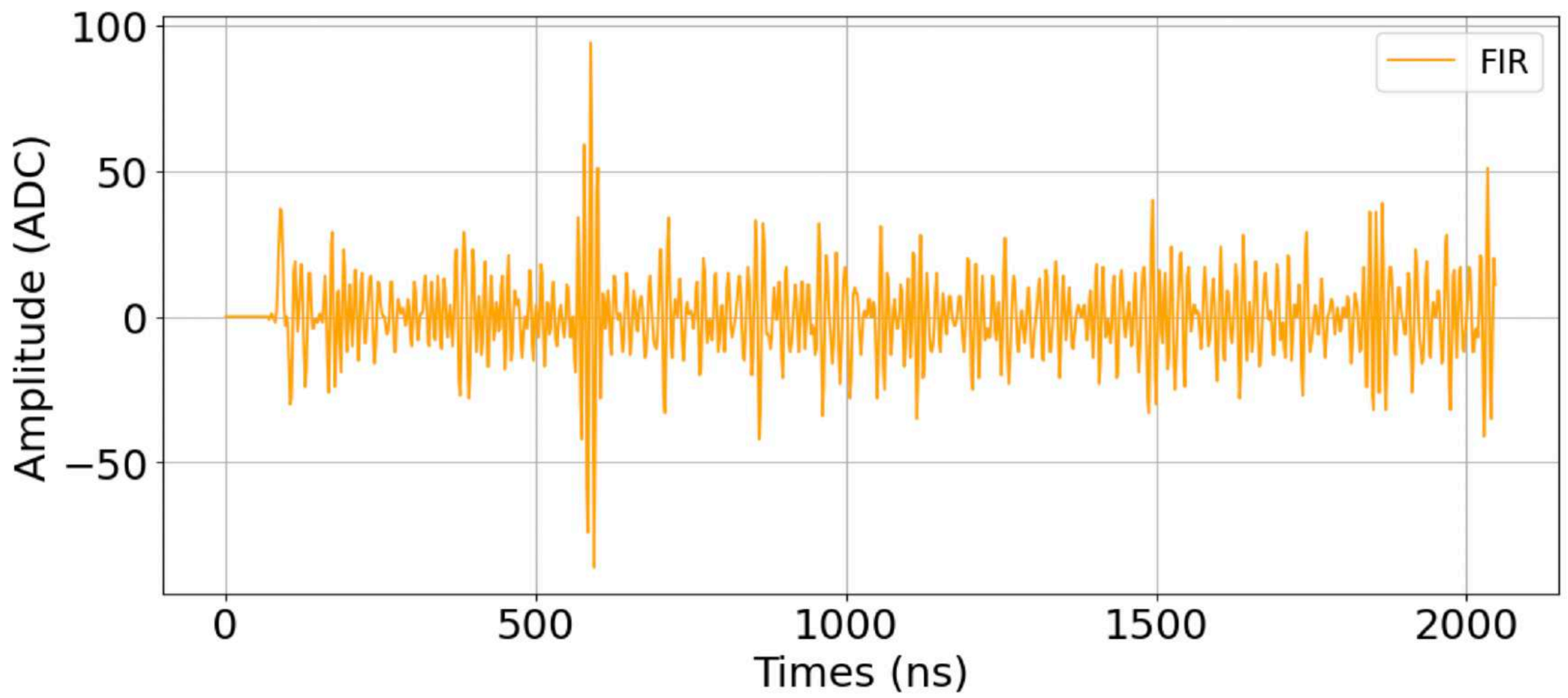

- **First systematic study** of First Level Trigger parameters
- Optimal parameters now **applied on site** (May 2025) and data ready for analysis
- Very positive effect of digital filtering on data rate

GRAND and the challenges of radio detection

I.Physical modeling of inclined air showers and their radio emission

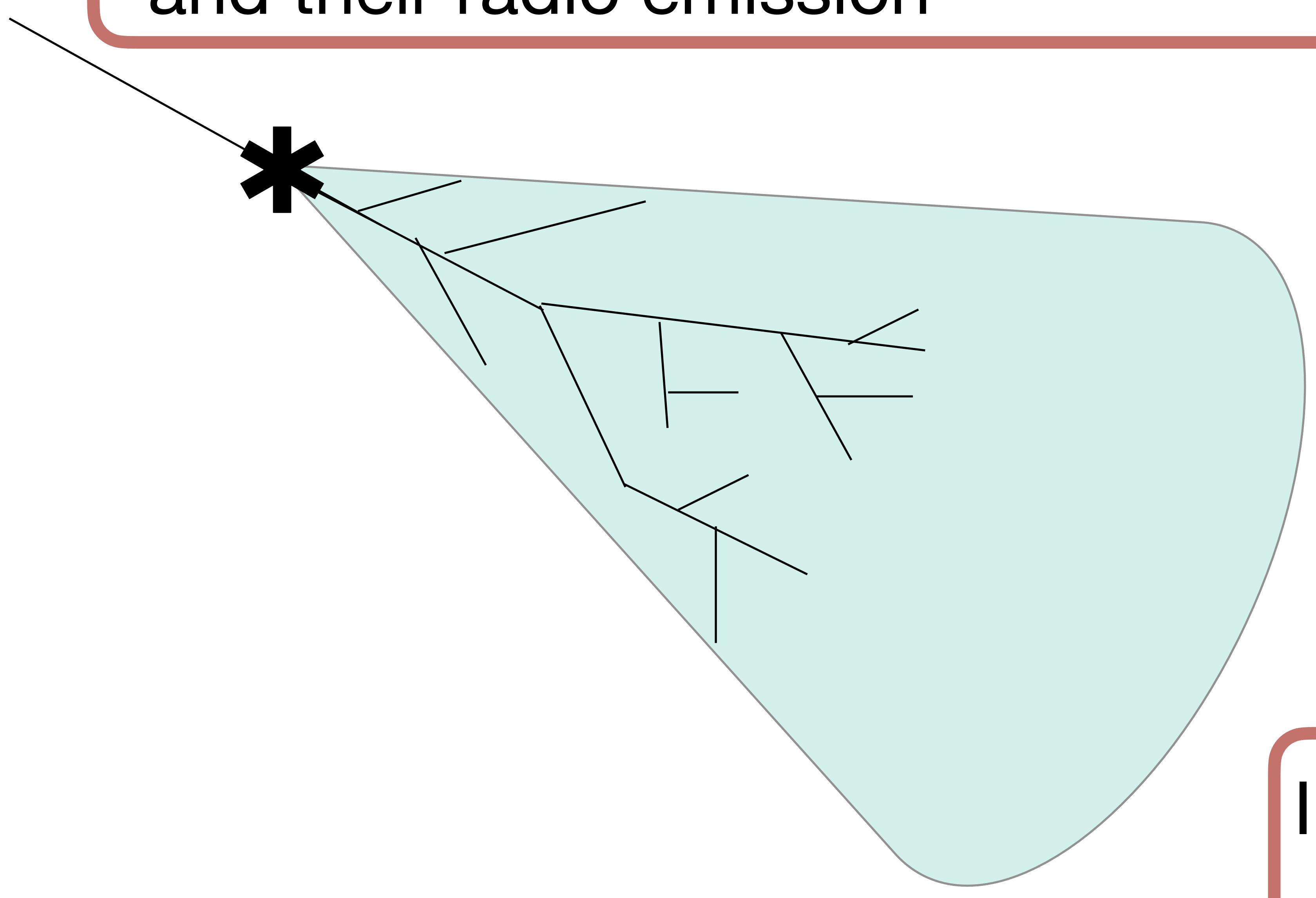

III. Reconstruction of cosmic particle properties for very inclined showers

II. Autonomous trigger: find the radio signal inside the noise

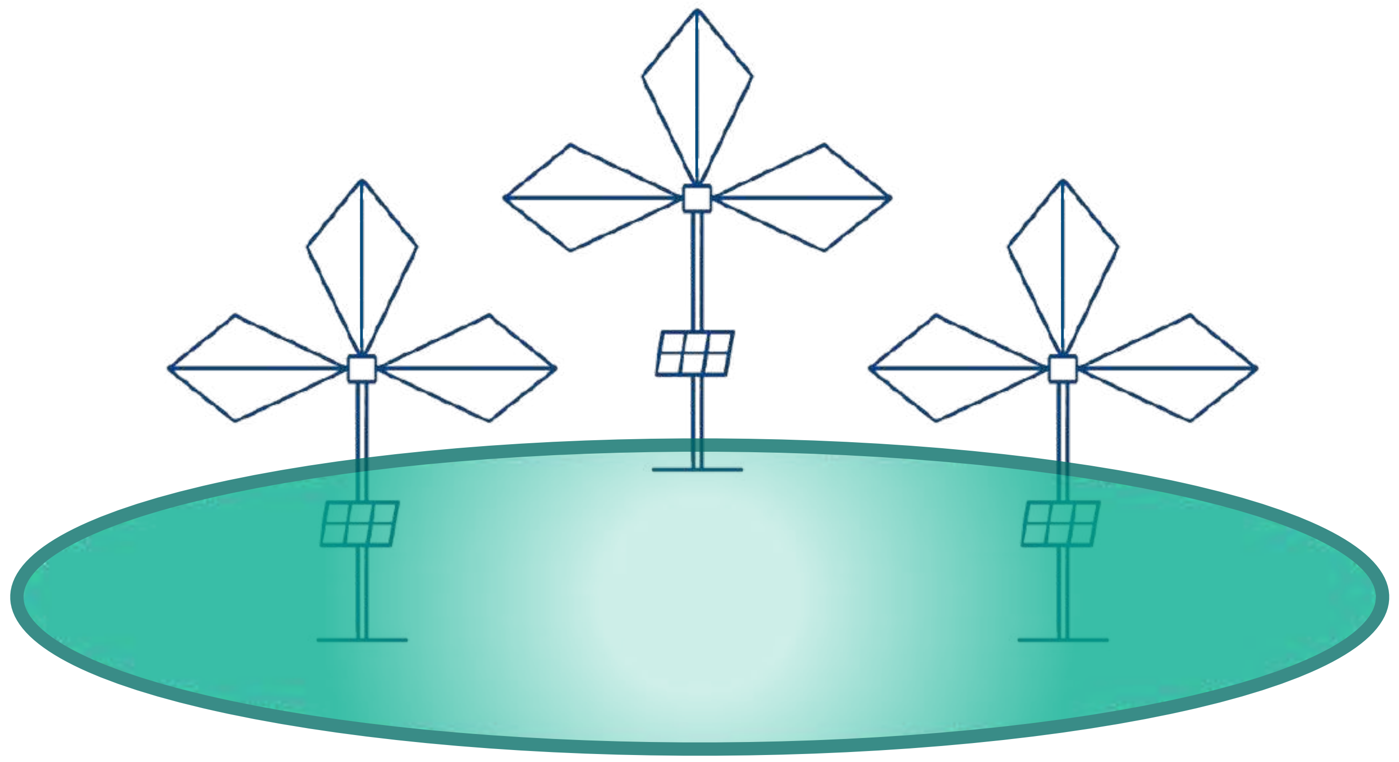

GRAND and the challenges of radio detection

III. Reconstruction of cosmic particles properties for very inclined directions

ADF model: validation and arrival direction reconstruction

Reconstruction of cosmic-ray properties (arrival direction)

Valentin Decoene Thesis, 2020

Hybrid model: timing t_i + **amplitude** A_i
at **electric field level** in 50-200 MHz frequency range

• **Radio emission point** X_{source}
Center of spherical fit using trigger times

V. Decoene et al. Astropart. Phys. (2021)

• Shower axis $\vec{k}(\theta, \phi)$ (intersects X_{source})
Analytical description of signal amplitude in radio footprint with Angular Distribution Function (ADF)

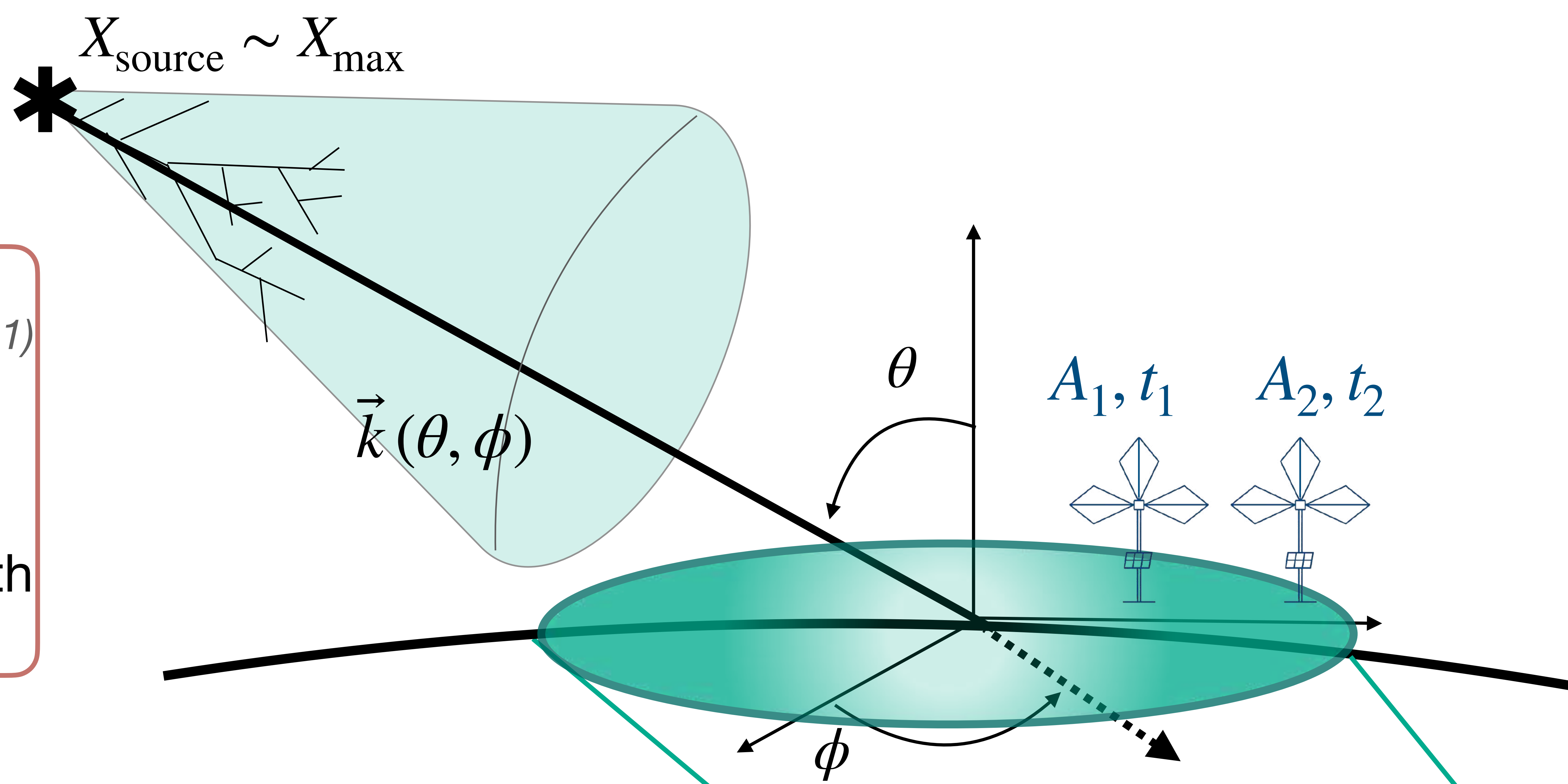

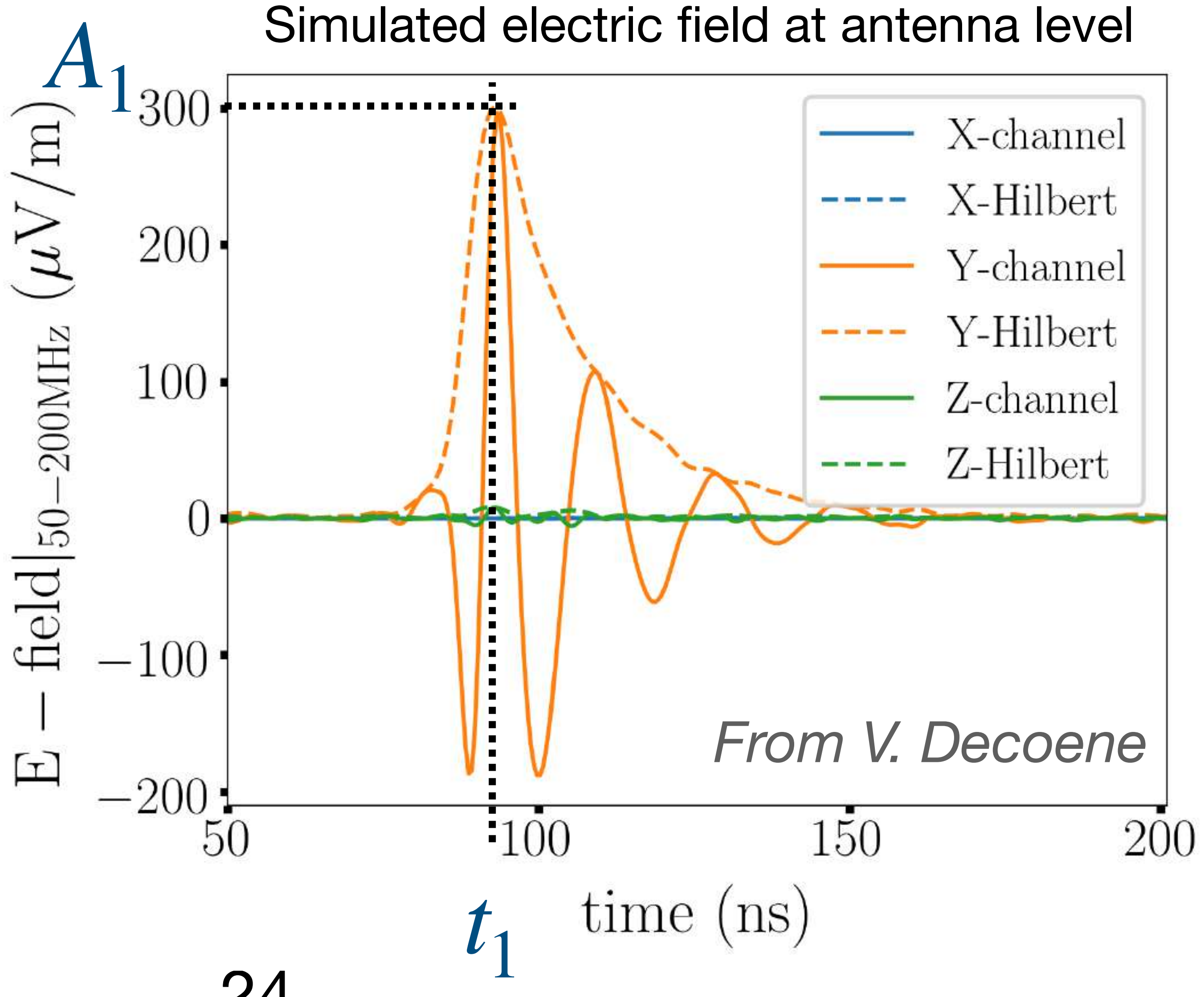

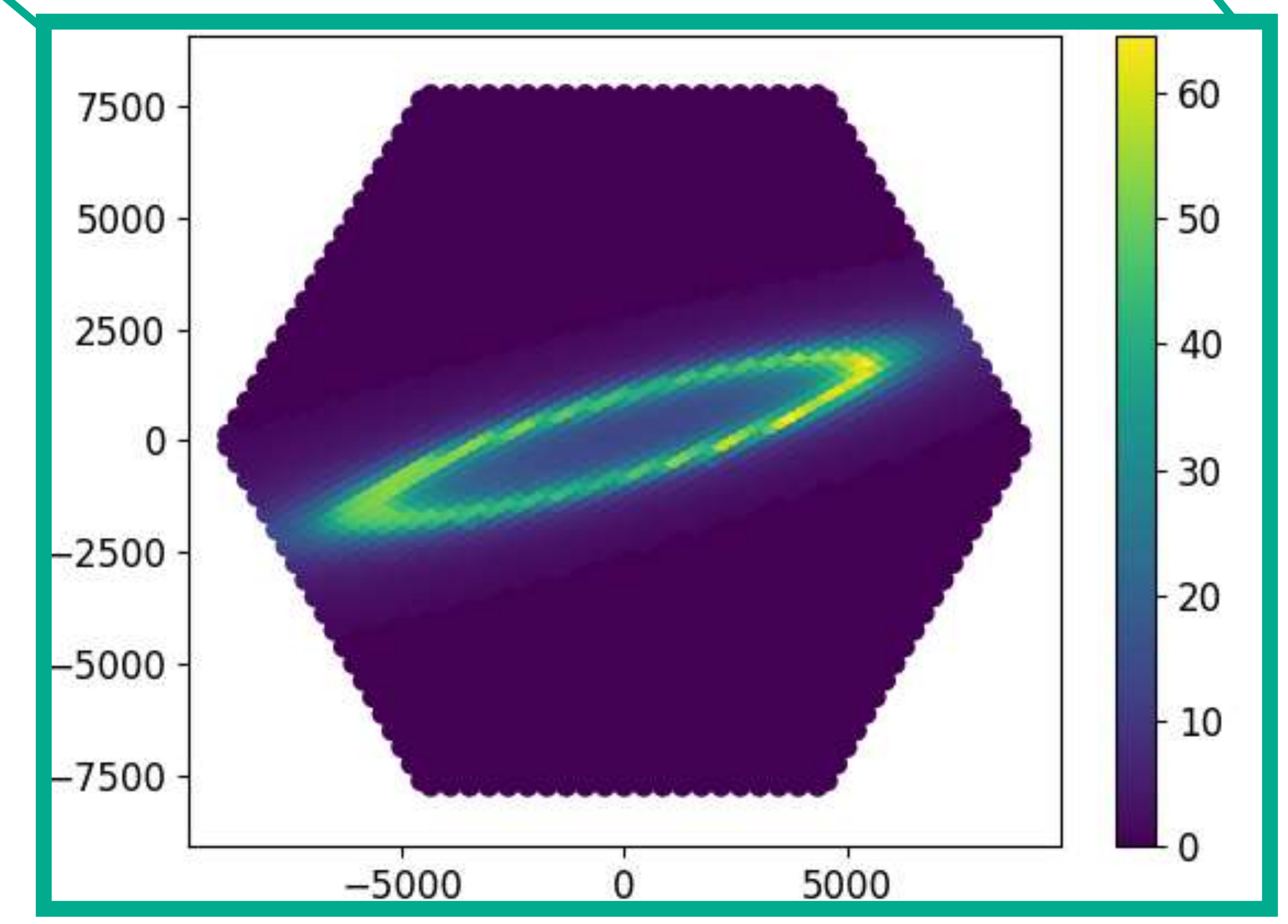

From A. Benoît-Lévy

Reconstruction of cosmic-ray properties (arrival direction)

Valentin Decoene Thesis, 2020

Hybrid model: **timing** t_i + **amplitude** A_i
at **electric field level** in 50-200 MHz frequency range

- **Radio emission point** X_{source}
Center of spherical fit using trigger times

V. Decoene et al. Astropart. Phys. (2021)

- Shower axis $\vec{k}(\theta, \phi)$ (intersects X_{source})
Analytical description of signal amplitude in radio footprint with Angular Distribution Function (ADF)

$$f^{\text{ADF}}(\omega, \eta, \alpha, l; \delta\omega, A) = \frac{A}{l} f^{GeoM}(\alpha, \eta, B) f^{\text{Cherenkov}}(\omega, \delta\omega)$$

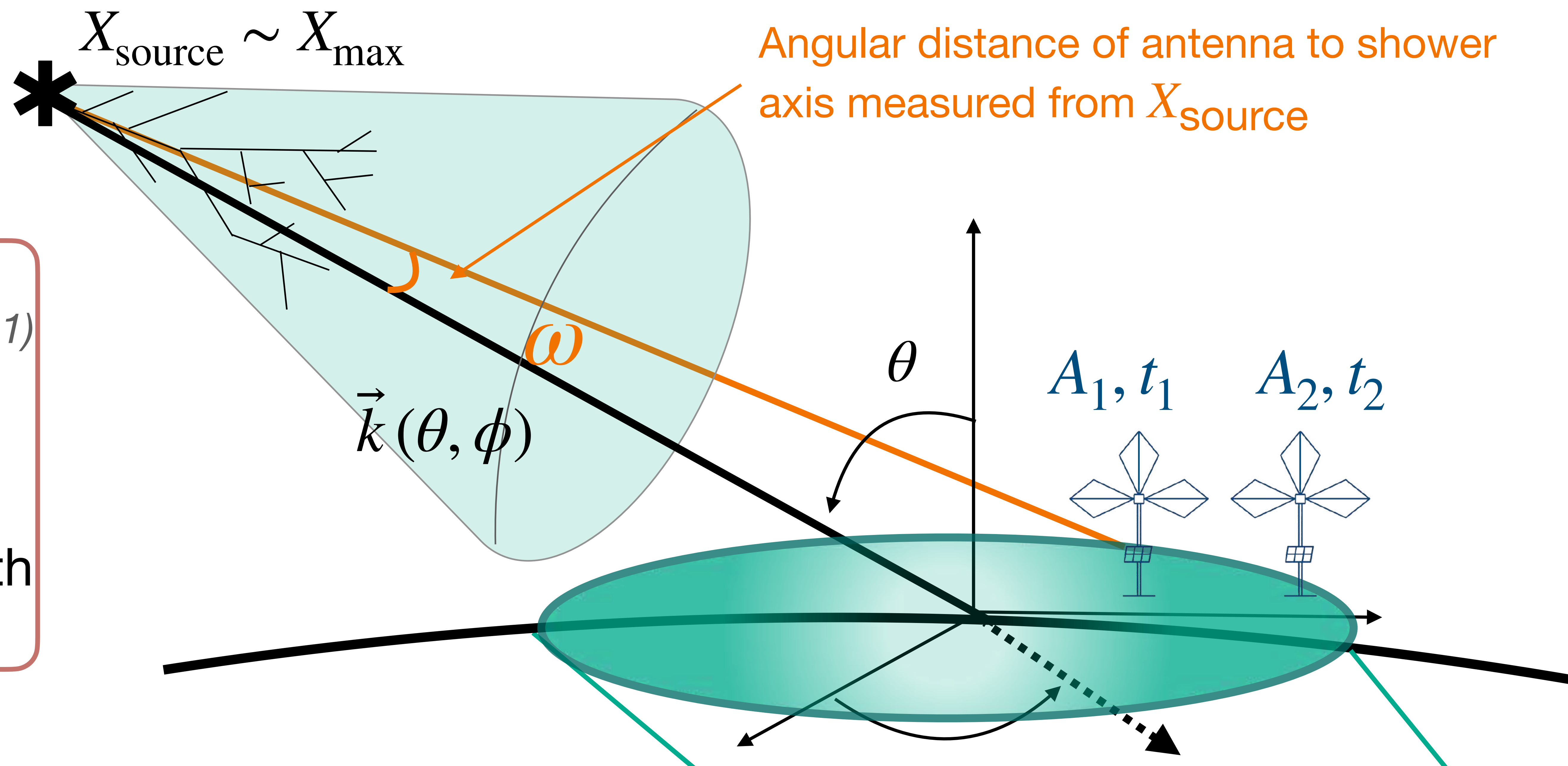

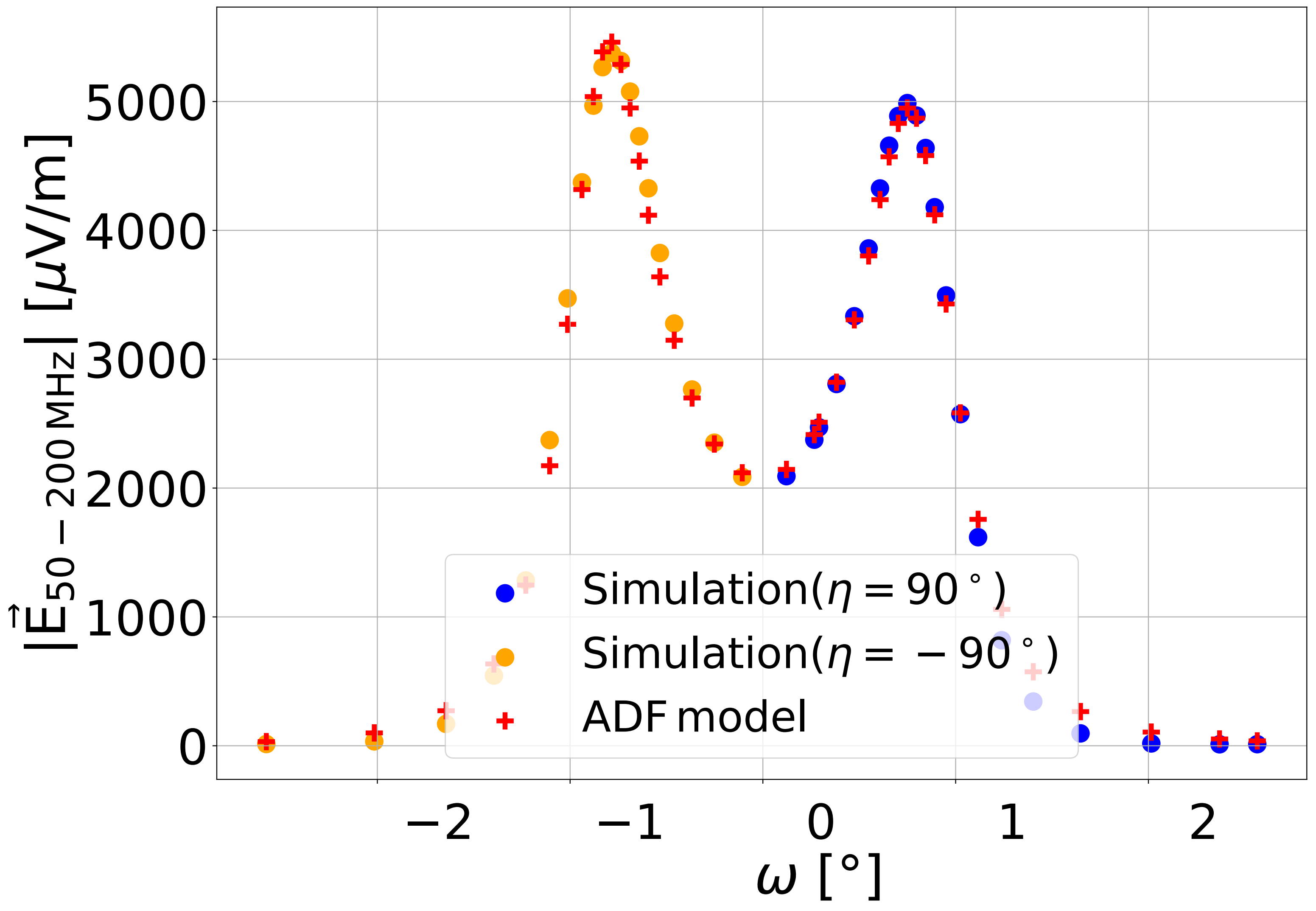

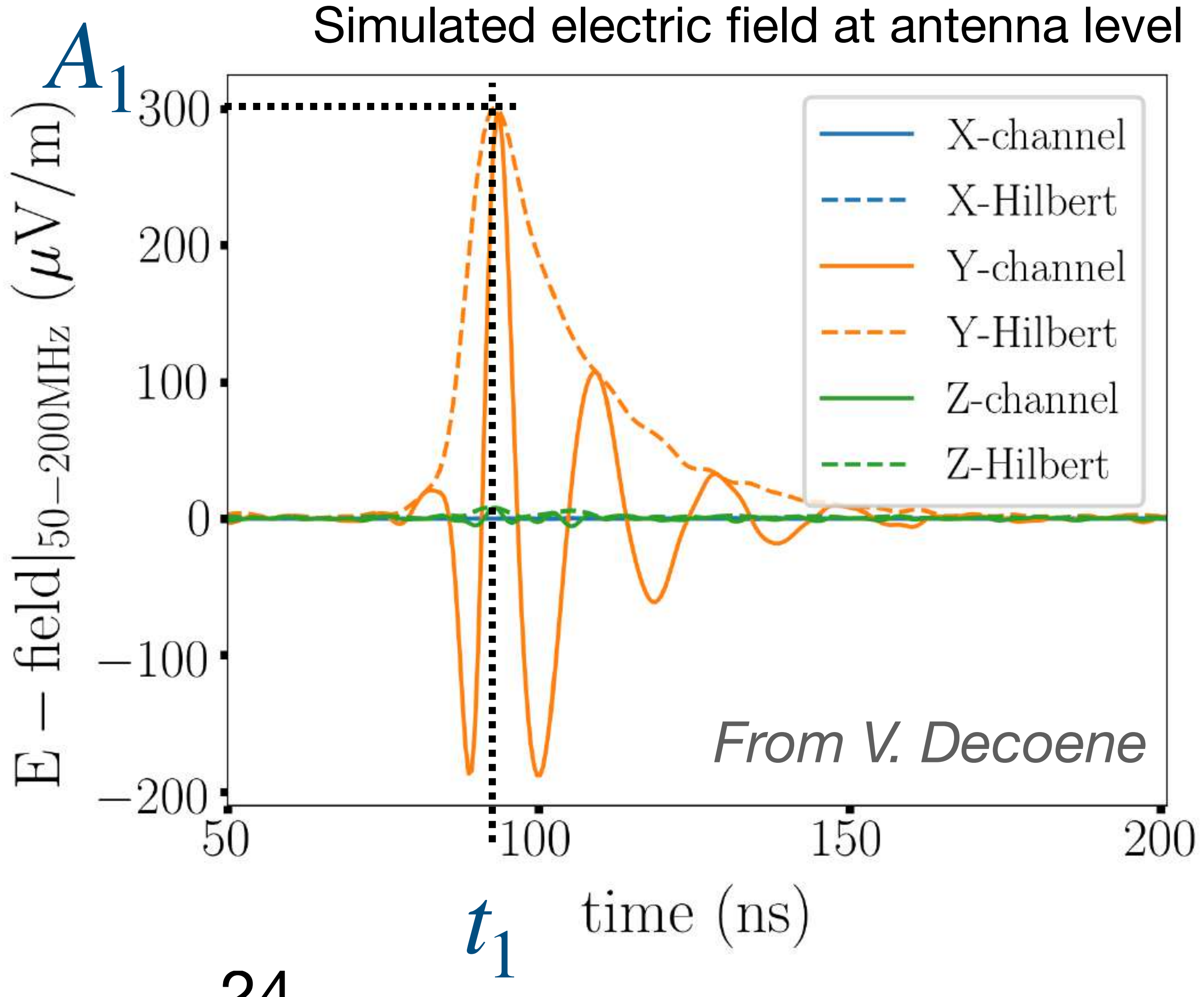

Cosmic-ray footprint simulation ($\theta = 80°$)

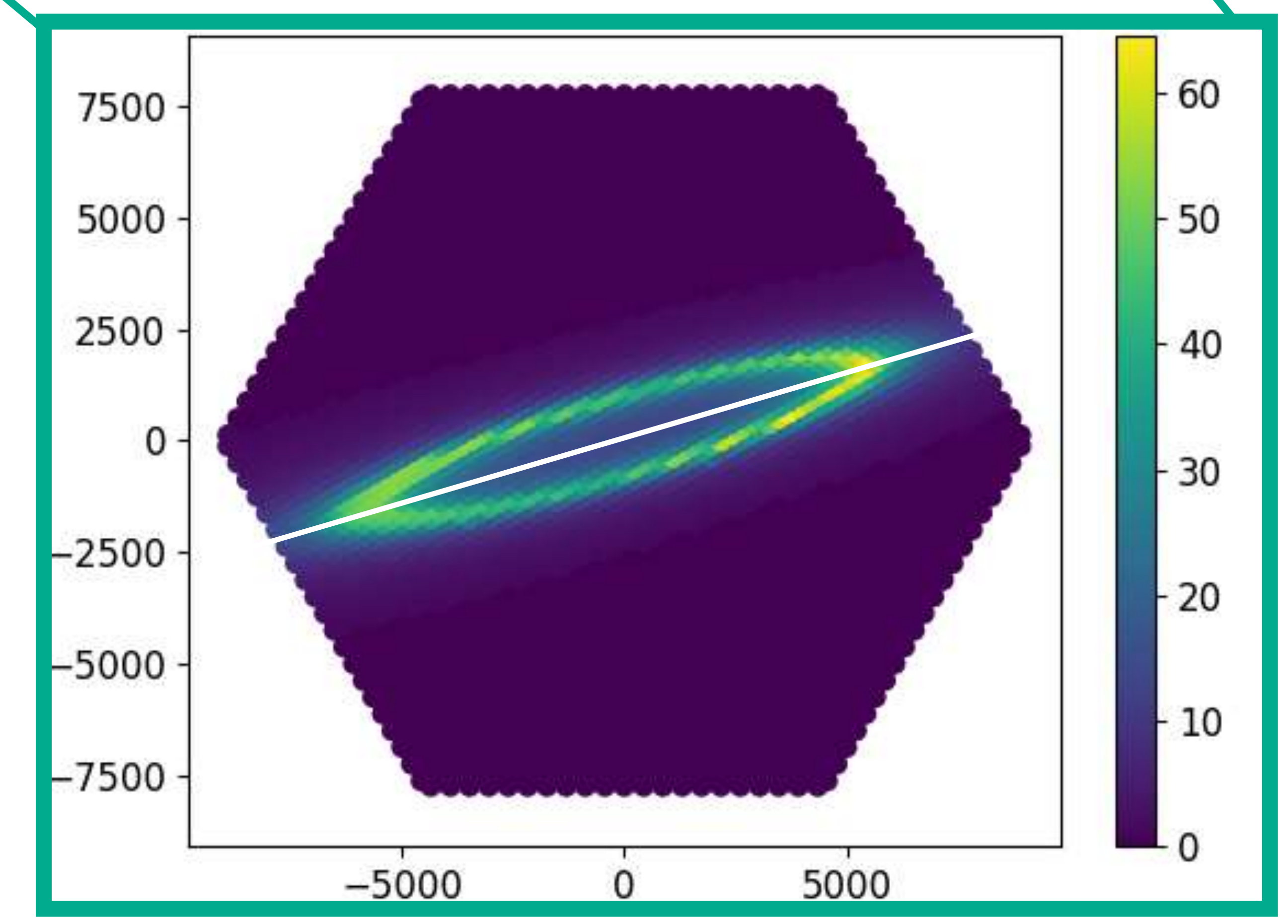

From A. Benoît-Lévy

Insight the ADF model

$$f^{\mathrm{ADF}}(\omega,\eta,\alpha,l;\delta\omega,A)=\frac{A}{l}f^{GeoM}(\alpha,\eta,B)f^{\mathrm{Cherenkov}}(\omega,\delta\omega)$$

Cherenkov pattern: shape of radio footprint (Lorentzian)

$$f^{\mathrm{Cerenkov}}(\omega,\delta\omega)=\frac{1}{1+4\left(\frac{(\tan(\omega)/\tan(\omega_c))^2-1}{\delta\omega}\right)^2}$$

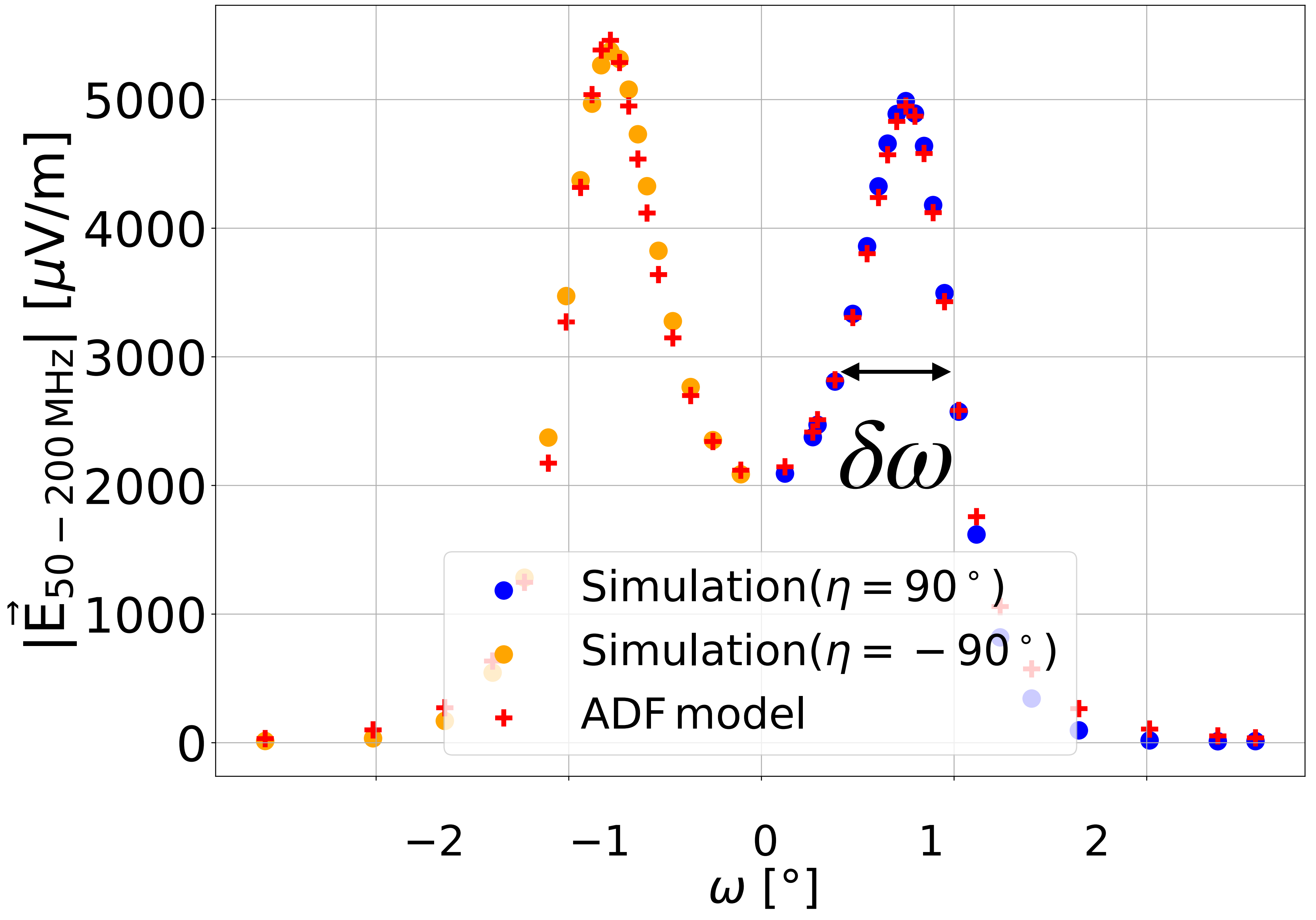

A/l: **Early-late asymmetry**: dilution effect

Insight the ADF model

$$f^{\text{ADF}}(\omega, \eta, \alpha, l; \delta\omega, A) = \frac{A}{l} f^{GeoM}(\alpha, \eta, B) f^{\text{Cherenkov}}(\omega, \delta\omega)$$

Cherenkov pattern: shape of radio footprint (Lorentzian)

$$f^{\text{Cerenkov}}(\omega, \delta\omega) = \frac{1}{1 + 4\left(\frac{(\tan(\omega)/\tan(\omega_c))^2 - 1}{\delta\omega}\right)^2}$$

ω_c
- described with dedicated model
- Not a free parameter

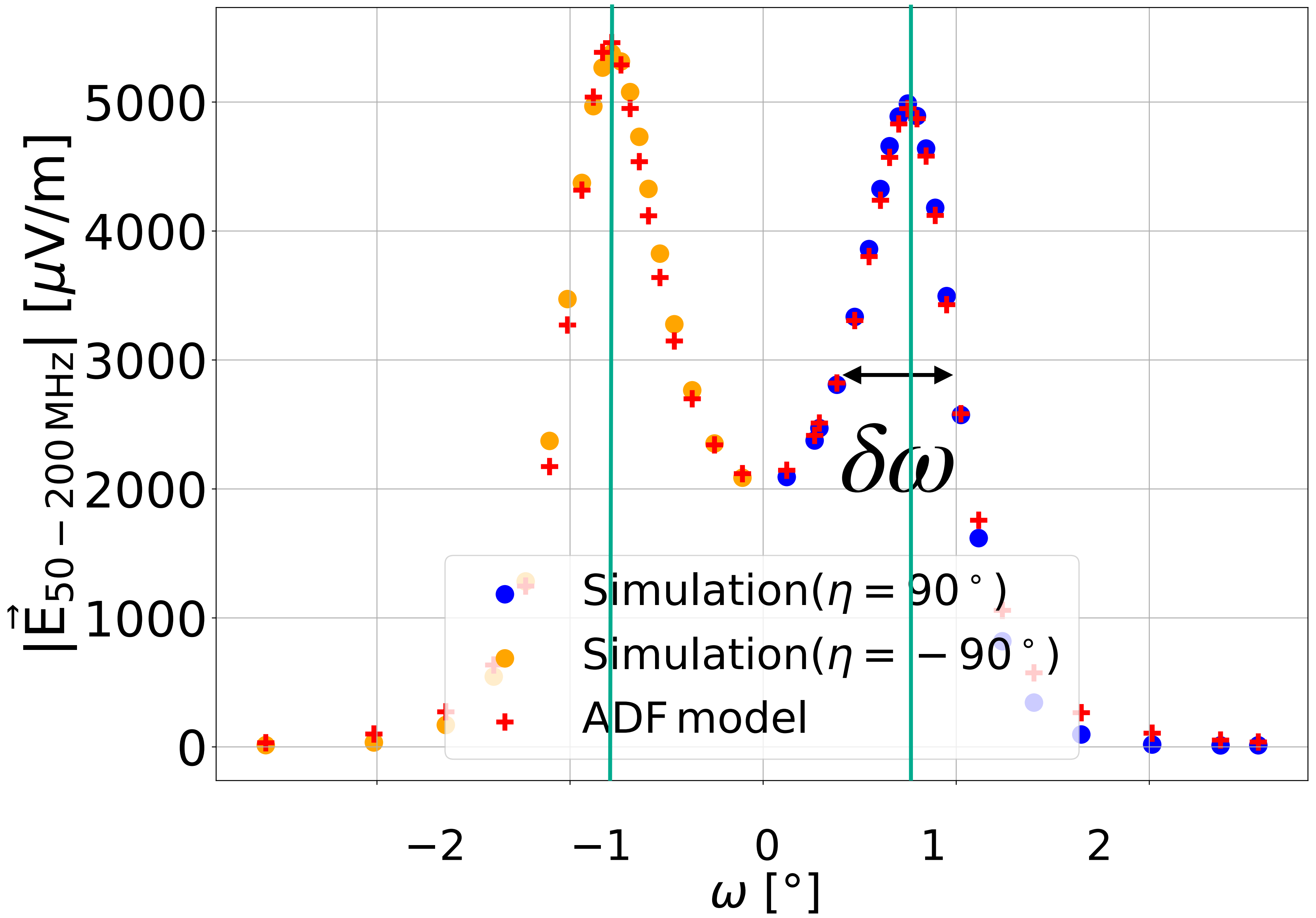

Cherenkov angle ω_c

Insight the ADF model

$$f^{\text{ADF}}(\omega, \eta, \alpha, l; \delta\omega, A) = \frac{A}{l} f^{GeoM}(\alpha, \eta, B) f^{\text{Cherenkov}}(\omega, \delta\omega)$$

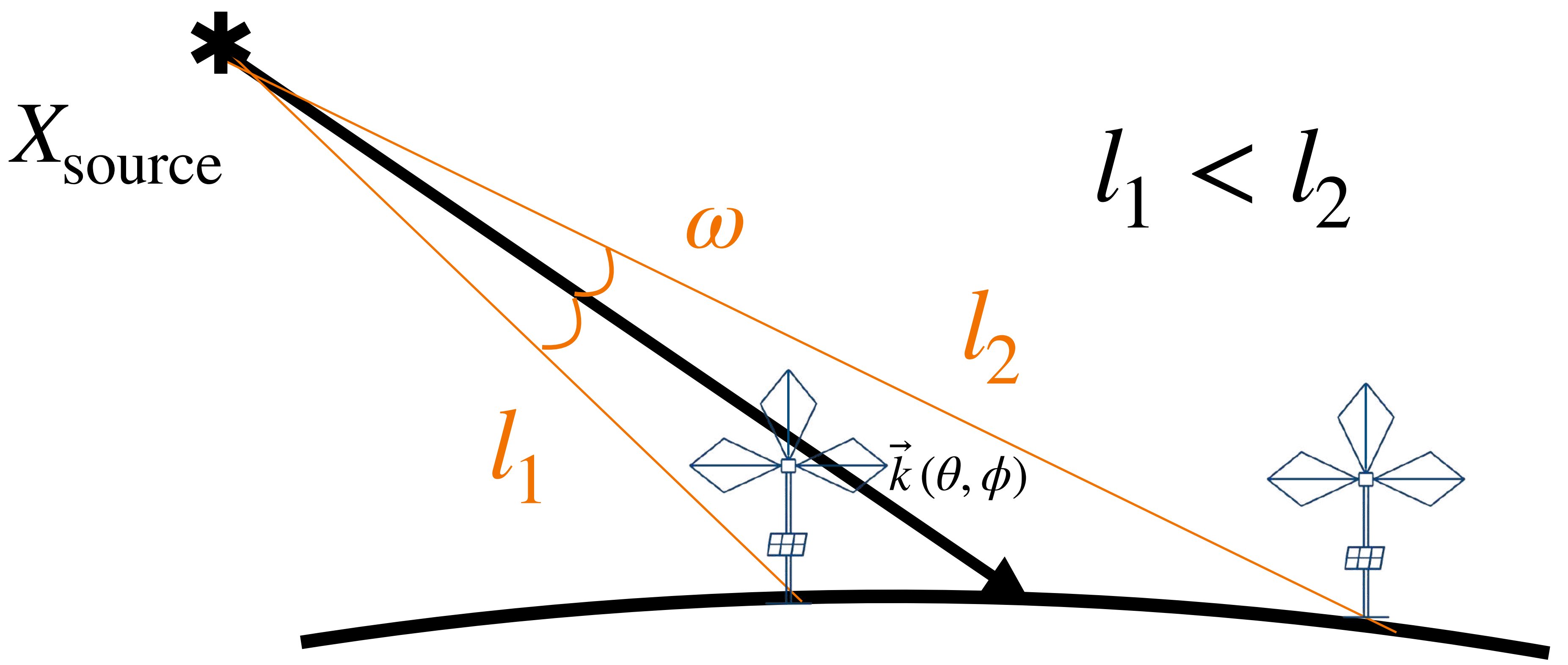

Cherenkov pattern: shape of there radio footprint (Lorentzian)

$$f^{\text{Cerenkov}}(\omega, \delta\omega) = \frac{1}{1 + 4\left(\frac{(\tan(\omega)/\tan(\omega_c))^2 - 1}{\delta\omega}\right)^2}$$

ω_c
- described with dedicated model
- Not a free parameter

l: **Early-late asymmetry**: dilution effect

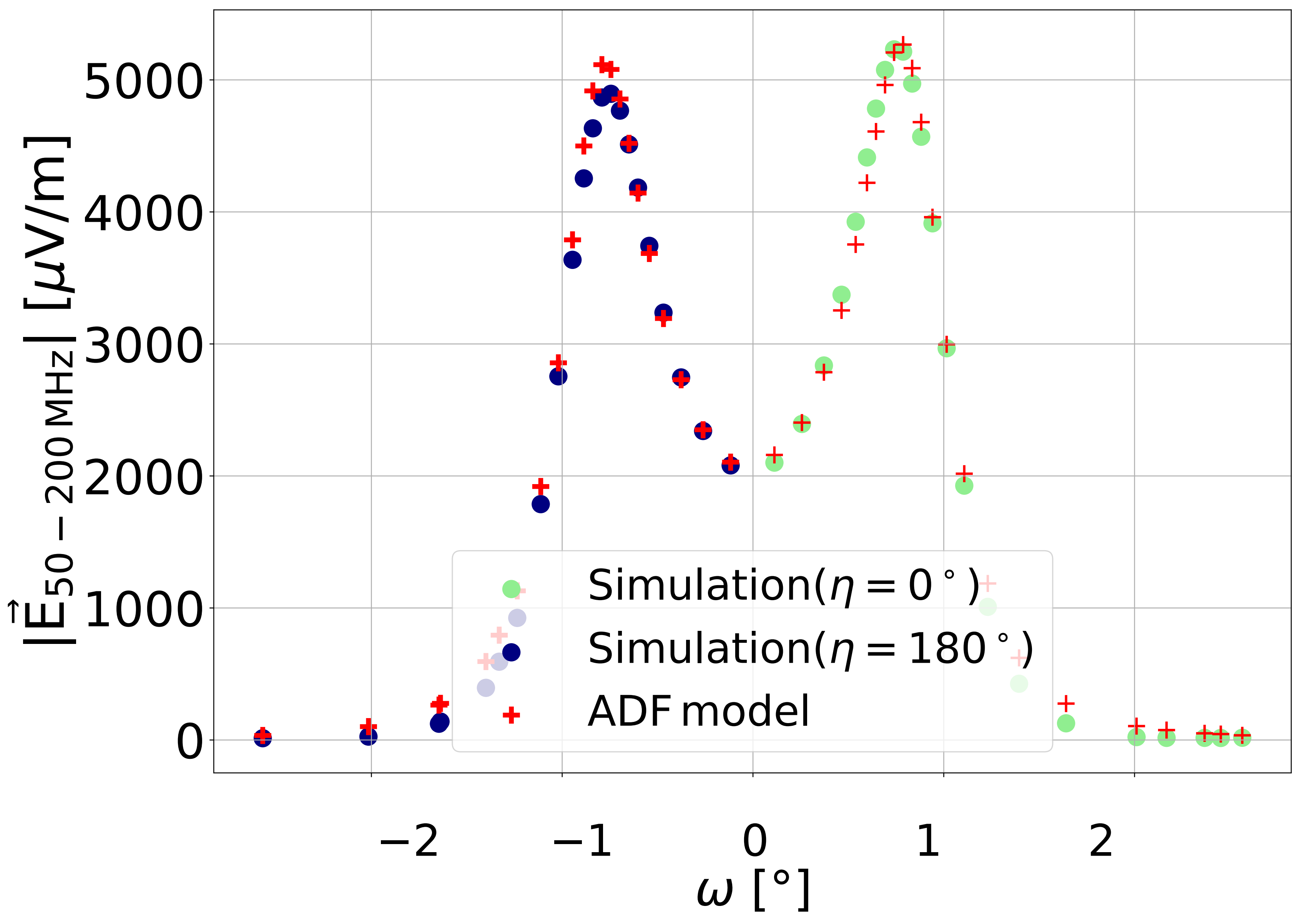

Insight the ADF model

$$f^{\mathrm{ADF}}(\omega, \eta, \alpha, l; \delta\omega, A) = \frac{A}{l} f^{GeoM}(\alpha, \eta, B) f^{\mathrm{Cherenkov}}(\omega, \delta\omega)$$

Cherenkov pattern: shape of there radio footprint (Lorentzian)

$$f^{\mathrm{Cerenkov}}(\omega, \delta\omega) = \frac{1}{1 + 4\left(\frac{(\tan(\omega)/\tan(\omega_c))^2 - 1}{\delta\omega}\right)^2}$$

ω_c
- described with dedicated model
- Not a free parameter

l: **Early-late asymmetry**: dilution effect

Geomagnetic asymmetry: interplay between geomagnetic effect and Askaryan effect (main emission mechanisms)

$$f^{\mathrm{Geom}}(\alpha, \eta, B) = 1 + G_A \frac{\cos(\eta)}{sin(\alpha)}$$

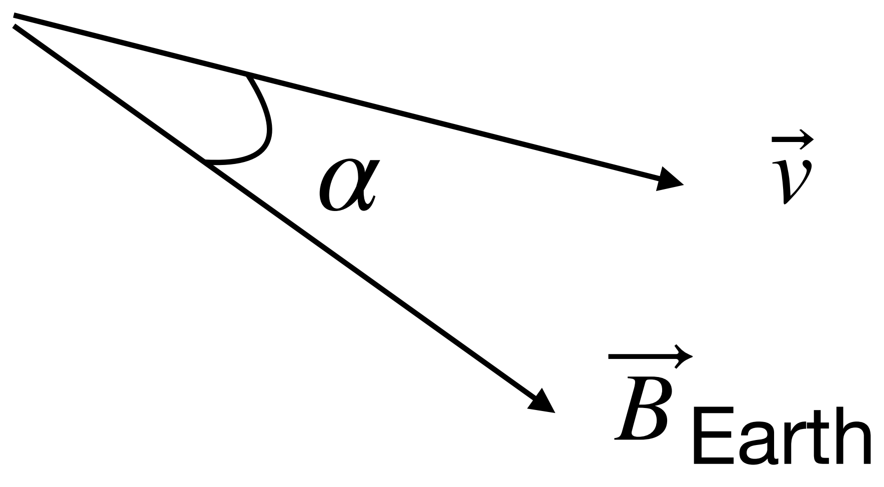

- α: geomagnetic angle
- G_A: geomagnetic strength

Geomagnetic emission | Askaryan emission

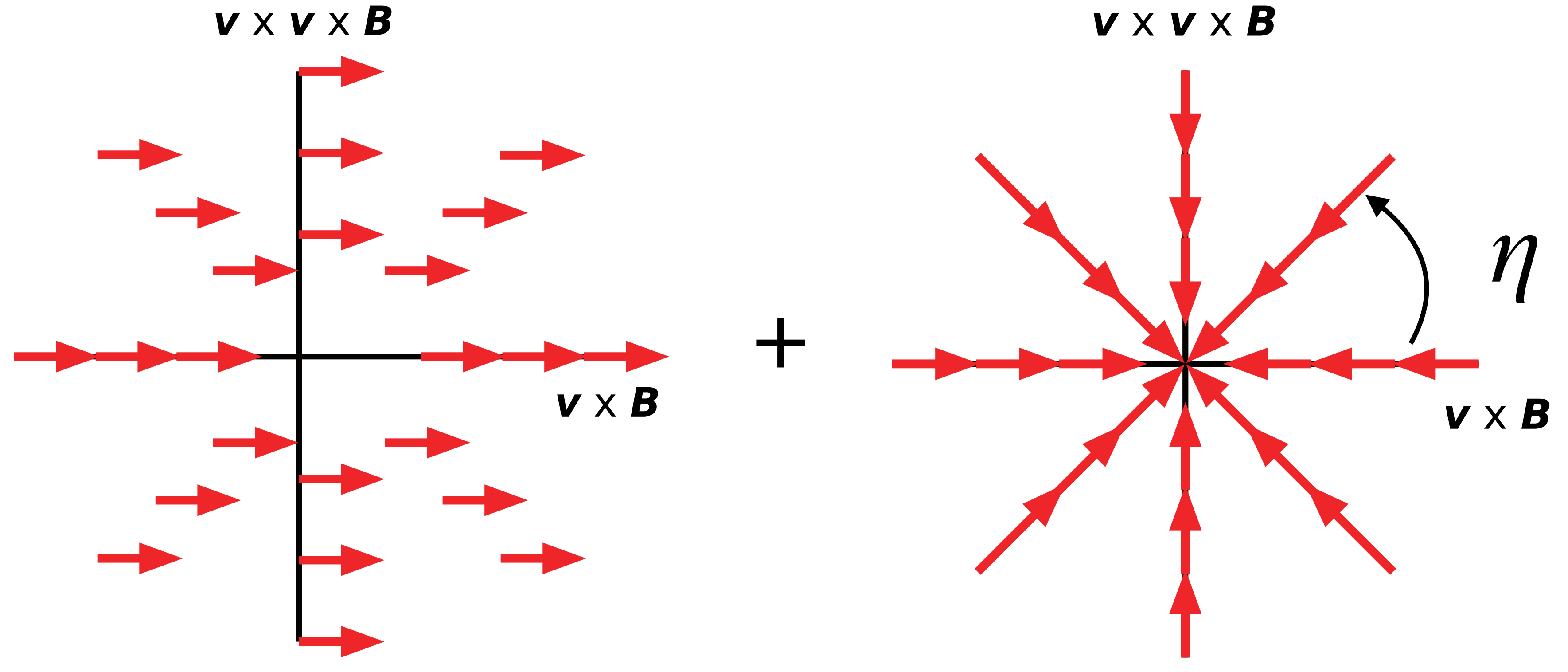

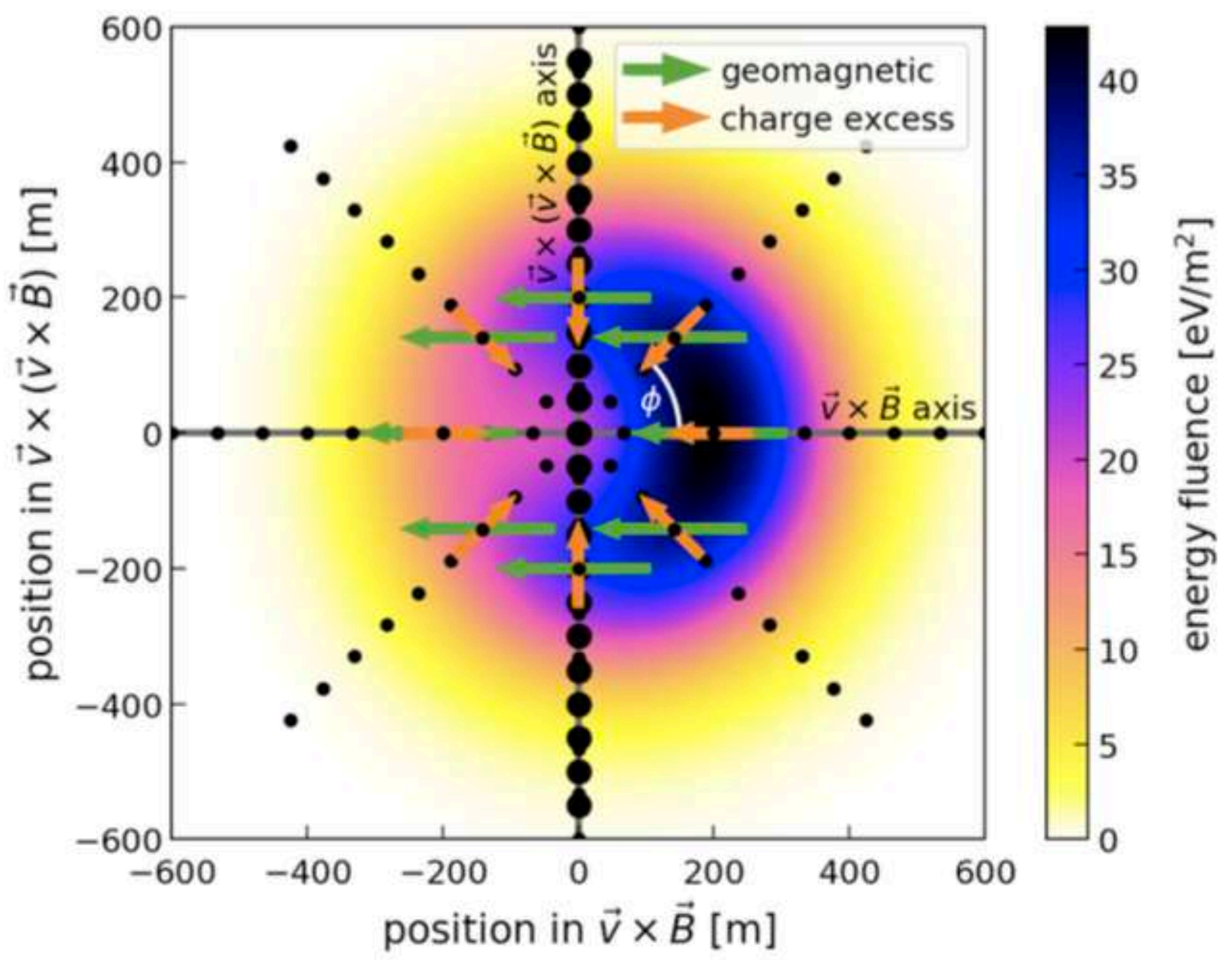

From Glaser et al. 2019

Insight the ADF model

$$f^{\mathrm{ADF}}(\omega,\eta,\alpha,l;\delta\omega,A)=\frac{A}{l}f^{GeoM}(\alpha,\eta,B)f^{\mathrm{Cherenkov}}(\omega,\delta\omega)$$

4 free parameters in ADF:

- **arrival direction θ, ϕ: direct reconstruction**
- scaling factor A and width $\delta\omega$

Cherenkov pattern: shape of there radio footprint (Lorentzian)

$$f^{\mathrm{Cerenkov}}(\omega,\delta\omega)=\frac{1}{1+4\left(\frac{(\tan(\omega)/\tan(\omega_c))^2-1}{\delta\omega}\right)^2}$$

ω_c
- described with dedicated model
- Not a free parameter

l: **Early-late asymmetry**: dilution effect

Geomagnetic asymmetry: interplay between geomagnetic effect and Askaryan effect (main emission mechanisms)

$$f^{\mathrm{Geom}}(\alpha,\eta,B)=1+G_A\frac{\cos(\eta)}{sin(\alpha)}$$

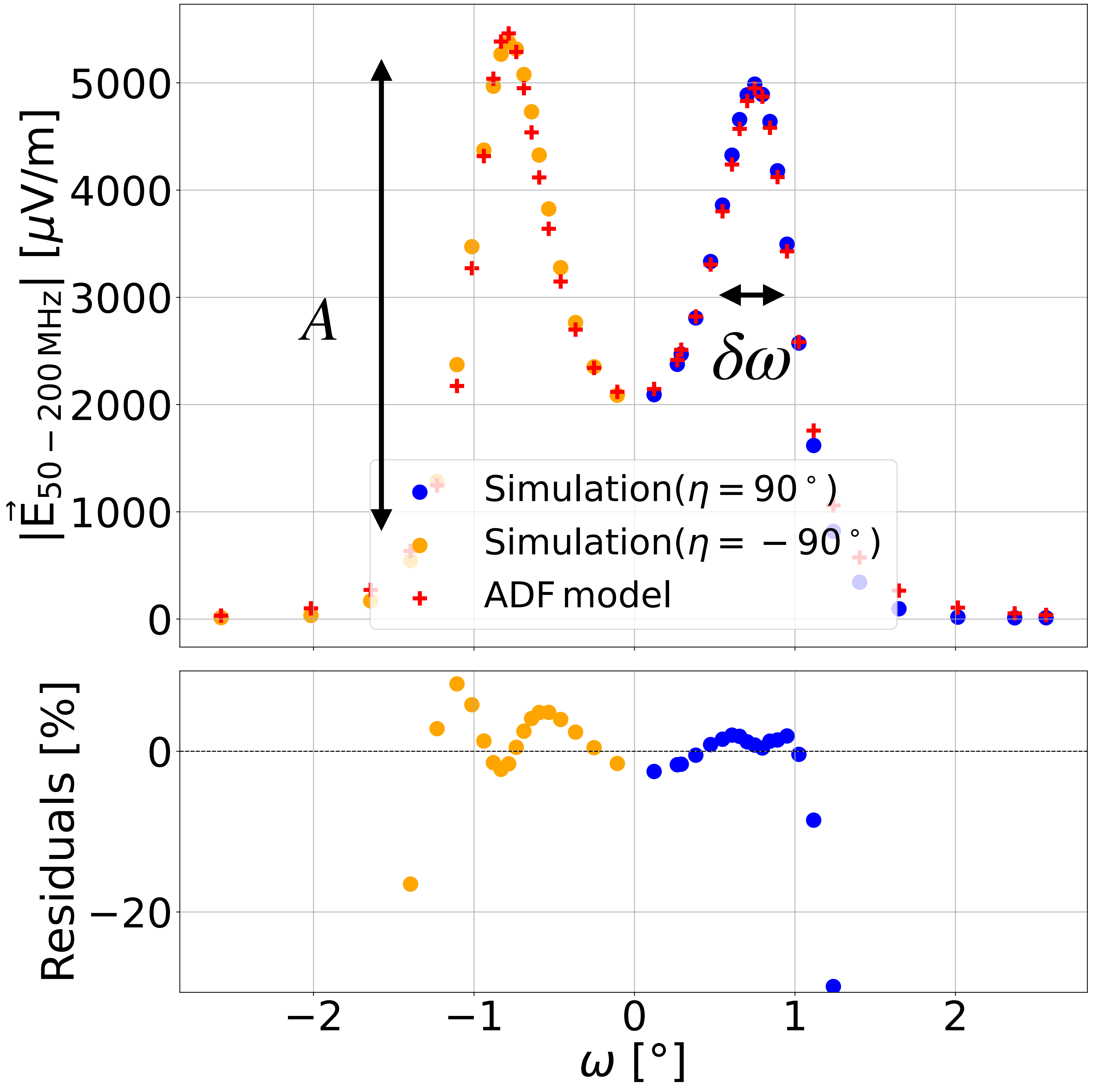

Validation of ADF model and arrival direction reconstruction

- Reconstruction code refactoring: from C++/FORTRAN to Python
- Numerical optimization: improve convergence & speed
- ADF model validation
- Validation on GRAND realistic simulations: performances

$\sim 10^4$ GRAND realistic simulations: Electric field
GRANDProto300 layout: 300 antennas
Simulated noise: 5ns on times + 7.5% on amplitudes
Trigger condition: $A \geq 5\sigma = 110\mu$V/m and ≥ 6 antennas

Guelfand et al., Astropart. Phys. (2025), arXiv:2504.18257

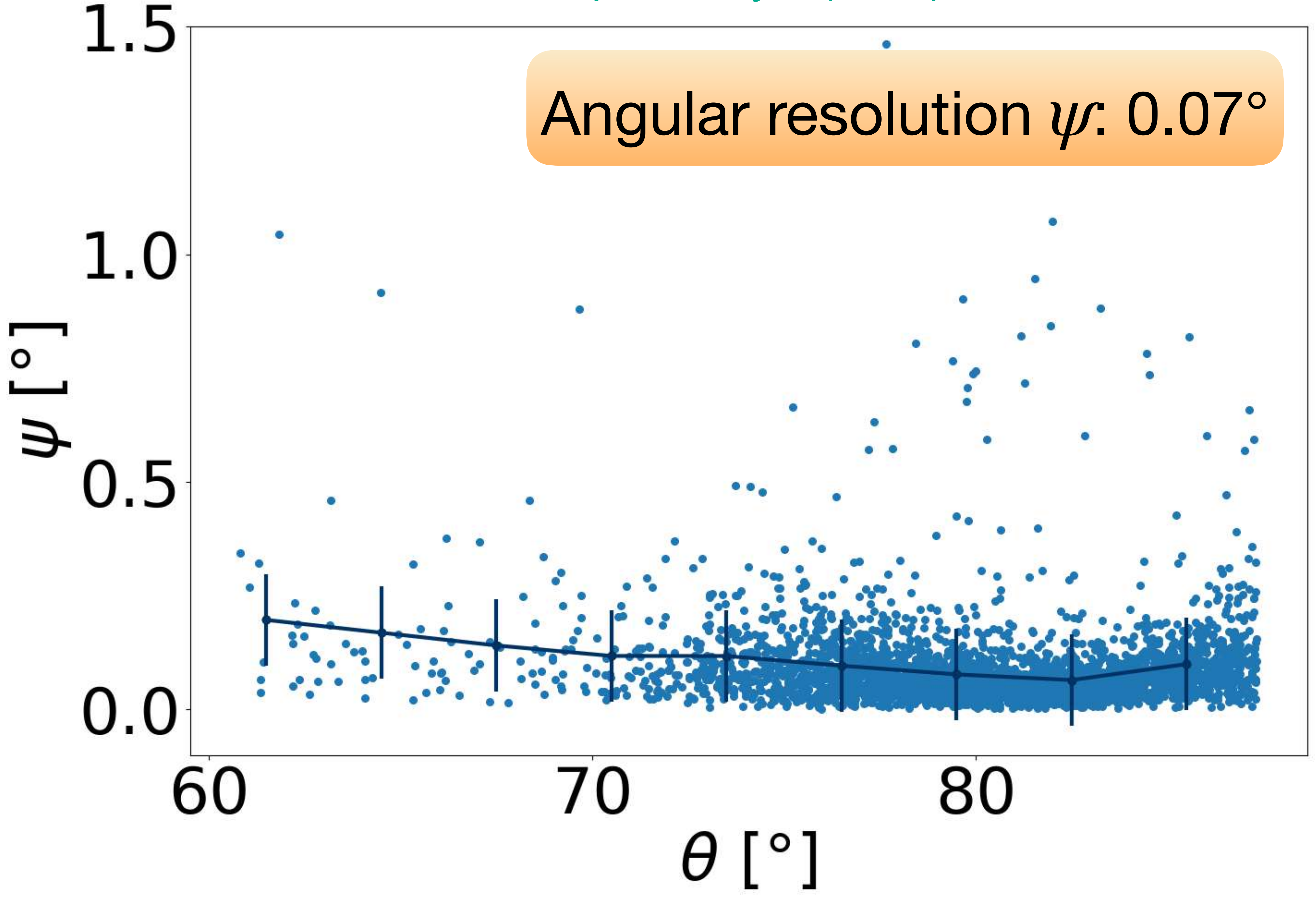

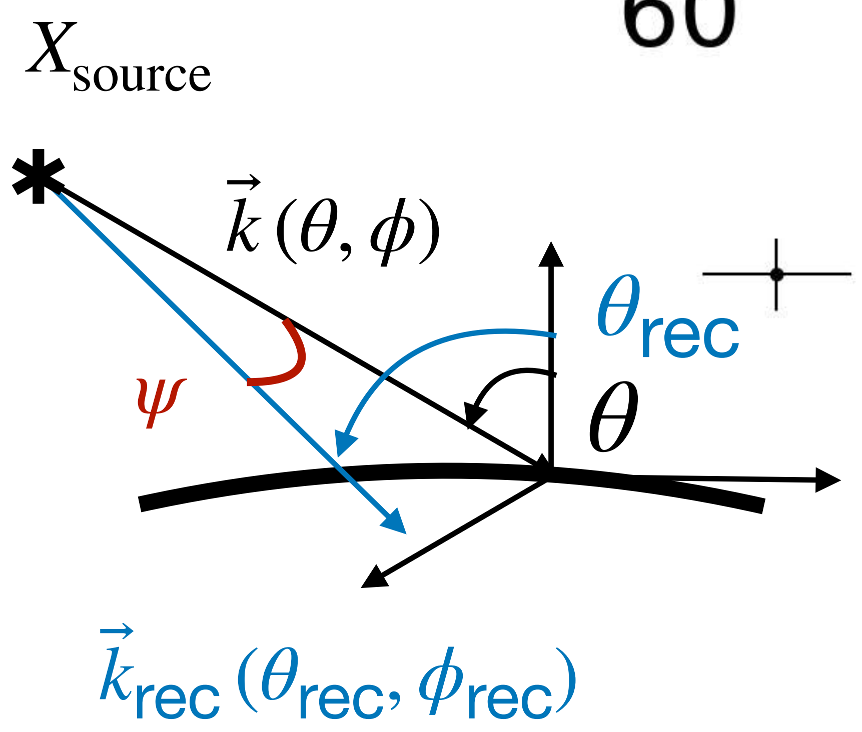

Efficiency $\epsilon = \frac{N_{\text{reconstructed}}}{N_{\text{trigger}}} = 88\,\%$ (40% in C++)

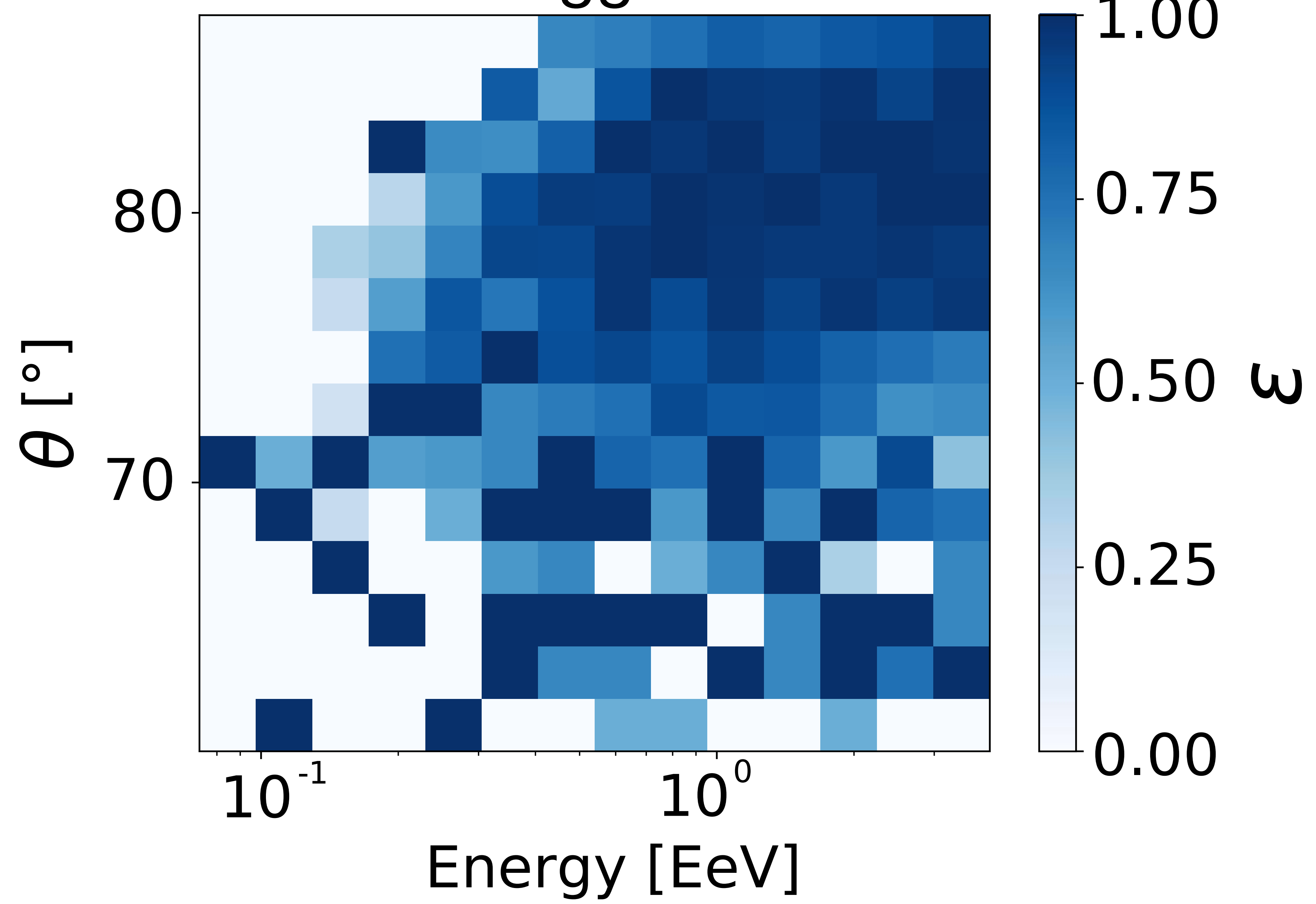

Sub-degree angular resolution allows to **pinpoint source** and perform ν **astronomy**
Only 4 free parameters
Fixed position of ω_c (dedicated model)

GRAND and the challenges of radio detection

III. Reconstruction of cosmic particles properties for very inclined directions

ADF model: validation and arrival direction reconstruction

Analytical modeling ω_c

The radio Cherenkov effect

Signal enhancement along specific directions
Cherenkov cone seen as a ring in radio footprints: **key signature** of cosmic particles
Time compression effects (refractive index $n > 1$)

For constant refractive index: $\omega_c = \mathrm{acos}(1/n)$
n changes with altitude: ω_c varies with inclination

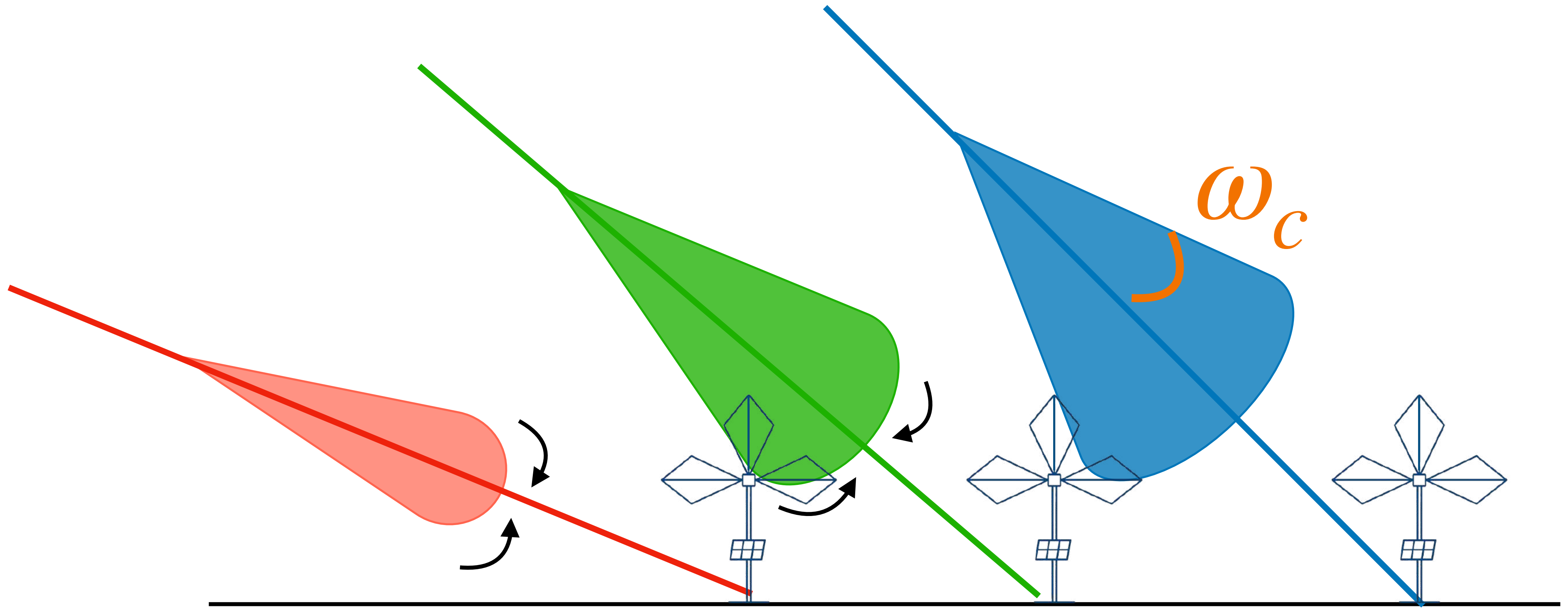

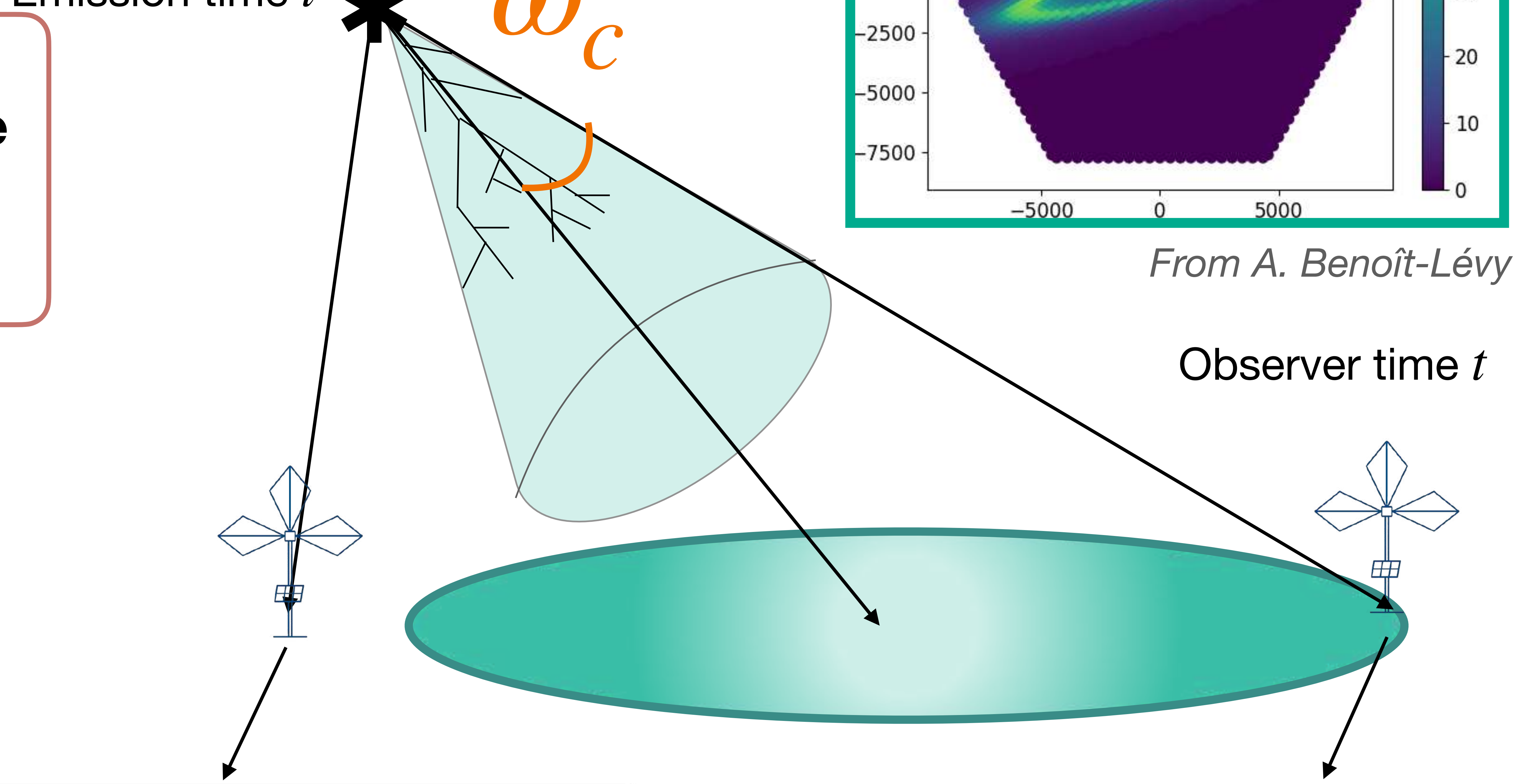

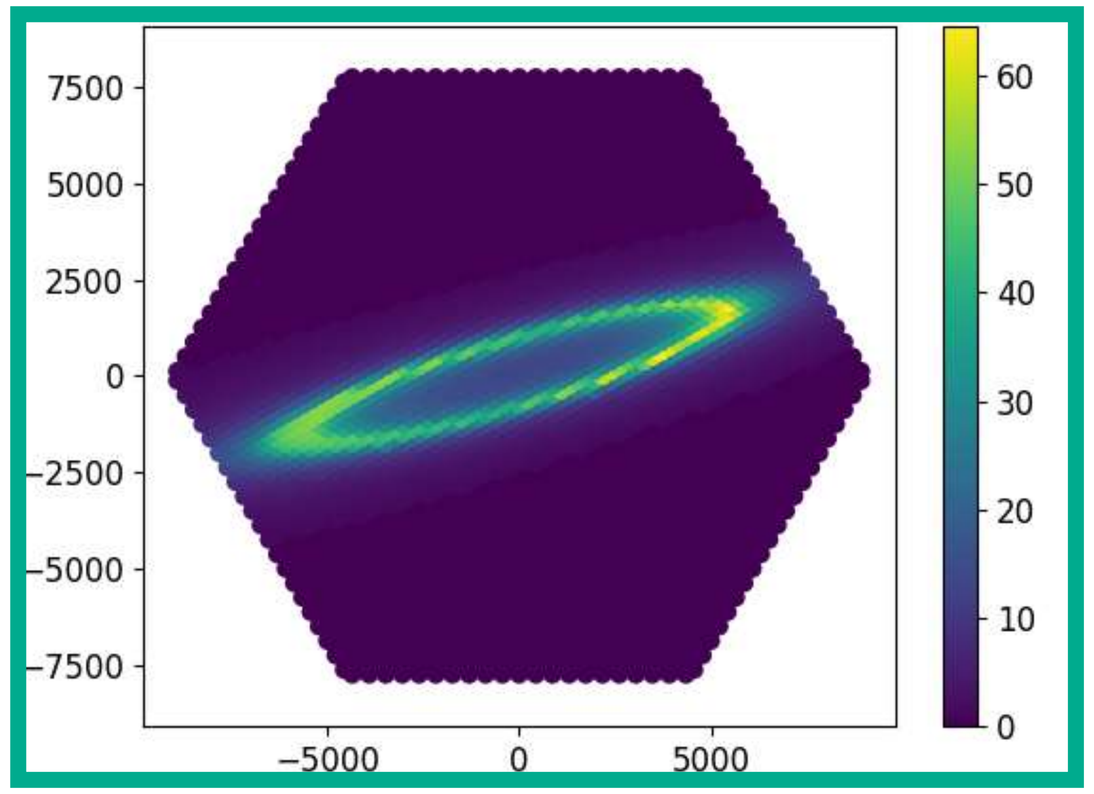

From A. Benoît-Lévy

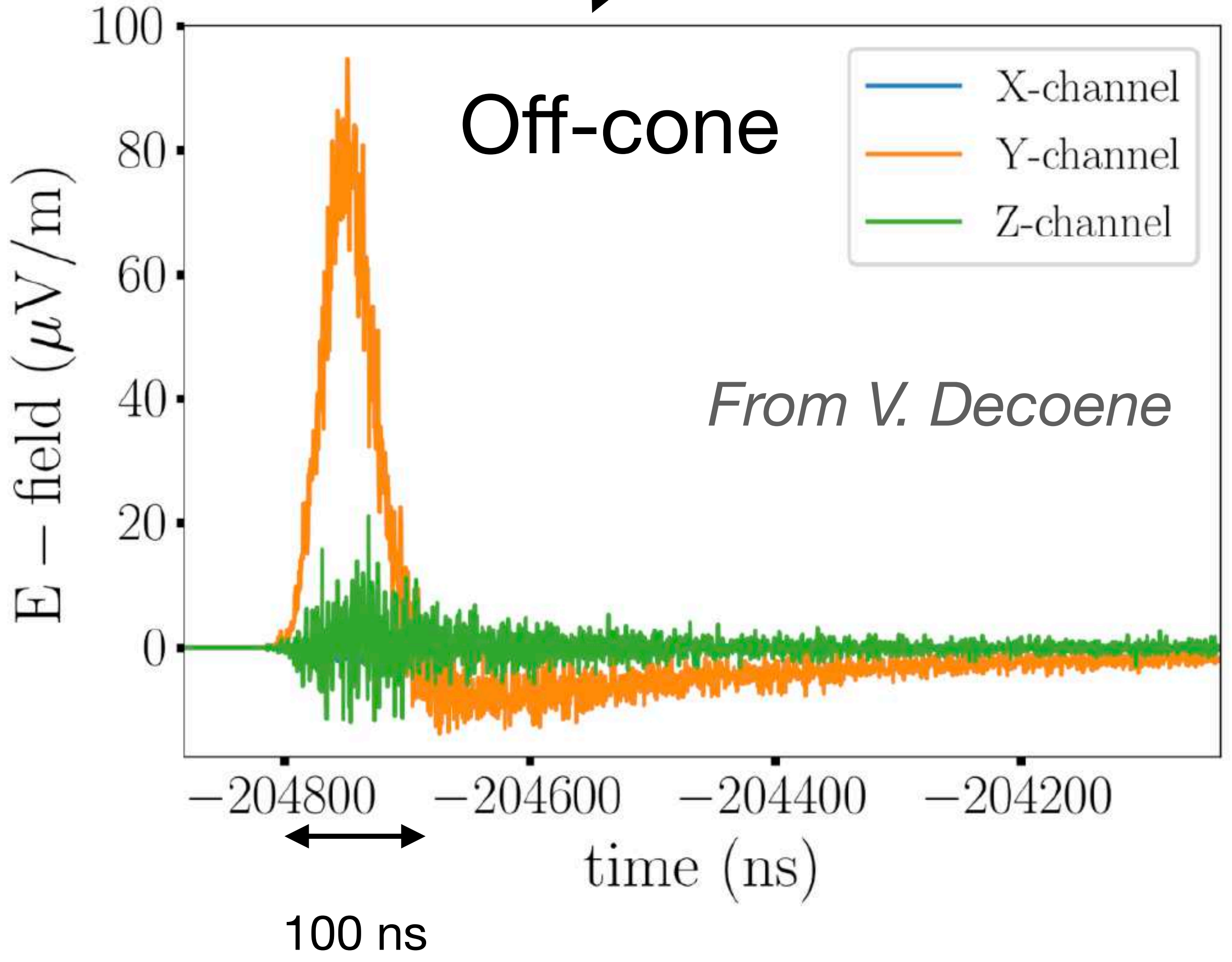

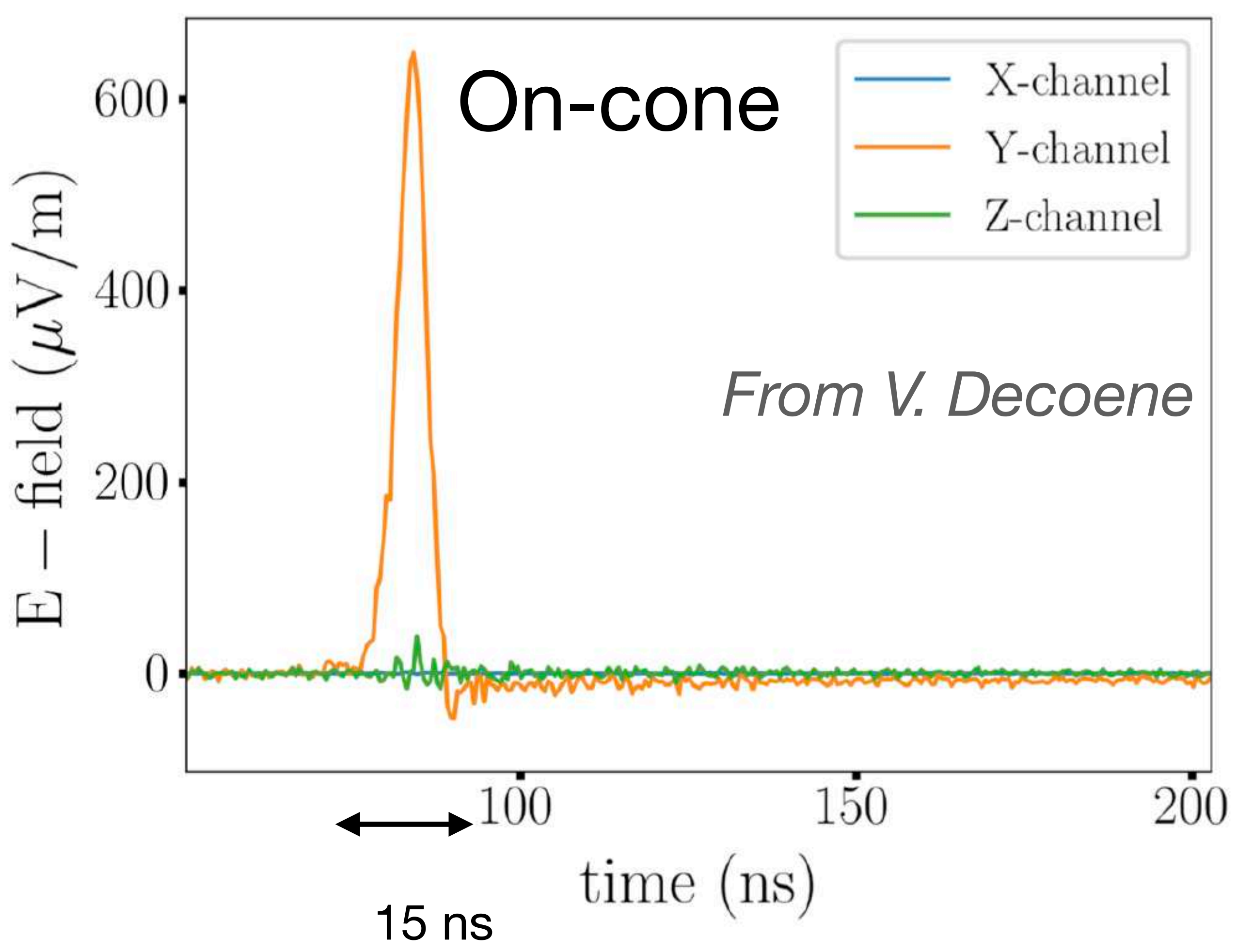

Analytical modeling of the radio Cherenkov cone

Causal relation: $c(t - t') = < n(R) > R$

Emission time t'

Origin from $X_{\max}(t' = 0)$

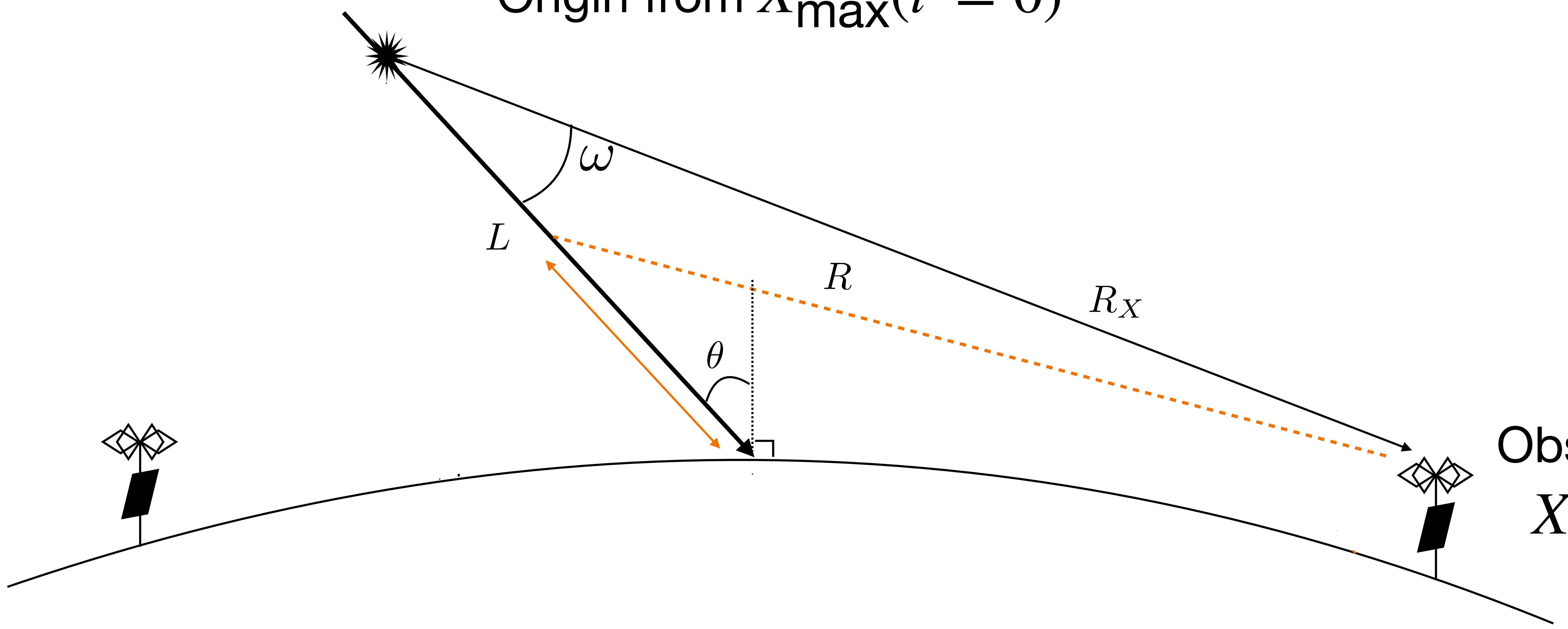

Observer time t

$X_{\max}$ frame

Effective refractive index $< n(R) > = \dfrac{\int_0^R dr\, n(r)}{\int_0^R dr}$

with $n(h) = 1 + ke^{-Ch}$ Alvarez-Muñiz et al., 2012

(analytically integrated)

Time compression effect:

$$\frac{\mathrm{d}ct'}{\mathrm{d}ct} \to \infty \leftrightarrow \frac{\mathrm{d}ct}{\mathrm{d}ct'} \to 0$$

- Time compression effect: $\dfrac{\mathrm{d}ct}{\mathrm{d}ct'} = 1 + [\dfrac{\mathrm{d} < n >}{\mathrm{d}R} R + < n >] \dfrac{\mathrm{d}R(\omega)}{\mathrm{d}ct'} = 0$ $\longrightarrow \omega_c$
- Maximum particle emission (altitude $X_{\max}$ i.e. $ct' = 0$)

Comparisons with simulations

*Decoene, **Guelfand**, Tueros, ICRC proc. 2025, arXiv:2507.05735*

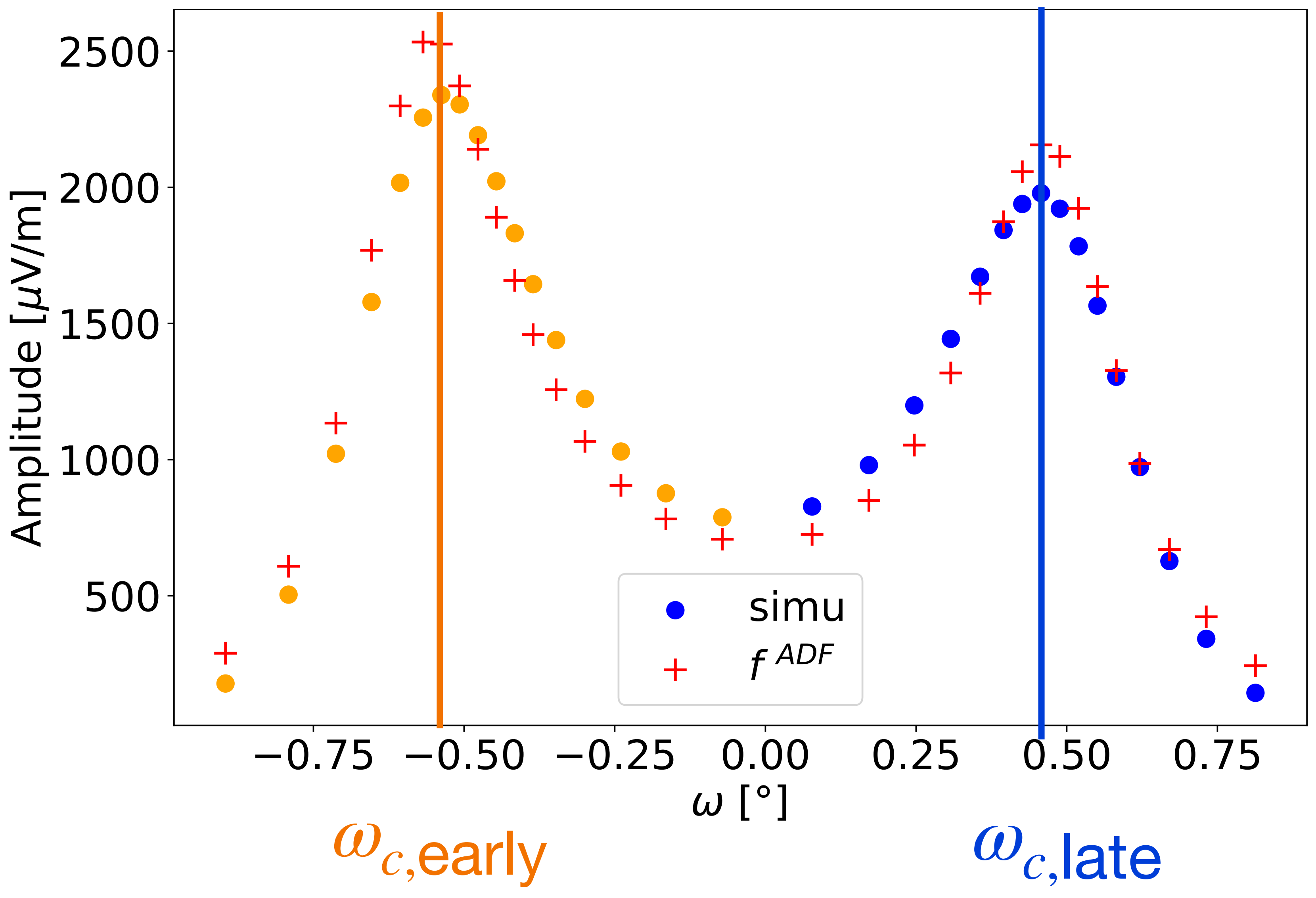

Monte Carlo codes: ZHAireS & CoREAS
No noise & no filter

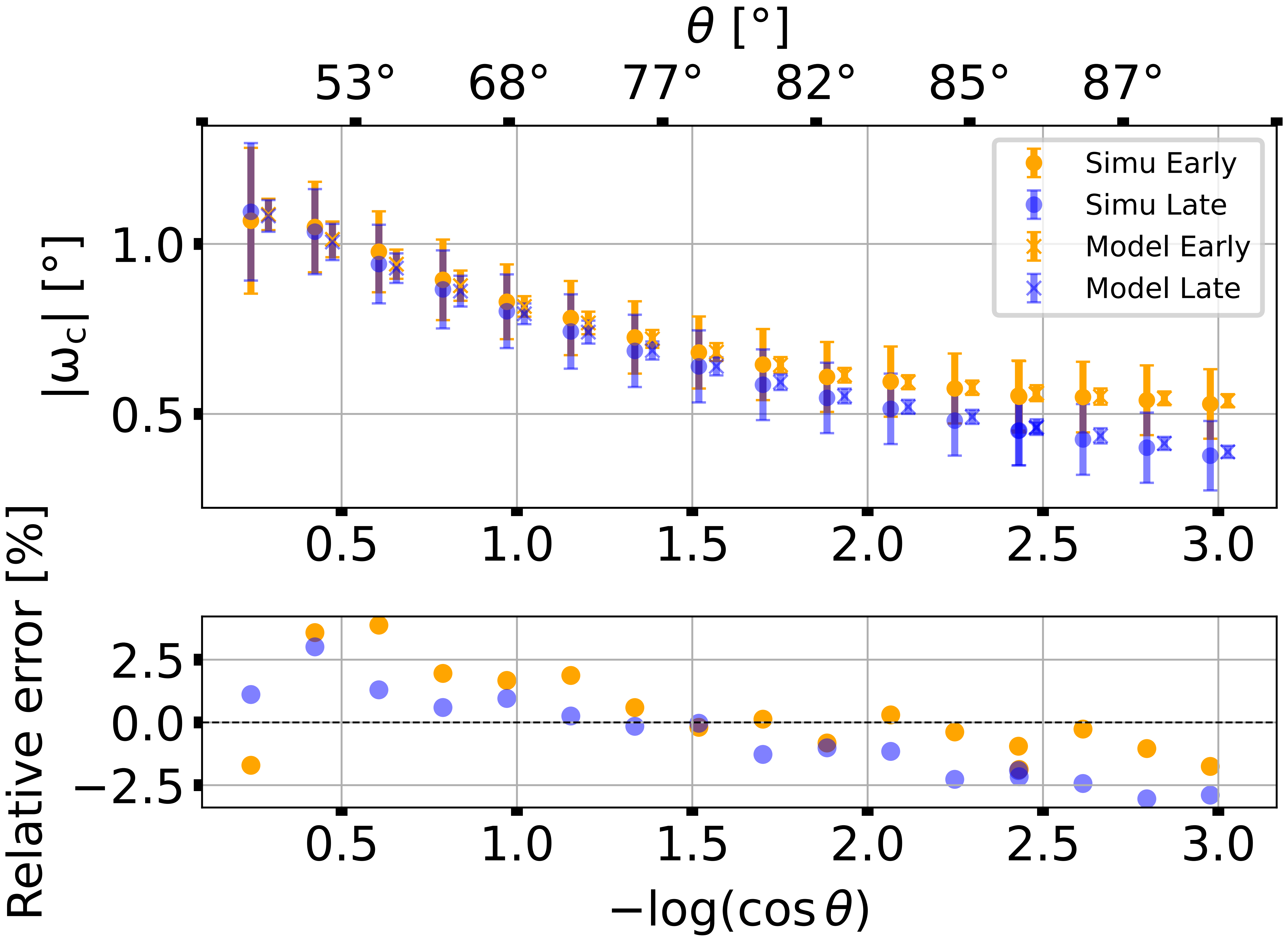

ω_c decreases with inclination

Asymmetry effect at high inclination: two distinct ω_c for early and late antennas: **optical path no longer equivalent**

‣ **Physical description of ω_c included in ADF**

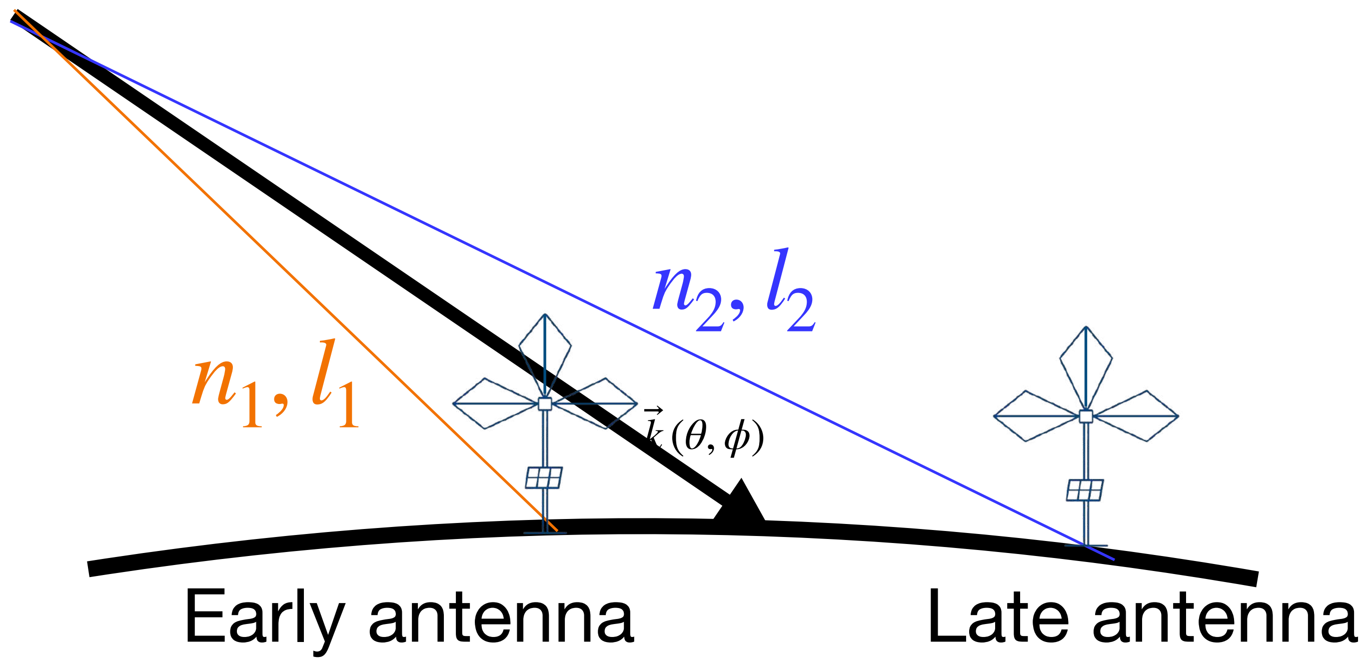

GRAND and the challenges of radio detection

III. Reconstruction of cosmic particles properties for very inclined directions

ADF model: validation and arrival direction reconstruction

Analytical modeling ω_c

ADF model: energy reconstruction

Reconstruction of cosmic ray energy with ADF model

$$f^{\mathrm{ADF}}(\omega,\eta,\alpha,l;\delta\omega,A) = \frac{A}{l} f^{GeoM}(\alpha,\eta,B)\, f^{\mathrm{Cherenkov}}(\omega,\delta\omega)$$

Radio signal amplitude (Scaling factor A) scales with electromagnetic energy E_{em}

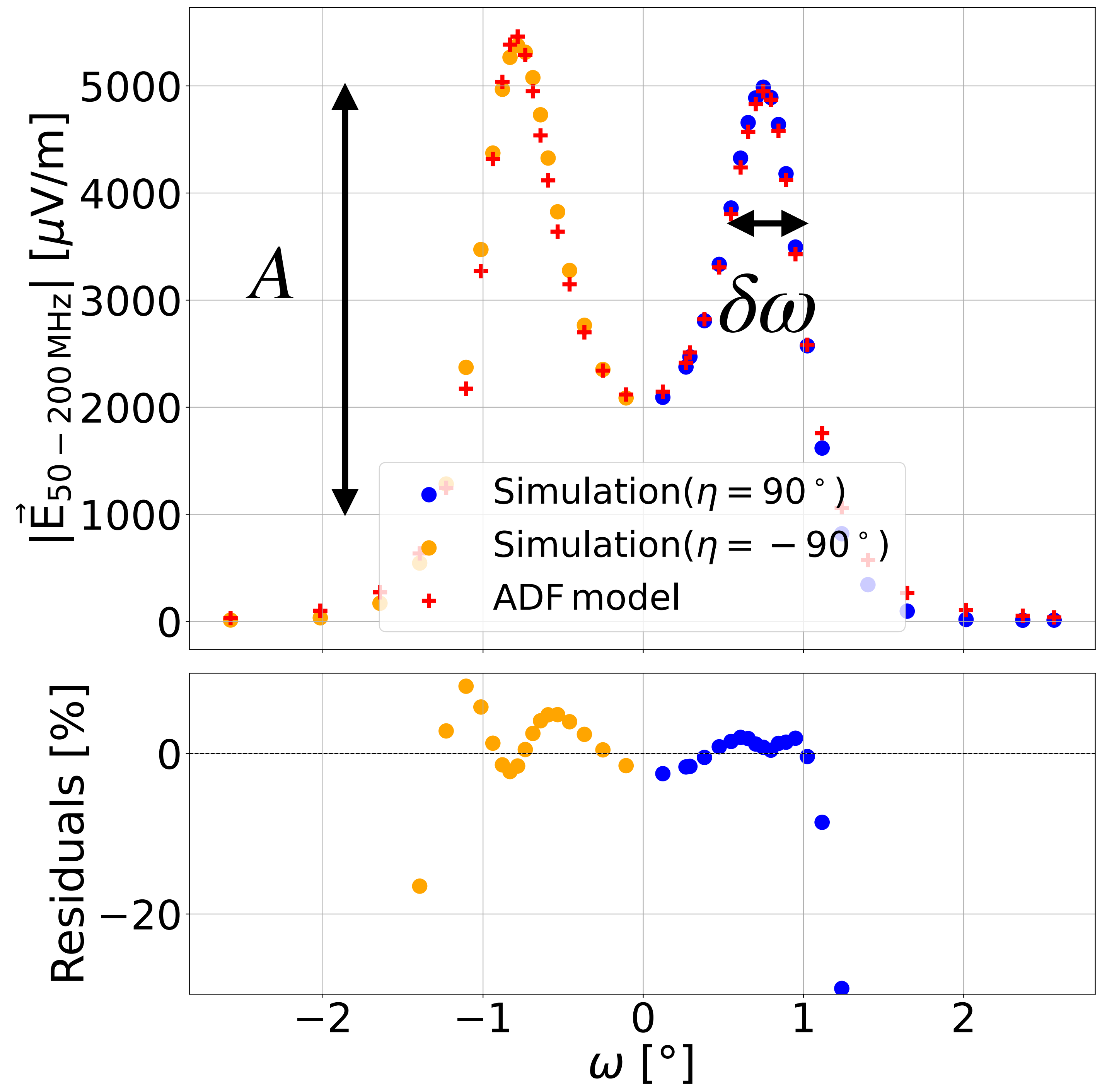

4 free parameters in ADF:

- **arrival direction θ, ϕ: direct reconstruction**
- scaling factor A and width $\delta\omega$

Reconstruction of cosmic ray energy with ADF model

$$f^{\mathrm{ADF}}(\omega, \eta, \alpha, l; \delta\omega, A) = \frac{A}{l} f^{GeoM}(\alpha, \eta, B) f^{\mathrm{Cherenkov}}(\omega, \delta\omega)$$

Radio signal amplitude (scaling factor A) scales with electromagnetic energy E_{em}

__Guelfand__ et al., Astropart. Phys. (2025), arXiv:2504.18257

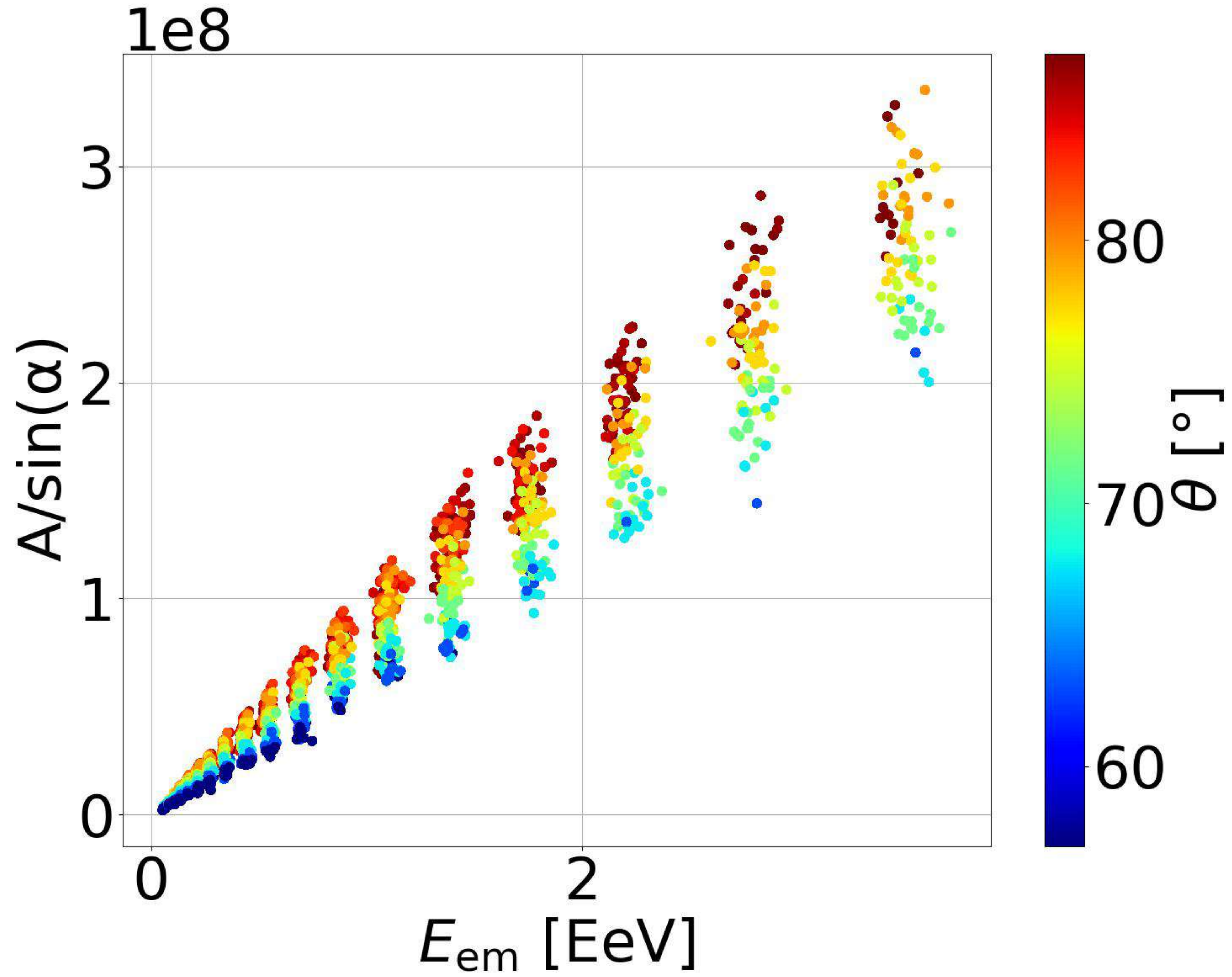

- Radio emission: dominated by **geomagnetic effect**

Driven by **Lorentz force**: $L_{\mathrm{Lorentz}} = q\vec{v} \times \vec{B}$

Amplitude $\propto qvB\sin(\alpha)$

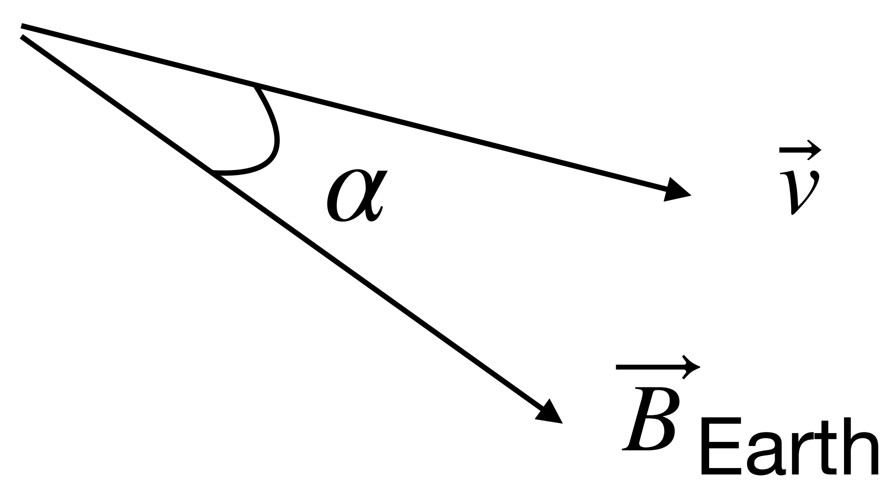

$$\frac{A}{\sin(\alpha)} = f(\theta) E_{\mathrm{em}}$$

Reconstruction of cosmic ray energy with ADF model

$$f^{\mathrm{ADF}}(\omega, \eta, \alpha, l; \delta\omega, A) = \frac{A}{l} f^{GeoM}(\alpha, \eta, B)\, f^{\mathrm{Cherenkov}}(\omega, \delta\omega)$$

Radio signal amplitude (scaling factor A) scales with electromagnetic energy E_{em}

Guelfand et al., Astropart. Phys. (2025), arXiv:2504.18257

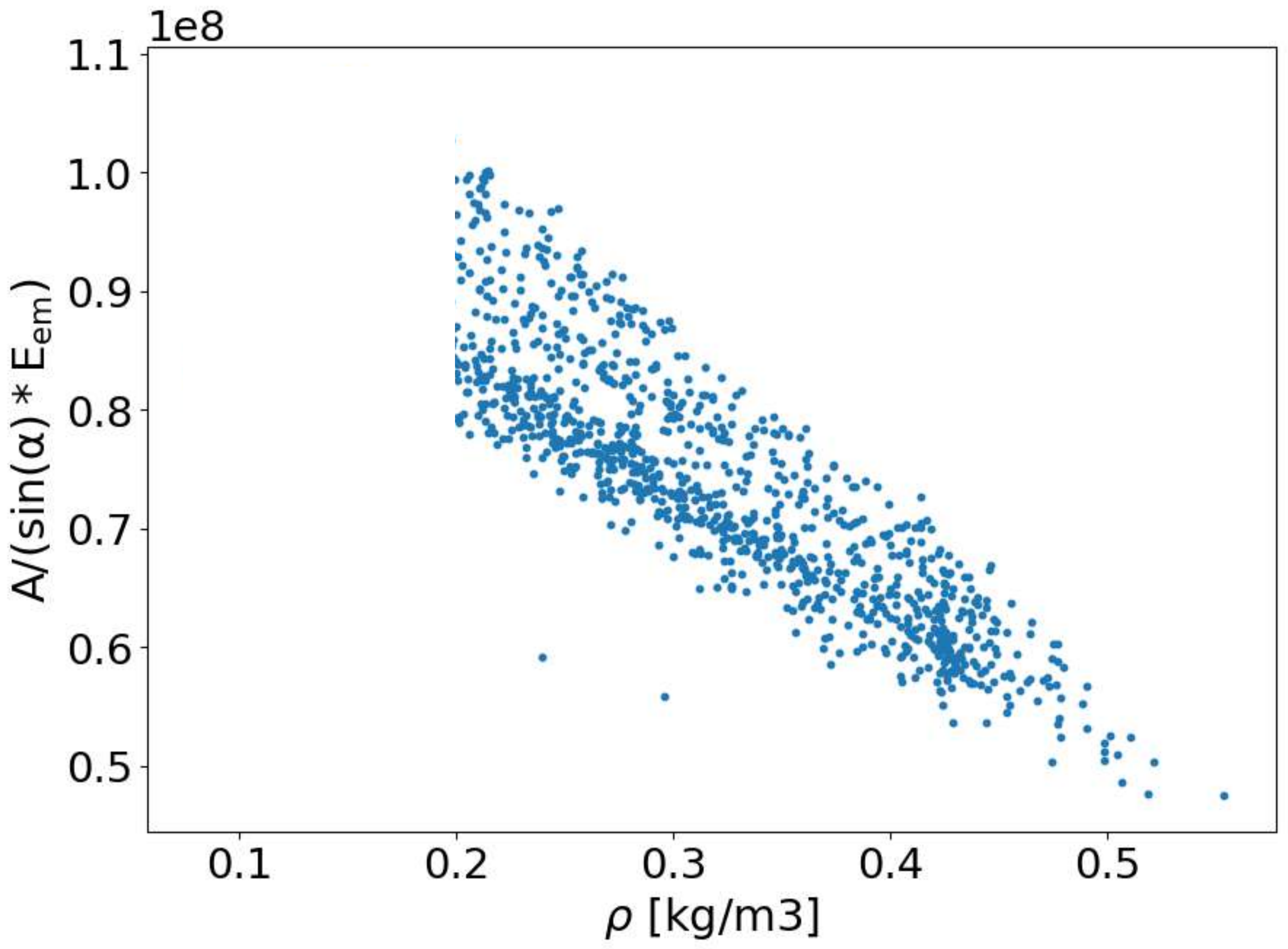

- Radio emission: dominated by **geomagnetic effect**

Driven by **Lorentz force**: $L_{\mathrm{Lorentz}} = q\vec{v} \times \vec{B}$

Amplitude $\propto qvB\sin(\alpha)$

- Geomagnetic effect: **larger for inclined EAS**

(Develop higher in atmosphere)

Reconstruction of cosmic ray energy with ADF model

$$f^{\mathrm{ADF}}(\omega,\eta,\alpha,l;\delta\omega,A) = \frac{A}{l} f^{GeoM}(\alpha,\eta,B)\, f^{\mathrm{Cherenkov}}(\omega,\delta\omega)$$

Radio signal amplitude (scaling factor A) scales with electromagnetic energy E_{em}

***Guelfand** et al., Astropart. Phys. (2025), arXiv:2504.18257*

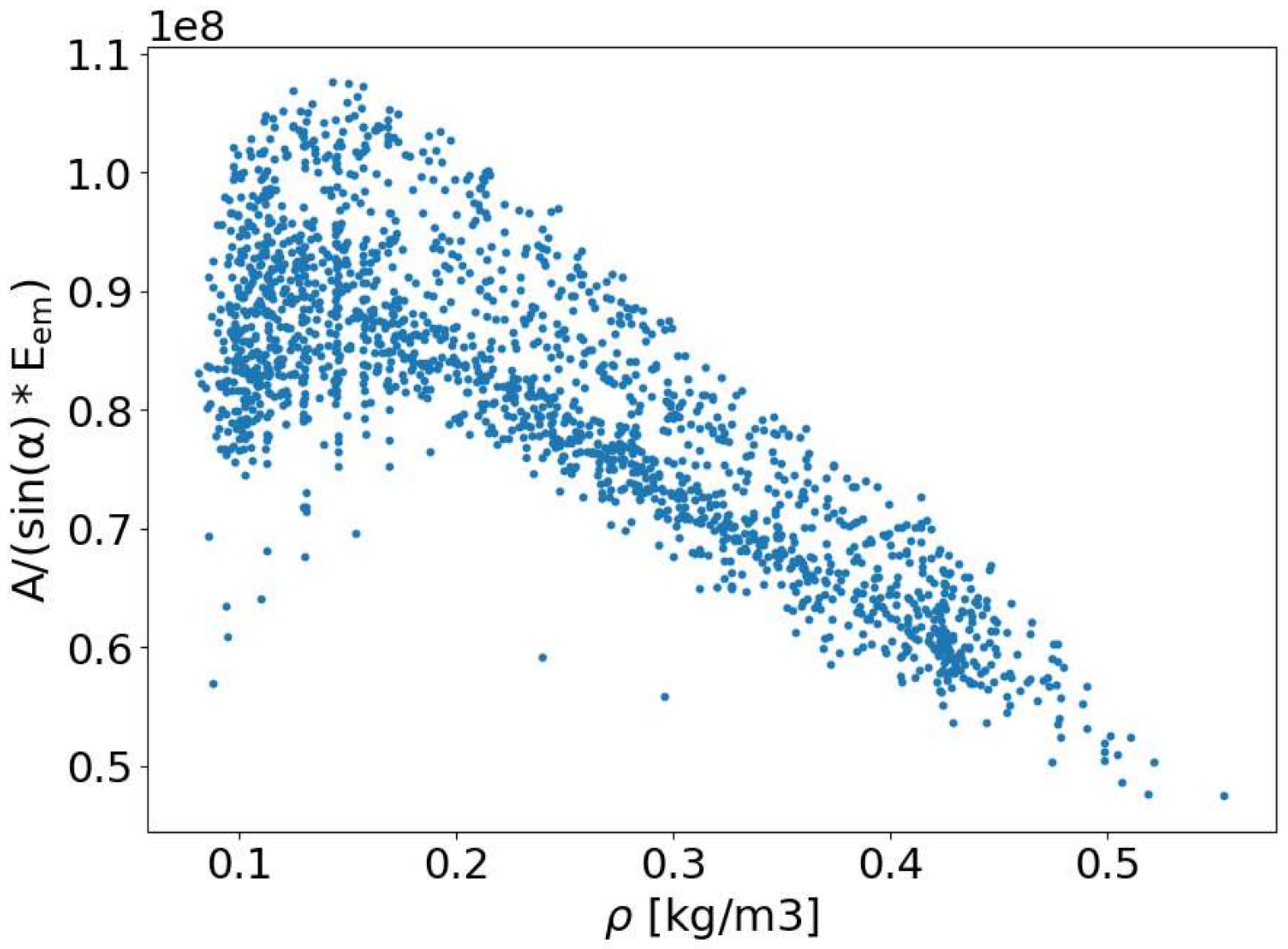

- Radio emission: dominated by **geomagnetic effect**

Driven by **Lorentz force**: $L_{\text{Lorentz}} = q\vec{v} \times \vec{B}$

Amplitude $\propto qvB\sin(\alpha)$

- Geomagnetic effect: **larger for inclined EAS**

(Develop higher in atmosphere)

- At very high inclination, **coherence loss**

See model Loss of coherence
*Chiche et al (incl. **Guelfand**), PRL 2023*
***Guelfand** et al., JCAP 2024*

$$\frac{A}{\sin(\alpha)} = f(\rho)E_{\text{em}}$$

Reconstruction of cosmic ray energy with ADF model

$$f^{\mathrm{ADF}}(\omega, \eta, \alpha, l; \delta\omega, A) = \frac{A}{l} f^{GeoM}(\alpha, \eta, B) f^{\mathrm{Cherenkov}}(\omega, \delta\omega)$$

Radio signal amplitude (scaling factor A) scales with electromagnetic energy E_{em}

Guelfand et al., Astropart. Phys. (2025), arXiv:2504.18257

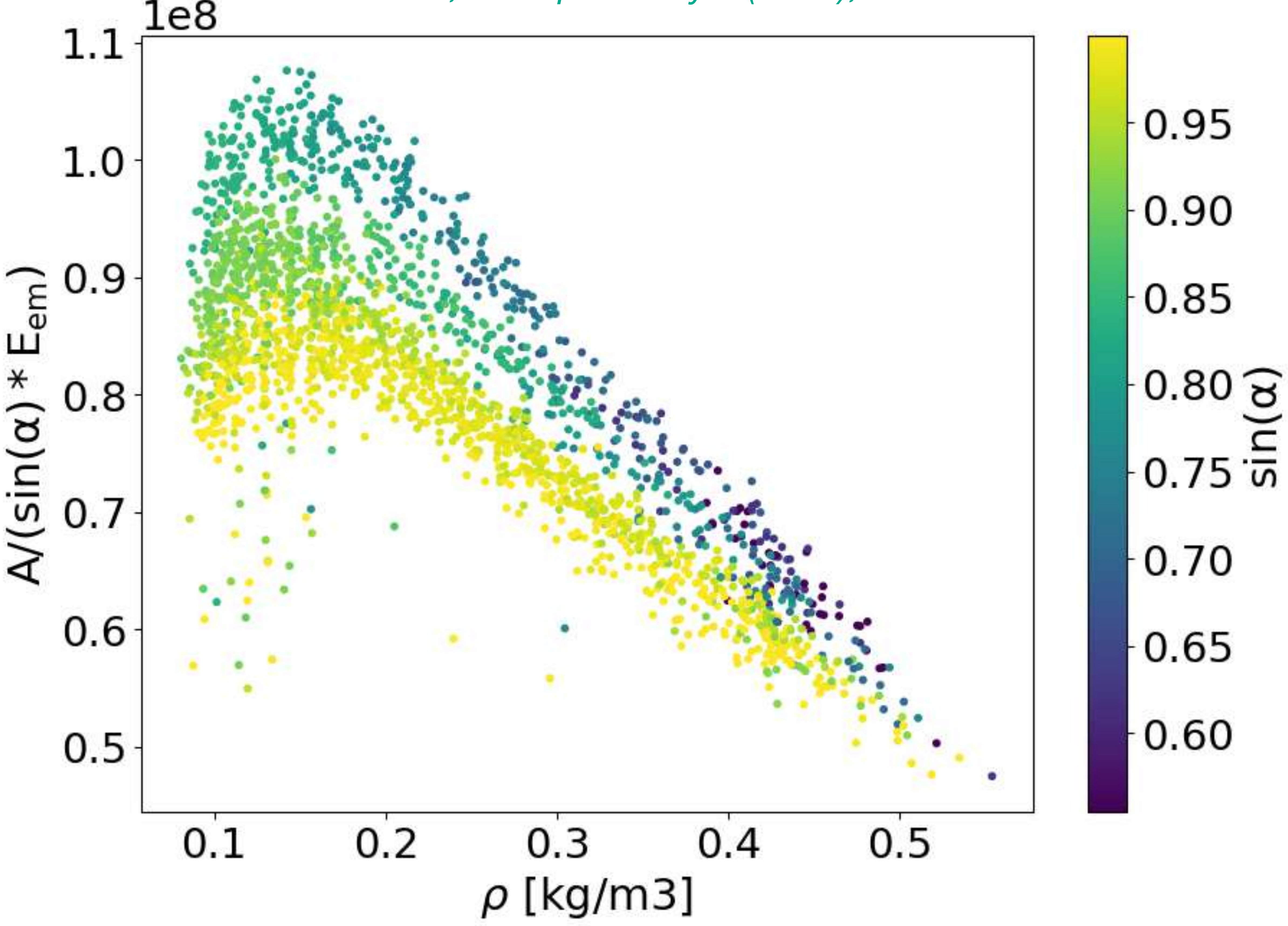

- Radio emission: dominated by **geomagnetic effect**

Driven by **Lorentz force**: $L_{\mathrm{Lorentz}} = q\vec{v} \times \vec{B}$

Amplitude $\propto qvB\sin(\alpha)$

- Geomagnetic effect: **larger for inclined EAS**

(Develop higher in atmosphere)

- At very high inclination, **coherence loss**

- Second order effect $\sin(\alpha)$: $B_{\mathrm{eff}} = B\sin(\alpha)$

Larger $\sin(\alpha)$: coherence loss

$$\frac{A}{\sin(\alpha)} = g(\rho, \sin(\alpha))E_{\mathrm{em}}$$

Reconstruction of cosmic ray energy: performances

Energy estimator: $E^*_{\mathrm{em}} = \dfrac{A}{\sin(\alpha)\, g(\rho, \sin(\alpha))}$

Ideal simulation set: intrinsic method resolution

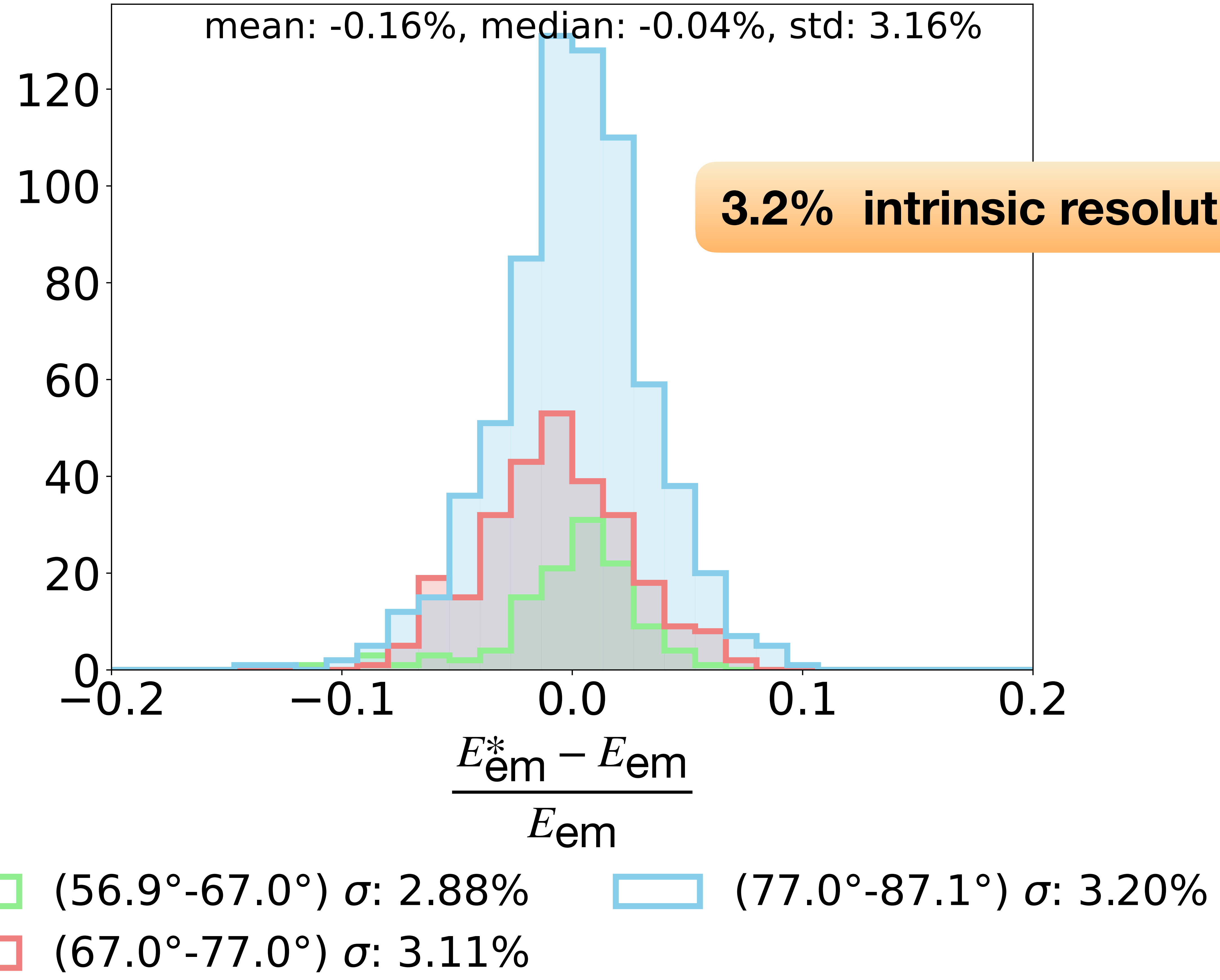

3.2% intrinsic resolution!

Reconstruction of cosmic ray energy: performances

Energy estimator: $E^*_{\text{em}} = \dfrac{A}{\sin(\alpha)\, g(\rho, \sin(\alpha))}$

$$E_{\text{primary}} = E_{\text{em}} + N_\mu E_c^\pi$$

Ideal simulation set: intrinsic method resolution

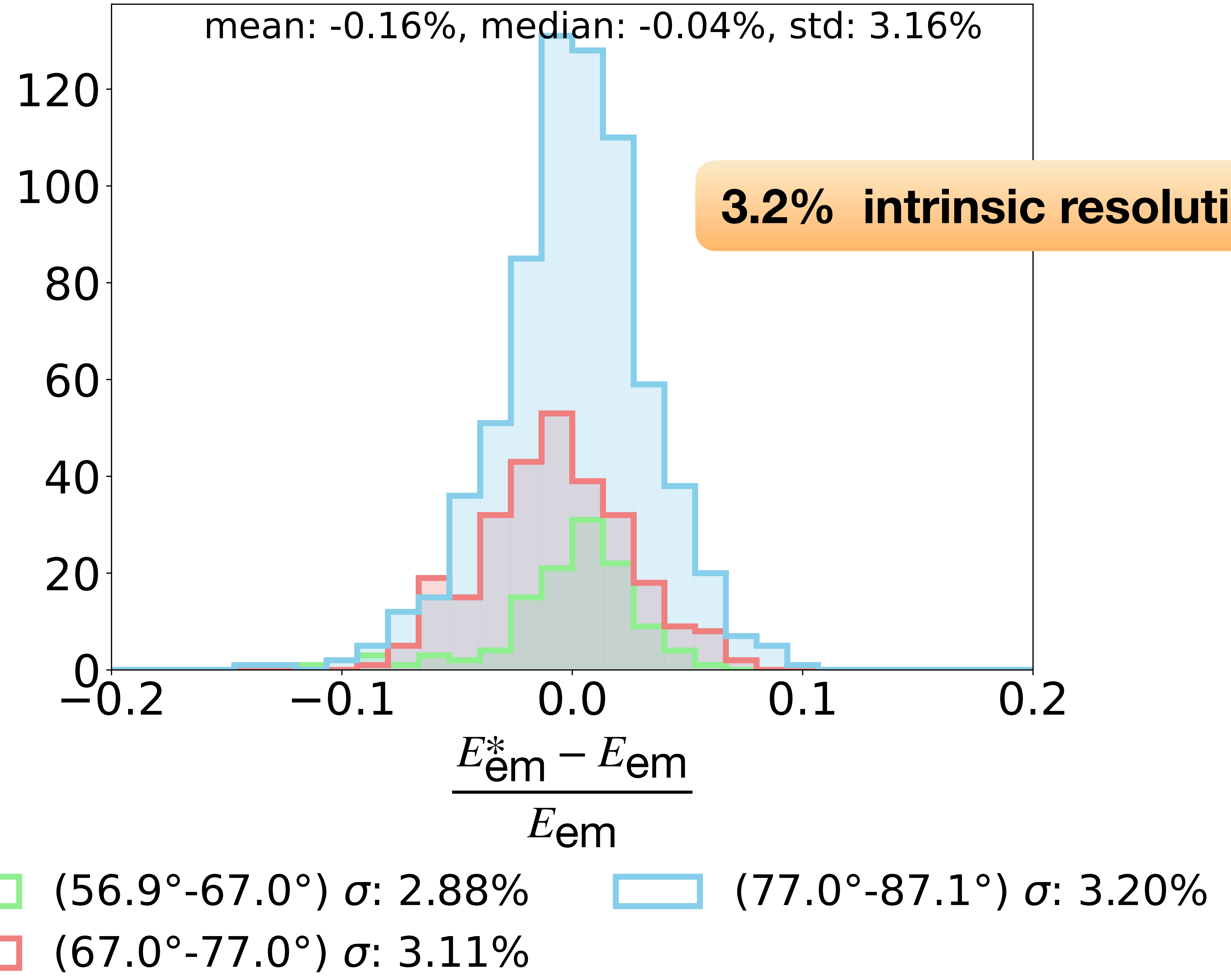

3.2% intrinsic resolution!

Realistic GRANDProto300 simulations with proton and iron nuclei

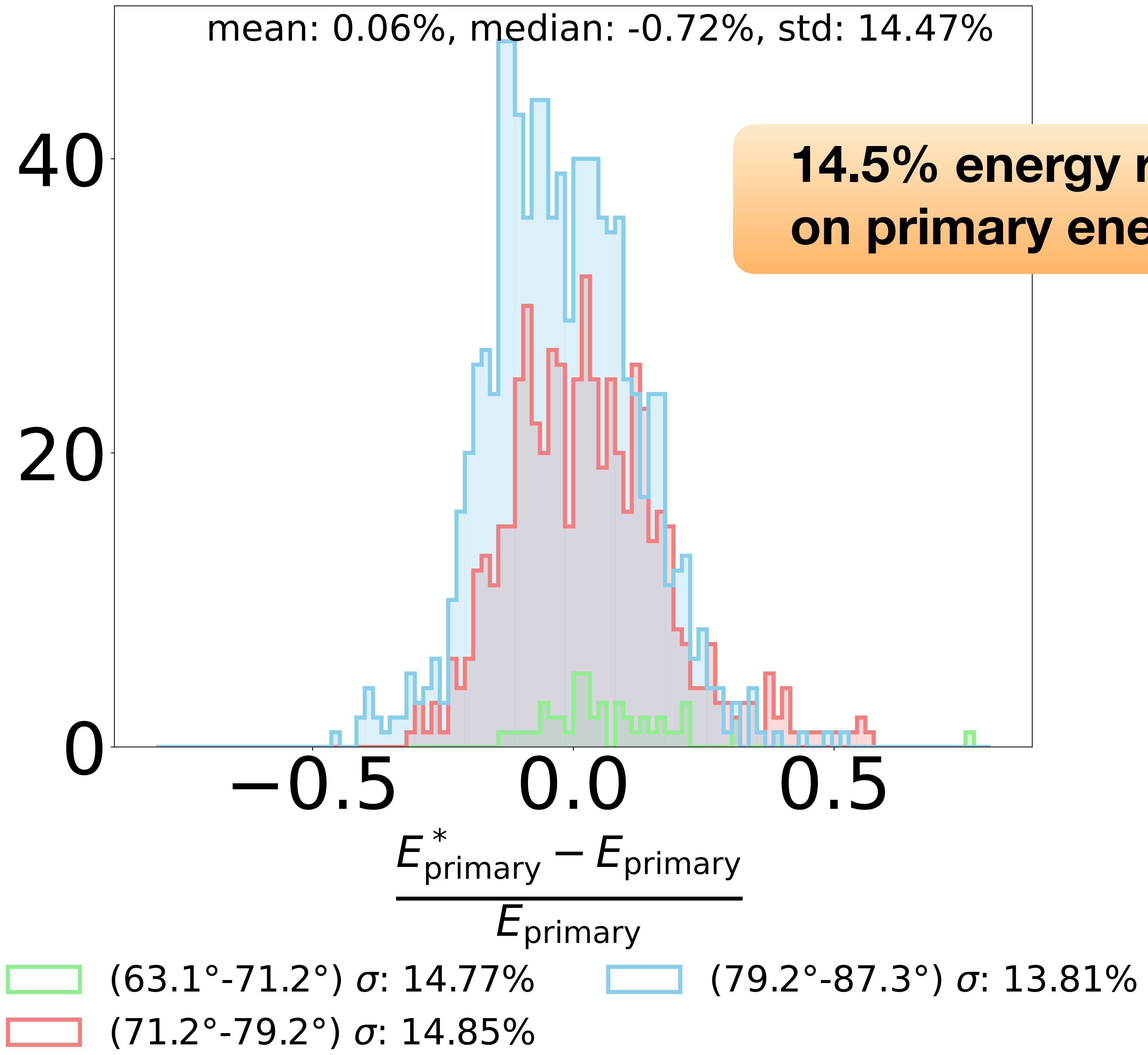

14.5% energy resolution on primary energy

Reconstruction of cosmic ray energy: performances

Energy estimator: $E^*_{\rm em} = \dfrac{A}{\sin(\alpha)\, g(\rho, \sin(\alpha))}$

$$E_{\rm primary} = E_{\rm em} + N_\mu E_c^\pi$$

Missing energy: invisible to radio detection
Heavier nuclei produce more muons

$$\frac{E_{\rm em}}{E_{\rm primary}}\Big|\ \text{Proton} \sim 88\ \% > \frac{E_{\rm em}}{E_{\rm primary}}\Big|\ \text{Iron} \sim 83\ \%$$

Resolution includes:

- Intrinsic method performances
- Realistic experimental conditions (noise, layout)
- Fluctuations (unknown particle nature)

Realistic GRANDProto300 simulations with proton and iron nuclei

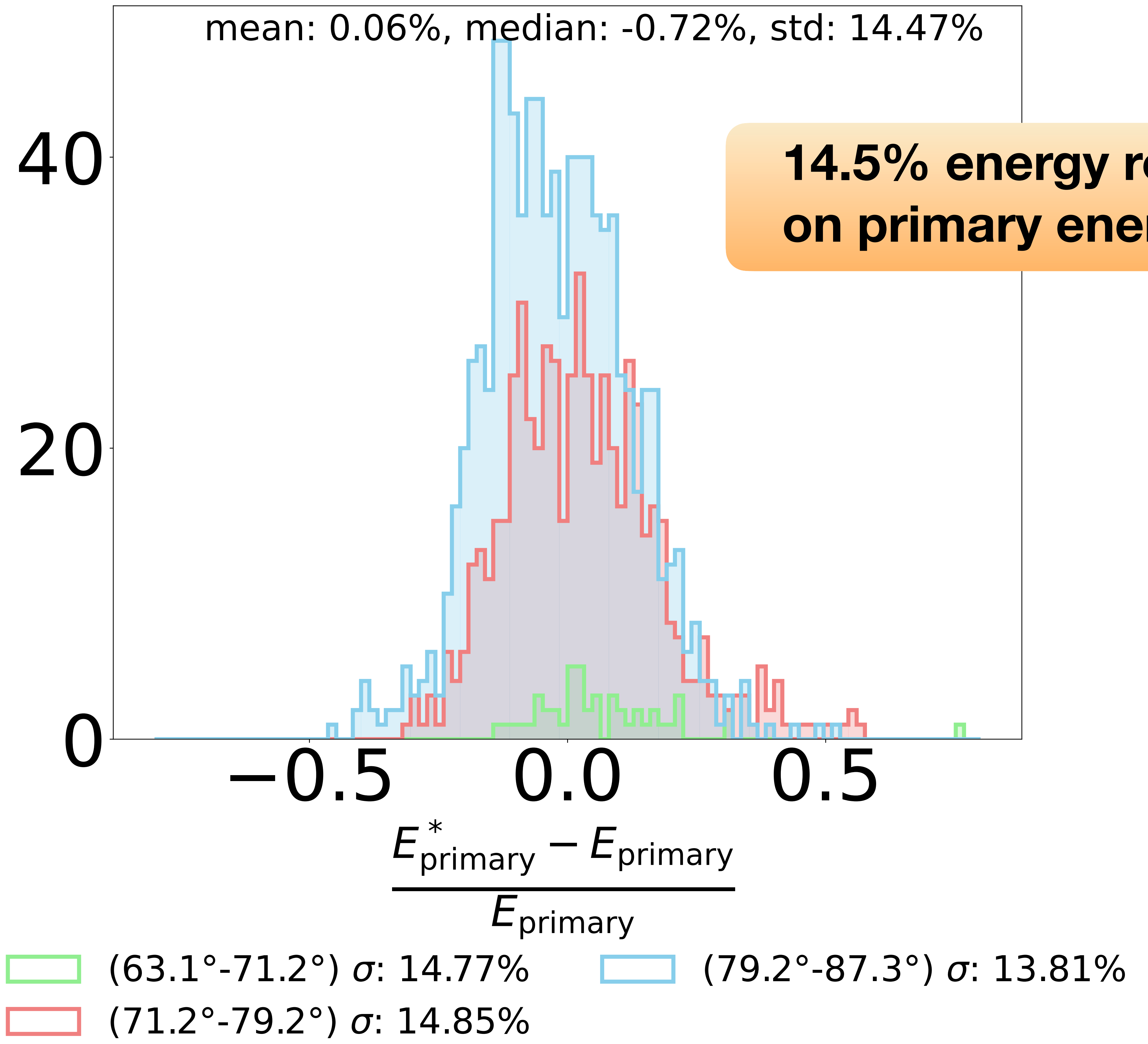

14.5% energy resolution on primary energy

GRAND and the challenges of radio detection

III. Reconstruction of cosmic particles properties for very inclined directions

ADF model: validation and arrival direction reconstruction

Analytical modeling ω_c

ADF model: energy reconstruction

Analysis pipeline on the first cosmic-ray candidates

Offline analysis pipeline

Coincident Data ← Trigger

↓

Cosmic ray search (cuts) → Electric field deconvolution → Reconstruction → Cosmic ray distribution

Since November 2024: 65/300 antennas running on GRANDProto300 site
December 2024 - March 2025: 533,466 Coincident Data stored

First Level Trigger (FLT) on FPGA
Signal-over-threshold trigger

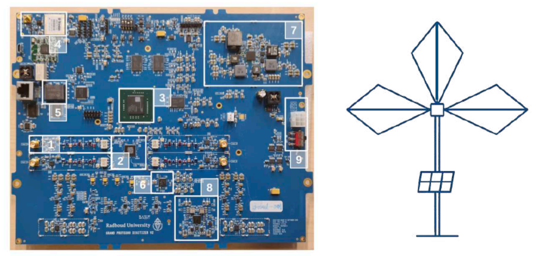

At the antenna level

Second Level Trigger (SLT)
Coincidences within 10 μs time window between at least 5 antennas

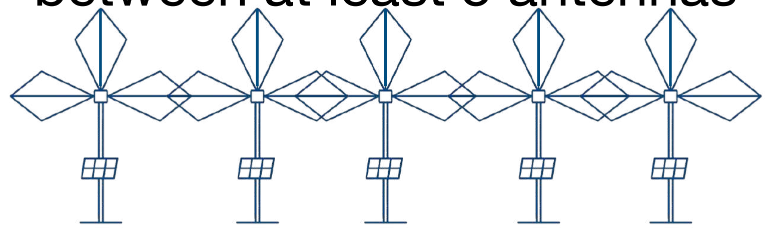

At the detector level

Wi-Fi

Central DAQ
Coincident data (CD) stored

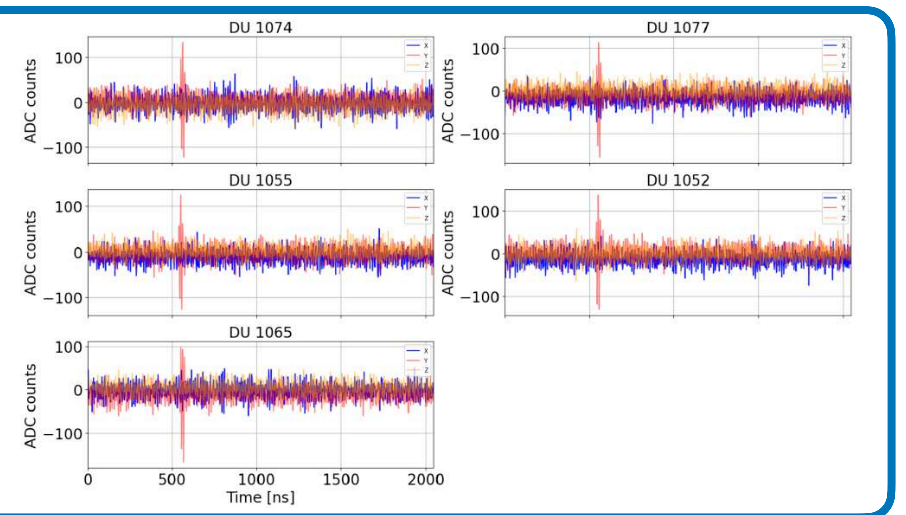

Cosmic ray search

Coincident Data ← Trigger

↓

Cosmic ray search (cuts) → Electric field deconvolution → Reconstruction → Cosmic ray distribution

533,466 Coincident Data (CD)

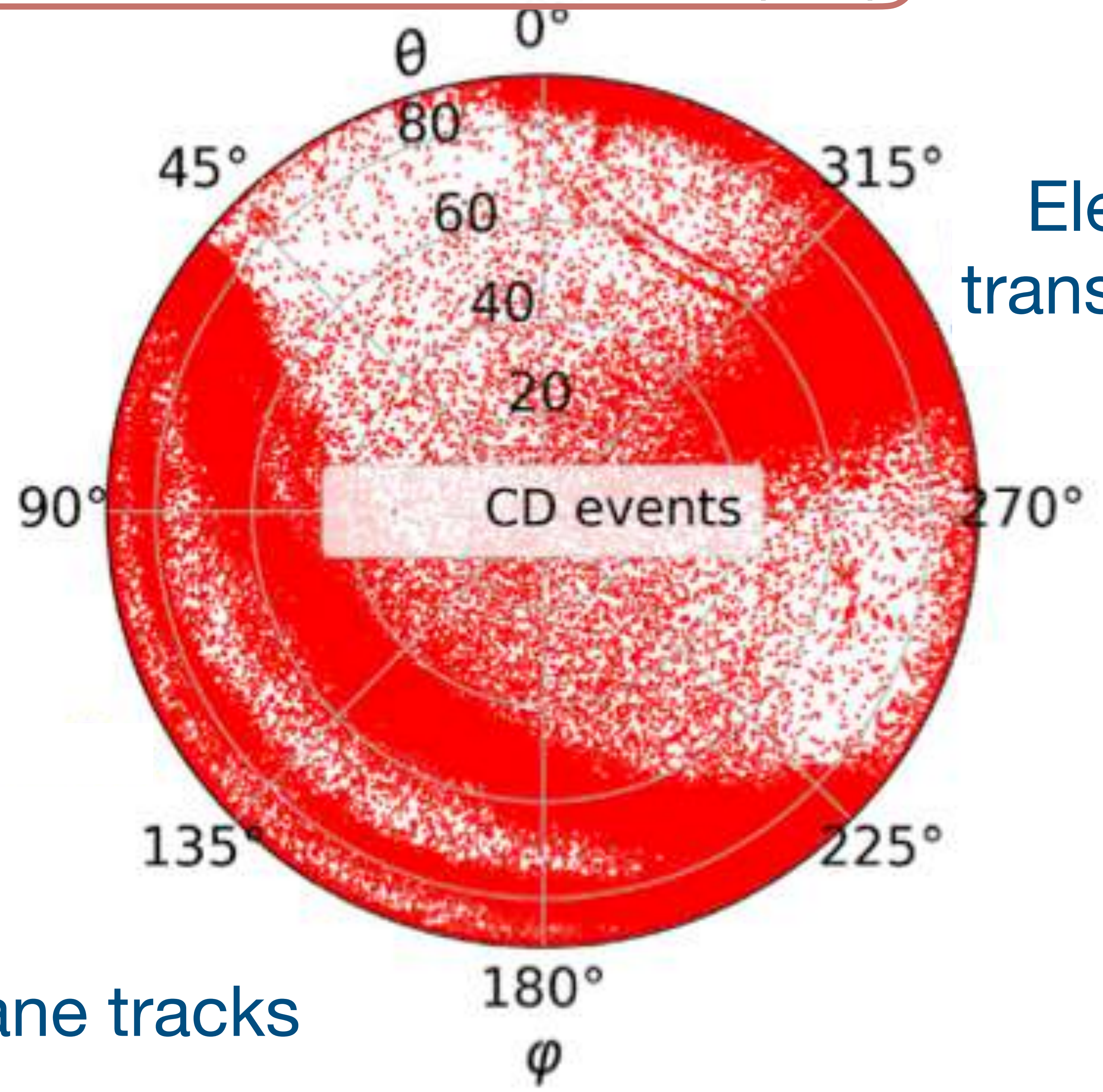

Electric transformer

Plane tracks

Lavoisier for the GRAND collaboration, ICRC proc. 2025

Cosmic ray search

Coincident Data ← Trigger

↓

Cosmic ray search (cuts) → Electric field deconvolution → Reconstruction → Cosmic ray distribution

533,466 Coincident Data (CD)

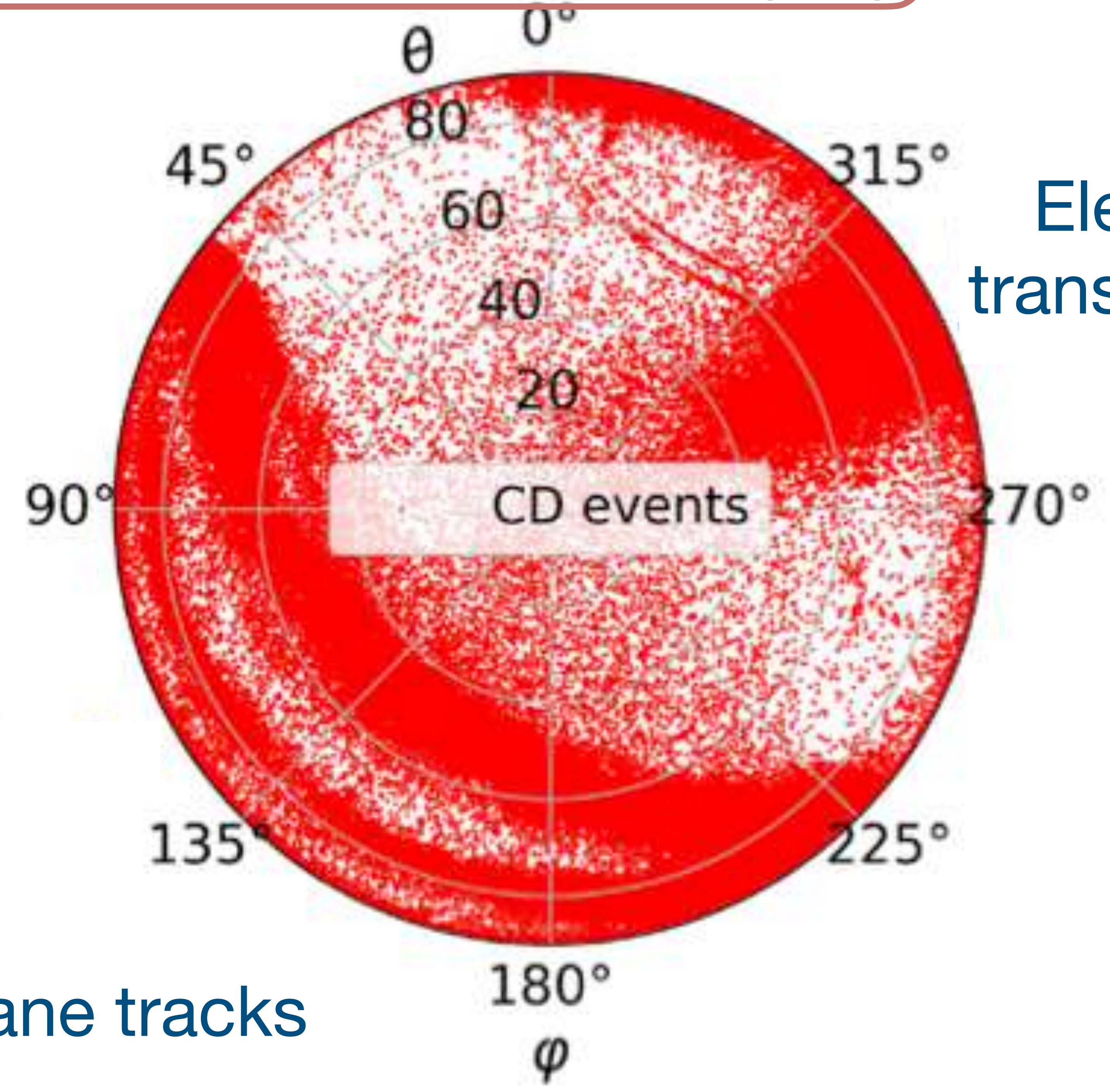

Electric transformer

Plane tracks

Clustering cut
Polarization cut
Visual cuts (footprint)

41 cosmic-ray candidates

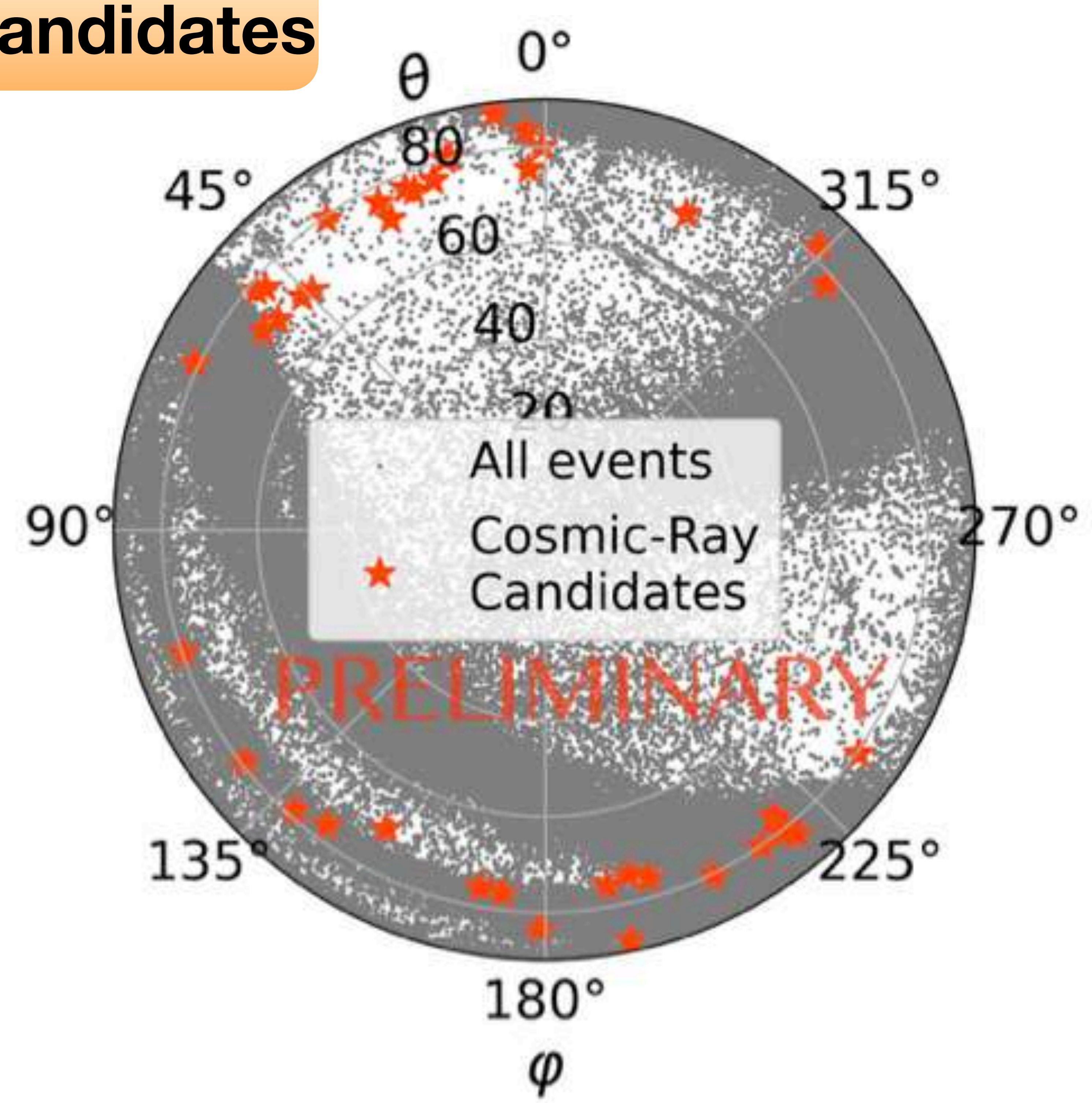

Lavoisier for the GRAND collaboration, ICRC proc. 2025

Refining the cosmic ray selection with ADF

Guelfand *for the GRAND collaboration, ICRC proc. 2025, arXiv:2507.04324*

Coincident Data ← Trigger

↓

Cosmic ray search (cuts) → Electric field deconvolution → Reconstruction → Cosmic ray distribution

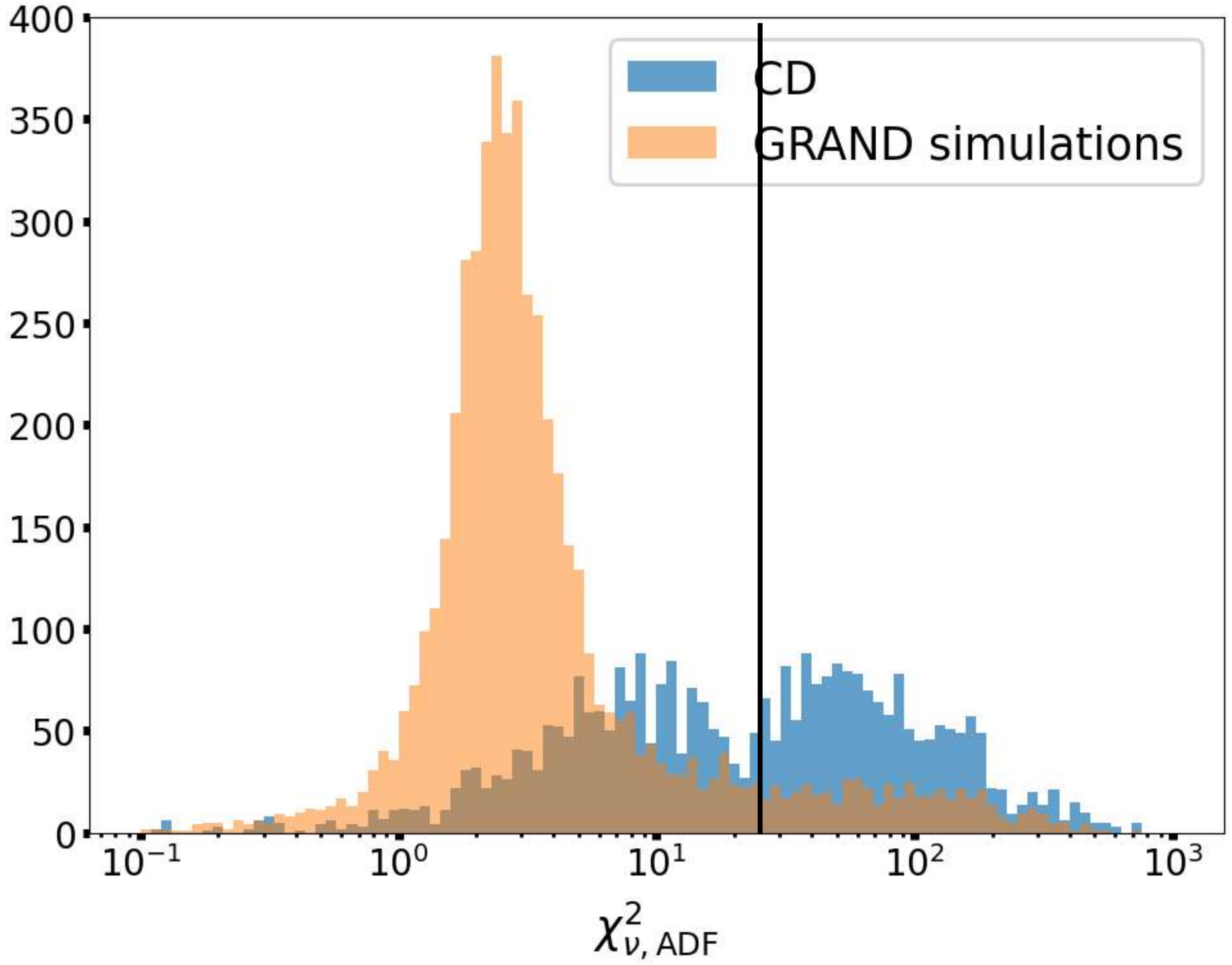

41 cosmic-ray candidates

↓

ADF model: **refine selection** using **amplitude Cherenkov enhancement: strong signature of radio signal induced by cosmic particles**

↓

29 cosmic-ray candidates ($\chi^2_\nu \leq$ 25)

ADF model: from Electric Field to Voltage

Coincident Data ← Trigger

Cosmic ray search (cuts) → Electric field deconvolution → Reconstruction → Cosmic ray distribution

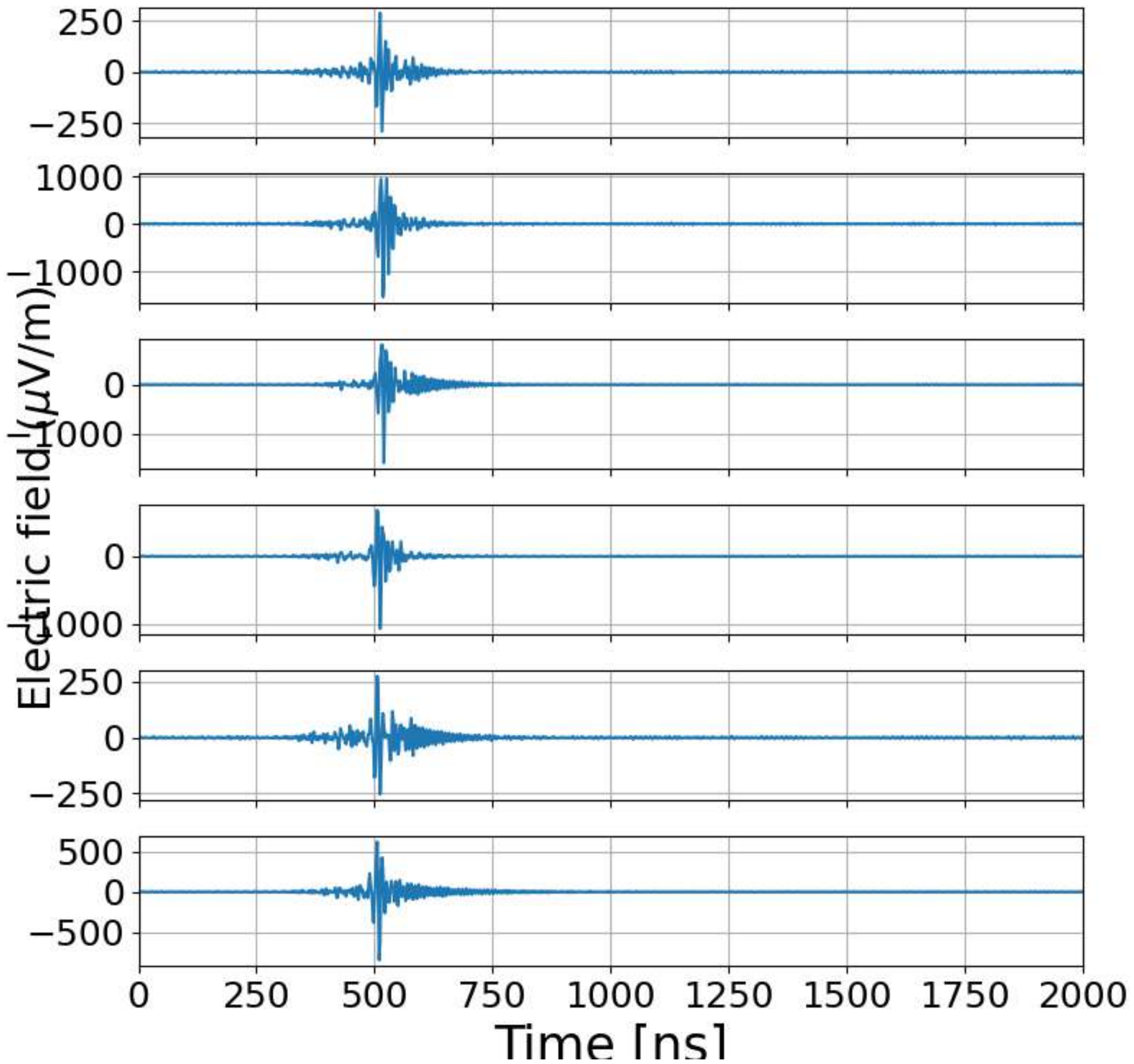

Motivations: reconstruction directly from raw detector data

Bypass electric field deconvolution

- Not robust
- Only one method: no crosscheck

Zhang for the GRAND collaboration , ICRC proc. 2025

ADF model: from Electric Field to Voltage

Guelfand *for the GRAND collaboration,*
ICRC proc. 2025, arXiv:2507.04324

Coincident Data ← Trigger

Cosmic ray search (cuts) → Electric field deconvolution → **Reconstruction** → Cosmic ray distribution

$$V(\nu) = \overrightarrow{\ell}(\theta, \phi, \nu) \, . \, \overrightarrow{E}(\nu)$$

Electric field

Voltage

Antenna effective length (response)

ADC amplitude distribution:
Almost uniform between antennas
‣ Reconstruction on raw ADC data

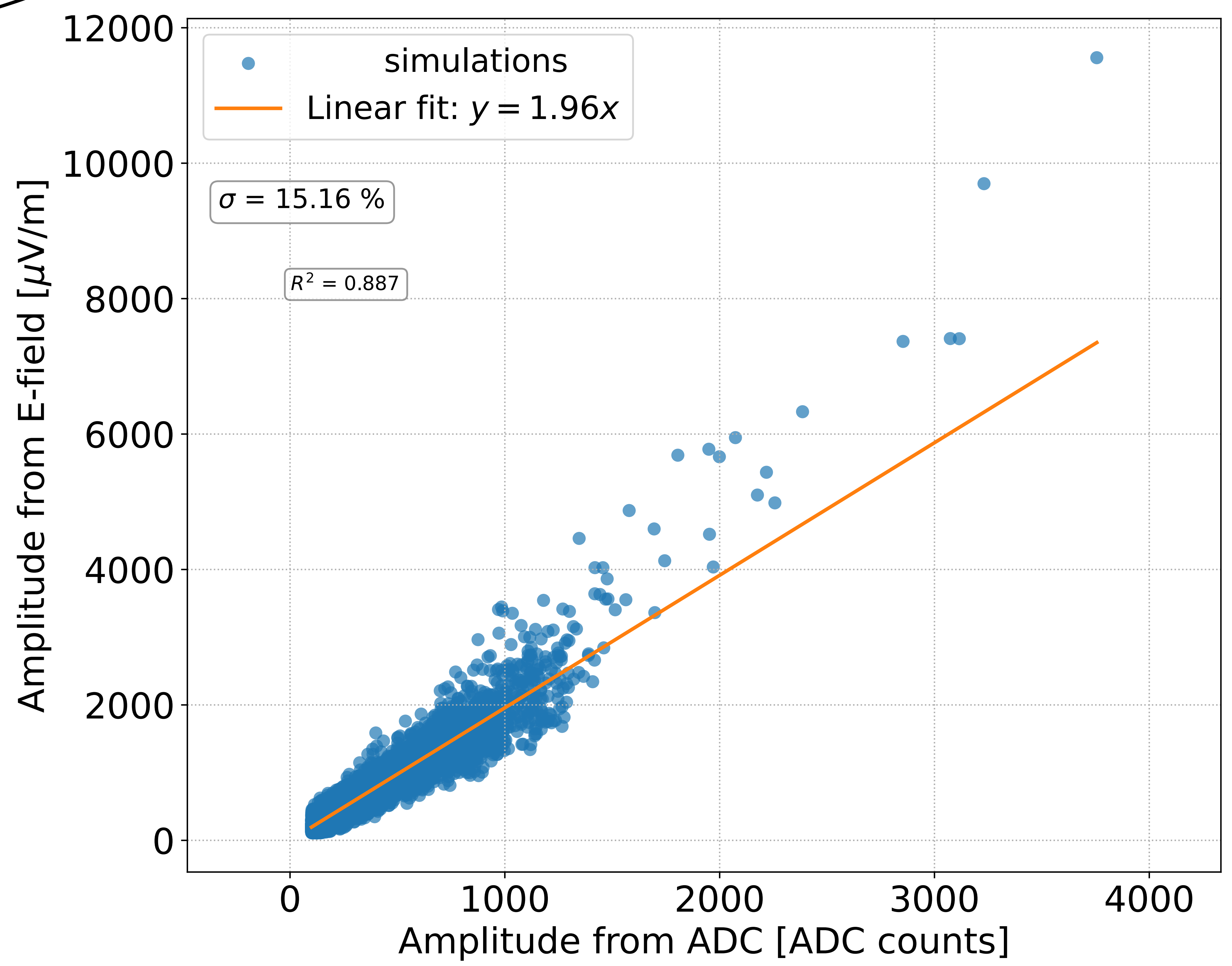

Reconstruction of cosmic-ray candidate

__Guelfand__ for the GRAND collaboration,
ICRC proc. 2025, arXiv:2507.04324

$\theta = 78.25^\circ, \phi = 137.76^\circ$

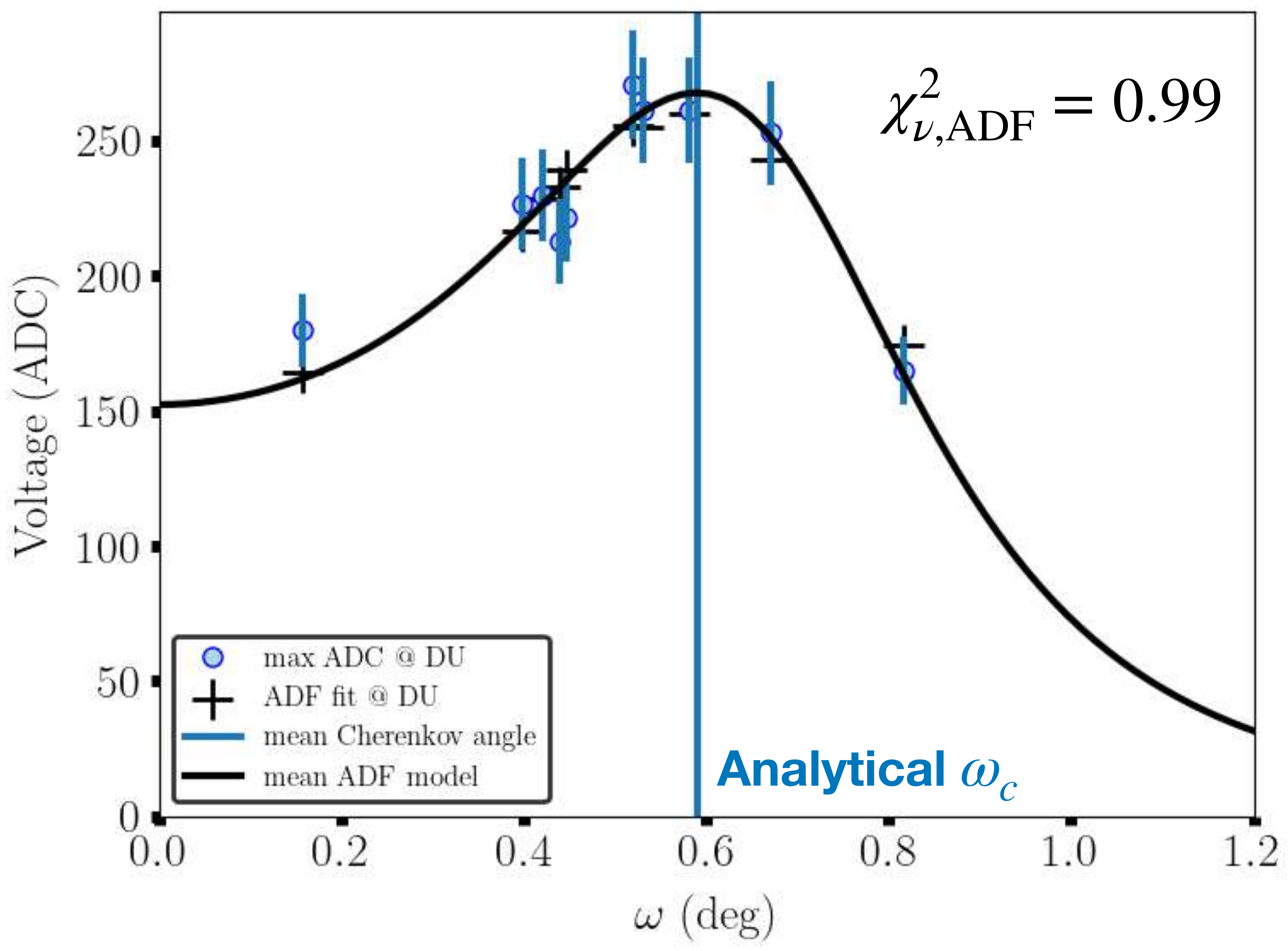

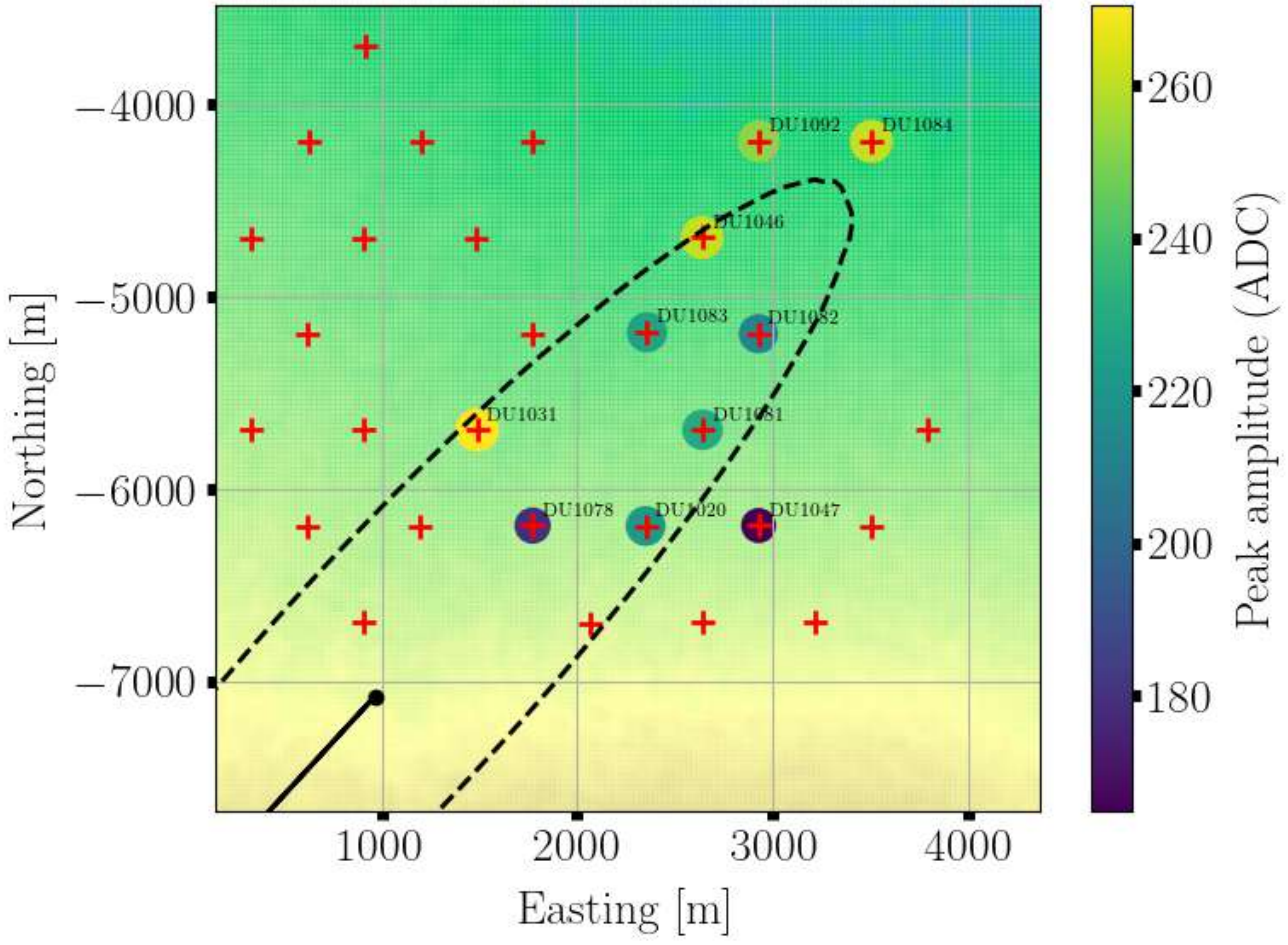

10 triggered antennas
Cherenkov enhancement: clear signature of EAS radio signal

Reconstruction of cosmic-ray candidate

__Guelfand__ for the GRAND collaboration,
ICRC proc. 2025, arXiv:2507.04324

$\theta = 78.25^\circ, \phi = 137.76^\circ$

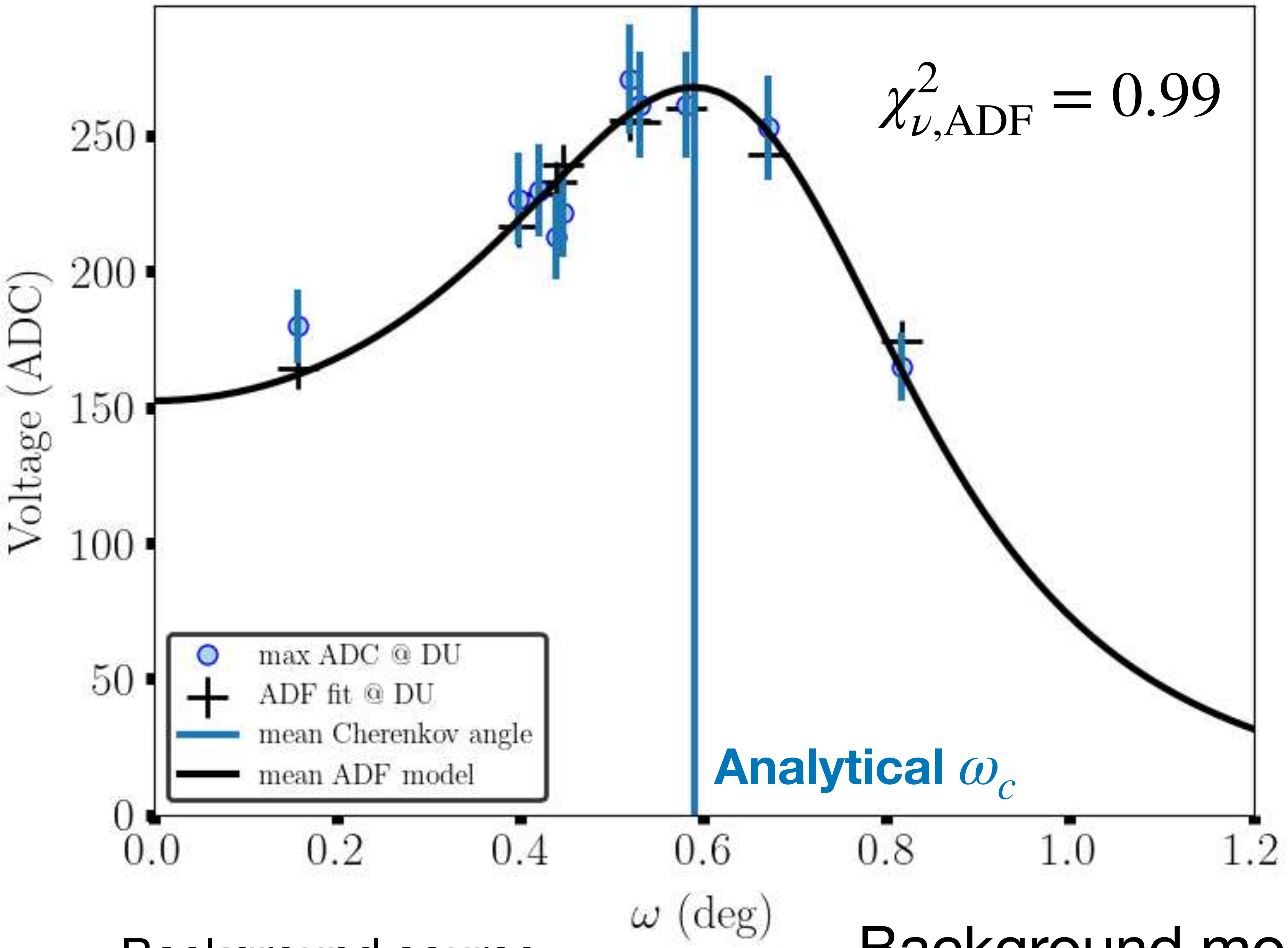

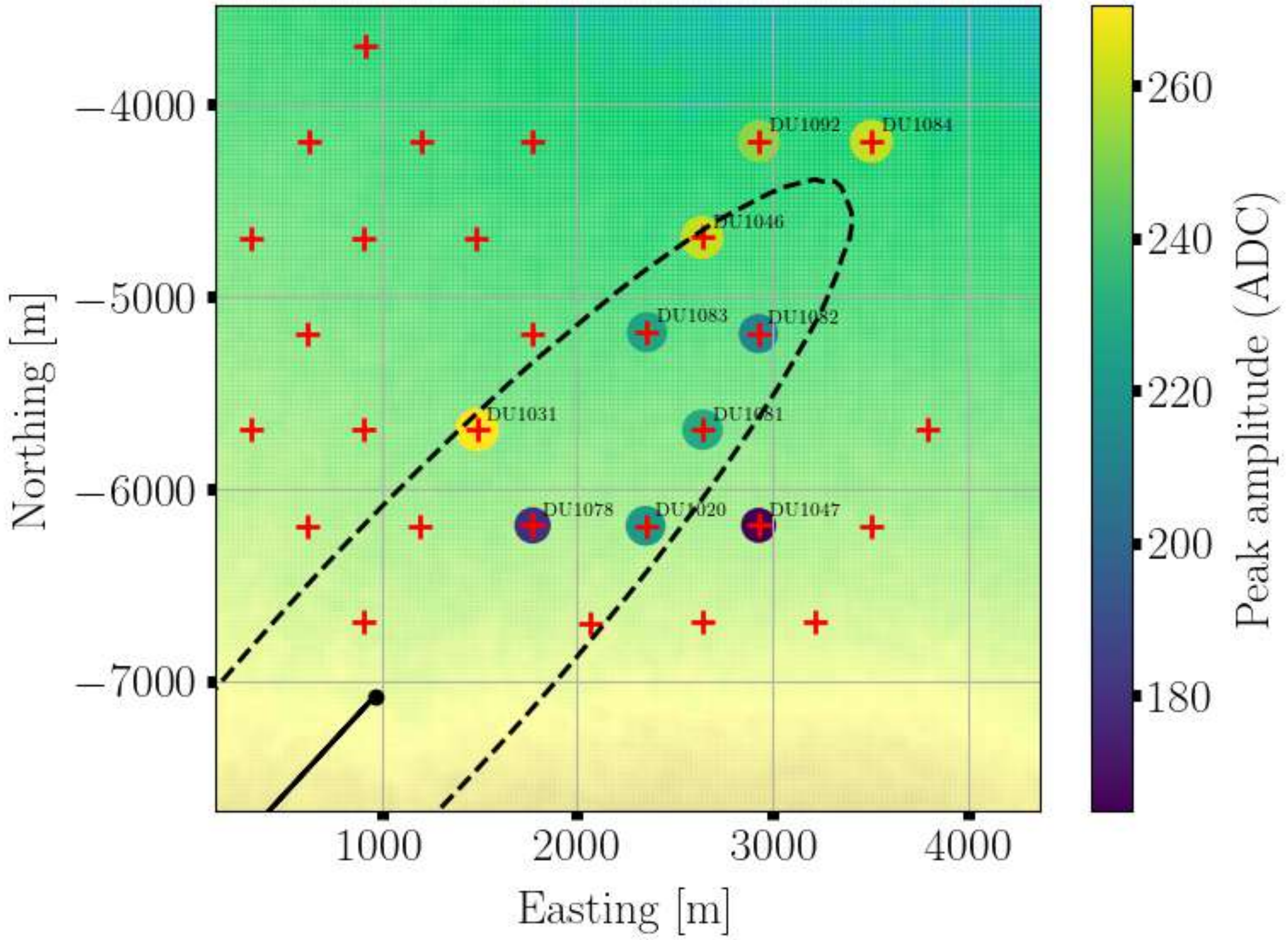

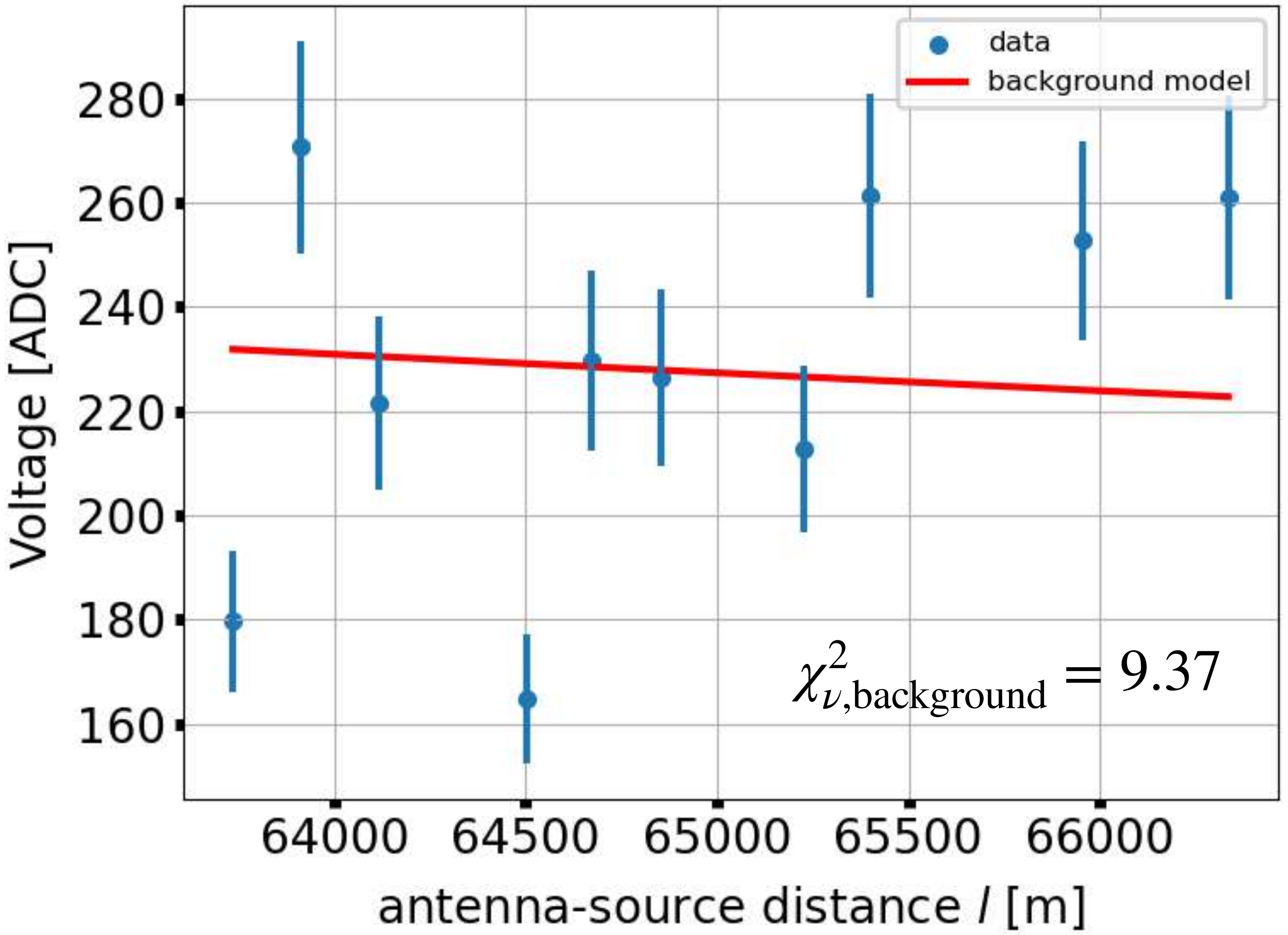

Background source
at X_{source} (from SWF)

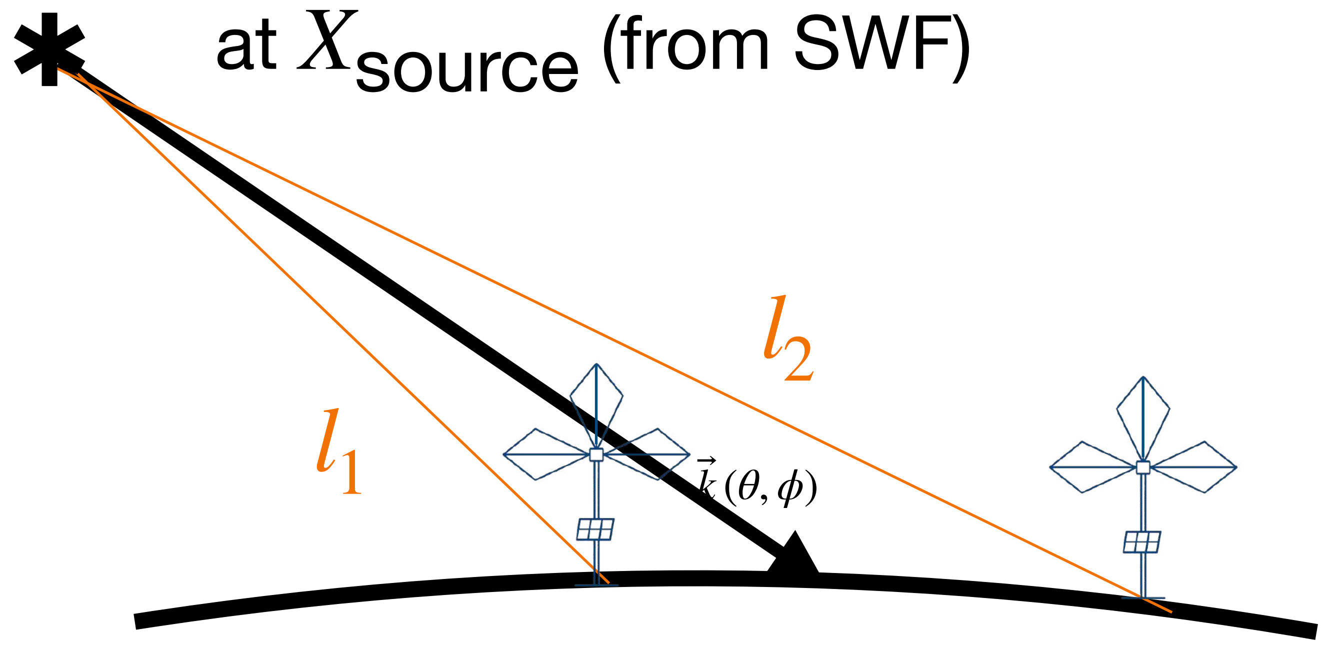

Background model (isotropic emission): $A = \kappa / l$

Free parameter

Reconstruction of cosmic-ray candidate

__Guelfand__ for the GRAND collaboration,
ICRC proc. 2025, arXiv:2507.04324

$$\theta = 76.8°, \phi = 195.9°$$

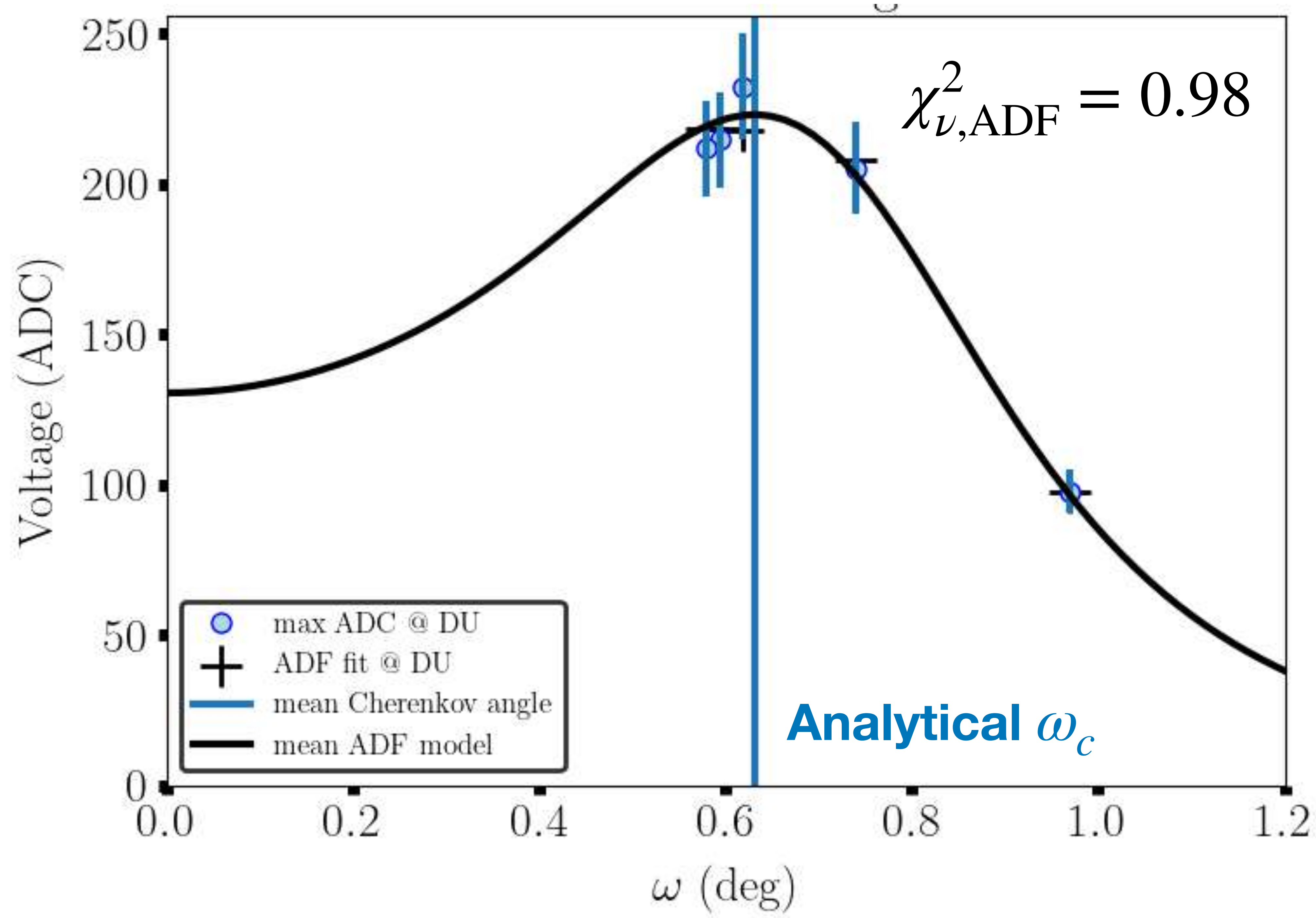

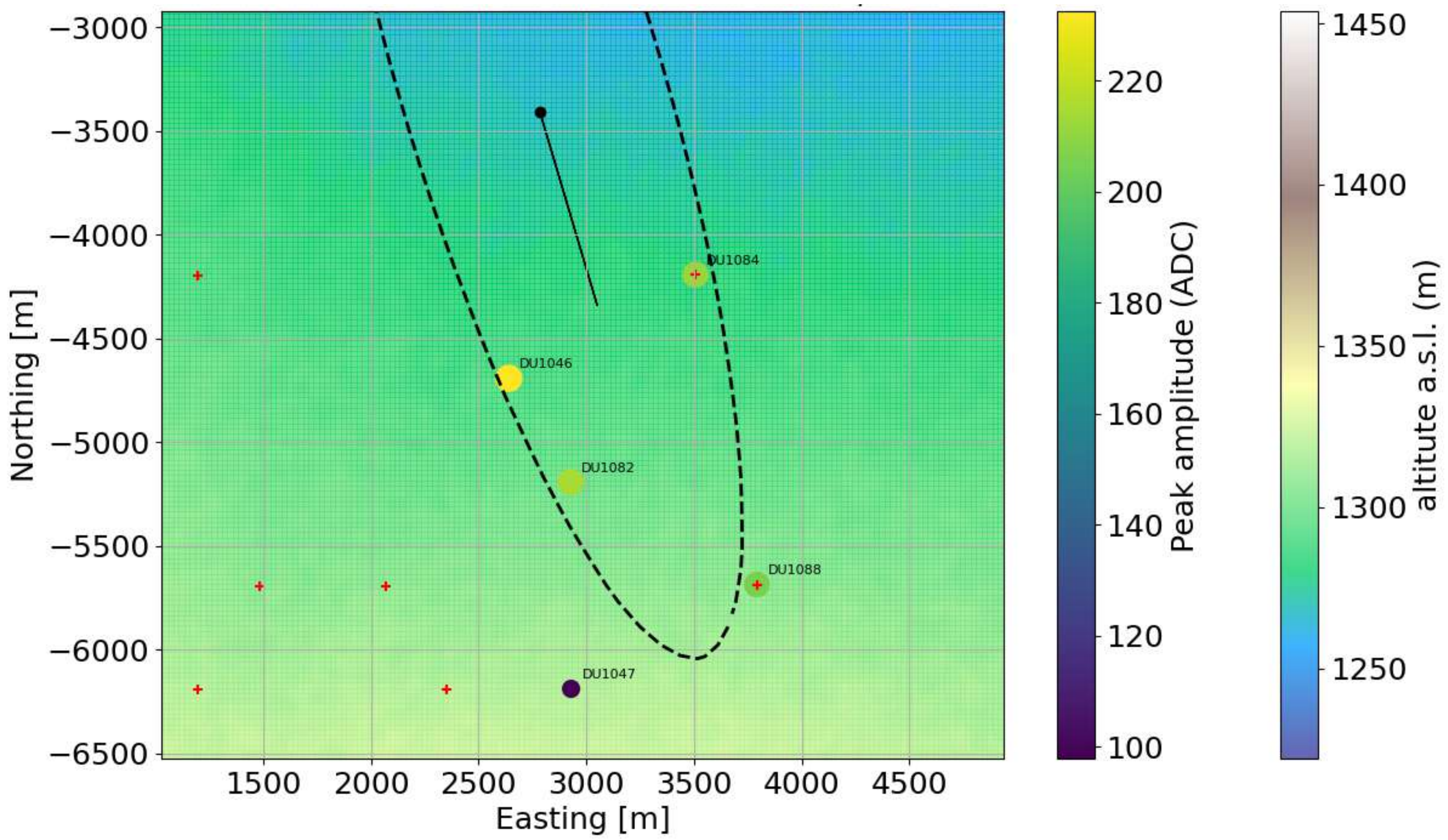

Background source
at X_{source} (from SWF)

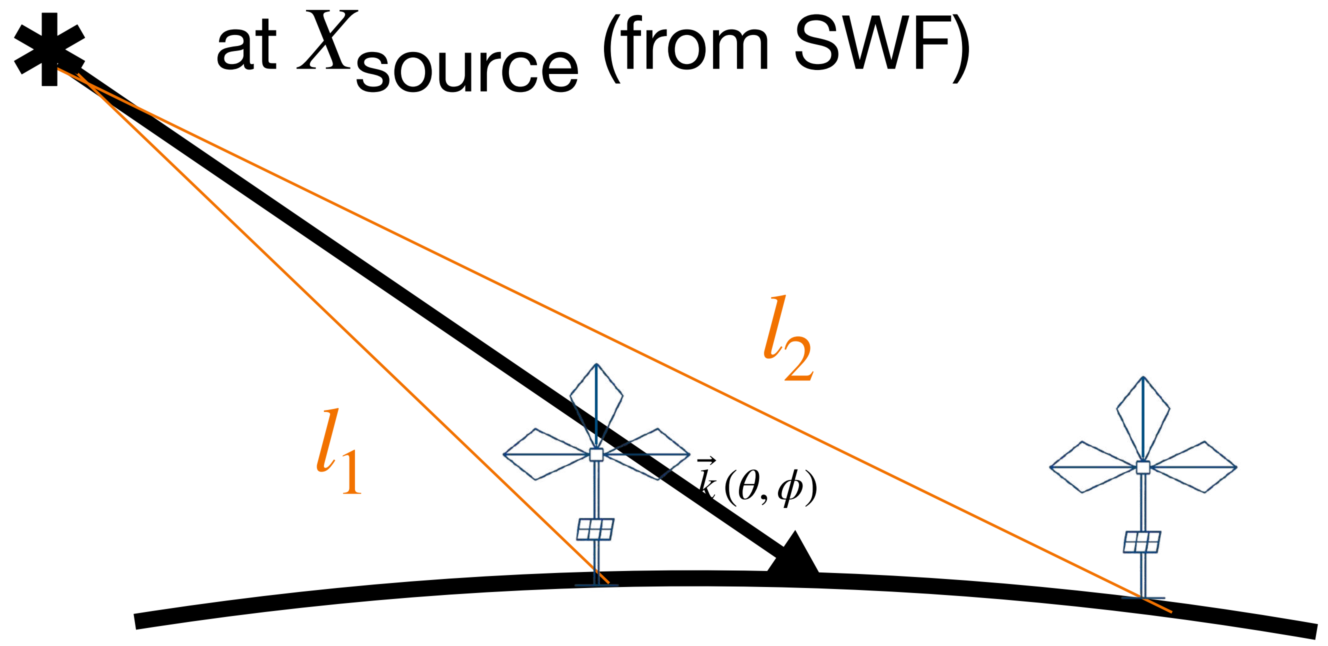

Background model (isotropic emission): $A = \kappa / l$

Free parameter

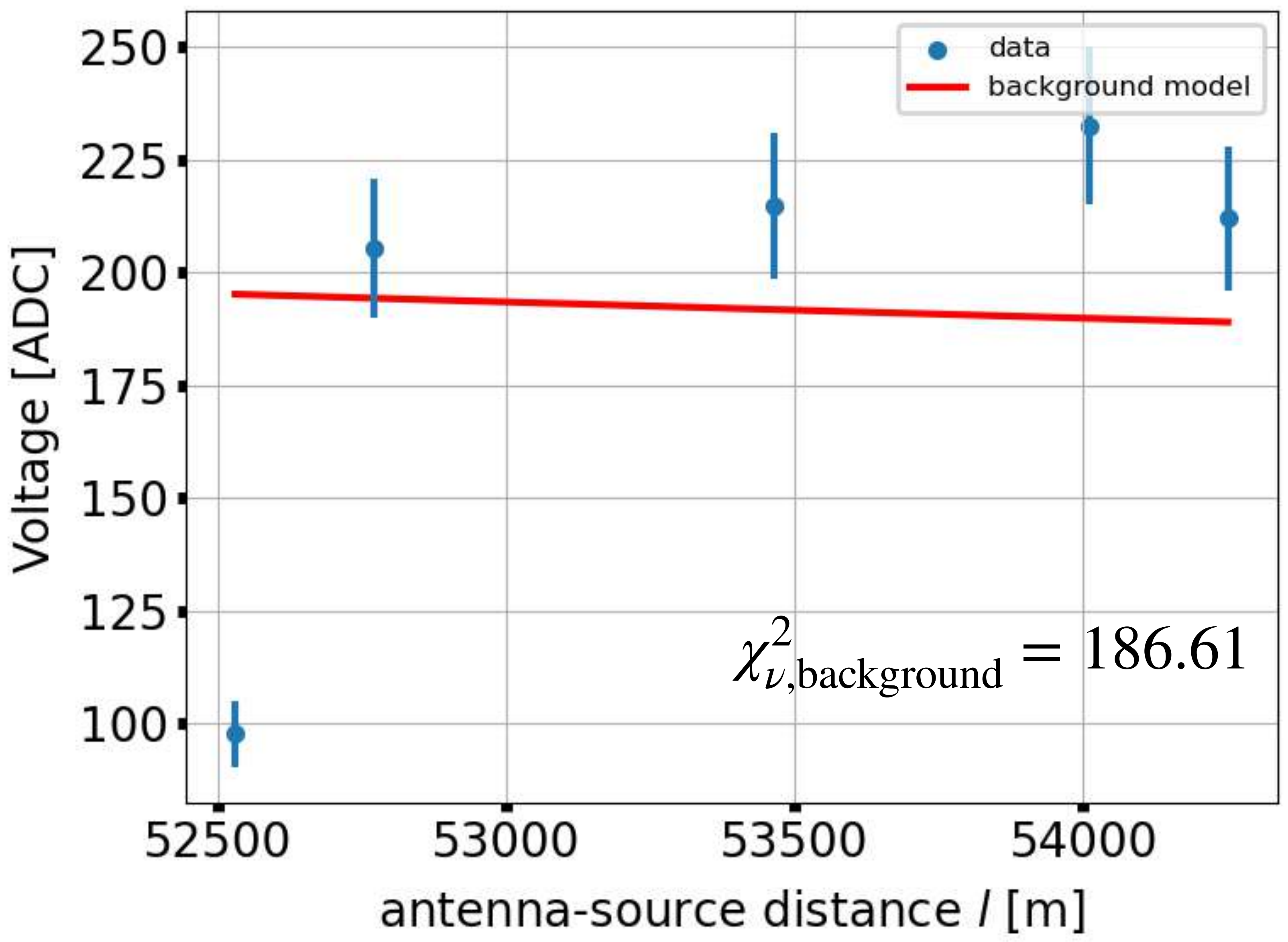

Candidate not passing ADF selection criteria

***Guelfand** for the GRAND collaboration,*
ICRC proc. 2025, arXiv:2507.04324

$\theta = 80.8^\circ, \phi = 178.5^\circ$

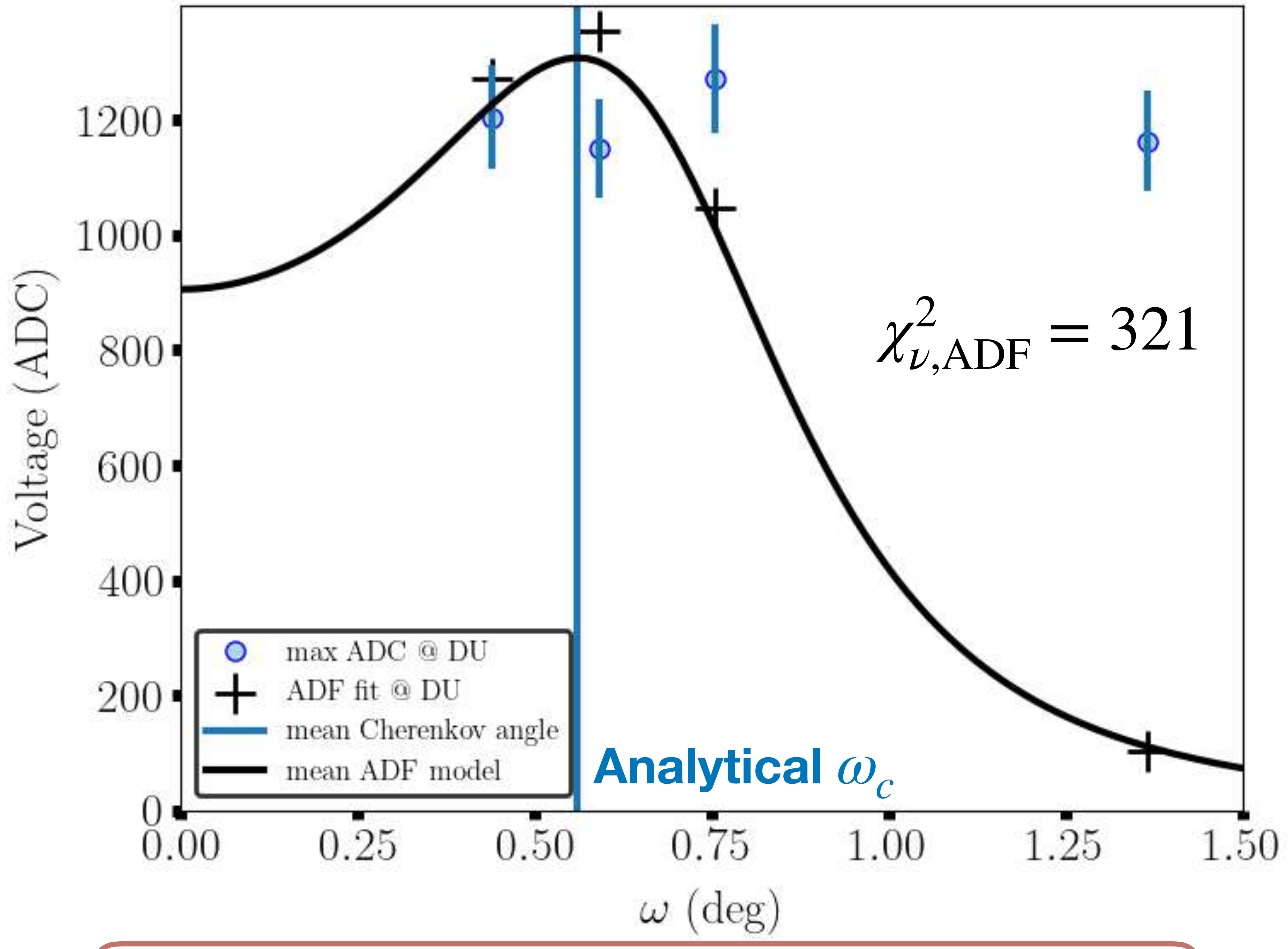

Amplitudes very similar along all antennas
Tagged as background event

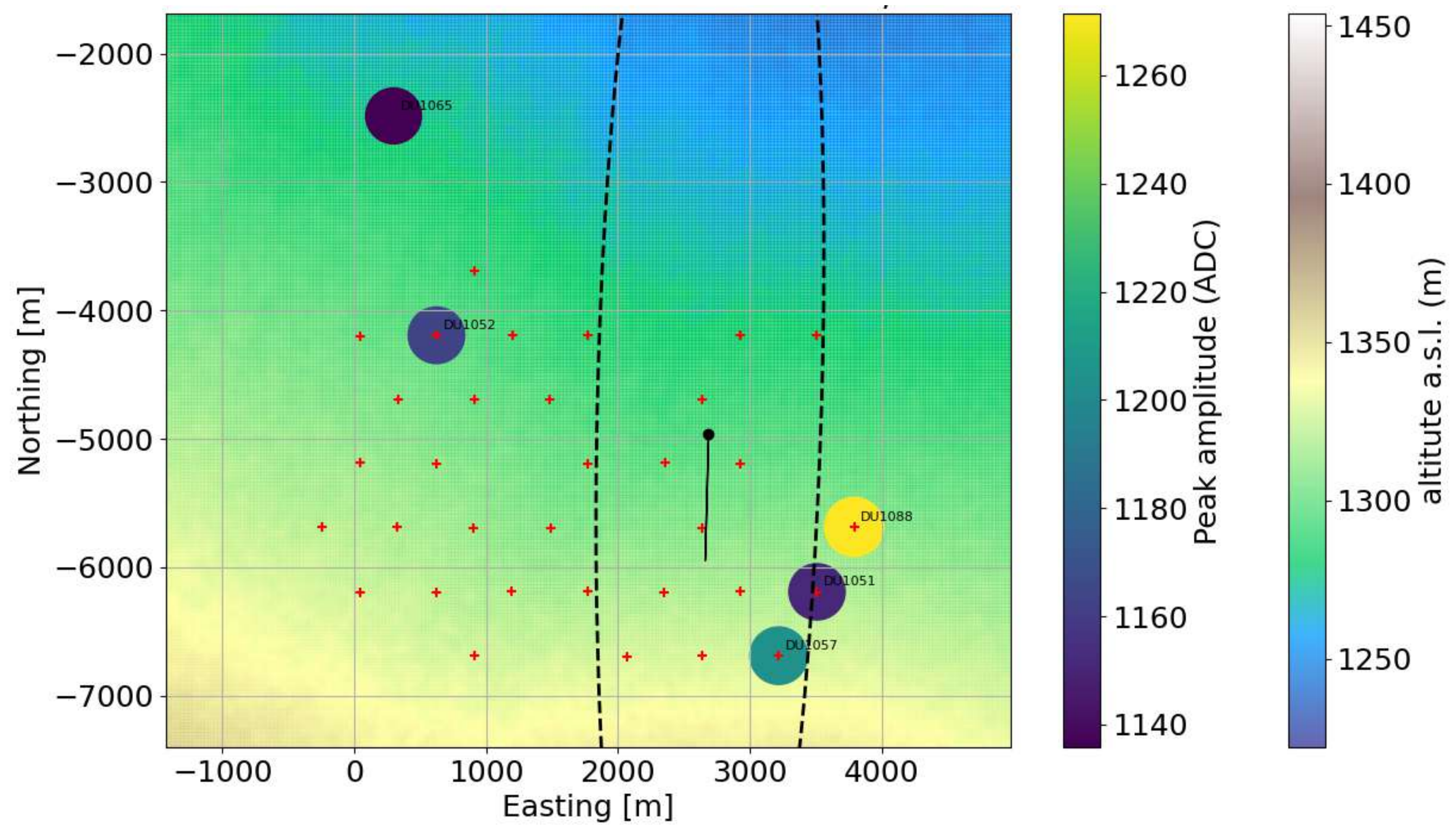

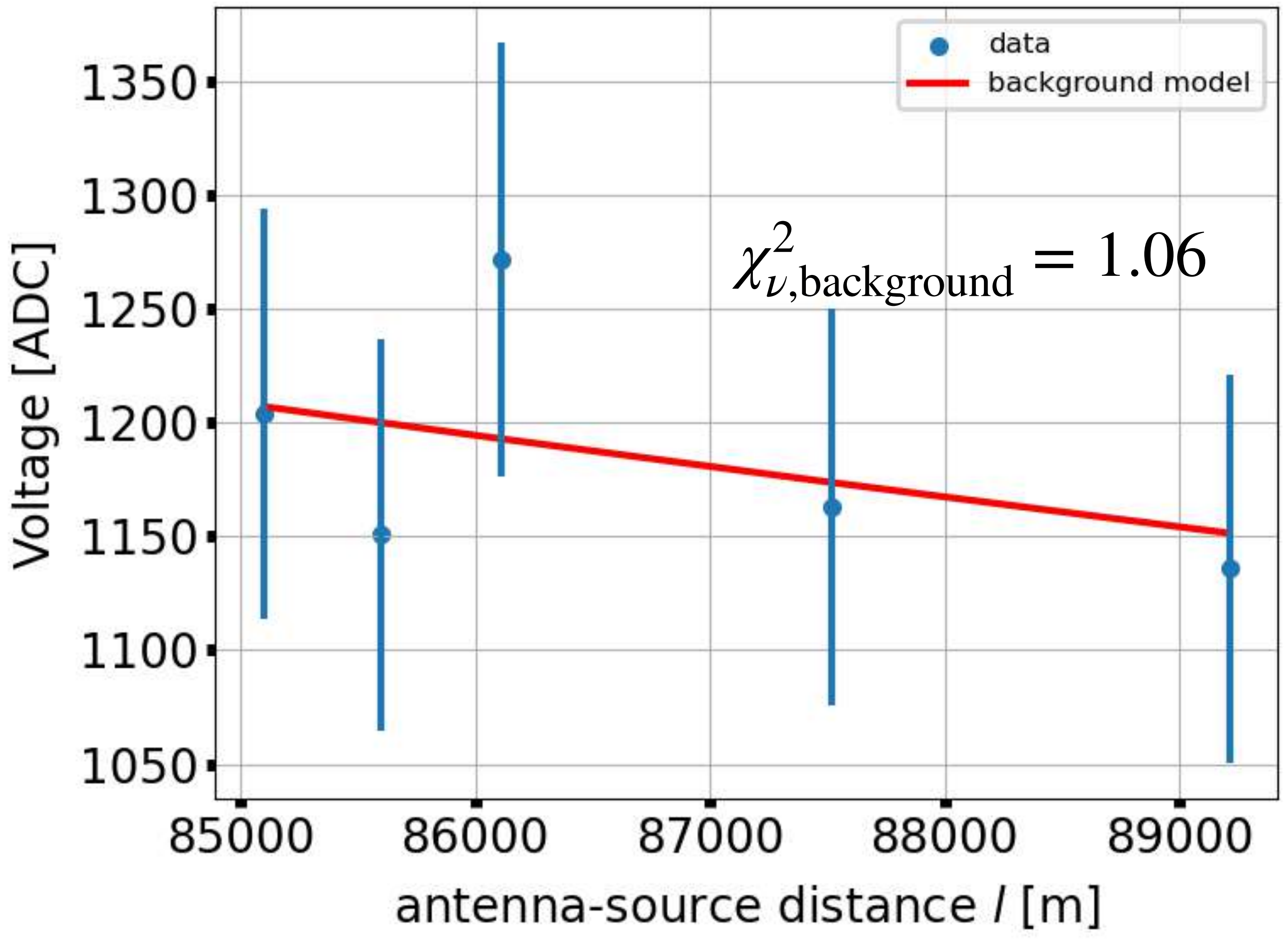

Reconstruction of cosmic-ray candidates

Arrival direction and energy reconstruction with voltage data
Three energy reconstruction methods in the collaboration: cross-check
Energy range consistent with expectations
Very preliminary results: no calibration

End of the commissioning phase
Next step: **build GRANDProto300 energy spectrum**

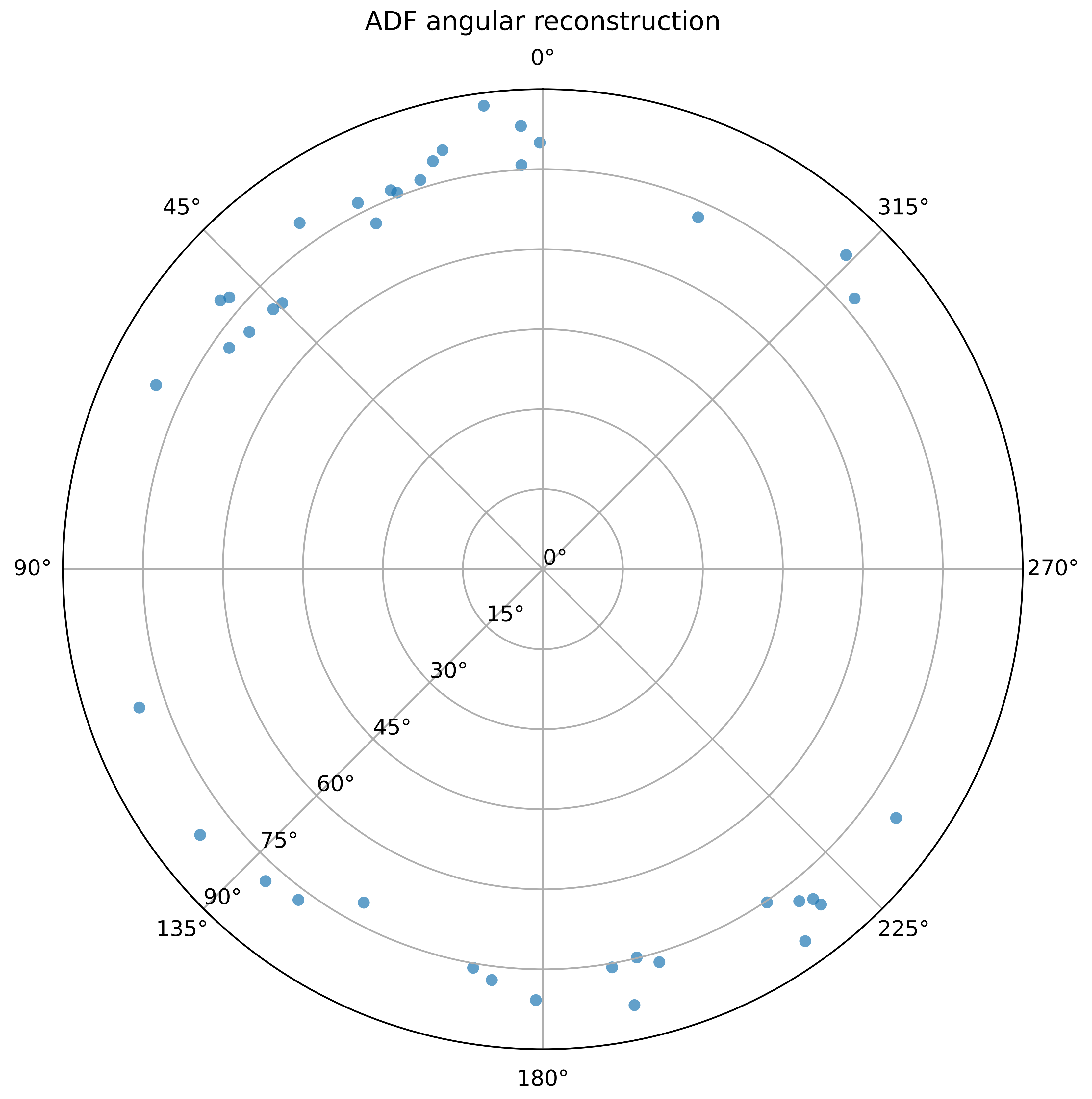

***Guelfand** for the GRAND collaboration, ICRC proc. 2025, arXiv:2507.04324*

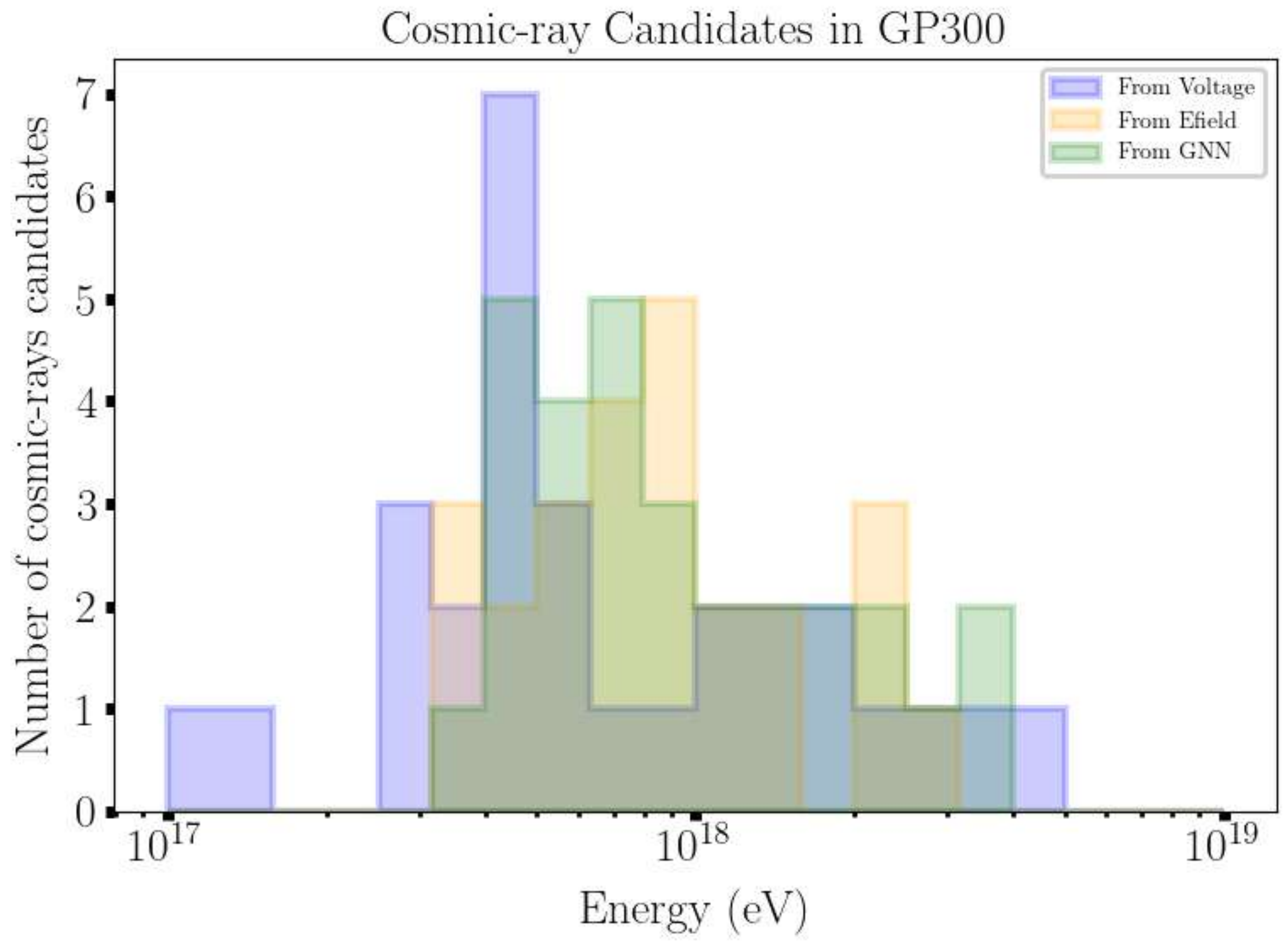

***Martineau** for the GRAND collaboration, ICRC proc. 2025*

Conclusion

What is the origin of UHECRs?
Radio antennas: ideal detector (vast surfaces to probe low fluxes)
Prototype: GRANDProto300: Validate detection principle & reconstruction of first commissioning data

I.Physical modeling of very inclined showers and their radio emission

II. Autonomous trigger: find the radio signal inside the noise

III. Reconstruction of cosmic particle properties for very inclined showers

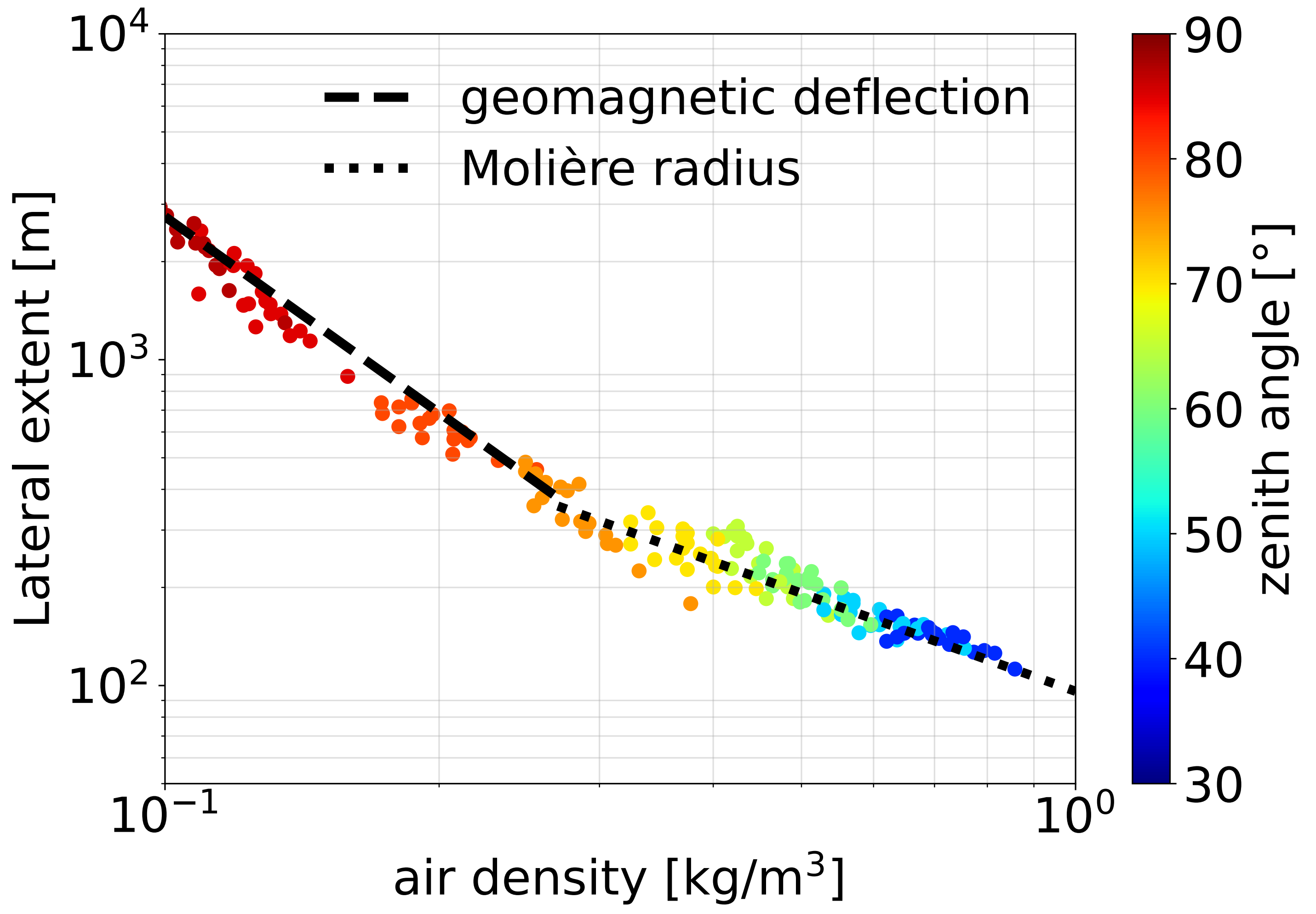

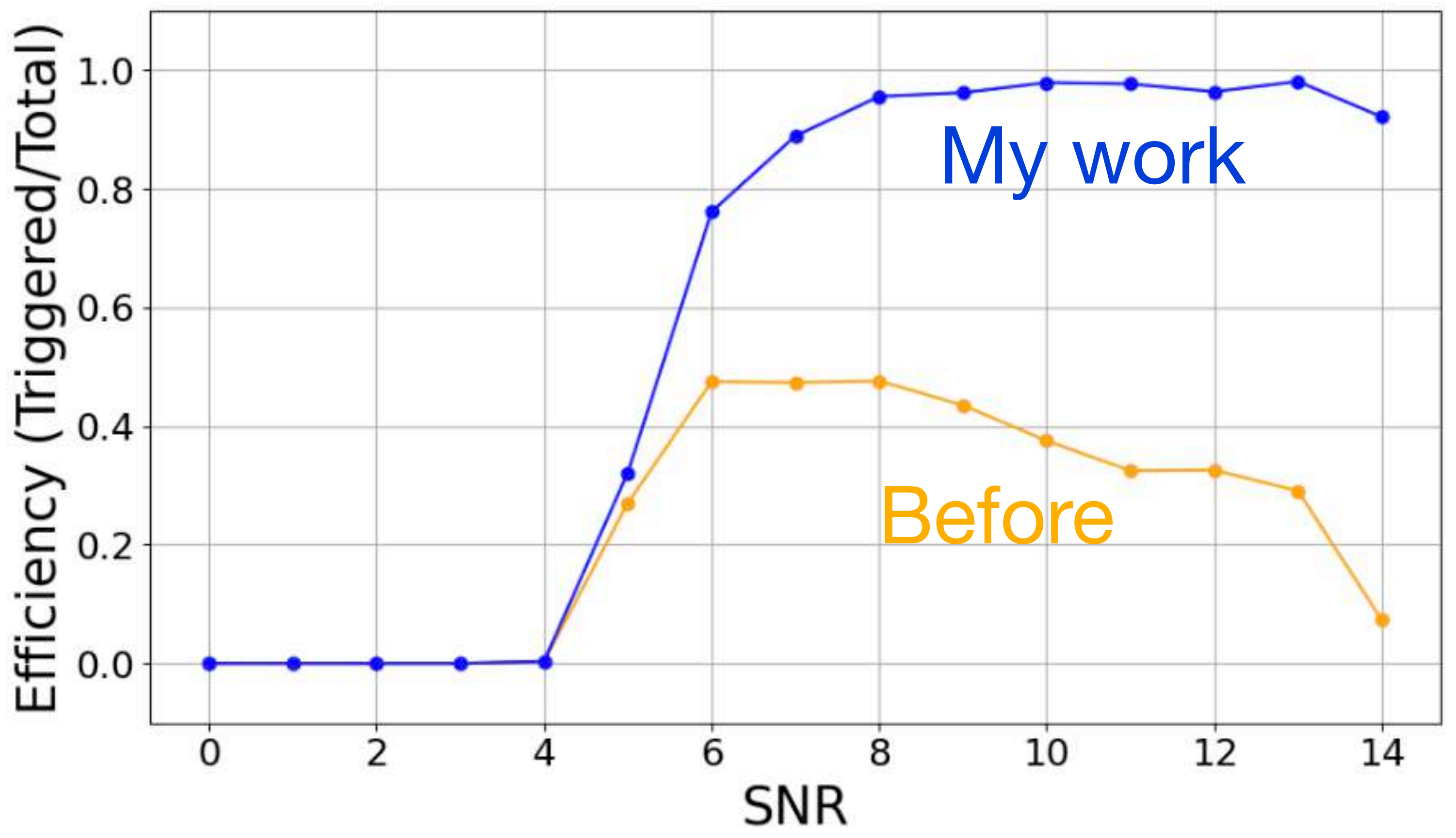

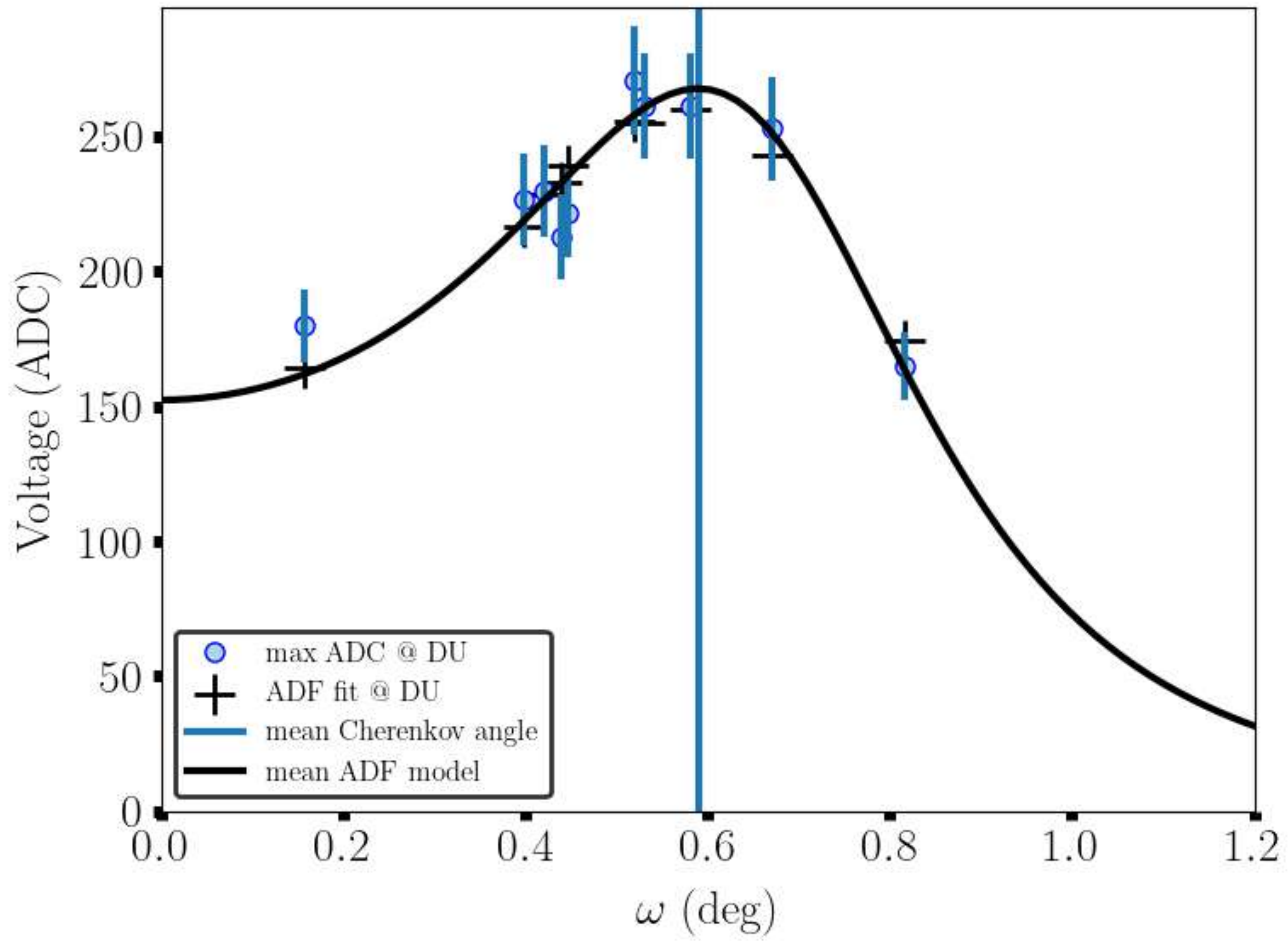

Better understanding of very inclined air showers & develop tools for data acquisition and analysis
Validation on first commissioning data: 29 cosmic-ray candidates!
GRANDProto300 now enters operational phase & GRAND enters R&D phase for the next stage

Backup slides

Alves Batista et al., 2019

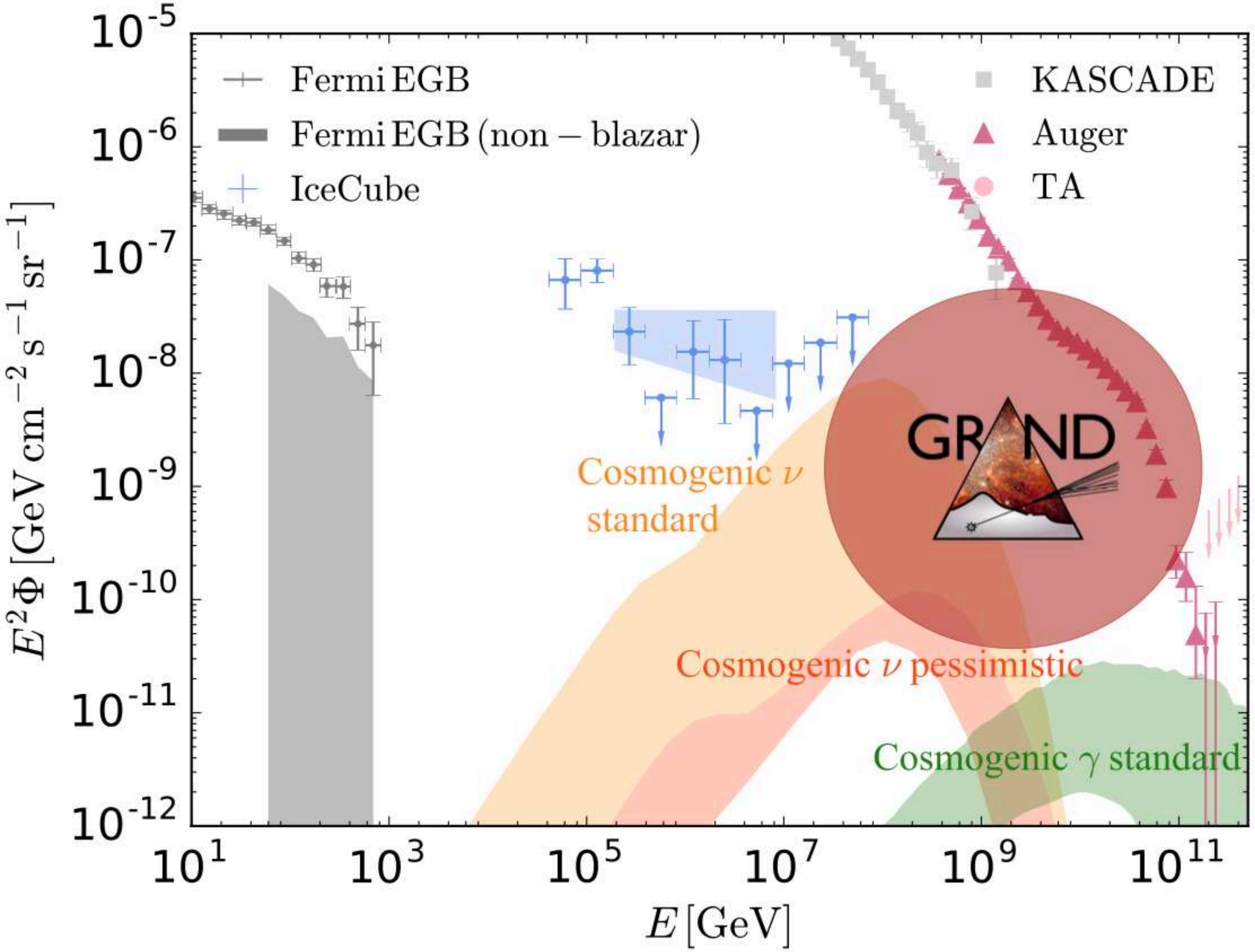

$$p + \gamma \rightarrow \Delta^+ \rightarrow p + \pi^0 \rightarrow p + \gamma\gamma,$$

$$p + \gamma \rightarrow \Delta^+ \rightarrow n + \pi^+ \rightarrow p + \nu_{e,\mu}$$

__Kotera__ et al, submitted to JCAP, arXiv:2504.08973

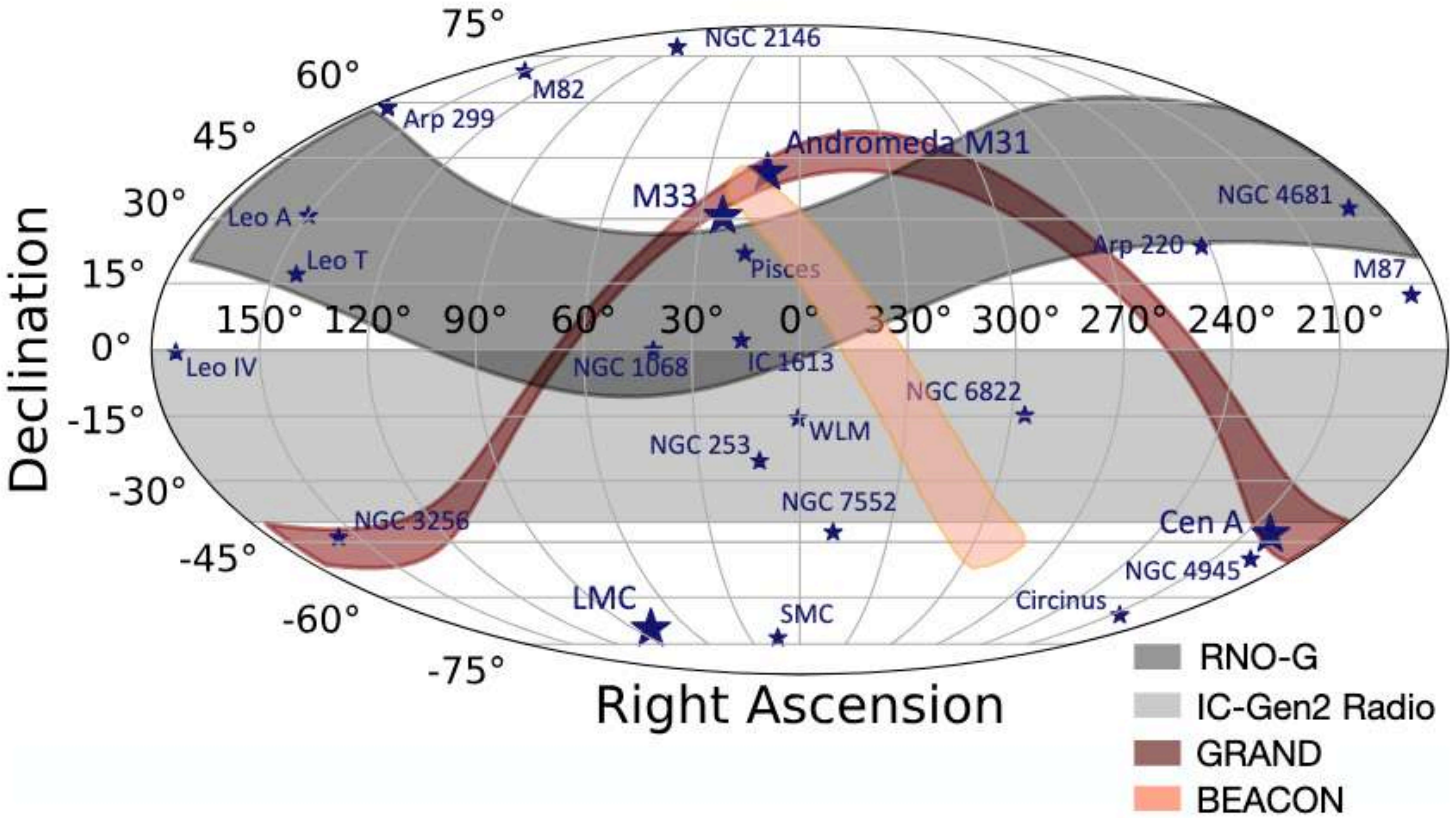

__Alvarez-Muniz__ et al, Sci. China-Phys, 2019

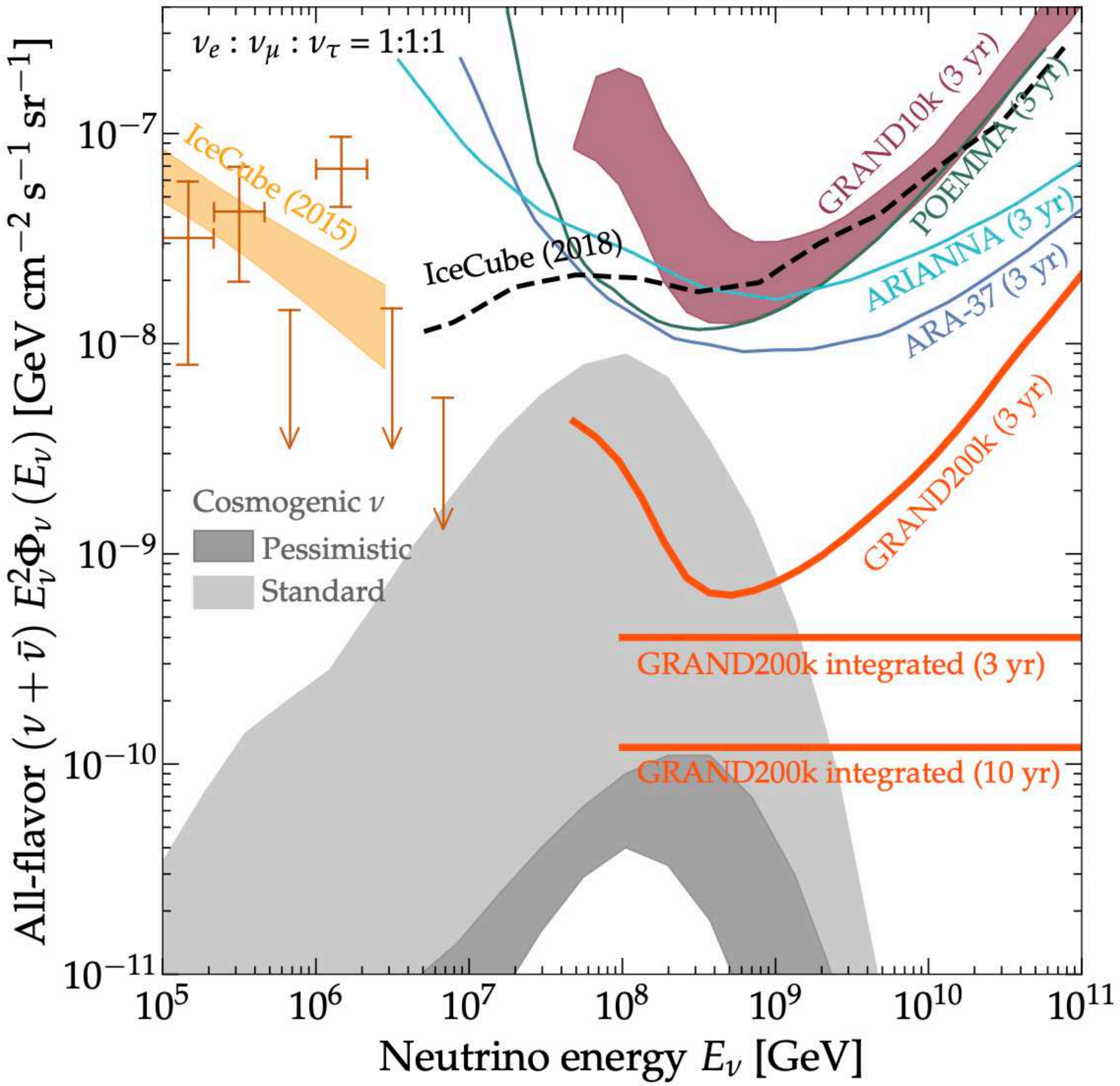

Guépin et al, Nature Reviews Physics, 2025

2021 2025 >2030	Minimum energy	Peak energy	Differential sensitivity limit [u.l.]	iFoV	dFoV	ang. res.
ANITA	0.1 EeV	100 EeV	[2.4×10^{-7} GeV cm^{-2} s^{-1} sr^{-1} in 24 d]	6% [7°×360°]	19% [26°×360°]	2.8°
PUEO	0.1 EeV	20 EeV	4.2×10^{-8} GeV cm^{-2} s^{-1} sr^{-1} in 30 d	6 %	20 %	<2.8°
ARA	10 PeV	1–3 EeV	3.6×10^{-9} GeV cm^{-2} s^{-1} sr^{-1} by 2030	35 %	35 %	5°
RNO-G	50 PeV	1 EeV	5×10^{-9} GeV cm^{-2} s^{-1} sr^{-1} in 10 yr	30% [45°×360°]	>50%	2°×10°
ARIANNA-200	30 PeV	1 EeV	4×10^{-9} GeV cm^{-2} s^{-1} sr^{-1} in 10 yr	50 %	>50%	2.9–3.8°
BEACON	30 PeV	1 EeV	6×10^{-9} GeV cm^{-2} s^{-1} sr^{-1} in 10 yr	6 %	19.5%	0.3°–1°
Auger	50 PeV	0.3–1 EeV	[1.5×10^{-8} GeV cm^{-2} s^{-1} sr^{-1} in 2019]	30 %	92.8%	<1°
POEMMA Cerenkov	10 PeV	0.5 EeV	3.5×10^{-8} GeV cm^{-2} s^{-1} sr^{-1} in 10 yr	0.6 %	18–36%	0.4°
fluorescence	10 EeV	100 EeV	1.5×10^{-9} GeV cm^{-2} s^{-1} sr^{-1} in 10 yr	?	?	1°
GRAND	50 PeV	0.4 EeV	2×10^{-10} GeV cm^{-2} s^{-1} sr^{-1} in 10 yr	45 %	100 %	0.1°
IceCube-Gen2 Radio	10 PeV	0.3 EeV	2×10^{-10} GeV cm^{-2} s^{-1} sr^{-1} in 10 yr	43% [55°×360°]	43% [55°×360°]	2°×10°
Ashra-NTA	1 PeV	0.1 EeV	10^{-10} GeV cm^{-2} s^{-1} sr^{-1} in 10 yr	25% [30°×360°]	>80%	0.1°
Trinity	0.1 PeV	0.1 EeV	5×10^{-10} GeV cm^{-2} s^{-1} sr^{-1} in 10 yr	6% [7°×360°]	62 %	<1°
TAMBO	0.3 PeV	10 PeV	?	27 %	62 %	1°
RET-N	10 PeV	0.1 EeV	1.5×10^{-10} GeV cm^{-2} s^{-1} sr^{-1} in 10 yr	50 %	>50%	?
ANTARES up(cascade)	20 GeV(1 TeV)	50(100) TeV	[2×10^{-8} GeV cm^{-2} s^{-1} sr^{-1} in 11 yr] (up+casc.)	50%(100%)	75%(100%)	0.3-0.4°(3°)
IceCube up(cascade)	300 GeV	100 TeV	[1.5×10^{-8} GeV cm^{-2} s^{-1} sr^{-1} in 3 yr] (up+casc.)	54%(100%)	54%(100%)	0.4°(10°)
IceCube-Gen2 up(cascade)	5 TeV	300 TeV	2×10^{-8} GeV cm^{-2} s^{-1} sr^{-1} in < 90 d (up+casc.)	54%(100%)	54%(100%)	0.3°(10°)
KM3Net ARCA up(cascade)	100 GeV(1 TeV)	100(100) TeV	5.8×10^{-9} GeV cm^{-2} s^{-1} sr^{-1} in 1.5(1 yr)	50%(100%)	75%(100%)	0.1°(1.5°)
Baikal-GVD up(cascade)	100 GeV(1 TeV)	100(100) TeV	(5.4×10^{-8} GeV cm^{-2} s^{-1} sr^{-1} in 10 yr)	50%(100%)	72%(100%)	<1°(4.5°)
P-ONE up(cascade)	1 TeV	100 TeV	1.4×10^{-8} GeV cm^{-2} s^{-1} sr^{-1} in 2 yr	50%(100%)	73%(100%)	0.1°(1–3°)

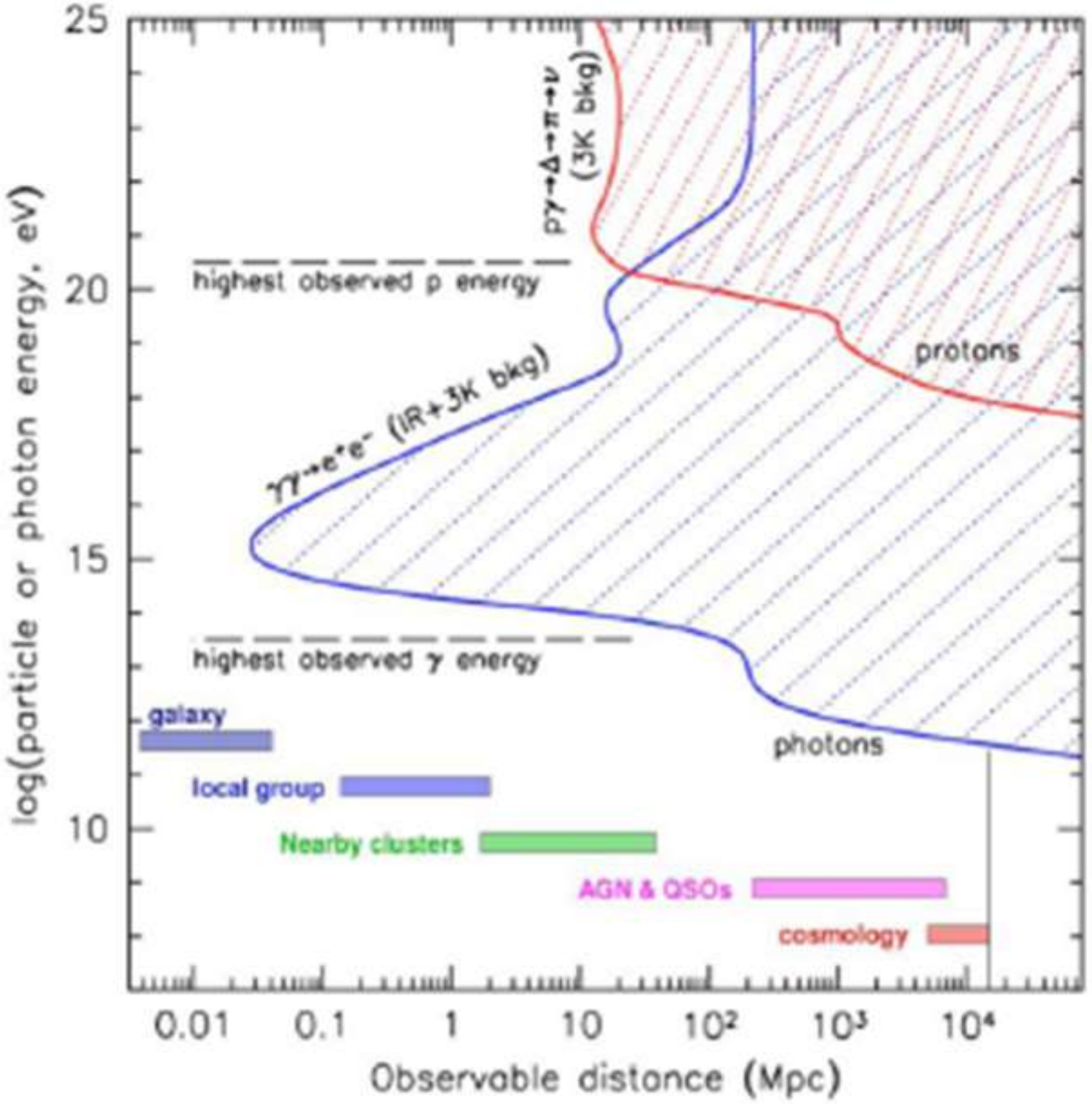

25
20
15
10
log(particle or photon energy, eV)
0.01
0.1
1
10
10^2
10^3
10^4
Observable distance (Mpc)
$p\gamma\to\Delta\to\pi\to\nu$ (3K bkg)
highest observed p energy
$\gamma\gamma\to e^+e^-$ (IR+3K bkg)
protons
highest observed γ energy
photons
galaxy
local group
Nearby clusters
AGN & QSOs
cosmology

Alvarez-Muniz et al, Astropart.Phys., 2015

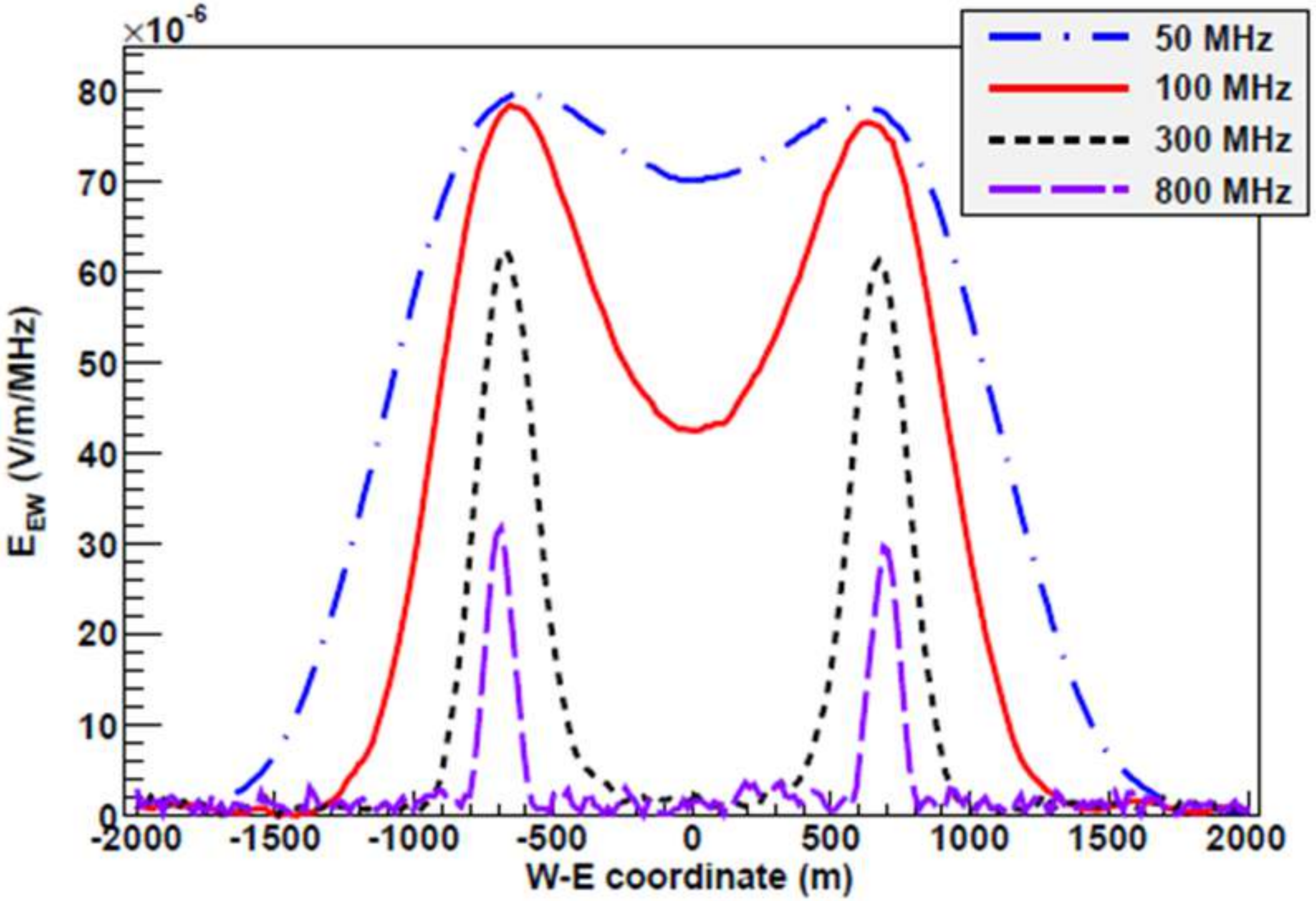

Digital Filtering

GRAND realistic simulations:
- Simulated electric fields with ZHAireS
- Process through simulated detector response
- Add **measured noise** on GP300 site
- Digital filtering: Finite Impulse Response (FIR)

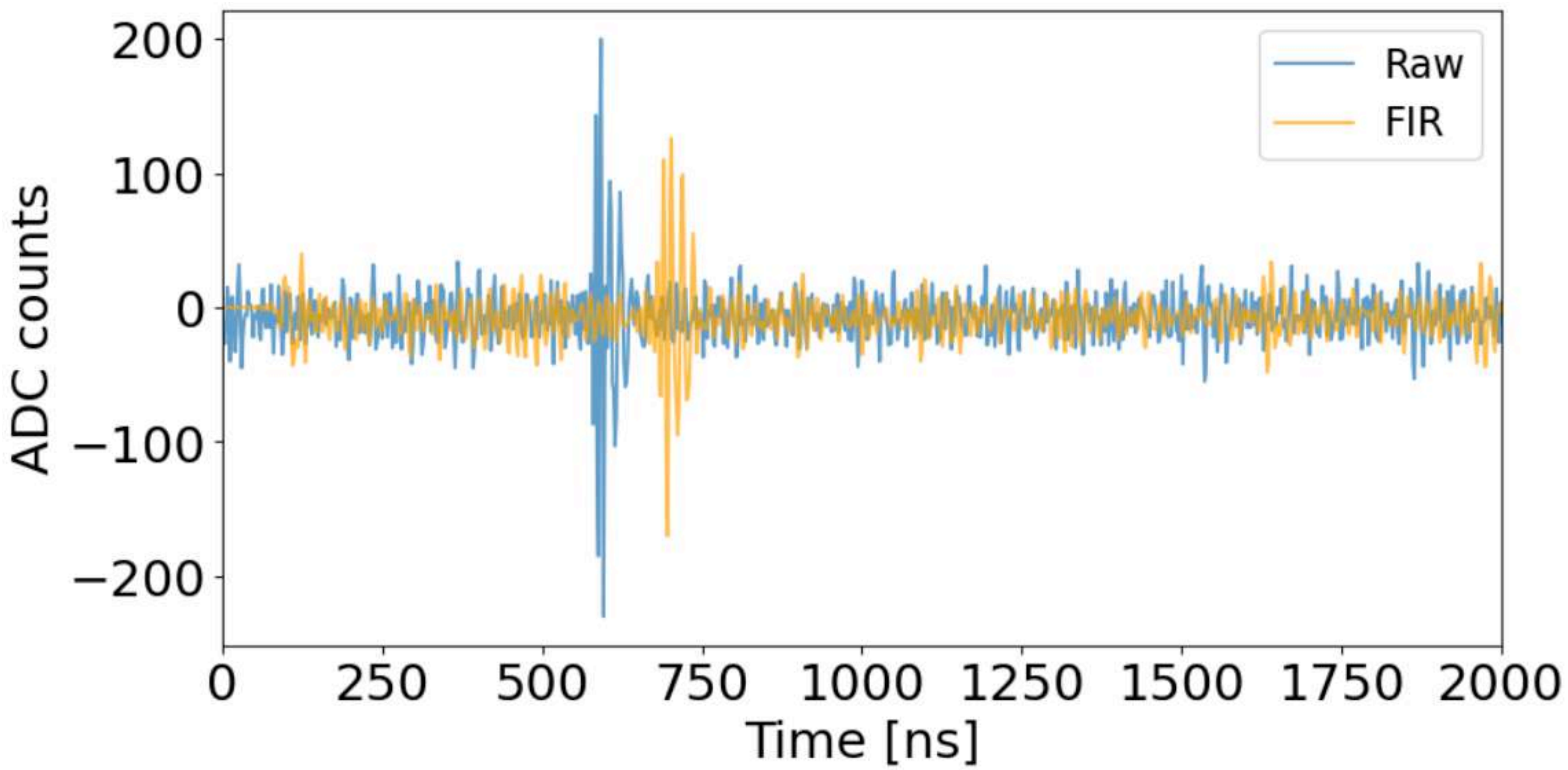

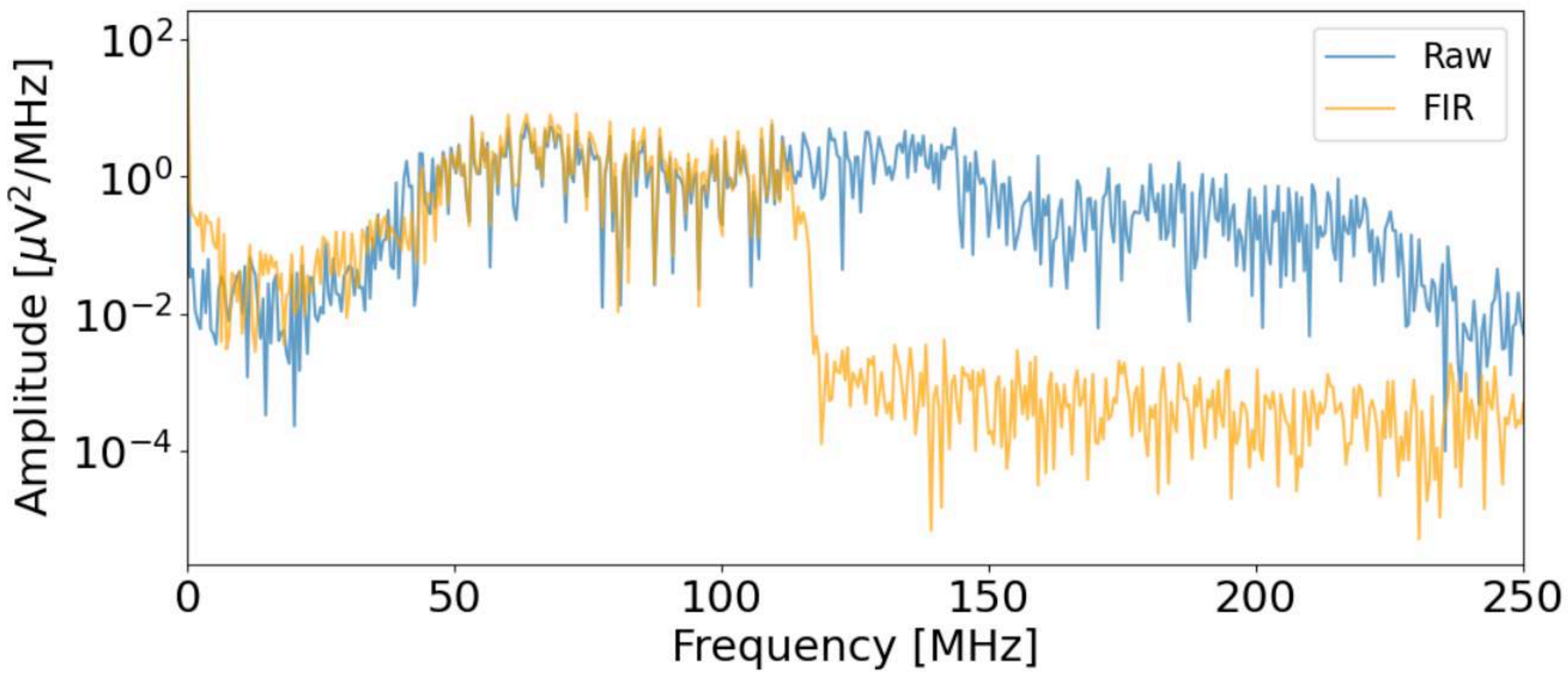

Number of crossings

GRAND realistic simulations:

- Simulated electric fields with ZHAireS
- Process through simulated detector response
- Add **measured noise** on GP300 site
- Digital filtering: Finite Impulse Response (FIR)

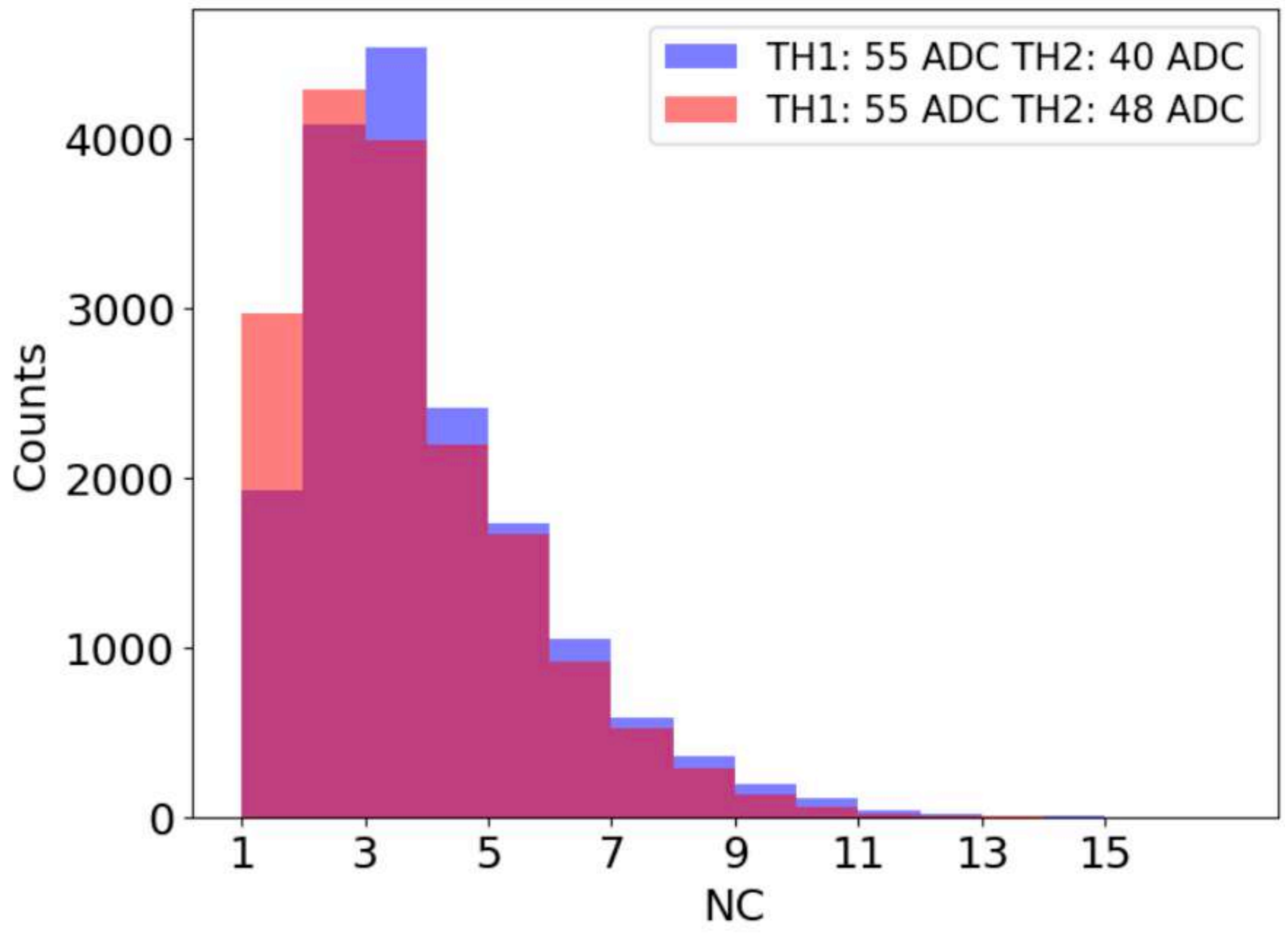

Optimization of First Level Trigger Parameters: purity

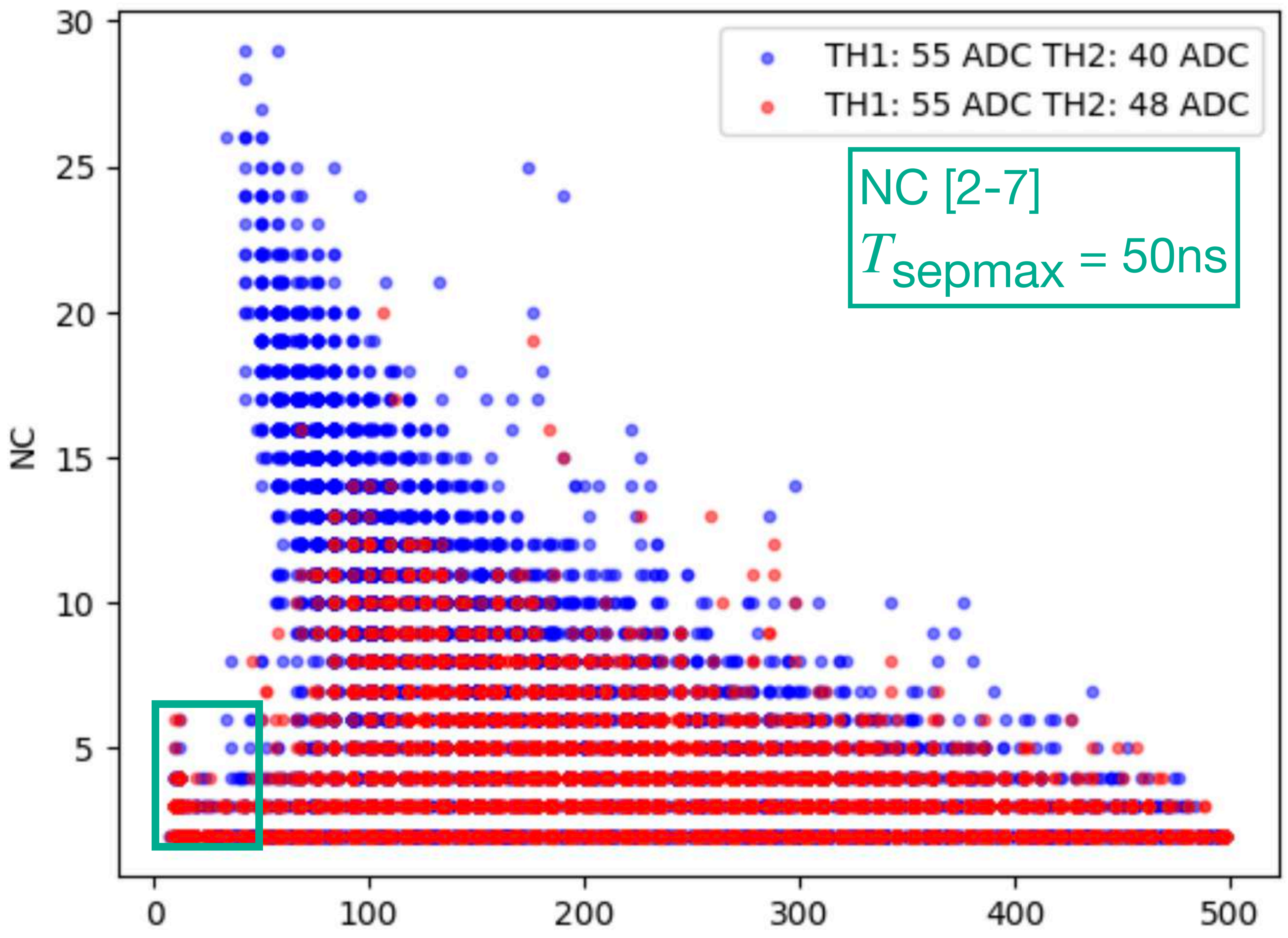

Maximum time separation between two consecutive crossings [ns]

Power Density Spectrum

PSD for 13 antennas at GP300 site with analog filtering 50-200 MHz

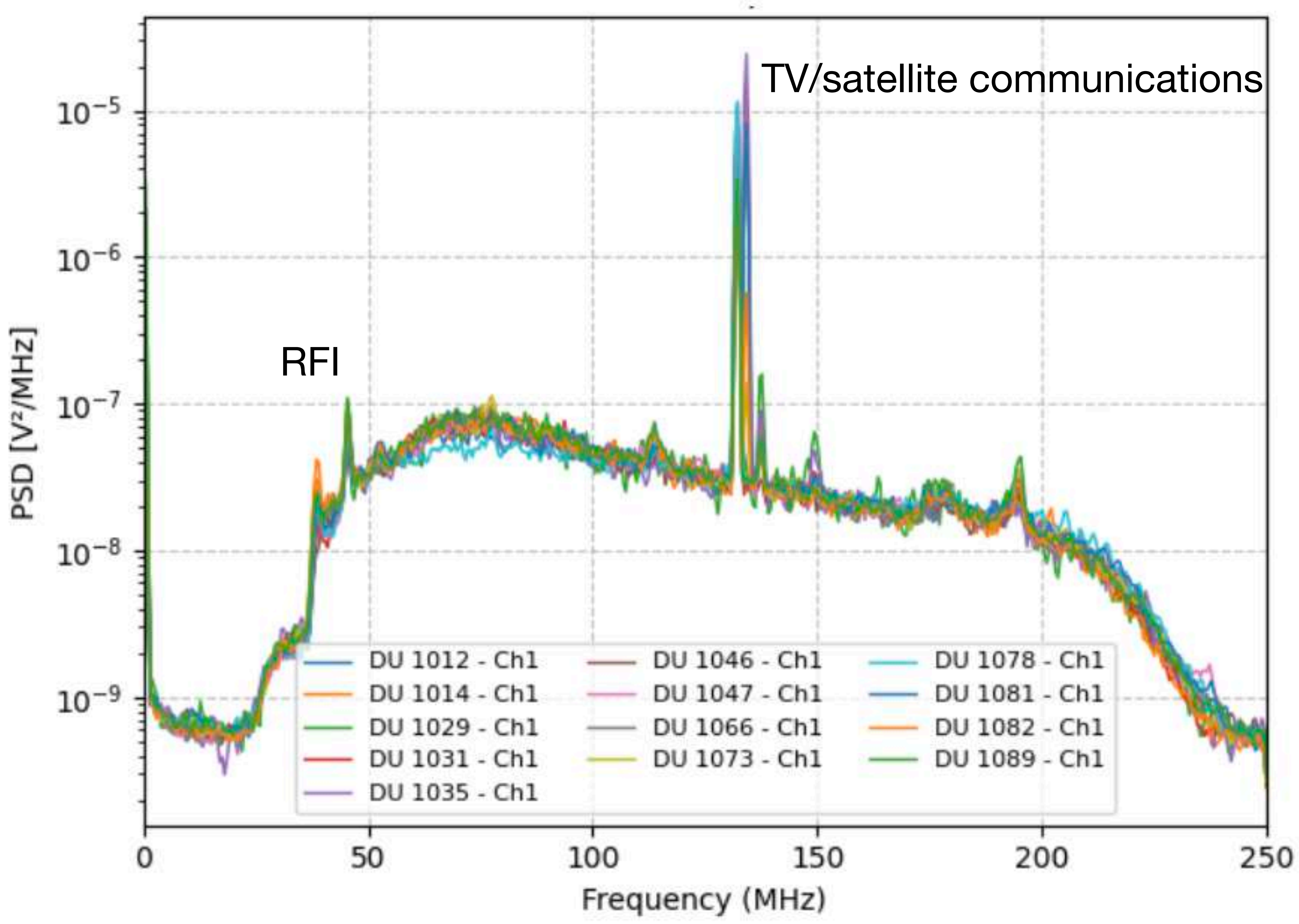

Power Density Spectrum

Monitoring data from 2024
No analog filter

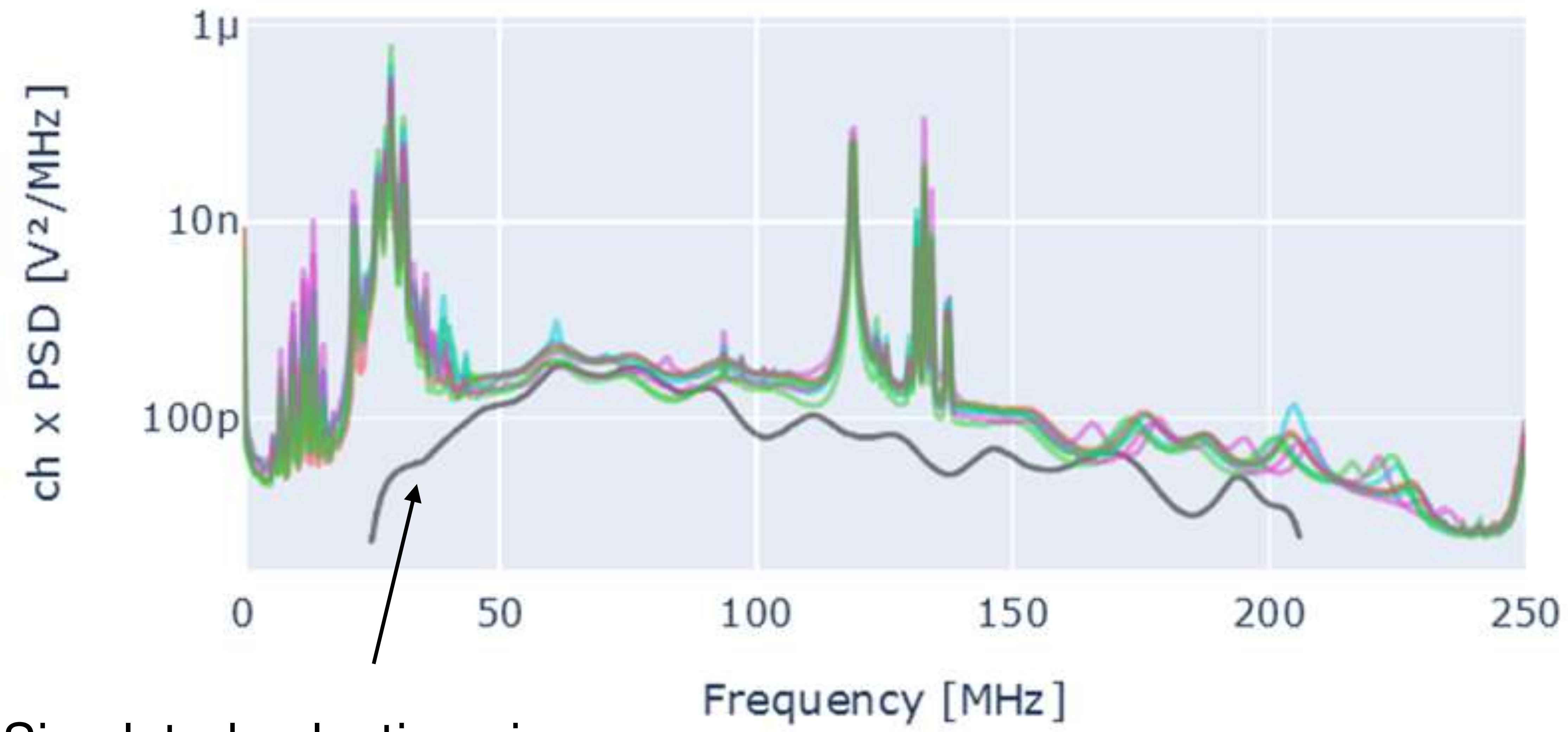

Simulated galactic noise

Data transmission and NUTRIG

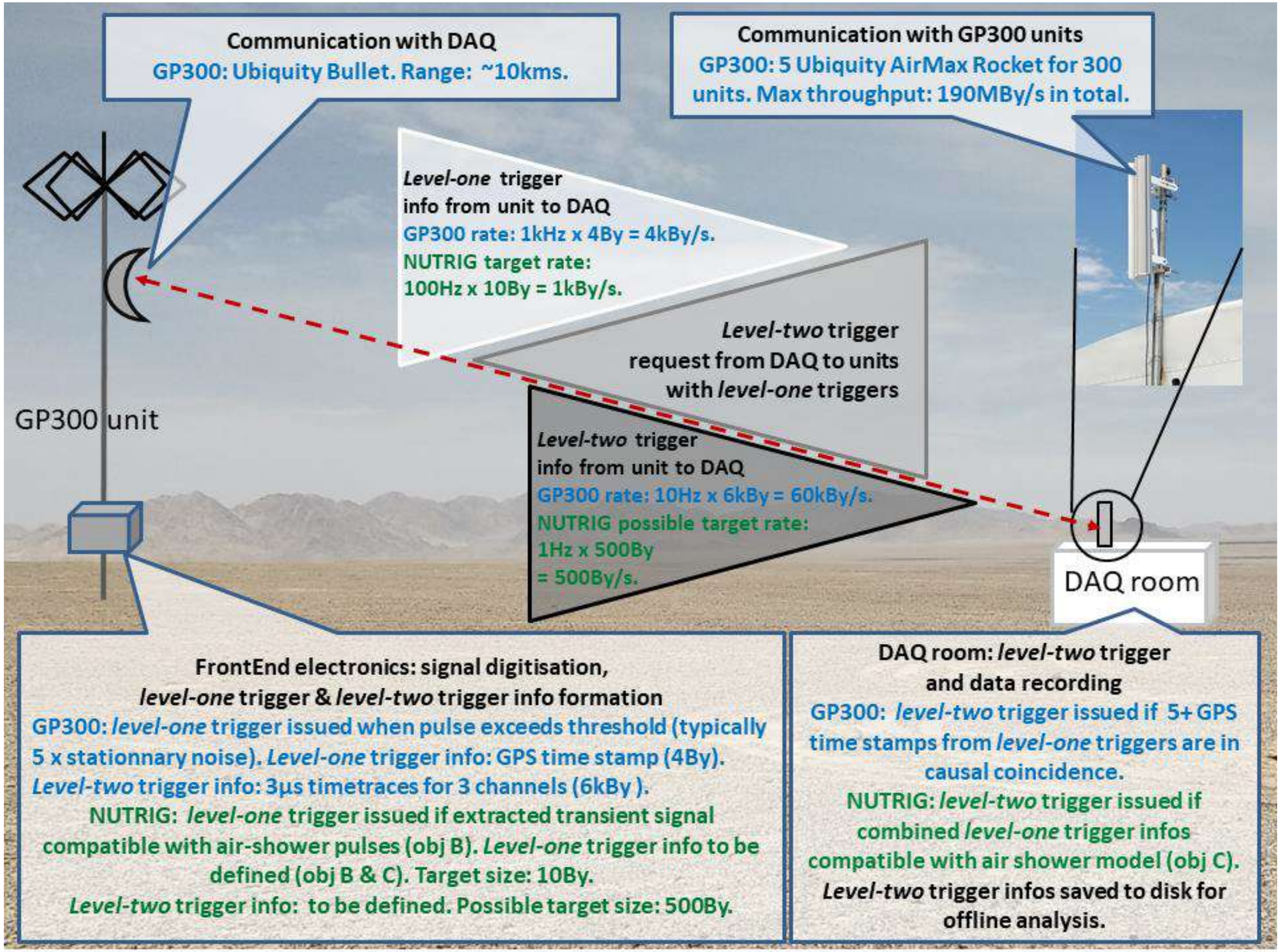

NUTRIG

From Pablo Correa

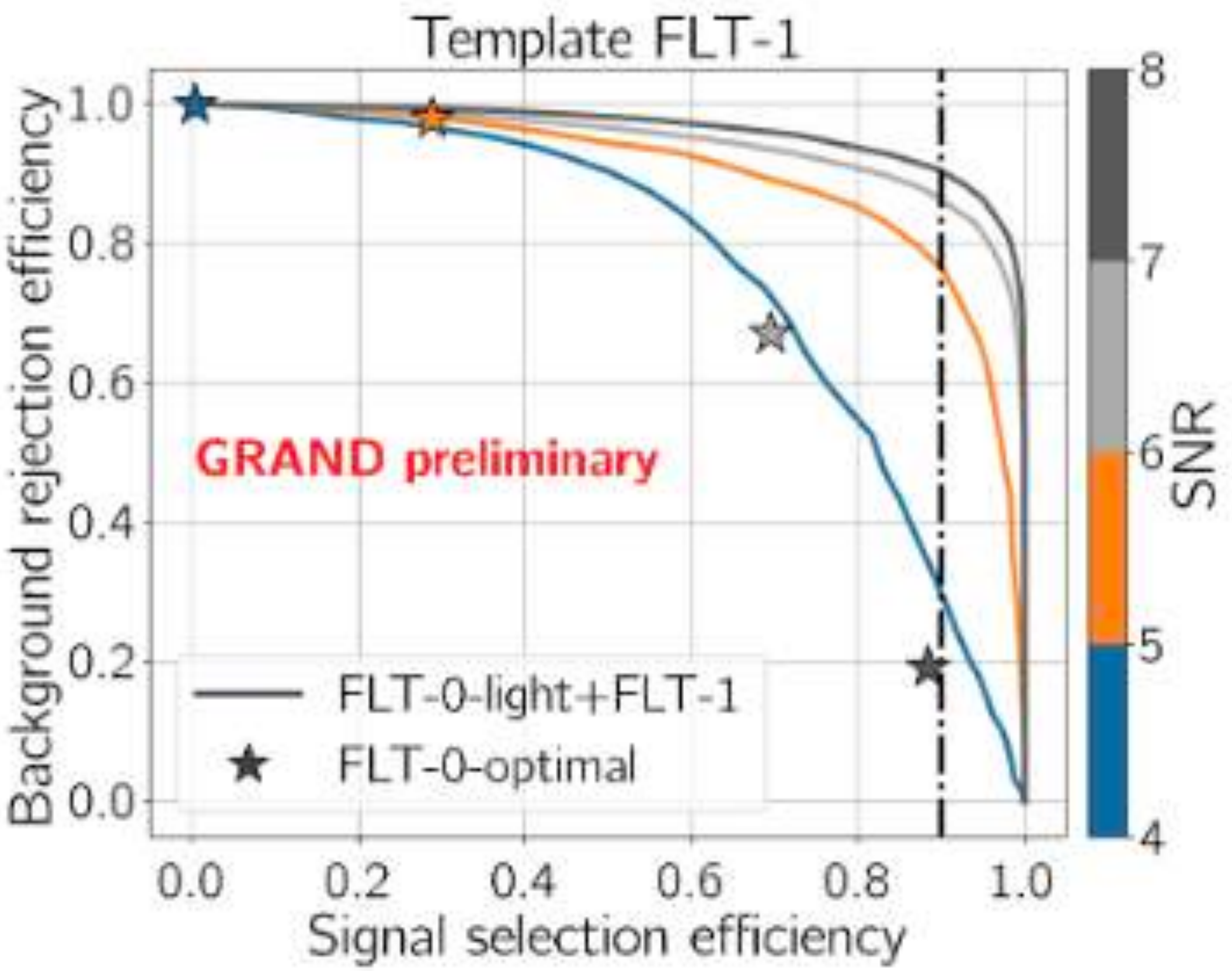

Cherenkov angle computation

Monte Carlo codes: ZHAireS
Filter: 50-200 MHz
From X_{source}

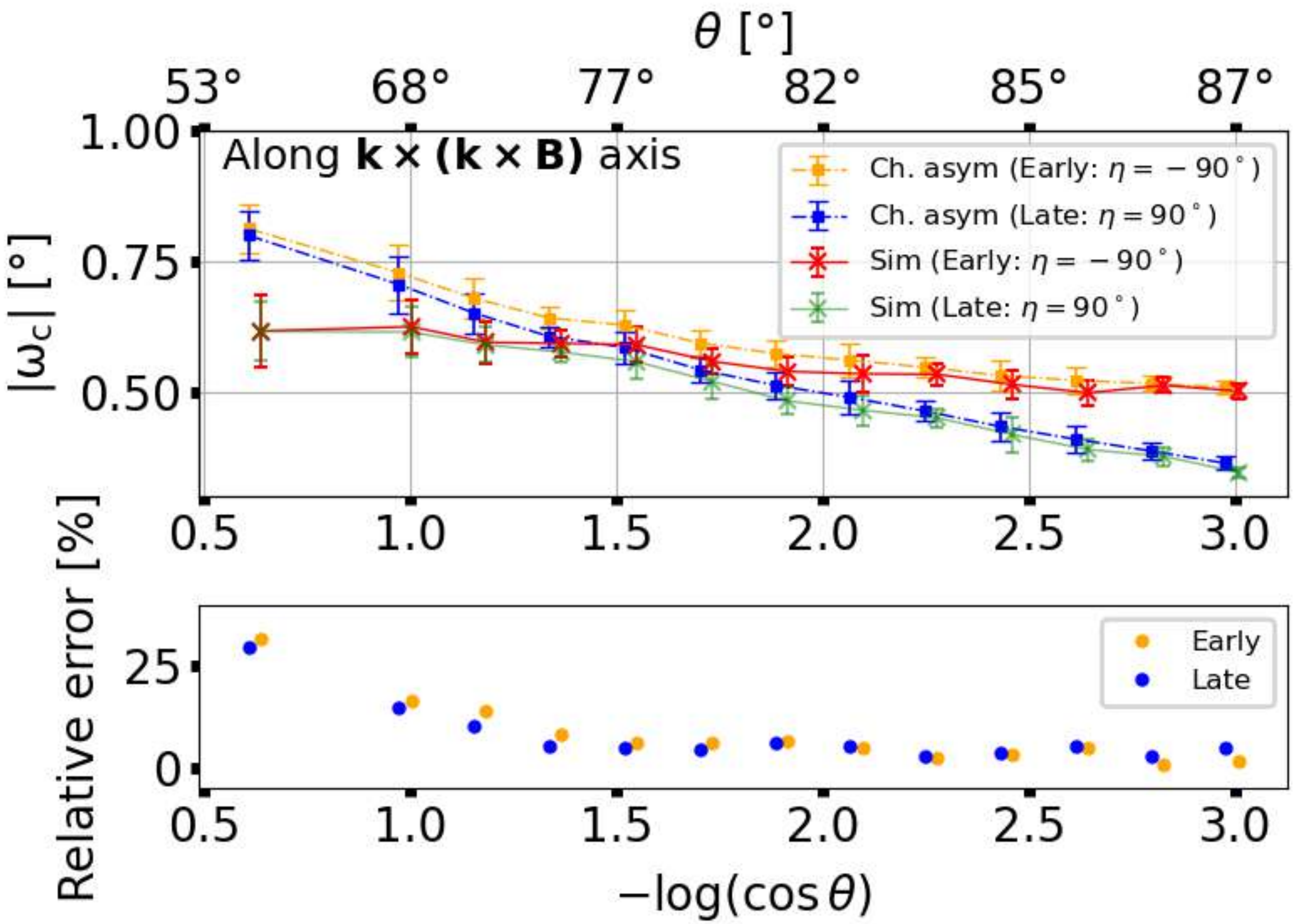

Cherenkov angle computation

Monte Carlo codes: ZHAireS
Filter: 50-200 MHz
From X_{max}

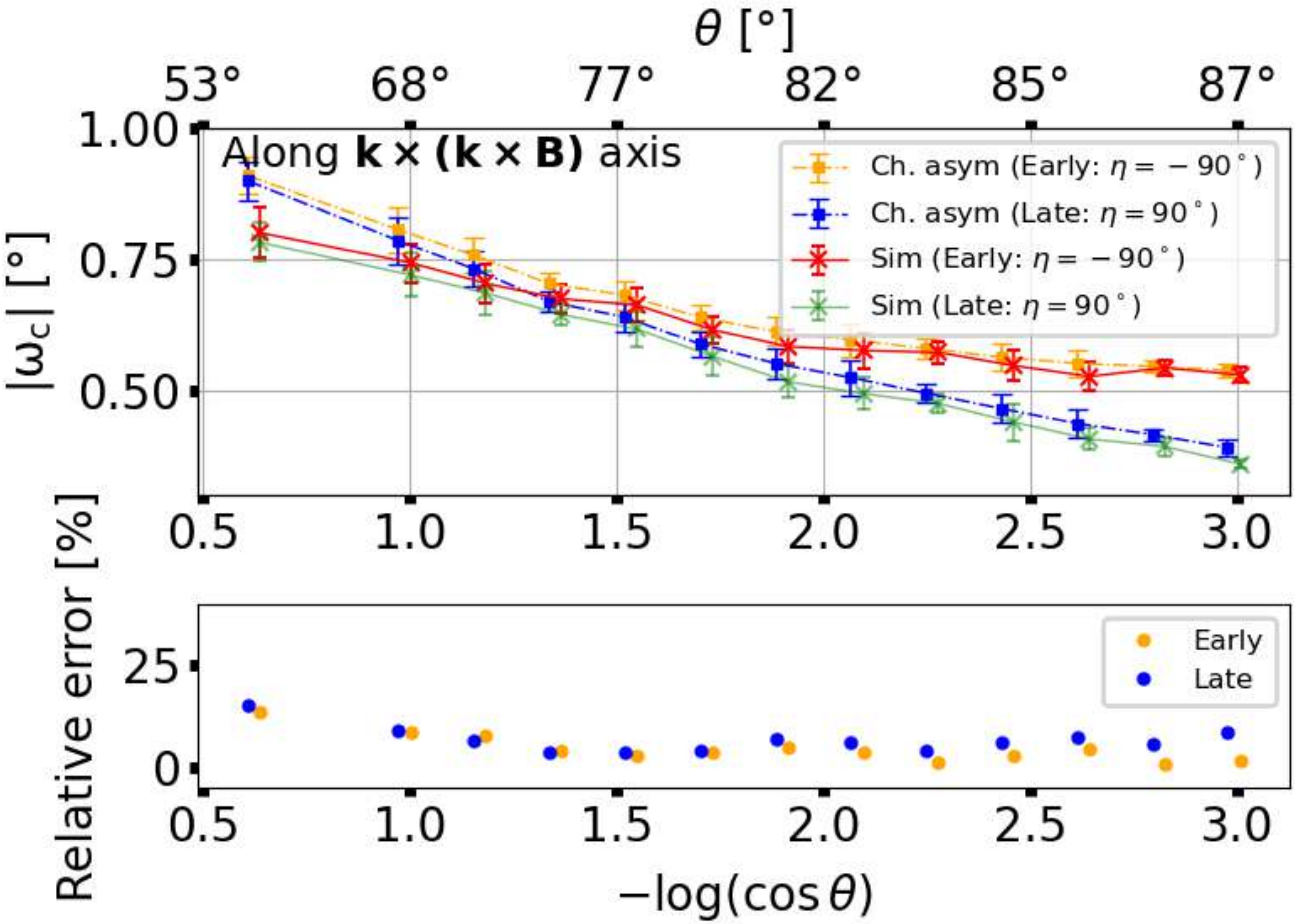

Frequency effect

Monte Carlo codes: ZHAireS
Filter: 50-200 MHz

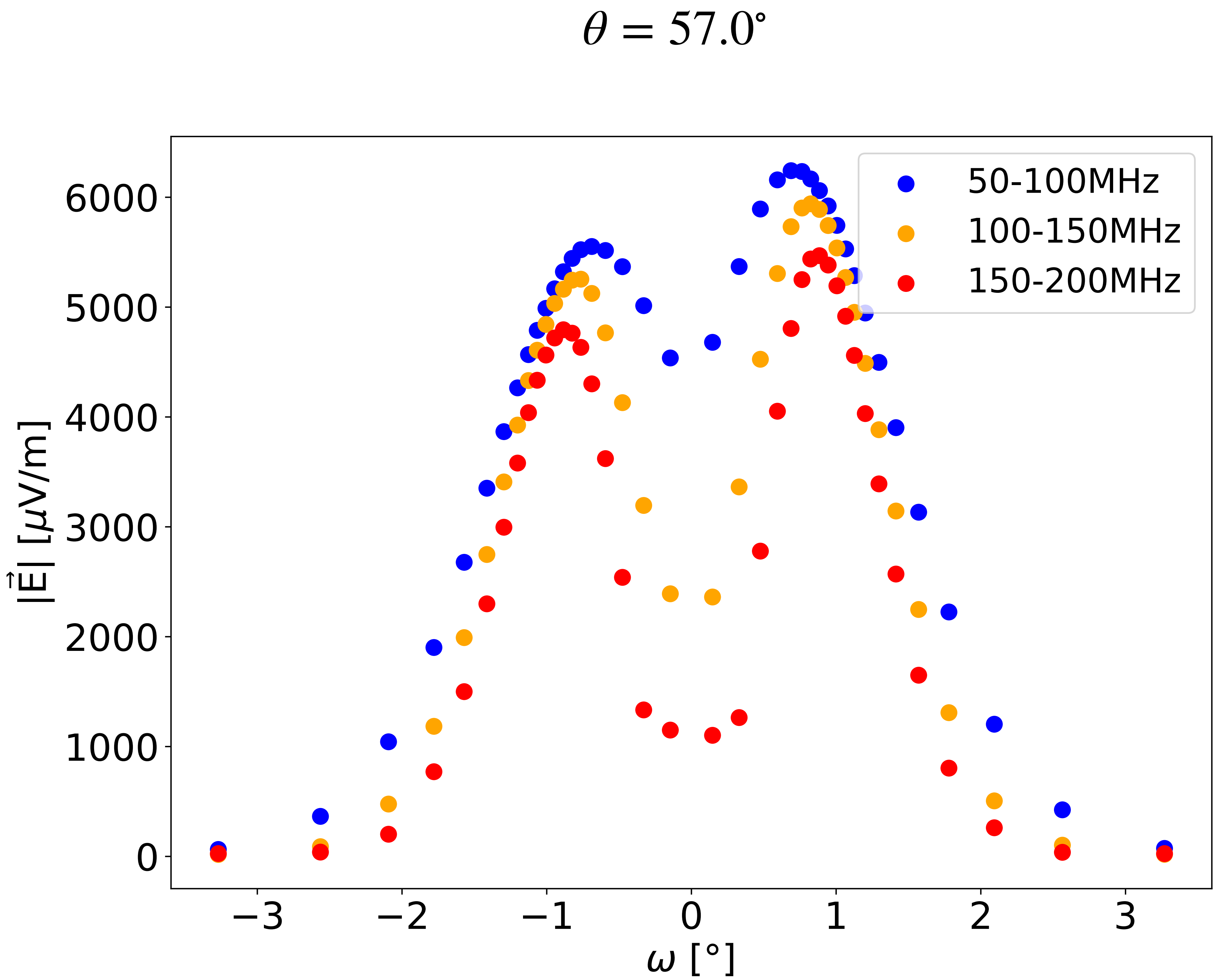

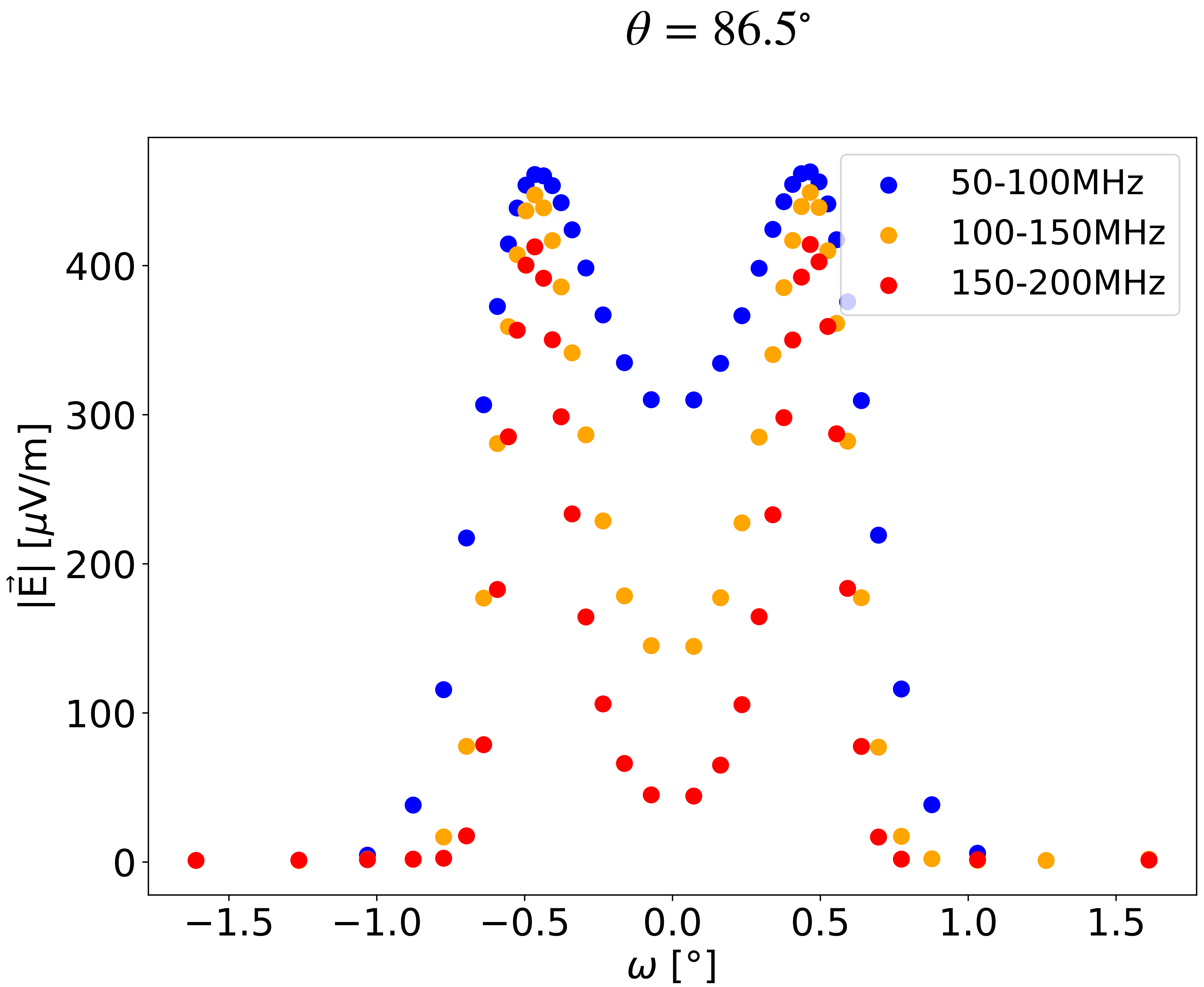

Cherenkov angle computation

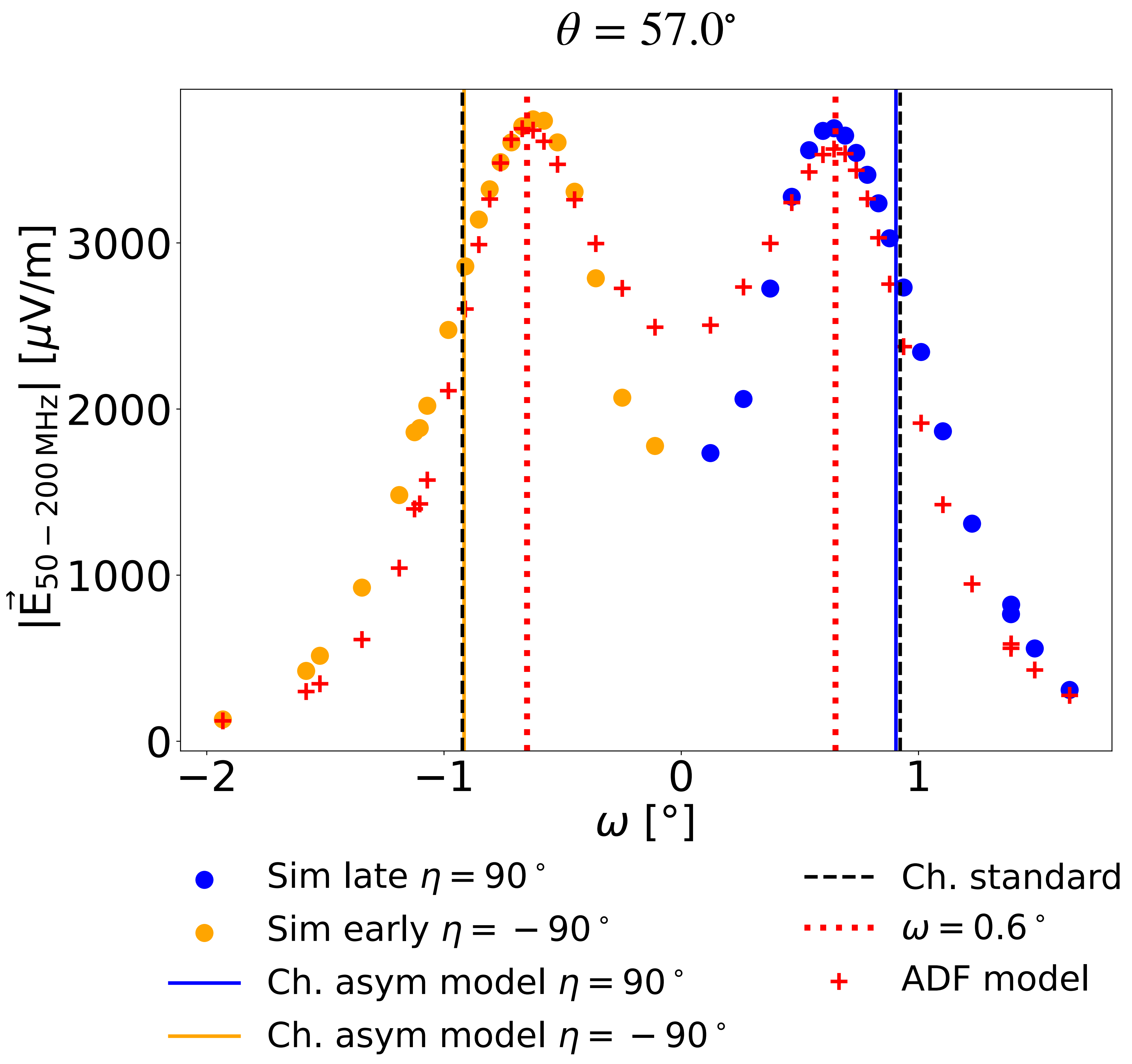

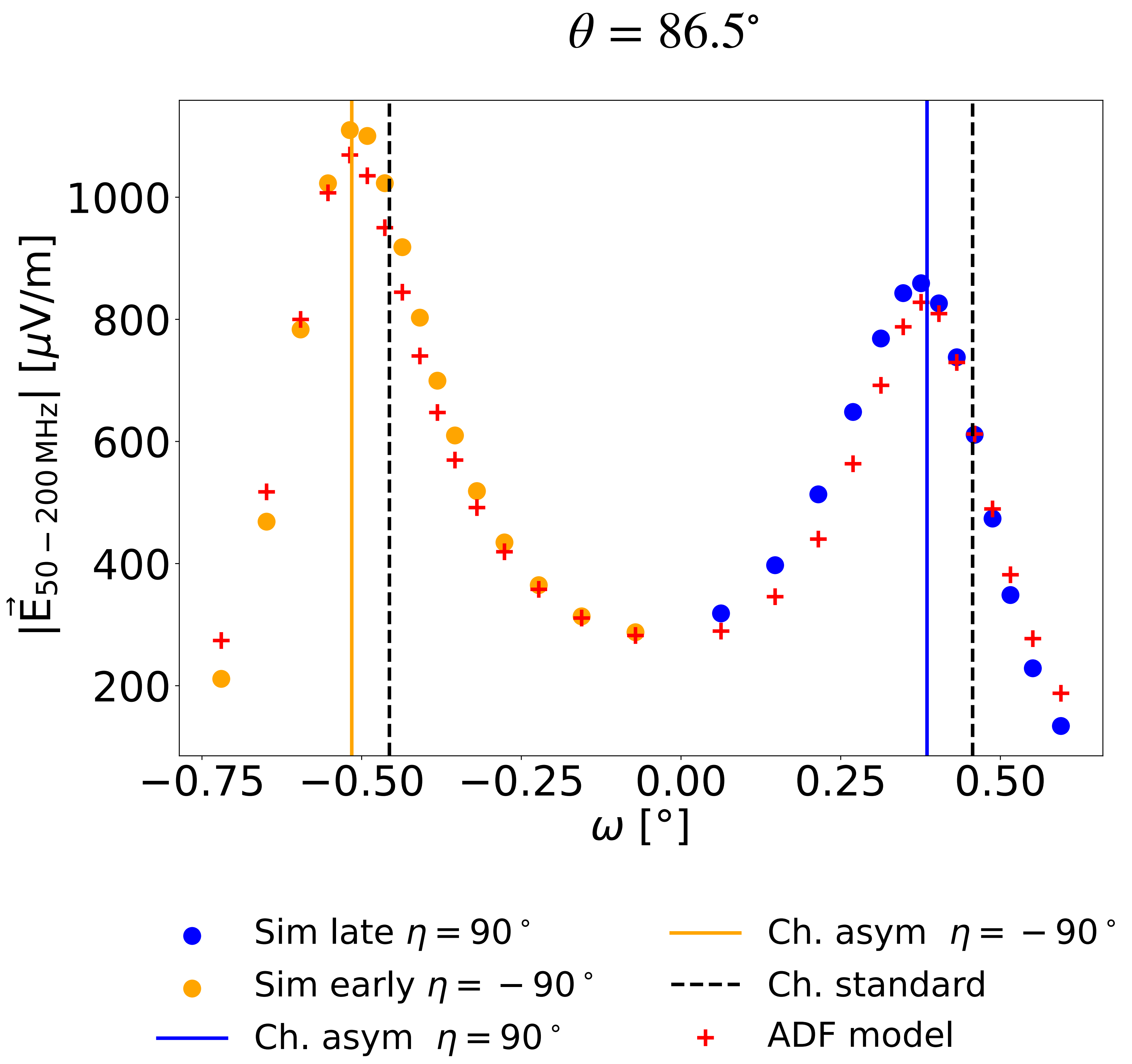

Layout

Starshape layout

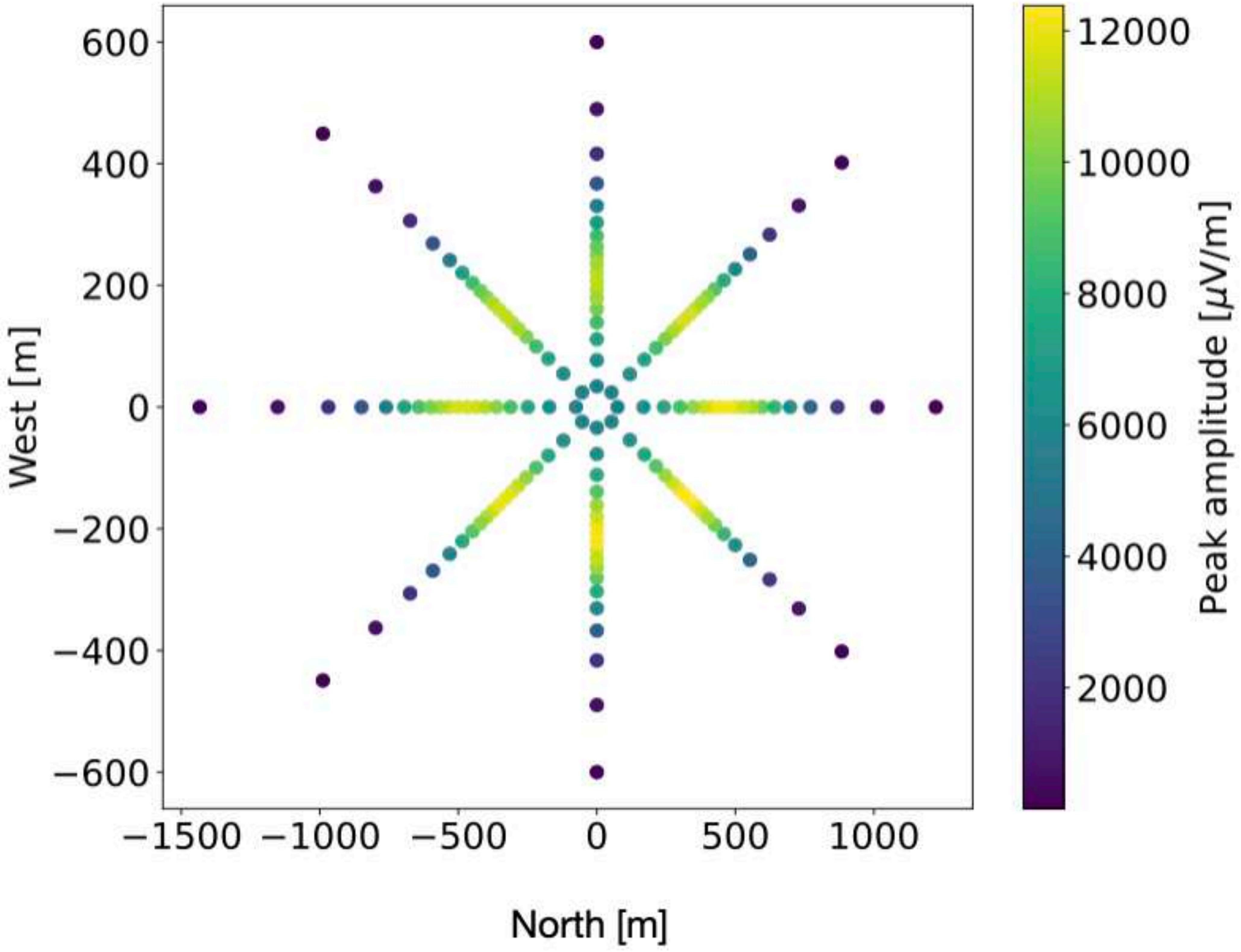

Realistic GRANDProto300 layout

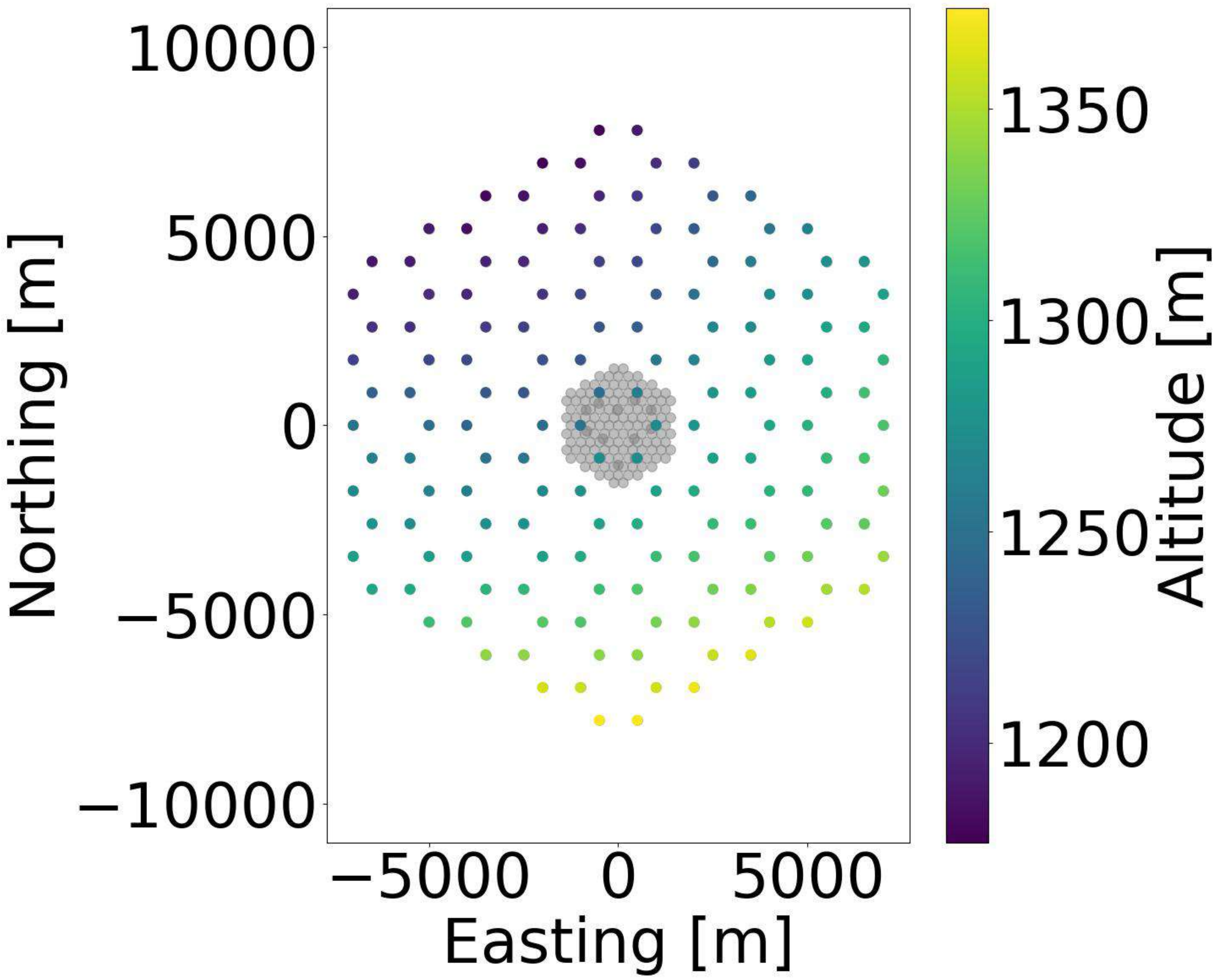

Angular resolution

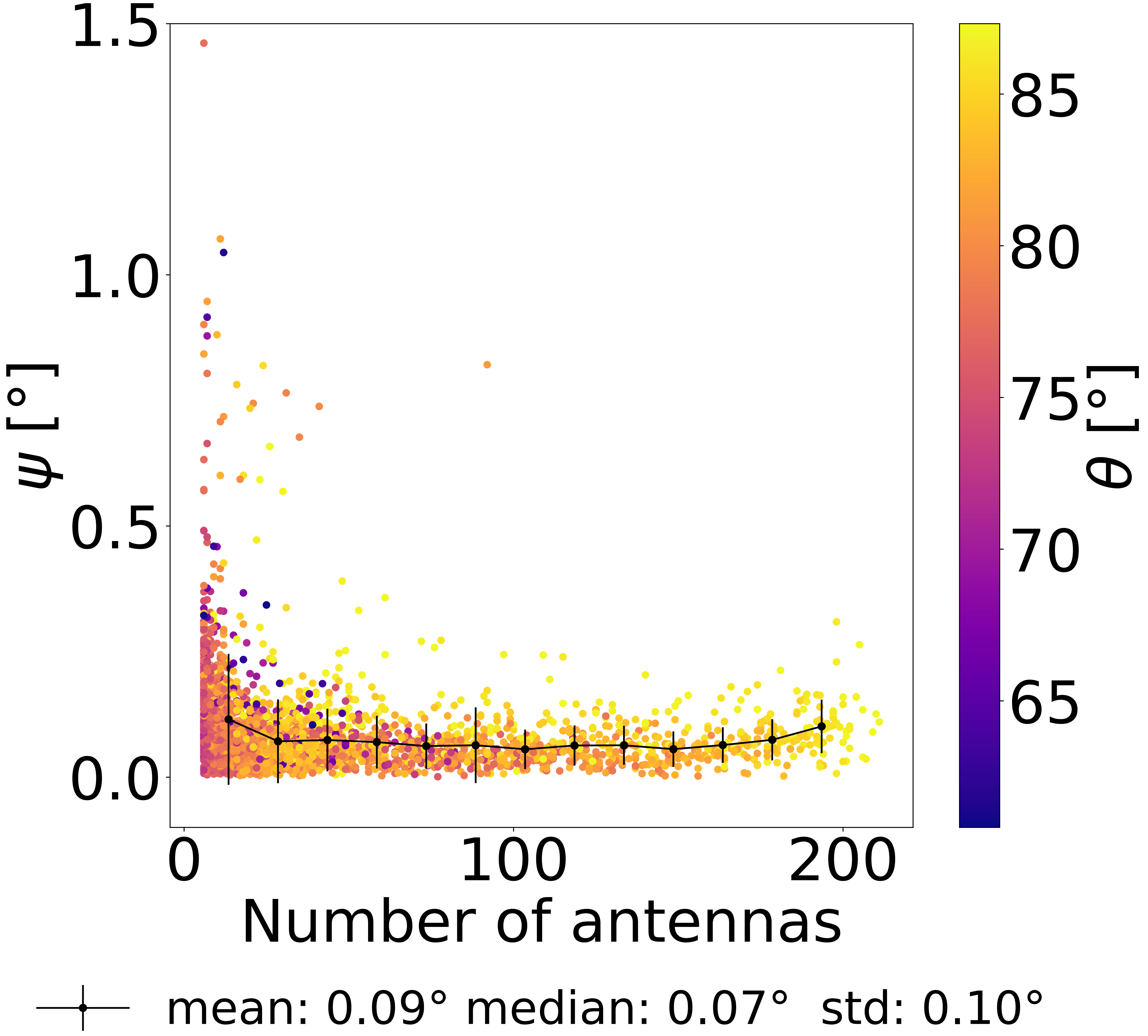

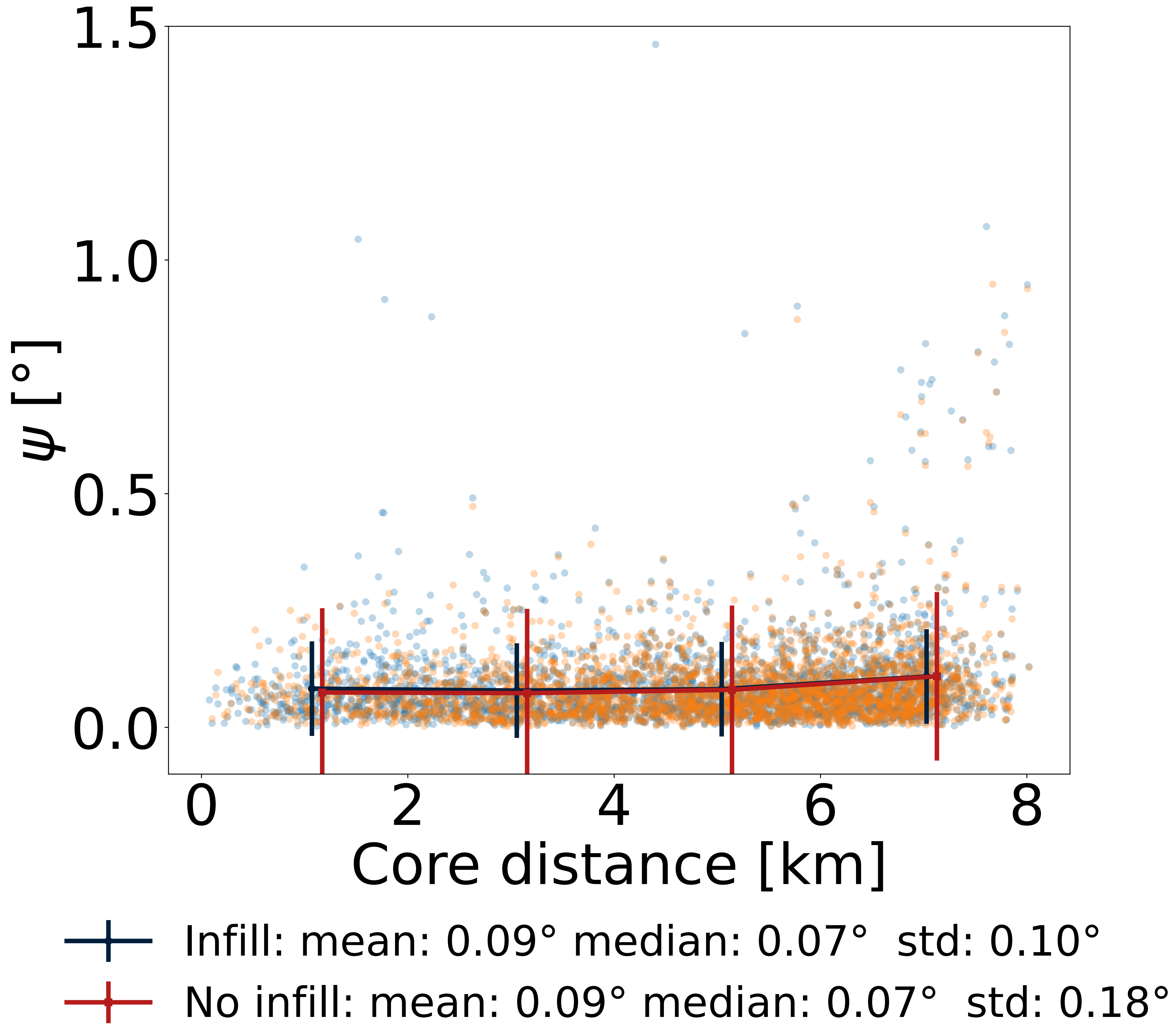

Energy resolution

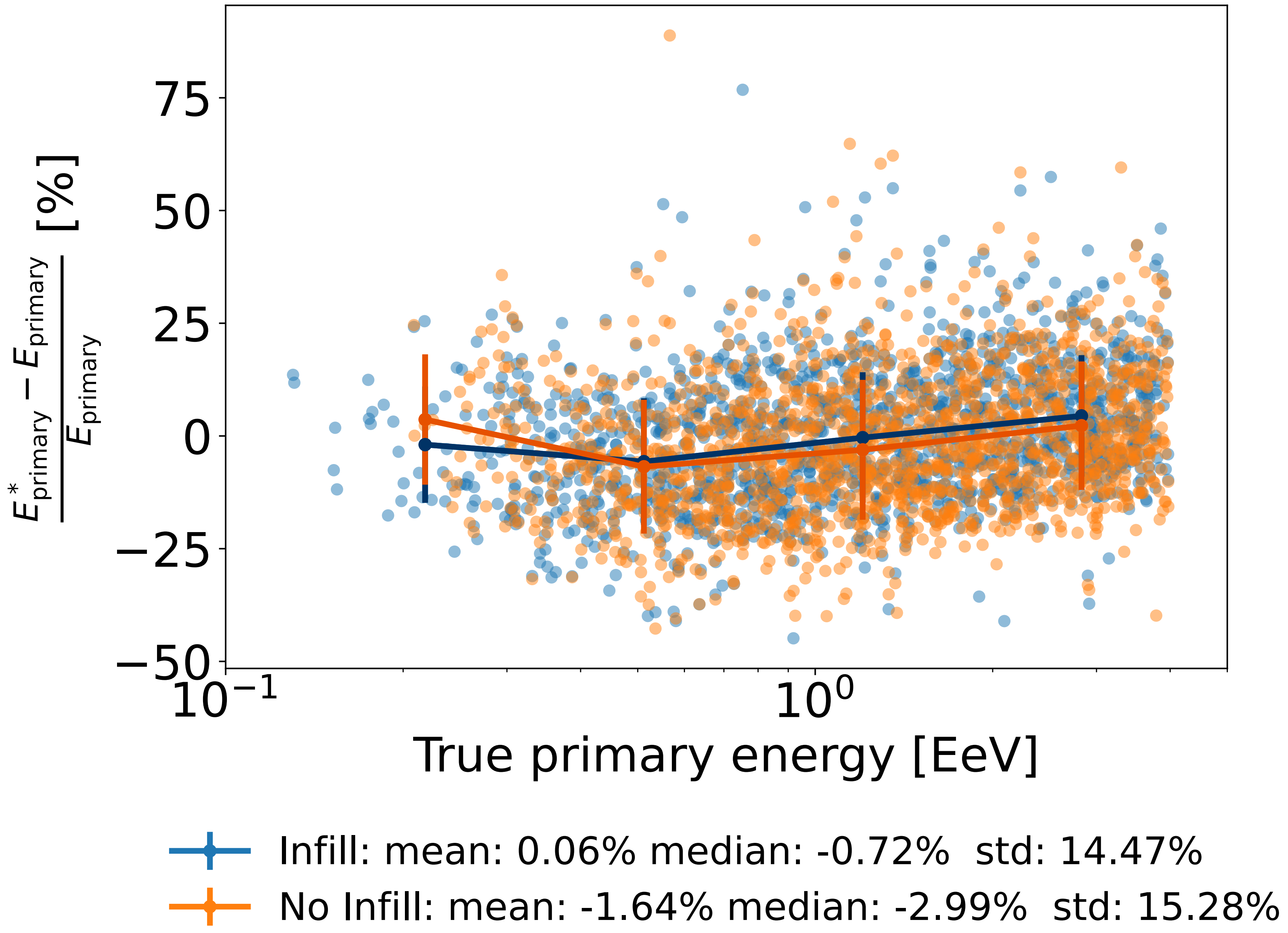

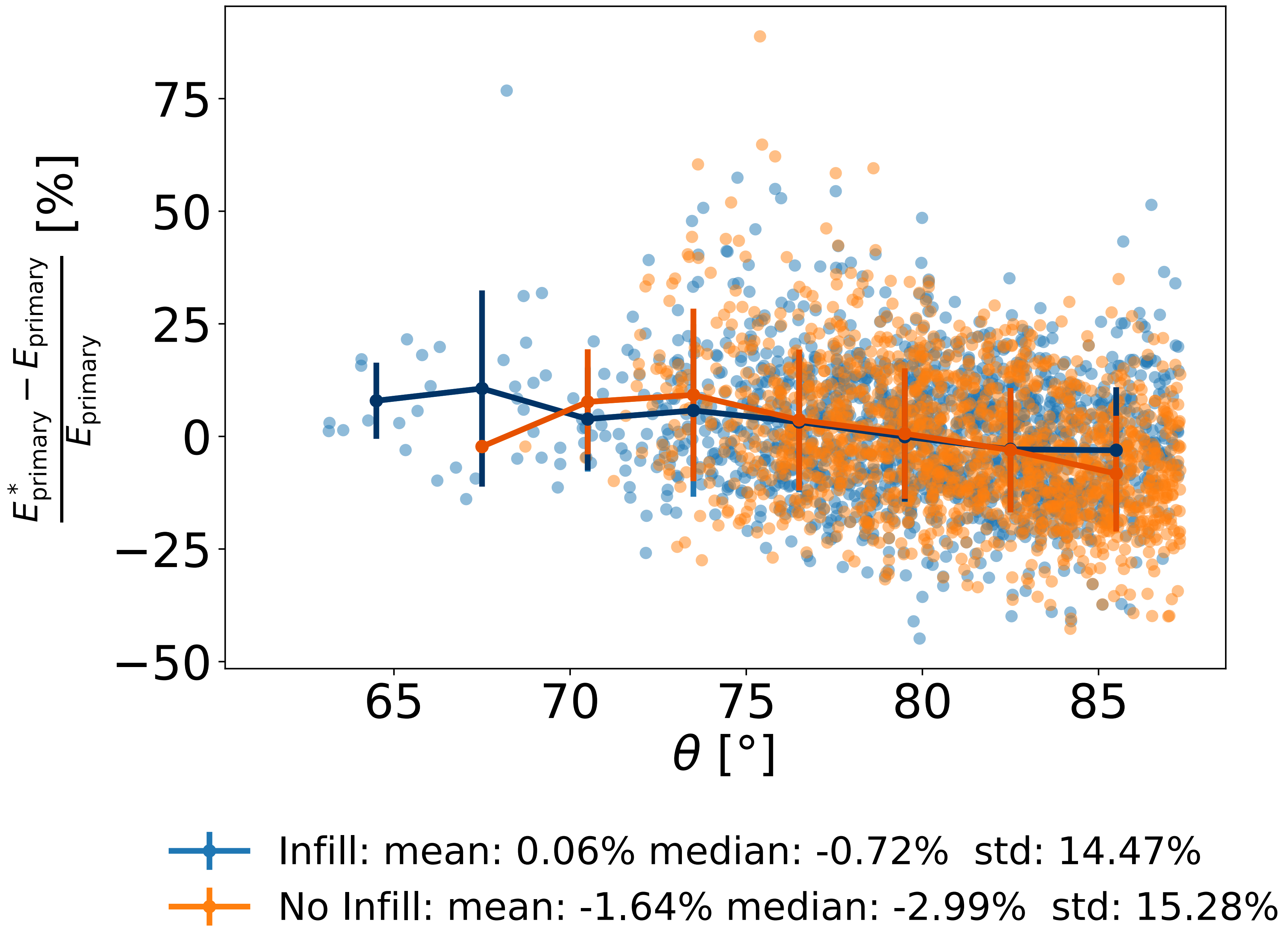

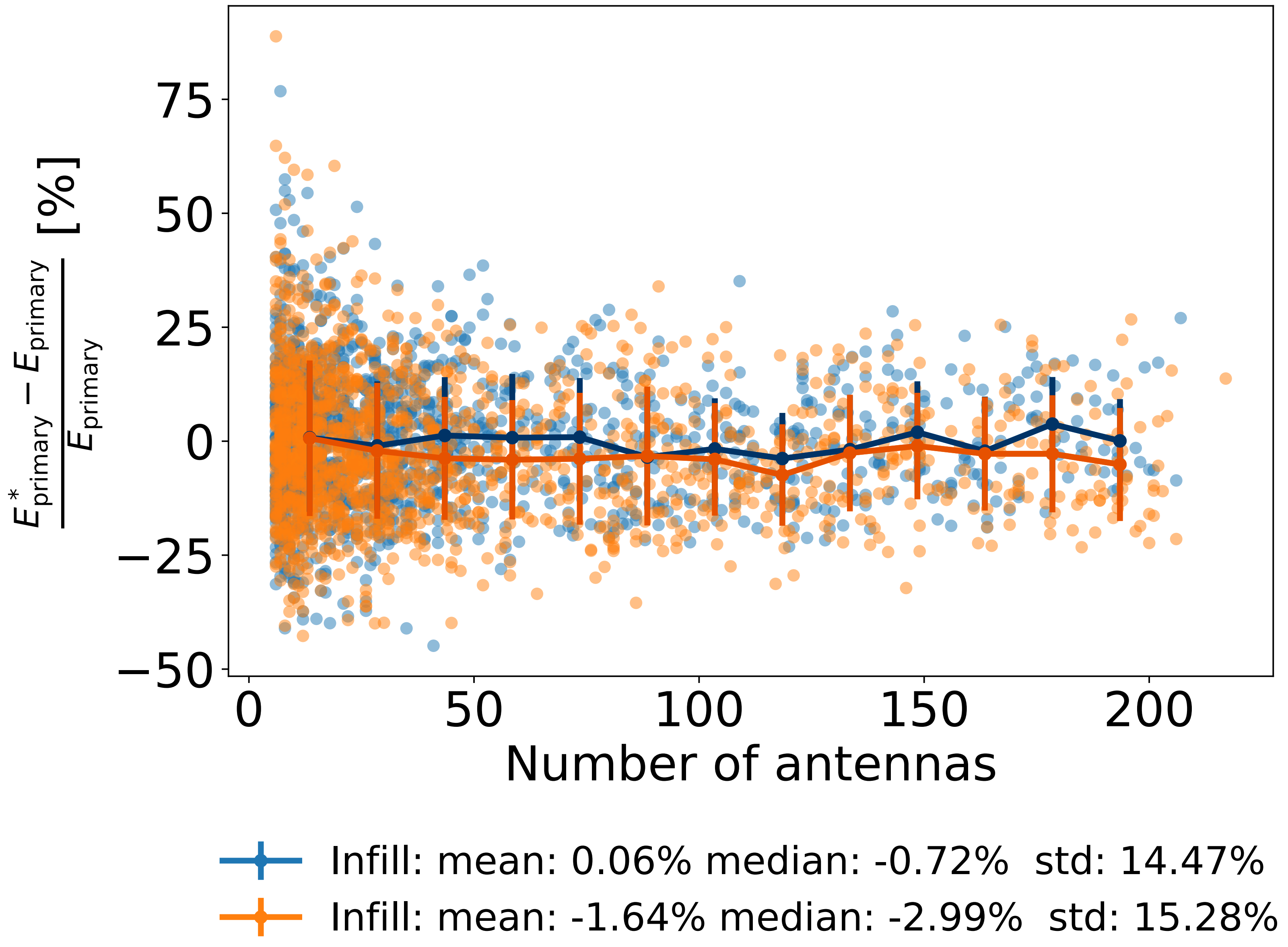

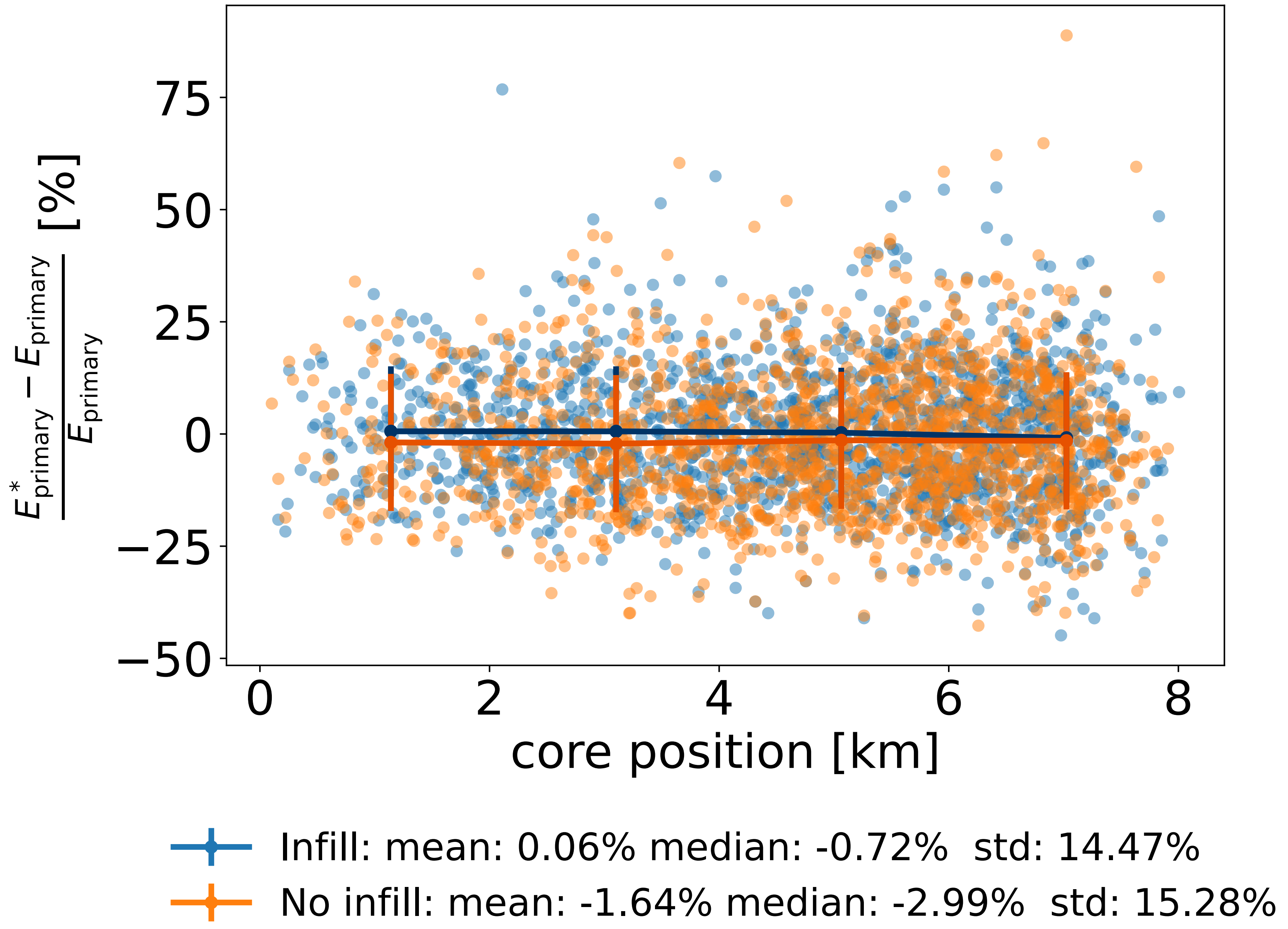

Energy resolution

Only Protons

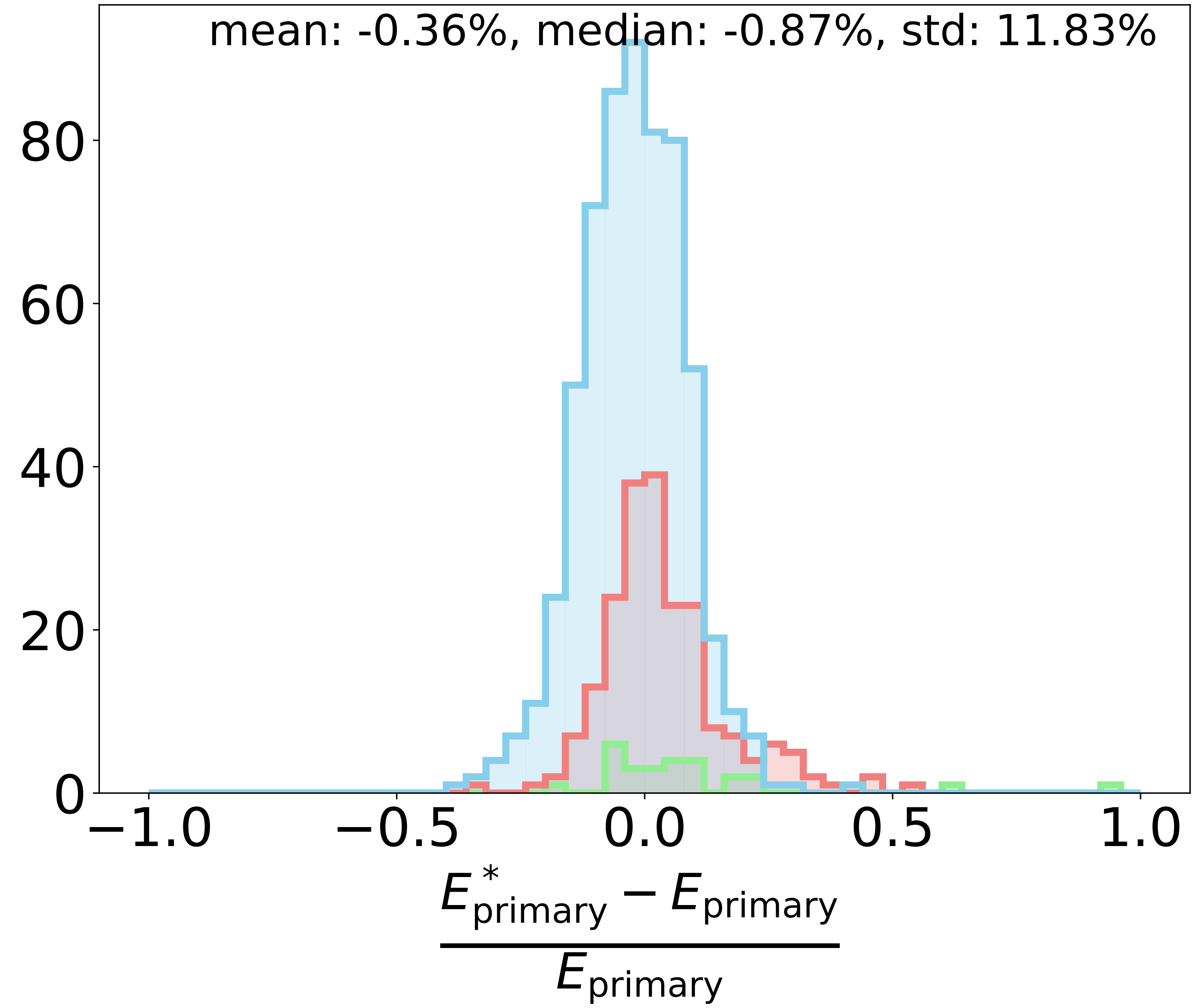

(61.3°-70.0°) σ: 22.03%
(70.0°-78.7°) σ: 12.28%
(78.7°-87.3°) σ: 10.35%

Only Irons

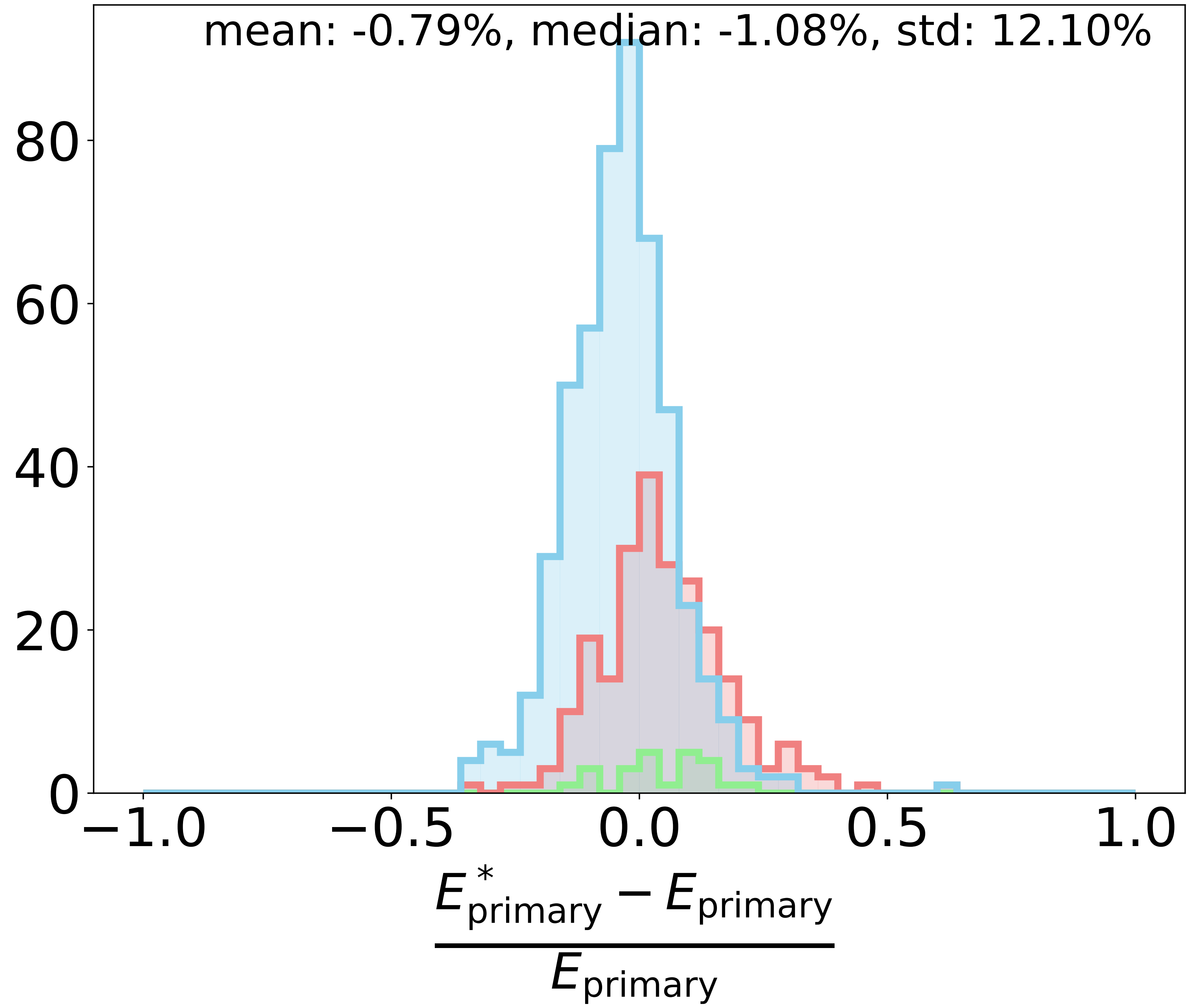

(61.8°-70.3°) σ: 9.33%
(70.3°-78.8°) σ: 12.85%
(78.8°-87.3°) σ: 10.69%

ADF fit and background fit

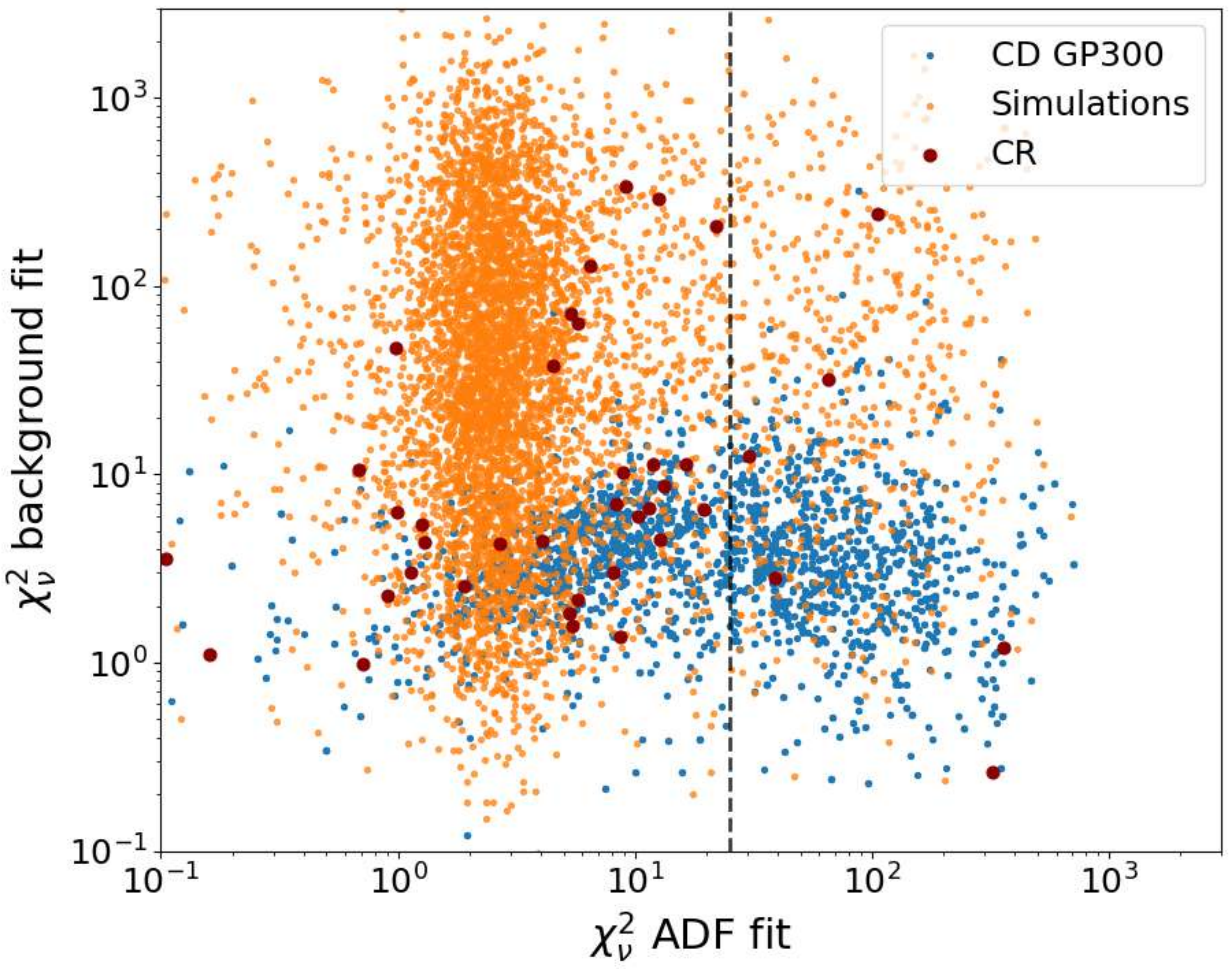

Reconstruction on ADC signal